

**Characterization of alteration and mineralization of the Moss gold
deposit, Shebandowan greenstone belt, Northwestern Ontario**

Michael Ugochukwu Nwakanma

A thesis submitted in partial fulfillment of the requirements

For the degree of Master of Science

Department of Geology

Lakehead University

December 2024

Abstract

The Moss Au deposit is an orogenic-style gold deposit hosted in felsic to intermediate rocks of the western Shebandowan Greenstone Belt, close to the terrane boundary between the Wawa-Abitibi terrane and the Quetico metasedimentary basin, ~120 km west of Thunder Bay. The deposit has an inferred mineral estimate of 140.07 Mt of ore averaging 1.09 g/t Au, which yields 4.91 Moz (Goldshore, 2024). The majority of the gold is hosted within diorite and dacite and is localized by shear zones and an array of quartz-carbonate-pyrite veins. The central-felsic metavolcanic belt of the Shebandowan Greenstone belt comprises felsic to intermediate units surrounded by late granitic intrusions, such as the Burchell Lake and Moss Lake stocks. This study focused on characterizing the alteration and mineralization at the Moss deposit and investigating any correlation between alteration and gold mineralization. A combination of petrography, geochronology, geochemistry, and mineral chemistry was used to achieve the objectives of this study.

Alteration occurs in different styles and intensities but generally comprises albite, biotite, sericite, chlorite, carbonate, and epidote alteration. Sulfide minerals are dominated by pyrite with minor chalcopyrite, sphalerite and molybdenite. Sulfide abundance is commonly 2 – 10% of the samples but can be up to 15% within sulfide-rich veins. Disseminated and vein-hosted pyrite are the two main textures in which pyrite occurs within the host rocks. A total of 12 vein types were observed, with quartz and carbonate being the most dominant veins occurring together in five of the vein types. Using the observed textural and crosscutting relationships of the alteration, sulfides, and veins, a paragenetic sequence was developed, highlighting the secondary processes associated with the formation of the Moss Lake deposit. Deformation textures were observed in early and late alteration phases, suggesting a long deformation history that was broadly coeval with mineralization.

Quartz-carbonate-pyrite ± sericite ± chlorite ± epidote veins are host to most of the observed gold occurrences, and are common within or in proximity to shear zones. Gold was rarely associated with disseminated pyrite away from veins. Gold grains occurred as inclusions in

pyrite, on the rims of pyrite grains and in the groundmass around pyrite grains within the host vein and are genetically related to pyrite.

A Re/Os age (2708 ± 12 Ma) from molybdenite from a Type 3 quartz-carbonate-pyrite vein is interpreted to be the age of mineralization. This age, when compared with the ages of the host rock from the Skimpole Lake area (2721 ± 4 Ma; Corfu, 1998), and the nearby Burchell Lake stock (2680 ± 3 Ma; Corfu, 1983), constrains the gold mineralizing event between 2725 Ma – 2694 Ma. The age of gold mineralization overlaps with the age of the Central Felsic Metavolcanic belt (CFB) and indicates that the mineralizing event is older than the nearby intrusions.

Hyperspectral data showed the presence of different species of white mica and chlorite. The white mica with a spectral range of 2208 – 2216 nm is associated with most of the high gold values and corresponds to white mica with a mixed phengite-muscovite composition. Chlorite with a spectral range between 2242 – 2249 nm is associated with gold-bearing samples. Mineral chemistry of chlorite and white mica varies with proximity to the center of the deposit. For white mica, Mg was highest in the samples proximal to the center of the deposit and lowest in the more distal samples. For chlorite, Mg and Si are highest in proximal samples and lower in distal samples, whereas Fe and Al are lower in the proximal samples and higher in the distal samples. These compositional changes in white mica and chlorite composition could be linked to the Tschermak substitution reaction, where Al is replaced by Si in the tetrahedral sites, while Mg or Fe is incorporated into the octahedral sites. This reaction can be attributed to temperature changes linked to interaction with mineralizing fluids during deposit formation. In general, the alteration intensity varies across the deposit with no clear vector towards mineralization. However, the mineral chemistry and spectral features of white mica and chlorite show a trend that can be used as a vector to ore, if properly applied.

Acknowledgments

Firstly, I thank God almighty for his infinite mercies and guidance throughout this journey and my life in general. I want to especially thank my supervisor, advisor, and teacher, Dr. Peter Hollings, for providing me with the guidance and support required to embark and complete this study with success. I also want to thank you for believing in me, Dr. Hollings.

I want to thank colleagues who have helped me during this study, Dr. Tobias Stephan and Dr. James Tolley; your contributions and advice were important. Thanks to Dr. Jonas Valiunas and Kristi Tavener for their help in the thin section preparation. I am also grateful for the effort of the staff at the Department of Geology to ensure the smooth running of student affairs and the important facilities that aid successful analysis and research work. Also thanks to the Goldshore team, Peter Flindell, Jason Pattison and others for providing me with all the important data needed to successfully conduct this study. Thankful to the EMPA lab team at the University of Toronto for their assistance in completing that analysis successfully.

Finally, I want to thank my sister, Mrs. Chioma Emeodume, for her good advice, and my family, friends, and loved ones for their support throughout the course of my study.

Table of Contents

Abstract	i
Acknowledgments	iii
Table of Contents	iv
List of Figures	vi
List of Tables	ix
1. Introduction	1
1.1 Introduction	1
1.2 Objectives.....	2
1.3 Orogenic Gold Deposits	2
2. Methods	7
2.1 Sampling.....	7
2.2 Petrography	8
2.3 4-Acid digest Geochemistry	8
2.4 Re/Os Geochronology.....	9
2.5 Short Wave Infrared (SWIR) Analysis.....	9
2.6 Electron Probe Microanalyzer (EPMA)	9
3 Regional Geology	11
3.1 Superior Province.....	11
3.2 Wawa-Abitibi Terrane.....	13
3.3 Shebandowan Greenstone Belt	14
3.4 Local Geology.....	19
3.5 Mineral Deposits and Exploration History.....	26
3.6 History of Moss Lake Deposit	27
4 Results	29
4.1 Sampling and Petrography.....	29
4.1.1 Dacite	31

4.1.2	Diorite.....	31
4.1.3	Andesite	32
4.1.4	Sulfides.....	33
4.1.5	Alteration	35
4.1.6	Veins.....	38
4.1.7	Au Mineralization.....	42
4.1	Re/Os Geochronology.....	44
4.2	Geochemistry and Spectral Data	45
4.3.1	Geochemistry	45
4.3.2	Spectral data.....	46
4.3	Mineral Chemistry.....	51
5	Discussion	56
5.1	Age Constraints of Au Mineralization	56
5.2	Paragenesis and Gold Occurrences	59
5.2.6	Paragenesis of Moss Lake Deposit.....	59
5.2.7	Sulfide and Gold.....	66
5.3	Alteration and Mineralization.....	69
5.4	Summary	78
6	Conclusions	80
	References	84
	Appendix I Thin Section Descriptions	90
	Appendix II 4 Acid-Digest Geochemistry	141
	Appendix III SWIR spectral data.....	152
	Appendix IV EPMA Mineral Chemistry data	156

List of Figures

<i>Figure 1.1: Location map of the Moss Lake deposit from Thunder Bay, Ontario</i>	<i>1</i>
<i>Figure 1.2: Detailed representation of the subduction-based model for the formation of orogenic gold deposits</i>	<i>3</i>
<i>Figure 2.1: Photos of drill core samples selected for the study</i>	<i>7</i>
<i>Figure 3.1: Geological map of the Superior Province showing the various terranes.....</i>	<i>12</i>
<i>Figure 3.2: Map of the western Wawa-Abitibi Terrane</i>	<i>14</i>
<i>Figure 3.3: A section of the geological map of the Shebandowan greenstone belt</i>	<i>15</i>
<i>Figure 3.4: Geological map of eastern Shebandowan Greenstone belt</i>	<i>17</i>
<i>Figure 3.5: Geological map of the Shebandowan Greenstone belt (SGB)</i>	<i>18</i>
<i>Figure 3.6: Simplified geological map of western Shebandowan greenstone belt.....</i>	<i>21</i>
<i>Figure 3.7: Geological map of the Moss Township.....</i>	<i>24</i>
<i>Figure 3.8: Geologic map showing the boundary of the Moss Lake Property</i>	<i>27</i>
<i>Figure 4.1: Plan view of the Moss Lake deposit</i>	<i>29</i>
<i>Figure 4.2: Downhole plots showing the different lithologies at the Moss Deposit</i>	<i>30</i>
<i>Figure 4.3: Photomicrographs of dacite from the Moss Deposit.....</i>	<i>31</i>
<i>Figure 4.4: Photomicrograph showing the diorites under cross-polarized light.....</i>	<i>32</i>
<i>Figure 4.5: Photomicrograph showing andesite in plane-polarized light.....</i>	<i>33</i>
<i>Figure 4.6: Photomicrographs of sulfides within the host rock</i>	<i>34</i>
<i>Figure 4.7: Hand sample photos showing different intensities of alteration</i>	<i>36</i>
<i>Figure 4.8: Photomicrographs of some alteration minerals</i>	<i>36</i>
<i>Figure 4.9: Photomicrographs and hand sample images of various alteration minerals.....</i>	<i>37</i>

<i>Figure 4.10: Drill core sample of different vein types</i>	<i>40</i>
<i>Figure 4.11: Sample photos of some major vein types at Moss Lake</i>	<i>41</i>
<i>Figure 4.12: Photomicrographs of some Au occurrences</i>	<i>43</i>
<i>Figure 4.13: Drill core photo of molybdenite bearing sample for Re/Os analysis</i>	<i>44</i>
<i>Figure 4.14: Jensen Cation Plots of the host rocks.....</i>	<i>45</i>
<i>Figure 4.15: white mica spectra showing the two main absorption features</i>	<i>48</i>
<i>Figure 4.16: Chlorite spectra showing the position of the Fe-OH absorption feature.....</i>	<i>49</i>
<i>Figure 4.17: Jensen Cation plot showing the distribution of white mica and chlorite.....</i>	<i>50</i>
<i>Figure 4.18: Downhole plots showing the sample distribution for EPMA analysis</i>	<i>51</i>
<i>Figure 4.19: Mica classification diagram</i>	<i>54</i>
<i>Figure 4.20: Chlorite classification diagram</i>	<i>55</i>
<i>Figure 5.1: Age distribution within the Shebandowan Greenstone Belt.....</i>	<i>56</i>
<i>Figure 5.2: Geological map showing the published ages of rocks in proximity to the Moss Lake deposit.....</i>	<i>57</i>
<i>Figure 5.3: Photomicrographs of alteration assemblages and their overprinting relationship ...</i>	<i>60</i>
<i>Figure 5.4: Photomicrographs and hand sample images of some vein types and relationships..</i>	<i>62</i>
<i>Figure 5.5: Ore minerals association from a paragenetic standpoint</i>	<i>64</i>
<i>Figure 5.6: Paragenesis of the Moss Lake deposit.....</i>	<i>65</i>
<i>Figure 5.7: SEM images of gold occurrences and their associated minerals.....</i>	<i>67</i>
<i>Figure 5.8: Ductile deformation at Moss Lake and associated gold occurrences.....</i>	<i>68</i>
<i>Figure 5.9: Different degrees of alteration at Moss Lake</i>	<i>69</i>
<i>Figure 5.10: Sc vs Mg plot of the host rock, colored by spectral alteration minerals.....</i>	<i>70</i>

Figure 5.11: Alteration indexes plotted against gold assay values 72

Figure 5.12: Comparison of the spectral characteristics of white mica and chlorite with rock compositions and gold distribution..... 74

Figure 5.13: Chlorite compositional variations with increasing distance away from the ore center 76

Figure 5.14: Plots showing compositional changes in white mica 77

List of Tables

Table 1.1: Mineralization and alteration styles of orogenic deposits worldwide	5
Table 1.2: Models for orogenic gold deposits from the superior province and Yilgarn cratons....	6
Table 3.1: Mineral deposits mined in the Shebandowan Greenstone Belt.....	26
Table 4.1: Vein types at the Moss deposits and their characteristics	39
Table 4.2: Re-Os isotopic and age data of molybdenite.....	44
Table 4.3: Distribution of different white mica types based on the wavelength of Al-OH absorption spectral feature	47
Table 4.4: Distribution of different chlorite types based on the wavelength Fe-OH absorption feature.....	49
Table 4.5: Sample mean values of EPMA analysis of white mica grains from Moss Lake Au deposit	52
Table 4.6: Sample mean values of EPMA analysis of chlorite grains from Moss Lake Au deposit	53

Chapter 1: Introduction

1.1 Introduction

Greenstone belts worldwide have historically been a significant source of precious and critical metals; such economic importance has fueled exploration and research projects toward finding more resources to supply the ever-increasing demand. The Shebandowan Greenstone Belt is no exception, with exploration activities dating back to the 19th century (Giblin, 1964). Gold, silver, nickel, and copper have been extracted over the years from different parts of the greenstone belt (Harris, 1970).

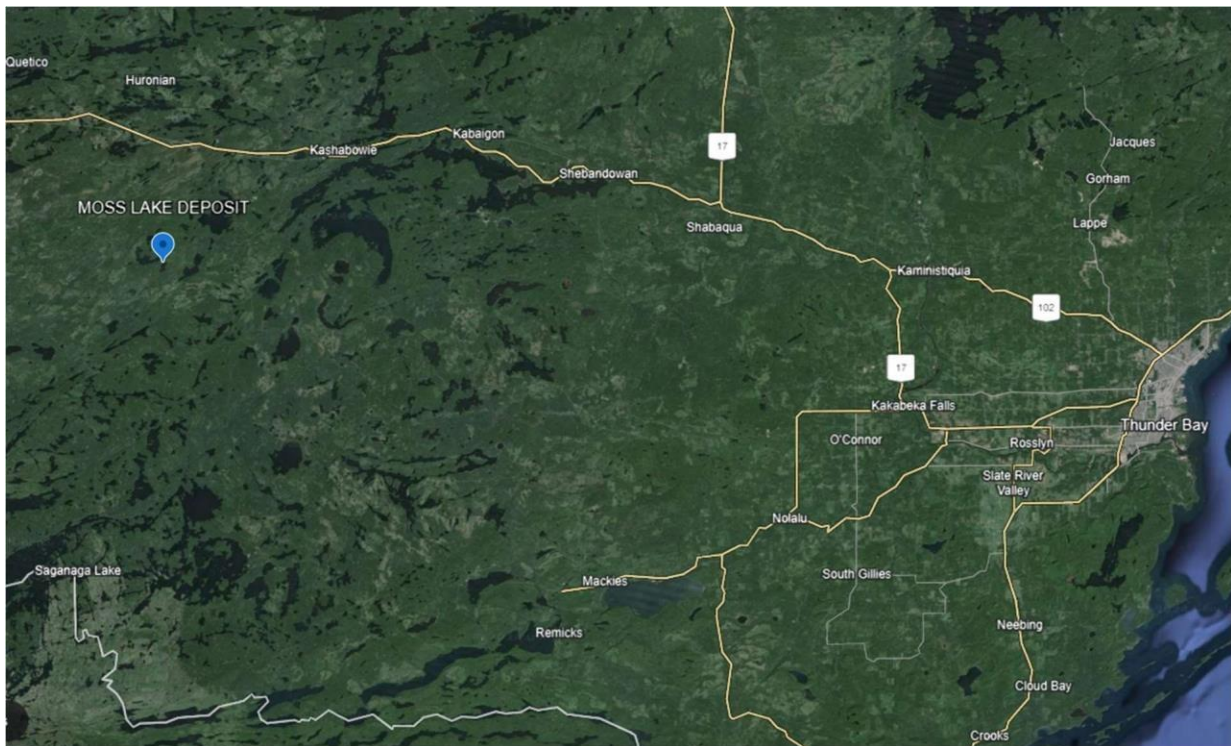


Fig. 1.1: Topographic map showing the location of the Moss Lake deposit (modified from Google Earth, 2024).

The Moss Lake deposit, located about 110km west of the city of Thunder Bay (Fig. 1.1), lies in a felsic to intermediate metavolcanic/intrusive segment of the Shebandowan Greenstone Belt (Osmani, 1997). The area has been the focus of several mapping projects by the Ontario

Geological Survey (OGS; Giblin, 1964; Hodgkinson, 1968; Harris, 1970; Osmani, 1997; Hart, 2007) and academic research (Shute, 2009; Forslund, 2012), which has led to a detailed understanding of the geology and petrology of the Moss Lake area. The Moss Lake area has been the focus of several exploration projects, the latest by Goldshore Resources who currently hold the Moss Lake property. The most recent exploration endeavors have reported an inferred resource of 4.91 Moz Au at 1.09 g/t Au within 140.07 Mt of ore (Goldshore Resources, 2024). This study is focused on understanding the relationship between alteration chemistry and Au distribution within the Moss Lake deposit.

1.2 Objectives

The main purpose of this study was to characterize the Moss Lake Au deposit and develop a vector to ore by investigating changes in the chemistry of alteration minerals, particularly chlorite and white mica, with proximity to Au mineralization. The aim was to characterize the deposit using petrography, geochemistry, and mineral chemistry to better understand the lithologies, alteration mineralogy and chemistry, as well as any chemical controls on Au distribution. The petrographic analysis was intended to characterize the host rock, vein relationships, alteration mineralogy and Au occurrence in order to develop a paragenetic sequence for the deposit. The geochemical data was used to investigate any trends between Au-rich zones and various rock compositions or elements. To understand the chemistry of the alteration minerals of interest (chlorite and white mica), Short Wave Infrared (SWIR) and Electron Probe Microanalyzer (EPMA) analyses were conducted on representative samples.

1.3 Orogenic Gold deposits

Gold is commonly associated with metamorphic belts, and its occurrence is attributed to various stages of orogenesis, which influences the nature of the deposit formed (Groves et al., 2003). The Moss Lake Au deposit can be classified as an orogenic gold deposit. These are a class of lode gold deposits that formed in metamorphic terranes during the later stages of regional-scale orogeny (Fig. 1.2; Groves et al., 1998; Sillitoe, 2020). They are generally related to major

structures (Fig. 1.2) or terrane boundaries and associated with hydrothermal alteration (Groves et al., 1998).

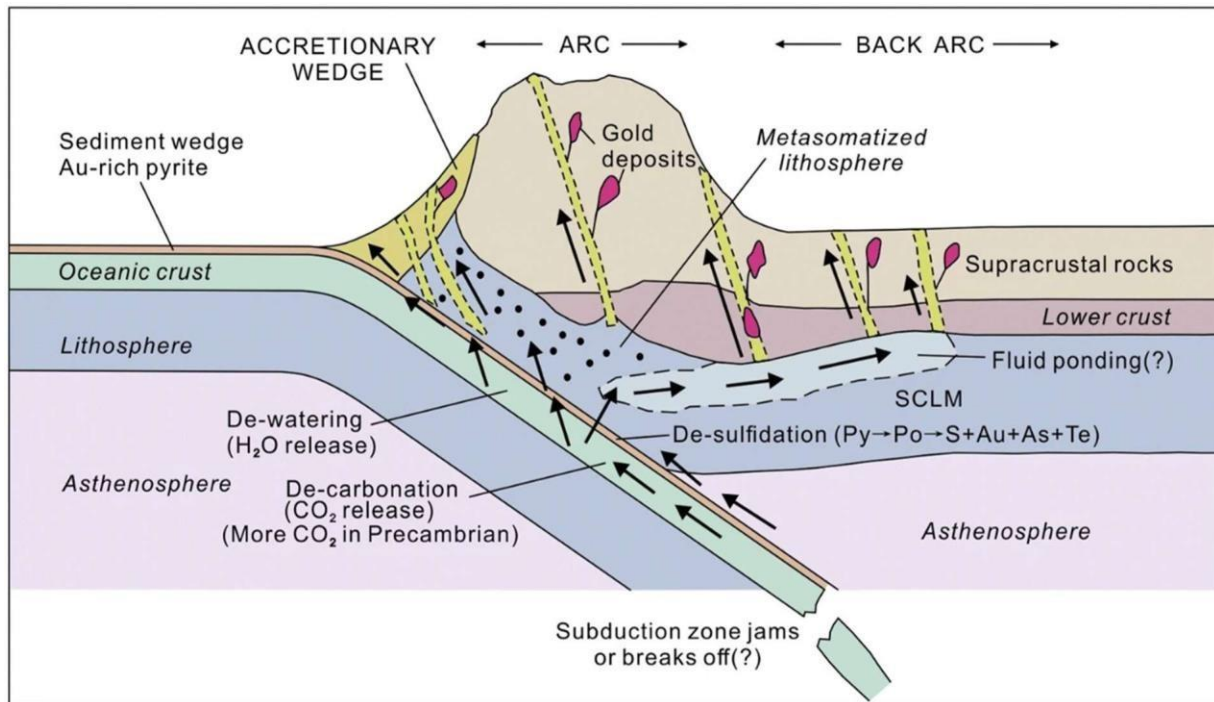


Fig. 1.2: Detailed representation of the subduction-based model for the formation of orogenic gold deposits. Black arrows show the travel path of mineralizing fluids through the interface between the slab and base of the lithosphere, then through second-order structures to form orogenic gold deposits (modified from Groves et al., 2020)

Orogenic gold deposits are widely considered to have formed in accretionary or collisional orogens at paleodepths of 5 to 15 km from low-salinity, gold- and arsenic-bearing aqueous carbonic fluids generated by devolatilization reactions that are associated with regional greenschist- to amphibolite-facies metamorphism (Sillitoe, 2020). The ore-bearing fluids in orogenic gold deposits transport the gold as a bisulfide complex in near-neutral pH and relatively reduced fluids (Goldfarb et al., 2005). Gold will remain in solution while these fluids travel upwards through major shear zones and structures (Goldfarb et al., 2005; Dubé & Gosselin, 2007), until changing conditions cause it to precipitate in either a chemical or structural traps, such as fold hinges, dilational jogs along faults or shear zones (Dubé & Gosselin, 2007), or carbon-rich rocks, rocks with high $Fe/(Fe + Mg) \pm Ca$ ratios (Groves et al., 2003).

Some factors, such as changes in temperature and pressure, fluid mixing, H₂O-CO₂ phase separation, salinity, and other physiochemical variations, can also influence the precipitation of gold from the ore-bearing fluids (Groves et al., 2003). Orogenic gold deposits occur with various mineralization and alteration styles, including quartz-carbonate veins, sulfidic replacement in banded iron formations (BIF), semi-massive to massive sulfide lenses, disseminated stockwork zones, sulfide-rich veins, and veinlets zones, sulfidic replacement and crustiform veins (Robert et al., 2005), these various occurrence styles are summarized in Table 1.1. Quartz-carbonate vein orebodies are very common and are characterized by elevated Au, Ag, As, W, B, Sb, Te, and Mo, with Au/Ag ratios typically between 5 and 10 (Groves et al., 2003). The alteration assemblage varies based on host rock and metamorphic grade, but commonly ranges from sericite-carbonate-pyrite at lower metamorphic grades to biotite-amphibole-pyrrhotite-arsenopyrite and biotite/phlogopite-diopside-pyrrhotite at higher metamorphic grades (Groves et al., 2003).

Various models have been used to explain the different orogenic gold occurrences around the world, as no single model fits all the different styles. These models include tonalite-trondhjemite-granodiorite (TTG) model, the granulization model, the cratonization model, the gold-shoshonite model, the crustal continuum model, the delayed thermal rebound model, and the late metamorphism model, and they are summarised in Table 1.2 (Kerrick and Cassidy, 1994).

Table 1.1: Mineralization and alteration styles of orogenic deposits worldwide, with selected examples (modified from Robert et al., 2005).

Mineralization style	Characteristics	Associated alteration assemblages	Metal association	Selected examples
Quartz-carbonate veins	Quartz veins with <25% carbonate, <10% sulfide, \pm albite, tourmaline, scheelite Vein types include laminated fault-fill and extensional veins. Sulfides are mainly pyrite, with arsenopyrite and pyrrhotite.	Carbonate-sericite- (albite)-pyrite (arsenopyrite), at greenschist grade Biotite-actinolite pyrite \pm carbonate, at lower amphibolite grade Biotite-calc-silicate pyrrhotite \pm pyrite at mid amphibolite grade	Au > Ag As, W \pm Te, Mo, B	Superior: Hollinger-McIntyre, Kirkland Lake, Sigma-Lamaque , San Antonio Yilgarn: Mount Charlotte, Victory-Defiance, Norseman , Centenary, Bayleys, Westonia
Sulfidic replacements in BIF	Strata-bound replacements of Fe-rich layers by mainly pyrite, arsenopyrite, or pyrrhotite. Associated with quartz veins or zones of veinlets or silica flooding.	Pyrite (arsenopyrite)-sericite-chlorite carbonate at greenschist grade Pyrrhotite (loellingite) grunerite-garnet at amphibolite grade	Au > Ag As \pm Cu	Superior: Musselwhite, Cockshutt-McLeod, Pickle Crow Yilgarn: Mount Magnet, Mount Morgans, Sunrise Dam (in part), Nevorlia
Sulfidic replacements and crustiform veins	Crustiform-colloform carbonate-quartz veins and breccias, with various proportions of sulfidic replacements of wall rocks or vein carbonates. Sulfides are pyrite or arsenopyrite; stibnite and tellurides abundant in some deposits.	Sericite-carbonate-(albite)-pyrite at greenschist grade Biotite-carbonate-silica \pm aluminosilicate at amphibolite grade	Au > Ag, As, Te, \pm Sb, Hg, W, Zn	Superior: Campbell-Red Lake (in part), Cochenour Yilgarn: Golden Mile, Jundee, Wiluna, Racetrack
Disseminated stockwork zones	Zones of 5 to 20% sulfides, as uniform disseminations or along foliation-parallel bands, with variably developed stockworks of sulfidic fractures or quartz veinlets, and crackle type breccias. Sulfides are pyrite or arsenopyrite, with molybdenite abundant at Hemlo.	Albite-carbonate-sericite-pyrite at greenschist grade Biotite-calc-silicate-pyrrhotite \pm pyrite at amphibolite grade K feldspar-muscovite \pm calc-silicates at Hemlo	Au > Ag, As, Te, \pm W, Hg, Cu, Mo, Sb	Superior: Malartic, Hemlo, Kerr Addison (Flow ore), Ross, Beattie, Madsen Yilgarn: Wallaby, Plutonic, Sons of Gwalia, Kanowna Belle, Binduli
Sulfide-rich veins and veinlet zones	Sulfide-rich (25–100% sulfide) veins and veinlet zones with Intervening disseminated sulfides. Sulfides include pyrite, sphalerite, chalcopyrite, and galena.	Sericite-chlorite \pm chloritoid at greenschist grade Biotite-garnet cordierite at amphibolite grade	Ag > Au, Cu, Zn, Pb \pm As, Te	Superior: Doyon, Mouska, Copper Rand, Sleeping Giant Yilgarn: Mount Gibson, Bellevue
Semimassive to massive sulfide lenses	Semimassive to massive sulfide lenses of pyrite, chalcopyrite, sphalerite, and galena, with pyrrhotite and magnetite in some cases.	Sericite-quartz \pm chlorite or garnet-biotite Quartz-andalusite-kyanite-pyrophyllite	Ag > Au, Cu, Zn, Pb, As \pm Te, Sb	Superior: Horne, LaRonde-Penna, Bousquet 2-Dumagami, Bousquet 1 Yilgarn: none

Table 1.2: Models for orogenic gold deposits from the Superior Province and Yilgarn Craton (modified from Kerrich and Cassidy, 1994).

Hypothesis	Terrane/time connotation	Process/evidence	Sources	Comments
TTG	Abitibi Subprovince ~2695 to 2685 Ma	- Gold from abundant TTG magmas in mid-crust	Burrows & Spooner, 1987	- Gold related in time to late accretion and shoshonites at -2680-2670 Ma - Pb, Sr, O, C isotopes of deposits are inconsistent with TTG source alone
Granulization	Superior Province ~2710 to 2670 Ma	- Granulization of mid-crust by mantle CO ₂ - Gold, LILE driven to midcrust	Cameron, 1988 Colvine et al., 1988 Card et al., 1989	- Pb, Sr isotopes of deposits, unlike Kapuskasing, C isotopes dissimilar to mantle C alone, LILE of deposits not complementary to LILE-depleted granulites
Cratonization	Superior Province ~2710 to 2670 Ma	- Empirical evidence for deposits forming in equilibrium with ambient metamorphic and rheological environment	Colvine, 1989	- Corroborative evidence from Archean Yilgarn and Zimbabwe deposits, and lode gold deposits of all ages
Gold-shoshonite (A)	Superior Province ~2710-2670 Ma	- Association of gold and shoshonites in space and time with terrane boundary structures marking accretionary tectonics - robust -2680 Ma vein zircon ages in Abitibi Subprovince - Young ages reflect disturbance	Wyman & Kerrich, 1988 Kerrich & Wyman, 1993 Claoue-Long et al., 1990	- Gold mineralization "flare-up" over 1,500,000 sq. km during restricted interval of 2710-2670 Ma based on robust ages - Explains sparsity of Au in early Archean; abundant Au in Cordilleran-type tectonics at -2680 Ma, and in the Mesozoic cordillera - Deposits in metamorphic and rheological equilibrium with host terrane - Stable and radiogenic isotope and field evidence for secondary resetting, aberrant young ages equilibrium with host terrane
Gold-shoshonite (B)	Superior Province ~2710 to 2670 Ma	- Relationships as in (A) - Shoshonites intrinsically Au-rich	Rock et al., 1989	- Consistent with accretionary tectonic models of Superior Province and Yilgarn Craton - Shoshonites have average crustal Au
Crustal continuum	Yilgarn Craton 2630 ± 10 Ma	-related to accretionary processes	Groves et al., 1992, 1994 and references therein	- Gold mineralization occurred over 1,000,000 sq. km in restricted intervals of 2630±10 Ma - Deposits in metamorphic and rheological equilibrium with host terrane
Delayed thermal rebound	Abitibi Subprovince ~2630 to 2580 Ma	- Based on variably young ages in Val d'Or area - Thermal rebound ~50-100 m.y.	Hodgson et al., 1989	- Young ages likely record isotopic resetting - Stable isotopes variably reset - Time constants of thermal rebound are <10 to 40 m.y., not 100 m.y.
Late metamorphism	Abitibi Subprovince ~2630 to 2580 Ma	- Gold related to young zircon metamorphic ages in Kapuskasing - Unrelated to greenstone belt metamorphic or magmatic evolution - Magmatic underplating provides late heat for young ages, and CO ₂ for ore fluids	Jemielita et al., 1990 Wong et al., 1991 Hanes et al., 1992 Zweng et al., 1993	- Young ages likely record isotopic resetting - Sr, Pb, and C isotopes of deposits, unlike Kapuskasing (Kerrich, 1991) - No evidence for magmatic underplating of Kapuskasing at ca. 2600 Ma - Inconsistent with province-wide accretion

Chapter 2: Methods

2.1 Sampling

Sampling of drill holes from the Moss Lake Au deposit was carried out in February and July of 2023. A total of 10 drill holes were sampled; four of these drill holes are from the main ore body, whereas six were from a less mineralized zone termed the northeast zone (NE zone). A total of 178 drill core samples were taken, and field notes were made for each sample, outlining the depth, sample description, and reason for sampling. Eighty-nine samples were taken in winter 2023 from the drill hole that intercepts the main ore body, whereas the other 89 samples were taken from drill holes in the NE zone. Sampling generally focused on representative host rocks, vein relationships, alteration, and highly mineralized zones within the drill holes (Fig. 2.1). Of all the samples collected, 62 were deemed the most representative and submitted for polished thin section (PTS) preparation.

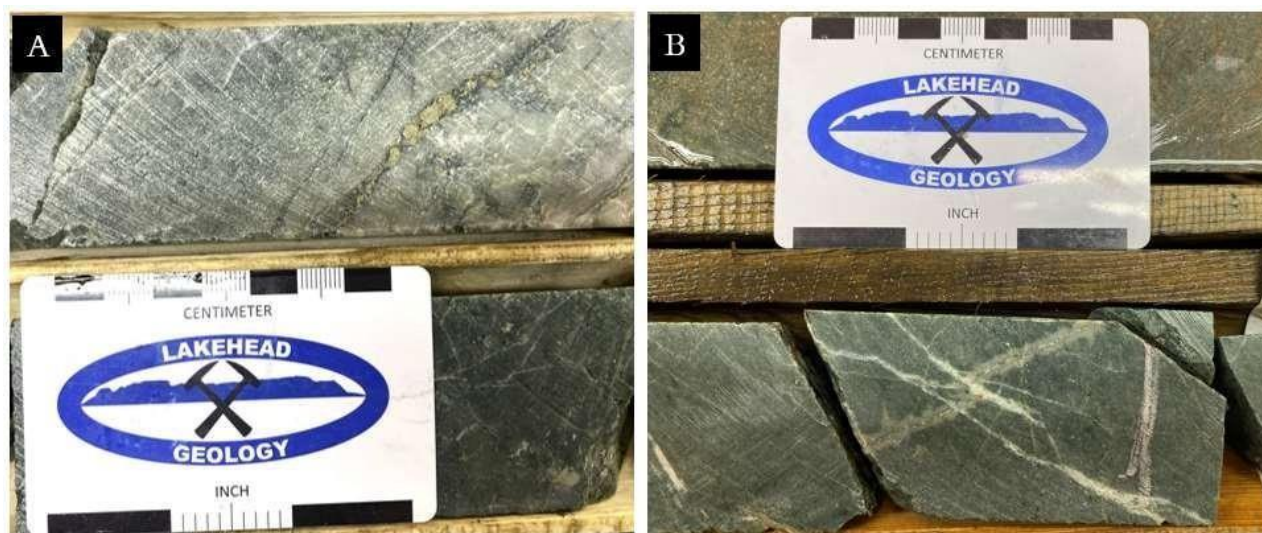


Fig. 2.1: Photos of drill core samples from sheared and altered rocks selected for the study. A (ML23-NM-010) is a sulfide-rich sample selected as a possible Au-bearing sample, whereas B (ML23-NM-001) is a sample with multiple veins showing a crosscutting relationship.

2.2 Petrography

A total of 62 samples were submitted to Lakehead University's lapidary facility for (PTS) polished thin sections preparation. Forty-two of the selected samples were from the main ore zone, whereas 20 samples were selected from the NE zone. The distribution of samples selected from individual drill holes reflects different proximity to ore and the different rock types intercepted by the drill holes. Petrographic analysis was carried out using a combination of an Olympus BX 51 microscope and the Zeiss Axioscope 5 Smart Microscope. However, all photomicrographs presented in this thesis were taken with the Olympus SC180 camera at Lakehead University. Additional petrographic observations were made using the Hitachi SU-70 Scanning Electron Microscope (SEM) equipped with the Oxford X-Max Aztec energy dispersive spectrometer (EDS) X-ray analyzer at the Lakehead University Instrumentation Laboratory. Minerals within thin-section photomicrographs and hand samples that appear in this thesis are labeled with their official abbreviations; these include Pl (plagioclase), Qz (quartz), Ep (epidote), Ser (sericite), Chl (chlorite), Cb (carbonate), Hem (hematite), Ab (albite). Full petrographic descriptions of all PTS can be found in Appendix I.

2.3 Whole rock Geochemistry

Four-acid digest geochemical analysis was conducted at ALS Geochemistry Vancouver by Goldshore Resources on all drill holes, including some of those sampled in this study; the drill core was sampled at an average interval of one meter. This analysis reported 49 elements at wt% and ppm concentrations. The geochemical data was acquired using the ICP-MS base metal analytical package ME-MS61, which also includes some major, minor, and trace elements, the validity of this data was verified by the company by the use of blanks and standards. This data was provided for all 89 samples from the drill holes within the ore zone. For the drill holes from the NE zone, the assay was conducted by Wesdome Gold at a similar location, using the Aqua Regia method, only the base metal composition was available for the samples collected from the NE zone. The full geochemical dataset for all the samples is reported in Appendix II.

2.4 Re/Os Geochronology

Re/Os geochronology was conducted at the Canadian Centre for Isotopic Microanalysis (CCIM) at the University of Alberta. Sample E927263 was selected for this analysis due to the presence of molybdenite. Molybdenite was chemically extracted from the sample, and molybdenum separates were made. Using isotope dilution mass spectroscopy, the rhenium and osmium concentrations in molybdenite were determined. The isotopic analysis utilized a ThermoScientific Triton mass spectrometer by Faraday Collector. The reference material 8599 Henderson molybdenite (Markey et al., 2007) was used as standard during the analysis. The ^{187}Re decay constant used for the analysis was $1.666\text{e}^{-11}\cdot\text{a}^{-1}$ (Smoliar et al., 1996).

2.5 Short Wave Infrared (SWIR) Analysis

SWIR analysis was conducted at Lakehead University on all 178 drill core samples collected. The point analysis was carried out using an ASD Terraspec 4 Hi-Res analyzer. The analysis involved utilizing a spectral gun on a flat surface of the sampled drill cores. For each core sample, three points were analyzed, and the point with the best spectral reflectance was selected as the representative spectrum for the sample. During data collection, white reference standard was analyzed every 20 minutes to ensure accurate spectra were being retrieved. All 178 samples produced spectra but not all had the relevant spectral features. The data retrieved from the Terraspec device were further analyzed using The Spectral Geologist (TSG) software. TSG analyzes the spectrum of individual samples and reports key mineral names and features. The full dataset for the SWIR analysis can be found in Appendix III.

2.6 Electron Probe Microanalysis (EPMA)

Seventeen polished thin sections were submitted to the Department of Earth Sciences at the University of Toronto for EPMA analysis of sericite and chlorite grains. The analyses were carried out on the JEOL JXA 8230 Electron Probe Microanalyzer using a wavelength-dispersive spectrometer (WDS) and an energy dispersive spectrometer (EDS) to determine the major and minor element compositions of sericite and chlorite. The operating conditions were an accelerating voltage of 15kV and a beam current of 20nA with a beam size of 10 μm . The analysis peak counting times were 10 seconds for Na and K, 20 seconds for Fe, Si, Mg, and Ti,

and 40 seconds for Cr, Al, Mn, and Ca. Standards used for the analysis include albite (Na), chromian augite (Mg, Ca), chlorite (Fe, Al, Si), sanidine (K), rutile (Ti), bustamite (Mn), and synthetic Cr_2O_3 (Cr), these standards were analyzed every two hours during the analysis. The EPMA data was filtered to eliminate data points that were non representative of the target mineral composition such as quartz and plagioclase; the full data from the EPMA analysis are reported in Appendix IV.

Chapter 3: Regional Geology

3.1 Superior Province

With a total surface area of 1,572,000 km², the Superior Province is one of the largest Archean cratons in the world (Thurston, 1991). With an approximate age of 3.0 to 2.70 Ga (Percival, 2003), it is one of the oldest Archean cratons. The final formation of the Superior Province is attributed to the Kenoran Orogeny, an accretionary event involving east-west trending subcontinental belts between 2.72 and 2.68 Ga (Card & Ciesielski, 1986).

These subcontinental belts are the basis for the division of the Superior Province into subprovinces by Card and Ciesielski (1986), a classification that was widely accepted for many years but has been revised recently based on new geologic and geophysical data (Thurston, 1991; Stone, 2005; Percival et al., 2006; Stott et al., 2007).

The subprovinces of the Superior Province are bordered by regional faults and characterized by similar rock types, structural style and patterns, age, metamorphic grade, and geophysical signature (Thurston, 1991). They have recently been redefined as terranes, which are regions defined by their tectonic boundaries with unique internal characteristics that distinguish them from surrounding regions prior to the Neoproterozoic assembly of the Superior Province (Fig. 3.1; Stott et al., 2010). The terranes may consist of lithologically distinct parts that are typically younger, known as domains, and they can be part of a younger crust or sit on the same basement as the rest of the terrane. Terranes and domains in the Superior Province are made up of smaller units known as tectonostratigraphic assemblages, which comprise one or more stratigraphic units or groups that share a distinct lithology, age and tectonic setting (Stott et al., 2010). The study area is located within the Wawa-Abitibi terrane shown in Figure 3.1.

A variety of lithologies are found within the Superior Province; they include granites, rhyolites, andesites, tonalite-trondhjemite-granodiorite (TTG) suites, komatiites, basalts, and iron formations. These are interpreted to have formed in different tectonic environments ranging from volcanic arc, continental arc, back-arc, ocean island basalt to plateau basalt (Thurston et al., 1991; Hollings, 1999; Whalen, 2002).

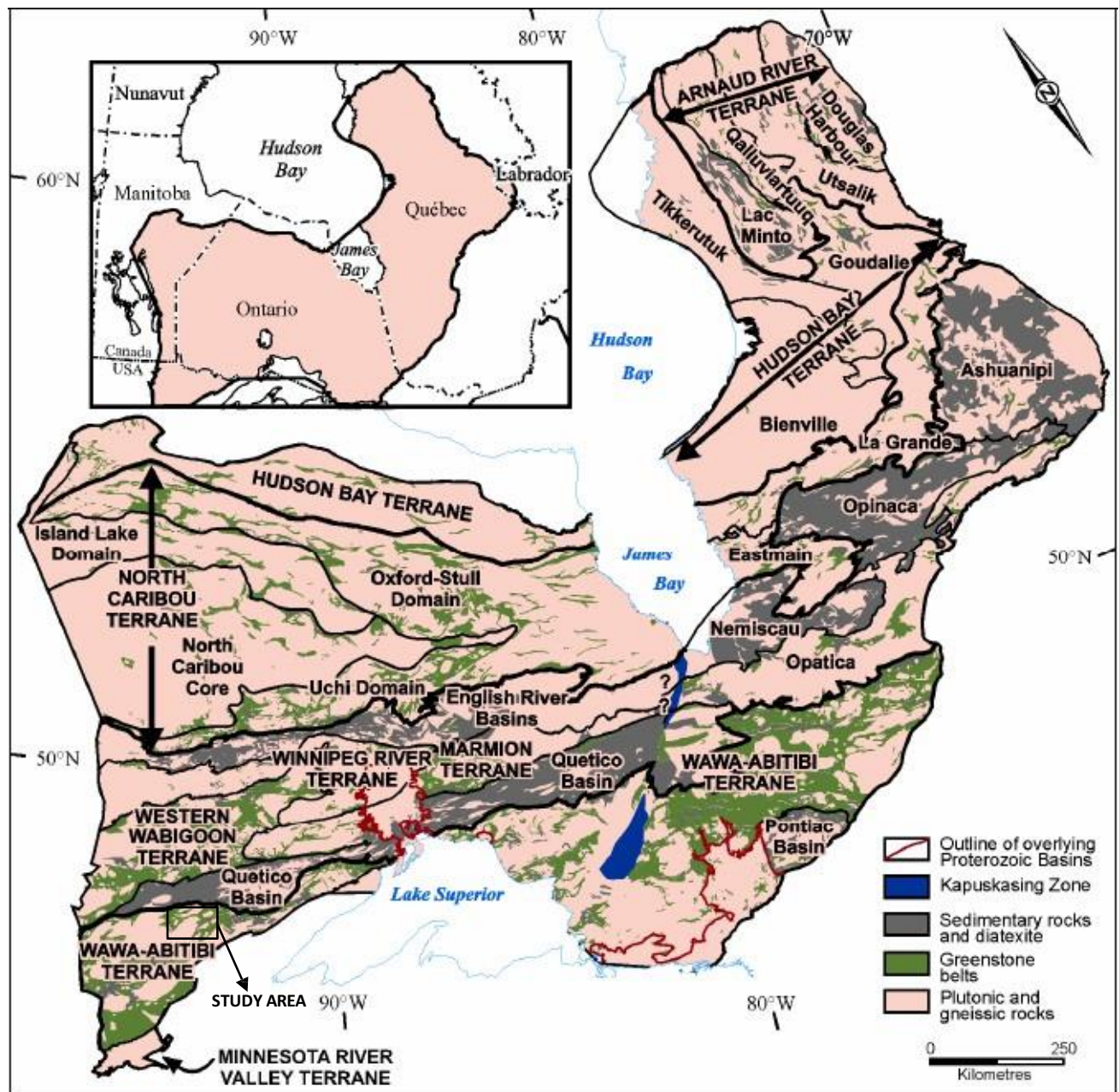


Figure 3.1: Terrane-scale geological map of the Superior Province showing the various terranes. The study area is shown by the black box in the western part of the Wawa-Abitibi terrane. modified from Stott et al. (2010).

3.2 Wawa-Abitibi Terrane

The Wawa-Abitibi terrane consists of the Wawa and Abitibi blocks that were once classified as two different subprovinces, separated by the Kapuskasing Structural Zone (KSZ) (Williams et al., 1991). However, based on geological correlations that have been identified between the Wawa and Abitibi, they are currently considered to be a single terrane (Stott et al. 2010).

The western Wawa-Abitibi Terrane consists of what was previously termed the Wawa subprovince and includes the study area. To the southwest, it is in contact with the Minnesota River Valley Gneiss Terrane (MVT), whereas to the north, it is bounded by the Quetico Basin (Corfu & Stott, 1998). The western half of the Wawa-Abitibi terrane extends westward from the Kapuskasing Structural Zone and is truncated at the contact with the Proterozoic Trans-Hudson Orogen in the west (Fig. 3.2).

Archean greenstone belts and granitoid plutons, with an age range from 2.9 Ga (Williams et al., 1991) to 2.68 Ga (Percival, 2007) dominate the geology of the western Wawa-Abitibi terrane. The greenstone belts are made up of supracrustal rocks that include komatiitic basalts, tholeiitic basalts, Fe- and Mg-rich tholeiite, submarine to subaerial calc-alkalic basalts, and felsic to intermediate volcanic rocks, as well as metasedimentary rocks, which occur interstitial to elongate domains of TTG plutons (Williams et al., 1991).

The geologic evolution of the Wawa-Abitibi terrane involved multiple stages of supracrustal development, including bimodal volcanism from 2.9 Ga to 2.7 Ga (Williams et al. 1991). A later stage of volcanism from 2.695 Ga to 2.689 Ga was coeval with regional deformation and was associated with Timiskaming-type sedimentation (<2.689 Ga) and followed by sanukitoid magmatism at 2.685 to 2.680 Ga (Percival, 2007). The plutonic rocks that make up the western Wawa-Abitibi Terrane were generally emplaced syn- to post-volcanism, mostly occurring interstitial to greenstone belts, with a few intruding the belts (Williams et al., 1991). The stratigraphy of the greenstone belts has been distorted by various episodes of deformation and alteration. Williams et al. (1991) noted that komatiites and associated tholeiitic basalts make up the basal section of the volcanic sequences in the early

event, whereas tholeiites and calc-alkaline basalts, andesites, rhyolites, and dacites dominate the upper stratigraphic levels.

The western Wawa-Abitibi Terrane is made up of several greenstone belts, of which the largest are the Saganagons, Shebandowan, and Michipicoten belts. The study area lies in the Shebandowan Greenstone Belt, which is connected to the Saganagons Greenstone Belt to the southwest (Fig. 3.2; Corfu & Stott, 1998).

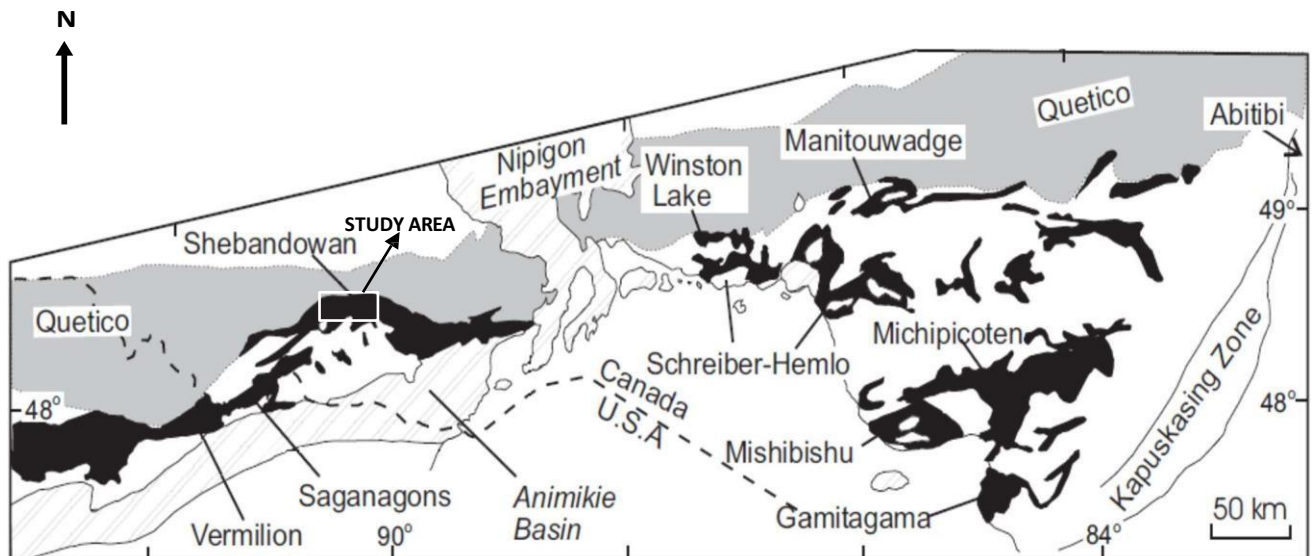


Figure 3.2: Western section of the Wawa-Abitibi Terrane (white), showing its greenstone belts (black), the Quetico Metasedimentary Basin (grey) to the north, the Kapuskasing structural zone to the east and the Animikie Basin and Nipigon Embayment. The study area is represented by the white box. (modified from Corfu & Stott, 1998).

3.3 Shebandowan Greenstone Belt

The Shebandowan Greenstone Belt is located in the western part of the Wawa-Abitibi terrane (Fig. 3.2). It lies southwest of the Nipigon embayment and is bordered to the north by the Quetico basin and to the south by the Northern Light-Perching Lakes Batholithic Complex (NLPG; Williams et al., 1991).

The 2.77-2.72 Ga Shebandowan Greenstone Belt comprises metavolcanic and metasedimentary assemblages associated with felsic to mafic intrusive rocks. The Shebandowan Greenstone Belt has been grouped into three main assemblages by Williams et al. (1991), who recognized two older assemblages known as the Burchell and Greenwater assemblages

separated by the Knife Lake Fault and overlain in part by the younger Shebandowan Assemblage (Fig. 3.3). The initial classification by Williams et al. (1991) was revised by Corfu and Stott (1998), who observed a similar age (2720 Ma) and younging direction for both Burchell and Greenwater assemblages and merged them into one assemblage. The Greenwater assemblage is characterized by cycles of volcanic activity, with tholeiitic basalt comprising the lower sequence and intermediate to felsic volcanic rocks making up the upper sequence (Corfu & Stott, 1998). The northern portion of the Burchell assemblage was observed to be distinct in age and termed the Kashabowie Assemblage, a 2695 Ma Timiskaming-type volcano-sedimentary assemblage that comprises heterolithic volcanoclastic units that are interpreted as debris flows (Corfu & Stott, 1998).

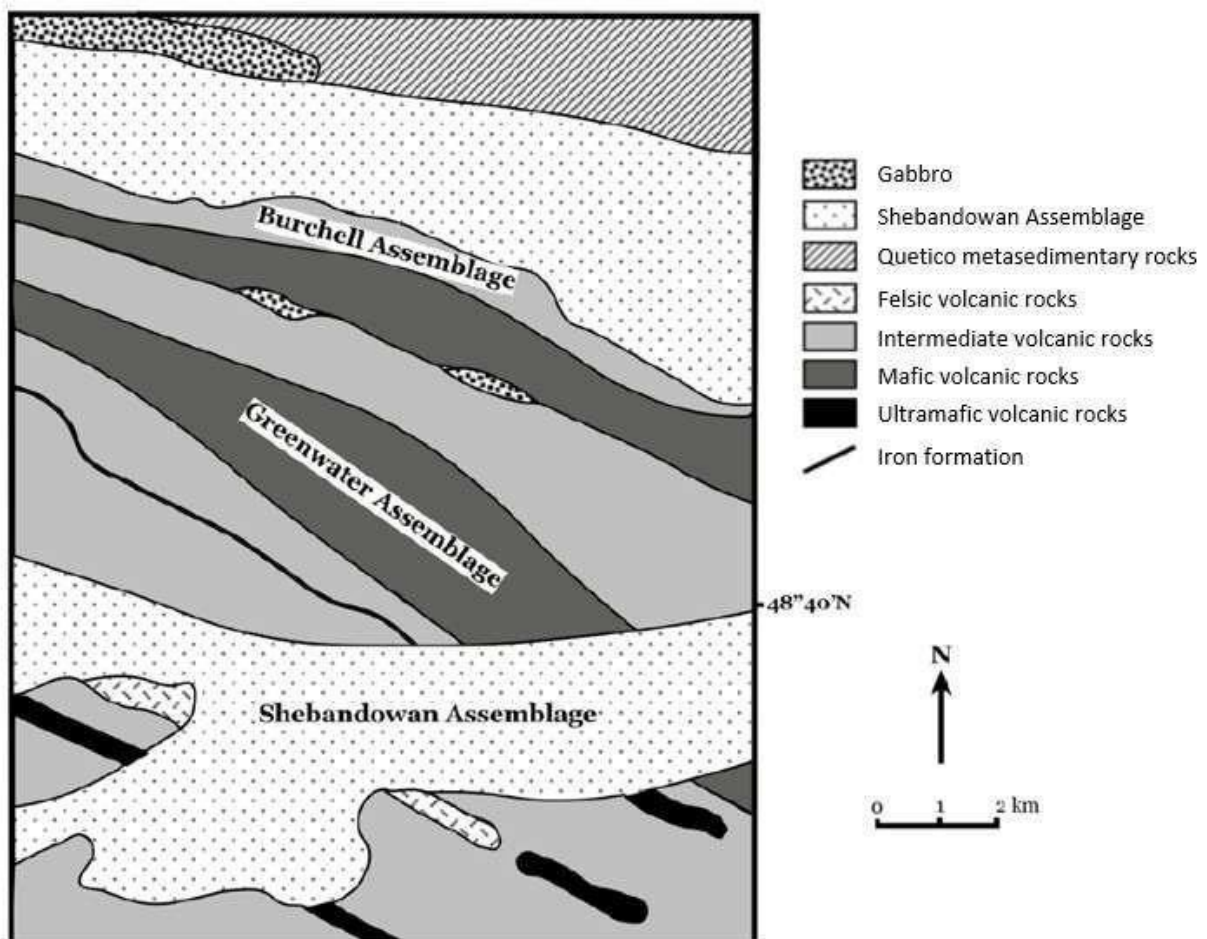


Fig. 3.3: Section of the geological map of the Shebandowan Greenstone Belt showing the relationship between the three assemblages (modified from Williams et al., 1991).

The Auto Road assemblage is the youngest assemblage in the Shebandowan Greenstone Belt, and it comprises conglomerate-sandstone units with clasts of volcanic and granitoid origin that lie within a sedimentary basin in the northeastern part of the belt (Fig. 3.5; Corfu & Stott, 1998).

The deformation history in the Shebandowan Greenstone Belt was first described by Corfu & Stott (1986), who observed two main deformation events, D1 and D2. D1 is characterized by vertical schistosity with west-southwest dipping mineral lineation and vertical to sub-vertical folds, appears to have affected the entire greenstone belt (Corfu & Stott, 1986). D2 was only observed in the northern segment of the belt and resulted from a large-scale subhorizontal compression along a northwest-southeast axis associated with the formation of the Quetico basin (Corfu & Stott, 1986). However, Williams et al. (1991), proposed that three deformational events were recorded in the Shebandowan Greenstone Belt. The first event, D1, is evident throughout the belt and is characterized by west-dipping lineation with a steep north-dipping schistosity. The second event, D2, is not obvious throughout the belt, but where evident is observed to overprint the first event. Williams et al. (1991) observed a similarity in the schistosity of D1 and D2 and a difference in the plunge of their lineations, as D1 lineations plunge westward, whereas D2 lineations plunge eastward. D2 is also characterized in some places by brittle/ductile shear zones that are spatially associated with gold mineralization (Stott & Schnieders, 1983). Lastly, D3 features steeply plunging kink folds that occur predominantly in the northern part of the belt (Williams et al., 1991). Structural features within the belt, such as faults, generally strike northeast or northwest; it has been suggested that some of the major faults are a result of crustal shortening associated with the cratonization of the Superior Province, which involved northwest-directed horizontal compression (Williams et al., 1991). The northeast-striking structures includes the Knife Lake Fault, which is the closest major fault to the Moss Lake deposit. The Knife Lake Fault is at least 60 miles long and serves as a contact between the biotite granite of the Myrt Lake Batholith and metavolcanic rocks to the northeast and southwest (Fig. 3.4; Harris, 1970).

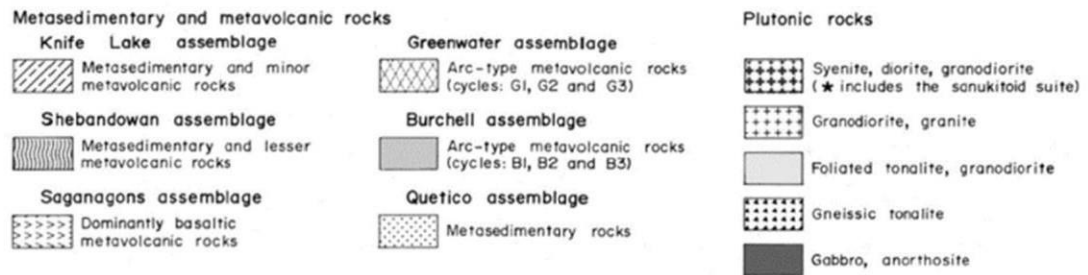
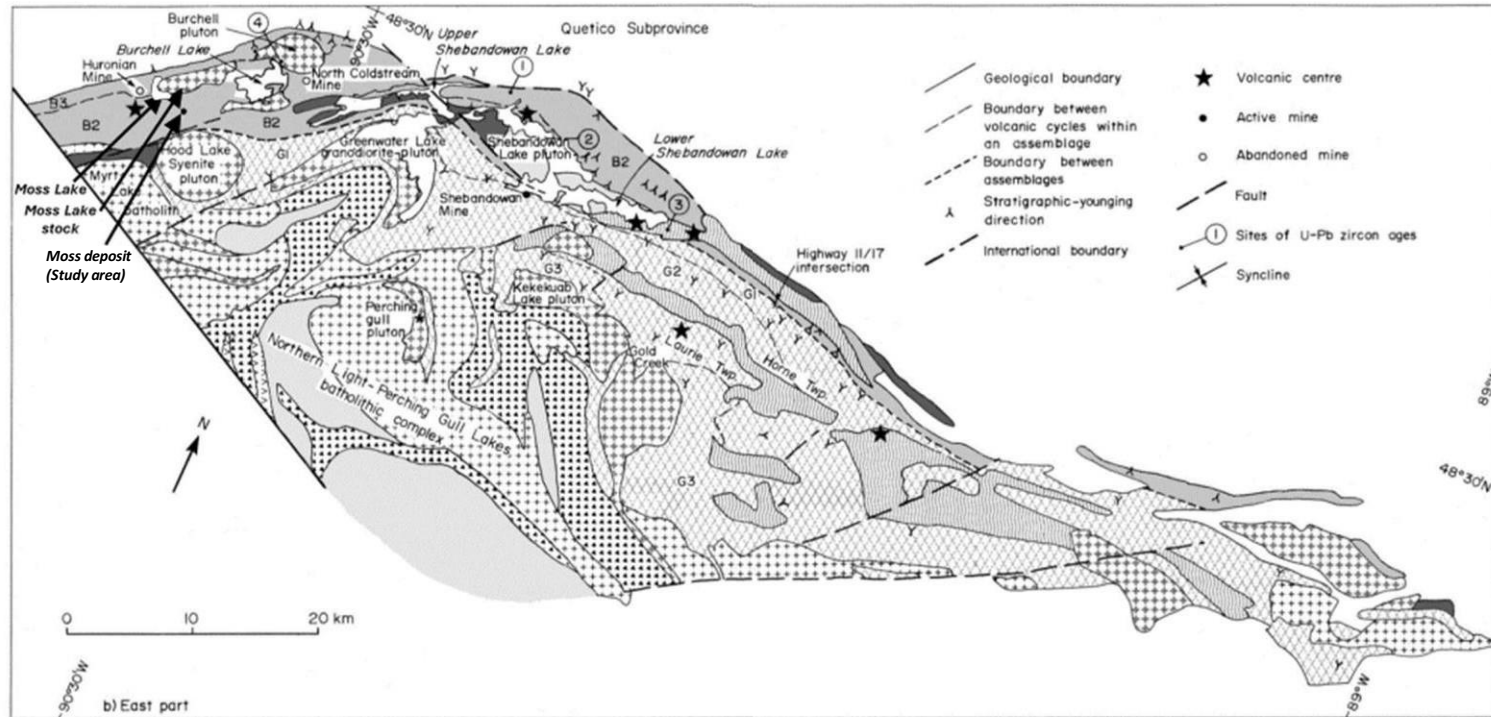


Fig. 3.4: Geological map of eastern Shebandowan Greenstone Belt showing the various lithologies, past producing mines, structural features as well as the Moss deposit (study area) (modified from Williams et al., 1991)

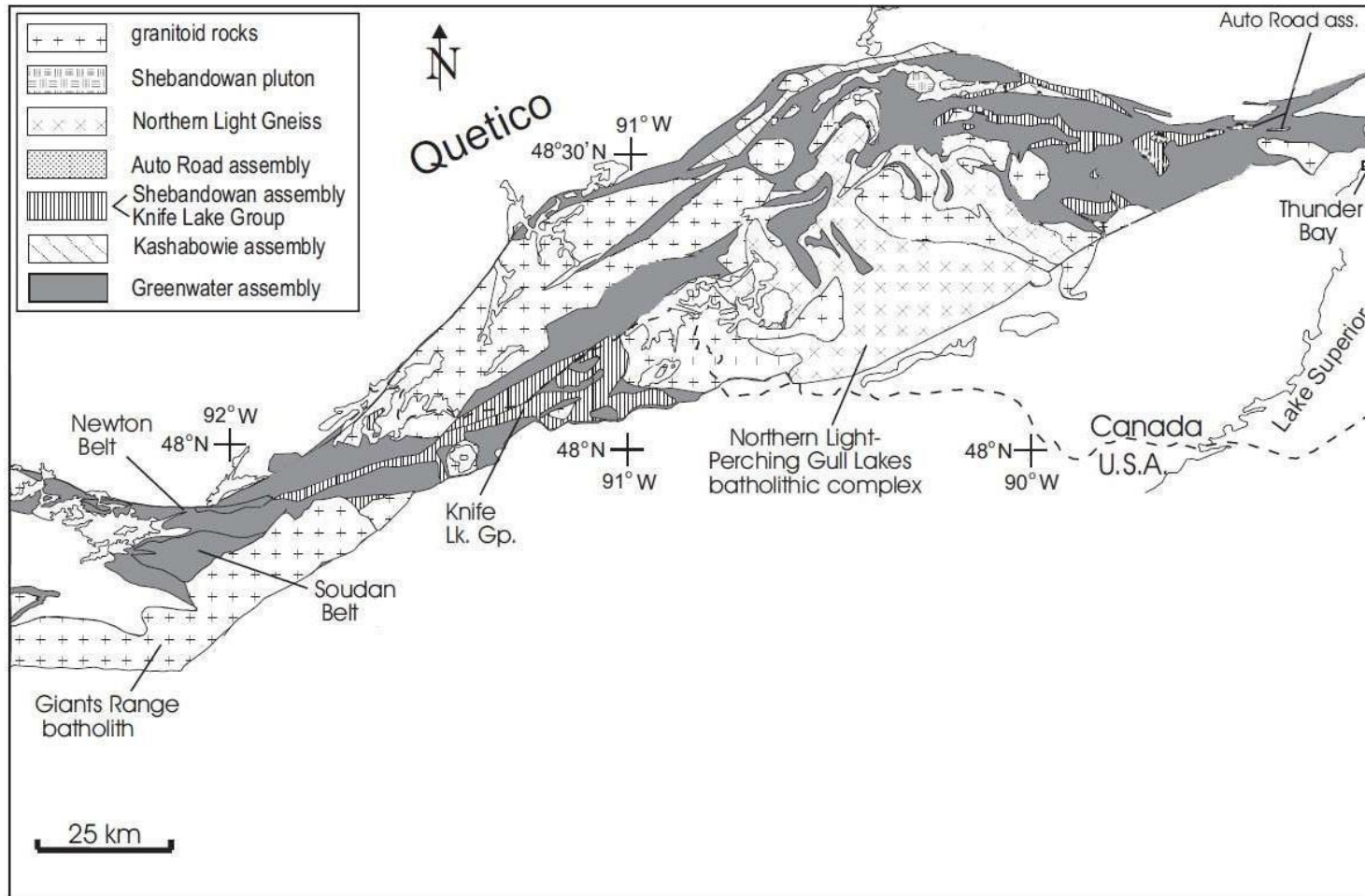


Fig. 3.5: Geological map of the Shebandowan Greenstone Belt (SGB) showing the various assemblages. The map also shows the Saganagons Greenstone Belt, which connects to the SGB to the southwest (modified from Corfu & Stott, 1986).

In the Shebandowan Greenstone Belt, the metamorphic grade ranges from lower greenschist to amphibolite facies (Osmani, 1997). Most of the metavolcanic rocks in the belt have been metamorphosed to greenschist facies, except those in proximity to late granitoid intrusions, which have been metamorphosed to lower amphibolite facies (Williams et al., 1991).

3.4 Local Geology

The Shebandowan area has been well studied over the years as a result of a number of mapping projects. The earliest studies followed gold discovery in 1871 at the Huronian Mine in Moss Township by Peter McKellar after which the first map of the Shebandowan Lake was prepared (McInnes, 1928; Hodgkinson, 1968).

The study area lies in the West-Central Shebandowan Greenstone Belt (Fig. 3.6). North of the study area, metasedimentary rocks occur, marking the boundary between the Quetico Basin and the western Wawa-Abitibi Terrane. The rest of the west-central Shebandowan Greenstone Belt comprises metavolcanic and intrusive rocks (Osmani, 1997).

Several detailed mapping projects have been carried out in the Shebandowan Greenstone Belt by the Ontario Geological Survey (OGS). Giblin (1964) mapped the Burchell Lake area and produced the Burchell Lake Sheet (Map 2036). Hodgkinson (1968) conducted a mapping project of the Kashabowie Lake Area and produced the Kashabowie (Map 2128) and the Greenwater Lake Sheets (Map 2127). Harris (1970) mapped the Moss Lake area and produced the Tilly Lake (Map 2203) and the Powell Lake Sheets (Map 2204). Osmani (1997) conducted a more detailed mapping project covering the Greenwater Lake area and other segments of the west central Shebandowan Greenstone Belt. Osmani (1997) covered a wider area than the previous OGS mapping programs within the Shebandowan Greenstone Belt. Most of the areas previously mapped by Giblin (1964), Hodgkinson (1964), and Harris (1970) were covered by Osmani (1997). More recently, Hart (2007) mapped the Hamlin-Wye lakes area, located southwest of the study area (Fig. 3.6).

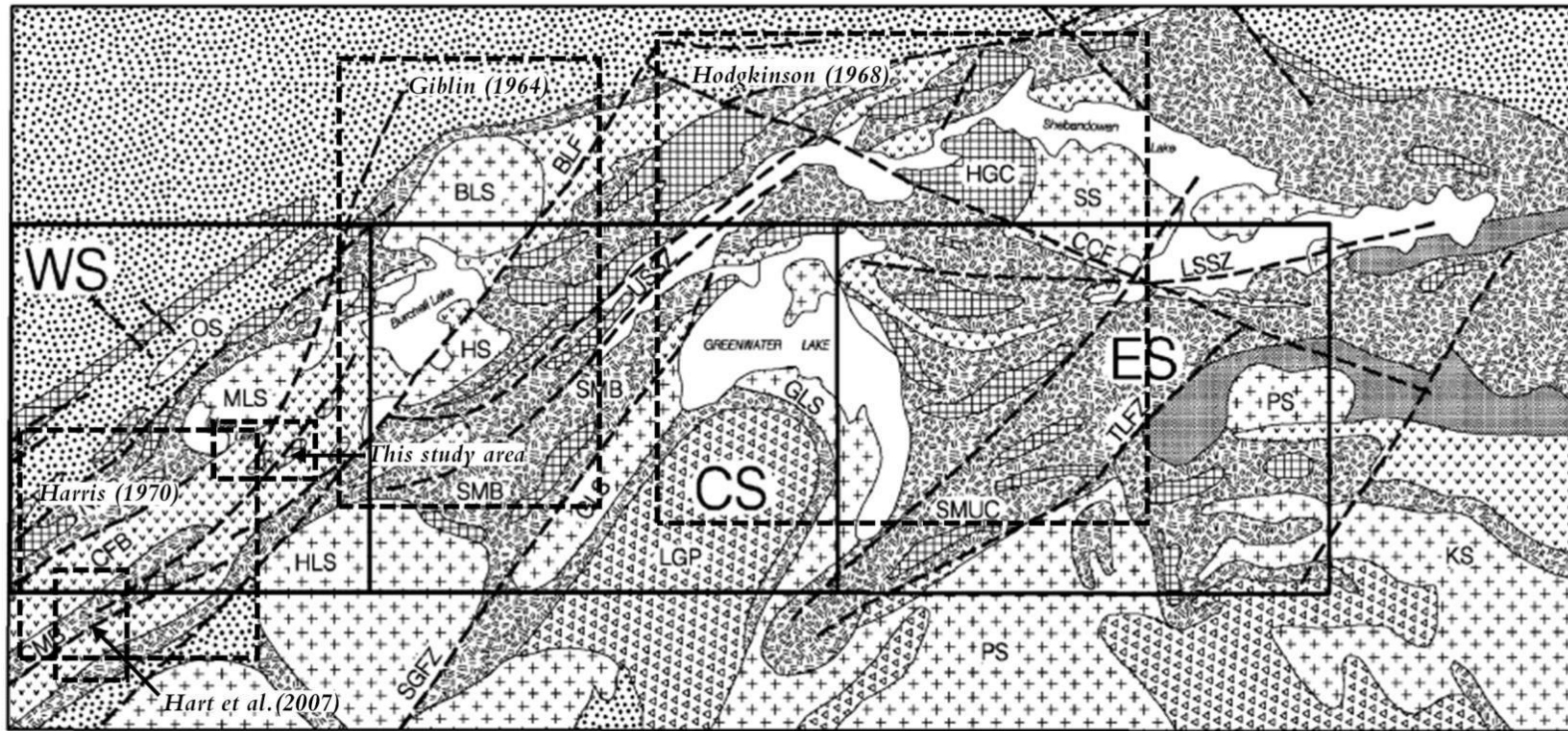
Osmani (1997) mapped the west-central Shebandowan Greenstone Belt and divided the map area into the western, central, and eastern areas (Fig. 3.6). For each area, maps were

produced describing lithologies and geological features. Map 2624 of the western study area covers Moss Township. Maps 2622 and 2623 of the central study area cover the Burchell-Greenwater Lakes area. Maps 2625 and 2626 of the eastern study area cover Begin, Lamport, and parts of Haines and Hagey townships (Fig. 3.6).

Mafic metavolcanic rocks are predominant in the map area (Fig. 3.6). The metavolcanic rocks have been divided into four belts: the Northern Mafic Metavolcanic Belt (NMB), the Southern Mafic Metavolcanic Belt (SMB), the Central Mafic Metavolcanic Belt (CMB) and the Central Intermediate to Felsic Metavolcanic Belt (CFB; Osmani, 1997). The NMB is in contact with metasedimentary rocks of the Quetico Metasedimentary Belt (QMB) to the northwest, which also occurs within the Osmani (1997) map area. The NMB and QSB form a sheared contact, which is suggested to be underlain by a major fault (Fig. 3.6; Osmani, 1997).

The three belts of mafic metavolcanic rocks (NMB, CMB and SMB) strike northeast to east, and comprise massive plagioclase-phyric, variolitic, spinifex-textured, and pillowed flows and associated pillow and flow top breccias (Osmani, 1997). Mafic to intermediate metavolcanic segments of these belts were observed within the western study area, and these include tuff, lapilli tuff, tuff breccia, and volcanoclastic rocks. They are commonly exposed as chlorite schists in high-strain zones, and rare amphibolite schists in proximity to large intrusive stocks (Osmani, 1997). The NMB and CMB also comprise mafic to intermediate fragmental metavolcanic rocks. The mafic to intermediate fragmental metavolcanic rocks within the belts are mainly block- to lapilli-sized, subangular to subrounded monolithic fragments set in a fine-grained mafic matrix (Osmani, 1997).

The CFB occurs between the NMB and the CMB. The CFB comprises intermediate to felsic metavolcanic rocks, and the belt extends for approximately 13 km and is widest between Fountain Lake and Snodgrass Lake with an approximate width of 2.9 km (Fig. 3.7; Osmani, 1997).



LEGEND

- Late- to post-tectonic granitoids.
- Tonalite-granodiorite gneiss.
- Metasediments (Quetico-type).
- Metasediments-metavolcanics (Timiskaming-type).

- Mafic to ultramafic intrusions.
- Intermediate to late felsic metavolcanics.
- Mafic to ultramafic metavolcanics.
- Fault/shear zones.
- Study area (1991-1993)

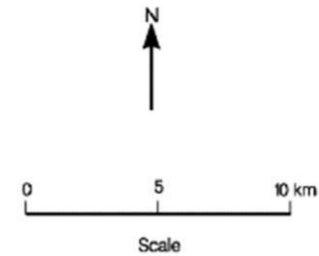


Fig. 3.6: Simplified geological map of Western Shebandowan greenstone belt. The map shows the area mapped by Osmani (1997), the western, central and eastern study areas of are represented by WS, CS and ES respectively. The map also shows areas covered by previous mapping projects and the current study area is represented by the dotted box (modified from Osmani, 1997).

The felsic to intermediate metavolcanic rocks of the CFB consist of aphanitic to fine-grained massive and porphyritic flows, with associated autoclastic breccias of similar composition. These rocks are white to beige on a weathered surface and greenish-grey on fresh surfaces (Osmani, 1997). Osmani (1997) observed some tuff units of intermediate composition that are greenish-grey on a weathered surface and grey to dark grey on a fresh surface. Some of the pyroclastic rocks occur as massive to bedded and poorly to well-sorted units. The stratigraphic sequence of the intermediate pyroclastic rocks northwest of Burchell Lake shows a northwest younging direction (Osmani, 1997).

West of Fountain Lake and proximal to the Snodgrass Lake area, pyroclastic rocks, such as tuff and pyroclastic breccias, tuff, and lapilli tuff, are common (Osmani, 1997). They are composed of 5 to 40% angular to subangular felsic clasts, set in a fine-grained intermediate to felsic matrix. In high-strain zones, sericite schist is the dominant derivative of the intermediate to felsic metavolcanic rocks. Schistosity and fracture planes within the sericite schists usually contain quartz and chlorite (Osmani, 1997).

Felsic metavolcanic rocks were mapped by Hodgkinson (1968) in the Shebandowan Lake area, and they include rhyolite, dacite, tuff, agglomerate, and sericite schist. The felsic metavolcanic rocks are white to light cream on a weathered surface and grey, green, pink or light cream on fresh surface (Hodgkinson, 1968). They form long and narrow metavolcanic belts parallel to regional schistosity and are interpreted to be Pelean-type avalanche deposits (Hodgkinson, 1968).

Osmani (1997) noted a felsic pyroclastic rock north of Greenwater Lake, with a strike length of about 5km and 450m thickness composed of coarse pyroclastic units, with block to lapilli-sized clasts in the middle of the pile, which fines to the east and west into tuff. Some of the felsic clasts have a pumiceous texture and occur within a felsic matrix (Osmani, 1997). The felsic metavolcanic rock grades northward to intermediate tuff to lapilli tuff, which then grades into mafic metavolcanic flows. This is interpreted to represent a complete volcanic cycle from a mafic base to a felsic top (Osmani, 1997). Based on this observation, the stratigraphy is suggested to young to the south-southeast. The mafic metavolcanic base of this unit is on strike

with mafic pillowed units mapped southwest of Upper Shebandowan Lake, which is a southeast-facing flow (Fig. 3.5; Osmani, 1997).

Ultramafic metavolcanic rocks are rare within the study area. They generally occur as discrete, narrow lenses adjacent to or grading into mafic metavolcanic rocks and are typically massive and lack diagnostic primary features, such as spinifex texture and pillows (Osmani, 1997). Some units of ultramafic metavolcanic rocks were observed north of Greenwater Lake (Fig. 3.6) and approximately 3km east of North Coldstream Mine, and in most outcrops, they occur as minor units within the mafic metavolcanic rocks (Osmani, 1997).

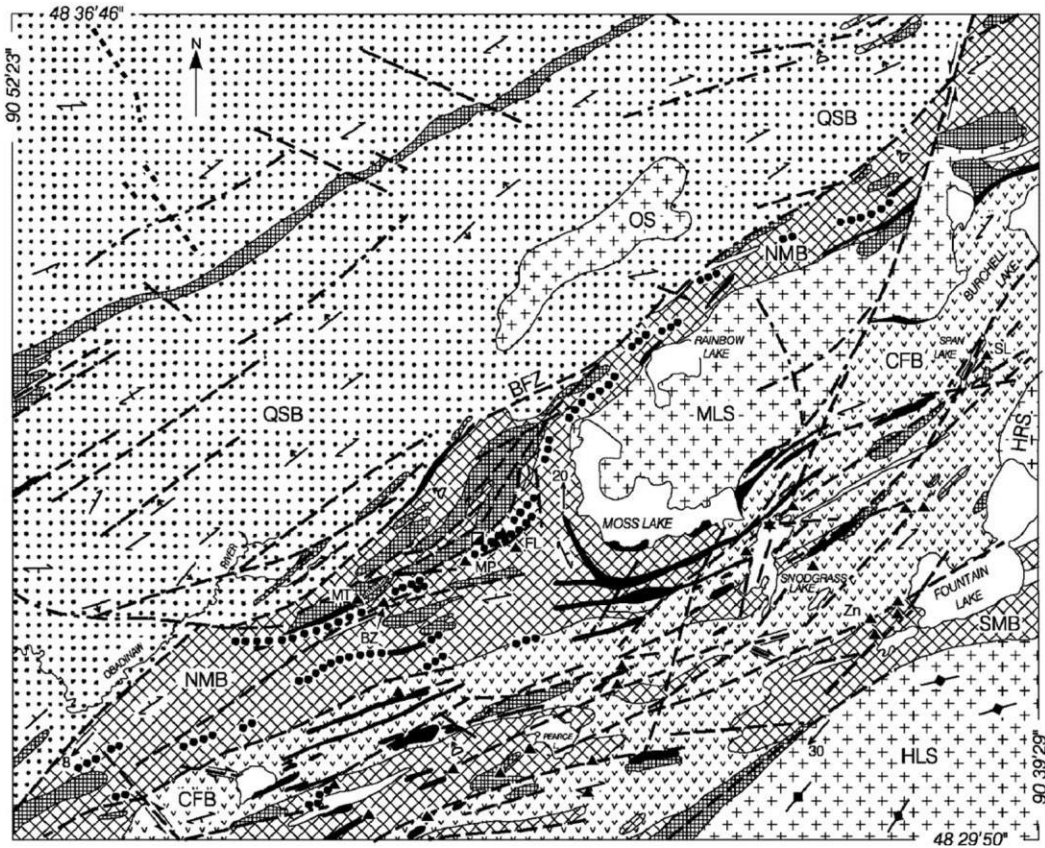
Northeast of Moss Township, metasedimentary rocks of the Quetico Metasedimentary Belt (QSB) occur (Fig. 3.7). These rocks include weakly graded metawacke, thinly bedded to finely laminated metasilstone, and metamudstone (Osmani, 1997). In proximity to the Obadinaw stock northwest of Moss Lake, migmatitic metasedimentary rocks occur, these rocks show intense deformation and display a well-pronounced foliation defined by biotite (Osmani, 1997). Chemical metasedimentary rocks form part of the mafic to intermediate metavolcanic and clastic metasedimentary successions within the area, and these include chert beds, chert with pyrite \pm pyrrhotite, chert \pm jasper-magnetite banded ironstone, and brecciated ironstone (Osmani, 1997).

Mafic and ultramafic intrusive rocks are observed throughout the area occurring as stocks, sills, and dikes. The mafic intrusive units include diorite, gabbro, leucogabbro, plagioclase-phyric gabbro, gabbro-anorthosite assemblage, and amphibolite (Osmani, 1997). Osmani (1997) noted that the mafic intrusive rocks mapped are commonly sheared and altered to chlorite \pm epidote-actinolite-hornblende schist, such as gabbroic units located at the south shore of Upper Shebandowan Lake and at the North Coldstream mine (Fig. 3.6). The ultramafic intrusive rocks mapped by Osmani (1997) include sills and dikes of peridotite, pyroxenite, and derived schists. These are predominant in the east of the study area. Massive peridotite sills host nickel, copper, and platinum group elements at the Shebandowan Mine (Osmani, 1997).

Several stocks of varying sizes were mapped by Harris (1970) within the study area, including mafic and felsic intrusive rocks. They include peridotite, gabbro, diorite, amphibolite, and granite. The stocks are intrusive into the metavolcanic rocks, suggesting that they post-date the metavolcanic rocks. The Knife Lake Fault marks the contact between the mafic intrusions and the granitic Myrt Lake Batholith, a fine- to medium-grained biotite granite (Fig. 3.6; Harris, 1970).

The Moss Lake Stock is a felsic to intermediate unit that ranges in composition from syenite to monzonite and granite with minor syenodiorite or diorite, which are generally medium-grained with minor fine-grained, porphyritic phases (Osmani, 1997). The stock intrudes into the NMB and the CFB within the western study area. Southeast of the Moss Lake Stock lies the Hood Lake Stock (Fig. 3.7). The Hood Lake Stock is a porphyritic hornblende \pm pyroxene monzonite and syenite intrusion (Osmani, 1997).

The segment of the CFB that hosts the Moss Deposit runs between the Hood Lake and the Moss Lake stocks (Fig. 3.7); the gold dominantly occurs within the CFB, mainly hosted by felsic to intermediate metavolcanic to intrusive rock, mainly of dioritic to dacitic composition as observed from petrographic analysis during the current study. An outcrop of felsic pyroclastic rock dated at 2696 ± 3 Ma (Corfu and Stott, 1998) occurs in the northeastern extension of the CFB within the Burchell Lake area. This rock shares similar geological features with the metavolcanic rocks in the study area and is considered to be a similar volcanic package.



LEGEND

- | | | | |
|--------------------|--|---|------------------------------------|
| PROTEROZOIC | | ★ | Snodgrass Lake prospect/deposit. |
| ⋯ | Diabase dike. | ▲ | Gold occurrence. |
| ARCHEAN | | ☒ | Huronian Mine (past producer). |
| + | Felsic to mafic intrusive rocks. | ⊕ | Pillow, top indicated by arrow. |
| ▨ | Younger metasedimentary rocks. | ⊖ | Bedding, top indicated by arrow. |
| ▩ | Mafic intrusive rocks. | ↔ | Bedding, parallel to foliation. |
| ⋯ | Metasedimentary rocks (Quetico-type). | ↗ | Foliation (inclined, dip unknown). |
| ● | Chemical metasedimentary rocks. | ↘ | Lination with plunge. |
| ⊕ | Intermediate to felsic metavolcanic rocks. | ↖ | Shear or fault zone. |
| ⊗ | Mafic to intermediate metavolcanic rocks. | ↗ | Lineament. |
| ■ | Feldspar porphyry, quartz-feldspar porphyry. | | |

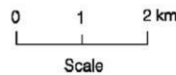


Figure 3.7: Geological map of the Moss Township. Mineral occurrences, lithologies, structural features, and mineral prospects are shown. Abbreviations: NMB, northern mafic metavolcanic belt; CFB, central intermediate to felsic metavolcanic belt; QSB, Quetico metasedimentary belt; OS, Obadinaw stock; MLS, Moss Lake stock; HLS, Hood Lake stock; HRS, Hermia Lake stock (modified from Osmani, 1997).

3.5 Mineral Deposits and Exploration History

The Shebandowan area has been explored for over a century, resulting in the discovery of a number of precious and critical mineral deposits. The first discovery of gold in Northwestern Ontario was in the Shebandowan area in 1871 at the Huronian Mine in Moss Township (Hodgkinson, 1968). The Huronian Au+Ag Mine was the first mine in the area to go into production. Subsequent exploration of prospects and occurrences led to the discovery of other mineral deposits within the Shebandowan Greenstone Belt that reached the production stage (Table 3.1).

Table 3.1: Mineral deposits mined in the Shebandowan Greenstone Belt

Mine	Huronian Mine	North Coldstream Mine	Shebandowan Mine
Deposit type	Orogenic Gold deposit	Volcanogenic Massive Sulfide (VMS) deposit	Magmatic Cu-Ni-PGE deposit
Resources	29,948 ounces of gold, 172,376 ounces of silver	984 tons of copper, 6,224 ounces of gold, 139,505 ounces of silver	8.7 million tonnes of ore at 2.07% Ni, 1.00% Cu and 3.0 g/t PGM + Au
Operation	1884-1885, 1932-1936 and 1942	1903, 1906, 1916-1917, 1957-1958 and 1960-1964	1972-1998
References	Hodgkinson (1968), Harris (1970).	Hodgkinson (1968), Giblin (1964).	Lavigne et al. (1990), Osmani (1997).

3.6 History of the Moss Lake Deposit

The history of the Moss Lake deposit described here is based on Risto and Breede (2010) and Poirier et al. (2013). The term Moss Lake deposit refers to the gold occurrence within the Moss Lake Property. The Snodgrass occurrence, which is located north of Snodgrass Lake, is the earliest gold discovery within the Moss Lake property boundary (Fig. 3.8). The earliest gold discovery within the Moss Lake property boundary (Fig. 3.8). The earliest exploration was in 1936 when seven trenches were dug along the mineralized zone just north of Snodgrass Lake by the Mining Corporation of Canada (Fig. 3.8; Harris, 1970). In 1945, the area was explored by Lobanor Gold Mines Limited who drilled 12 holes totaling a length of 4,695 ft (1431.0 m). Three zones of Au and Ag mineralization were delineated as a result of the drilling program (Harris, 1970).

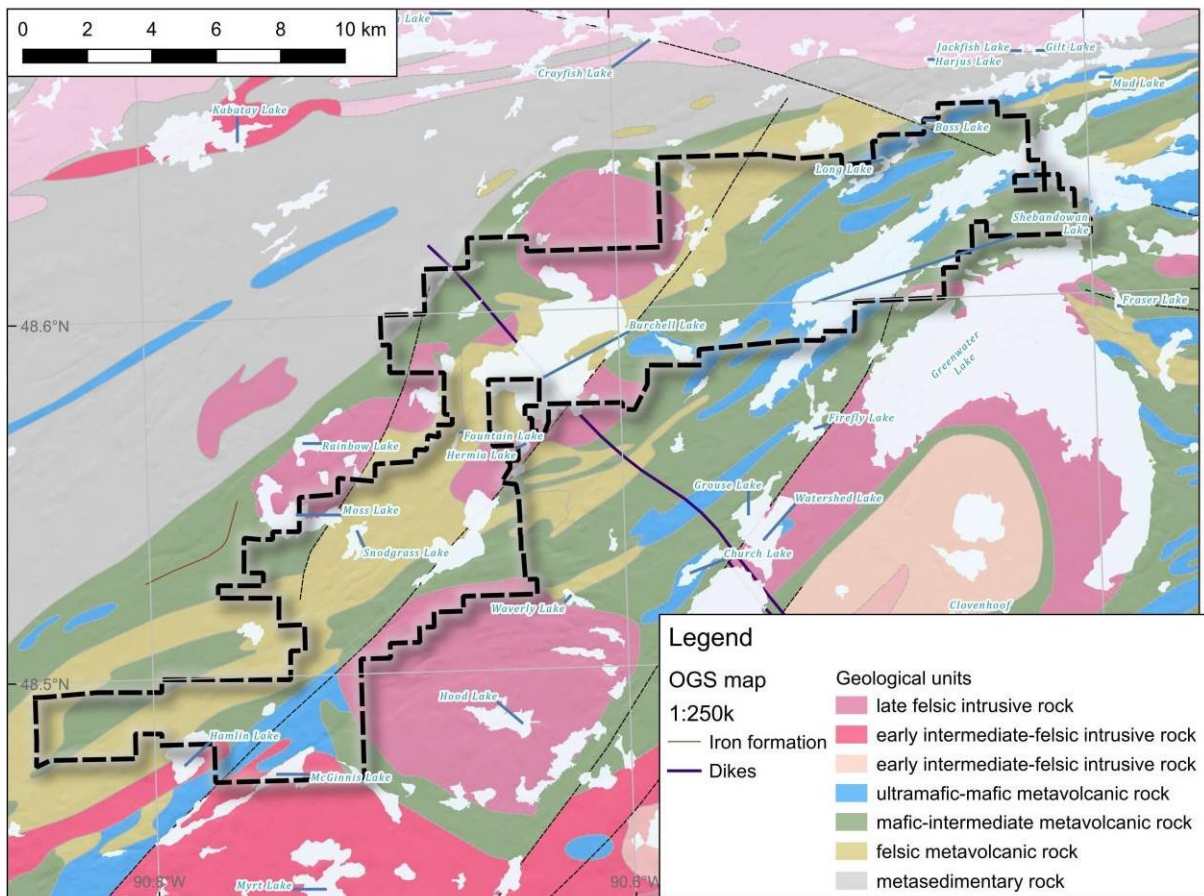


Figure 3.8: Geologic map showing the boundary of the Moss Lake Property (modified from Goldshore Resources, 2022).

Gold was discovered west of Fountain Lake around the same time as the Lobanor Gold Mines Ltd. drilling program (Fig. 3.7). This showing was drilled in 1947 by Airways Exploration Ltd., and later, the claims were optioned to Great Lakes Copper Mines Limited in 1952. Between 1974 and 1976, the areas west and north of Snodgrass Lake were explored using a combination of geological and geophysical surveys and diamond drilling; this exploration program was carried out by Falconbridge Nickel (Falconbridge Limited). From 1983 to 1987 Tandem Resources Limited conducted mapping, geophysical surveys, and diamond drilling in the Snodgrass Lake Prospect and surrounding areas (Osmani, 1997). As of 1988, the Tandem/Storminin JV, having drilled 204 surface holes and 32 underground drill holes on the Snodgrass Lake prospect, reported a drill-indicated reserve estimate of 338,722 t grading 5.35 g Au/t (Elliot, 1988). This was the earliest reserve estimate made for the deposit.

In 1996, Moss Lake Gold Mines Ltd. carried out more drilling in the Main and QES zones; by 1999 they acquired the Fountain Lake Property and conducted a geophysical survey covering 56.6 line km over the property; several anomalies were reported. From 1999 to 2006, Moss Lake Gold Mines Ltd. conducted geological and geophysical surveys, as well as drilling programs from Snodgrass Lake to Fountain Lake. By 2010, two 43-101 compliant reports had been prepared for the Moss Lake property, one in 2006 and the second in 2010. The 2010 report provided an updated Mineral Resource estimate with an indicated grade of 0.93 g Au/t from 36,569,769 t of ore and an inferred 18,783,976 t grading at 0.86 g Au/t.

In 2014, Moss Lake Gold Mines' ownership was amalgamated by Wesdome Gold Mines, who conducted more drilling to confirm the extent of the mineralization along the strike. In 2021, Goldshore Resource Inc. acquired the Moss Lake Property and is conducting a more intensive exploration program on the Moss Lake Deposit and surrounding occurrences within their property. A more recent mineral estimate of the gold at Moss Lake was published by Goldshore Resource (2022) after a detailed drilling program, stating that the deposit holds an inferred resource of 4.17 Moz of Au from 121.7 Mt of ore at 1.1 g/t Au.

Chapter 4: Results

4.1 Sampling and Petrography

The sampling conducted in this study focused on altered rocks, in order to investigate vein distribution and Au distribution. The samples were selected from the Mineralized and Northeast zones (NE zone). The mineralized zone includes samples from drill holes that cut the main ore body, whereas the NE zone includes samples from drill holes in a less mineralized zone northeast of the main ore body (Fig. 4.1). Petrography was used to characterize the host rocks, mineralogy, alteration assemblages, and the degree of alteration and mineralization present in the samples (Appendix I). Based on the petrographic analysis, the host rocks in the study area were identified; they include, in decreasing order of abundance, diorite, dacite, and andesite. Plagioclase, quartz, and amphibole are the primary minerals present in all rock types. Figure 4.2 shows a representative stratigraphic column through the deposit, highlighting the distribution of gold within drill hole MQD-22-070 and where some key samples were collected.

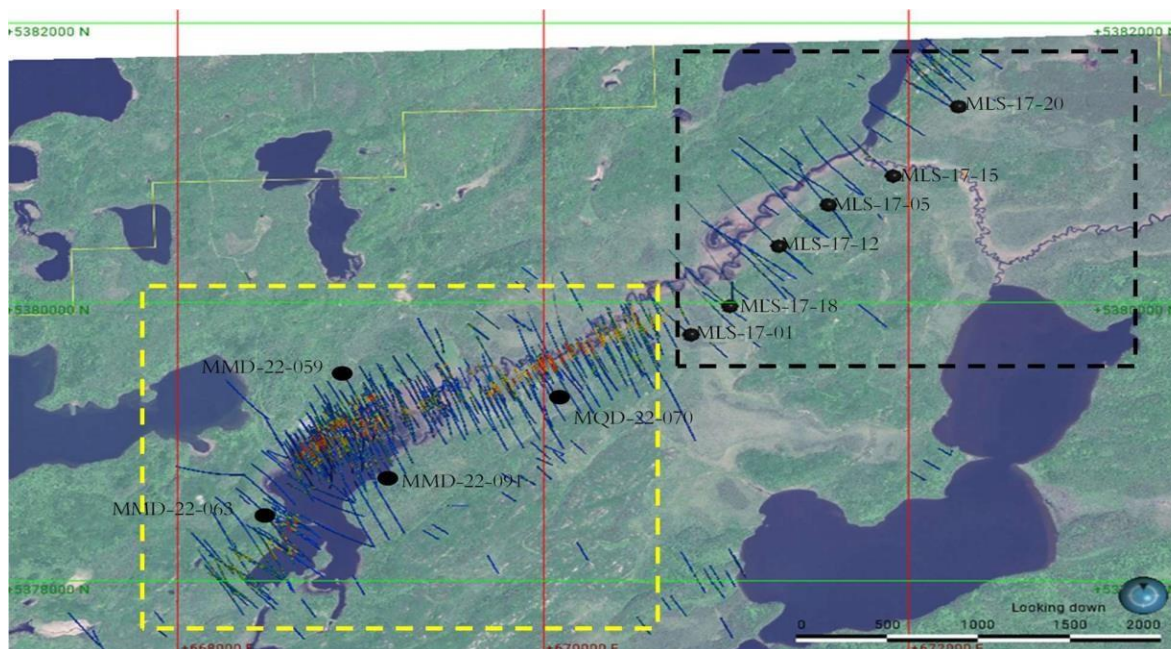


Fig. 4.1: Plan view of the Moss Lake deposit showing the Mineralized (yellow box) and NE zone (black box) zones from which samples have been collected for this study (modified from Goldshore Resources, 2022).

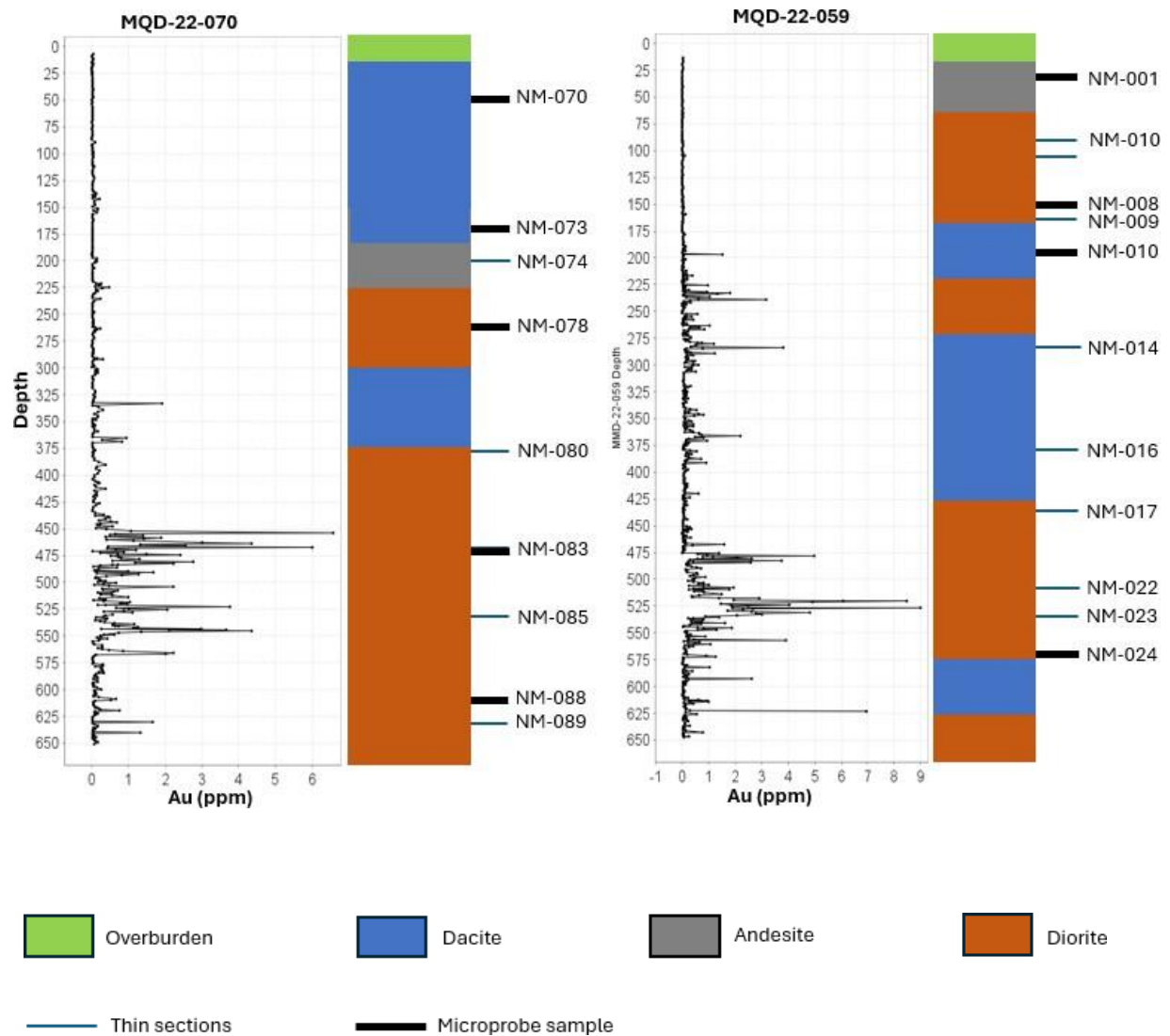


Fig: 4.2: Downhole plot of drill hole MQD-22-070 and MMD-22-059 highlighting the different lithologies and the distribution of gold within the rock types using a representative drill hole. Also shown are the sample locations.

4.1.1 Dacite

The dacites are weakly altered rocks that comprise fine grains of plagioclase and quartz, with minor sericite, chlorite, carbonate, and pyrite (Fig. 4.2).

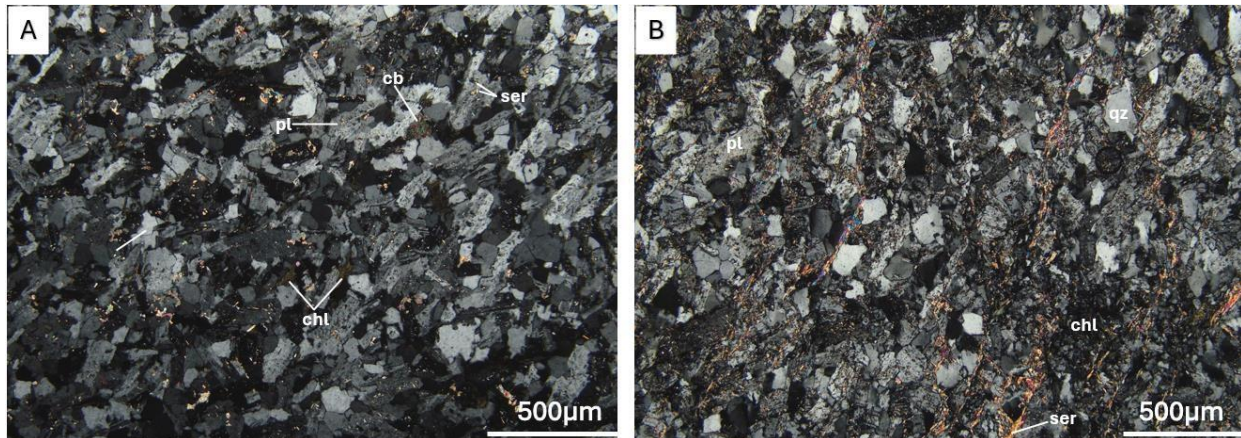


Fig. 4.3: Photomicrographs of dacite from the Moss deposit showing (a) a less altered dacite (ML23-NM-026) and (b) more altered dacite (ML23-NM-030) under cross-polarized light.

The plagioclase grains can be up to 300 micrometers across, and they exhibit simple and polysynthetic twinning with weak to moderate sericite alteration. The grains are randomly oriented throughout the rock. The quartz grains are anhedral up to 150 micrometers across, commonly ranging between 50 to 100 micrometers. Sericite grains are anhedral up to 20 micrometers across and they occur as an alteration phase affecting plagioclase grains. Sericite grains also occur elongated parallel to the fabric of the host rock. Chlorite grains are anhedral up to 100 micrometers, commonly occurring as pervasive alteration or as chlorite veinlets. The carbonate grains are up to 500 micrometers and occur mainly within veins that cut the host rock.

4.1.2 Diorite

The diorites are variably altered and vary from fine to medium grained (Fig. 4.3). The diorites comprise plagioclase and quartz, with minor amphibole, chlorite, sericite, biotite, epidote, carbonate, pyrite, and chalcopyrite. Plagioclase phenocrysts up to 5mm across occur within the diorites associated with a groundmass of quartz and plagioclase.

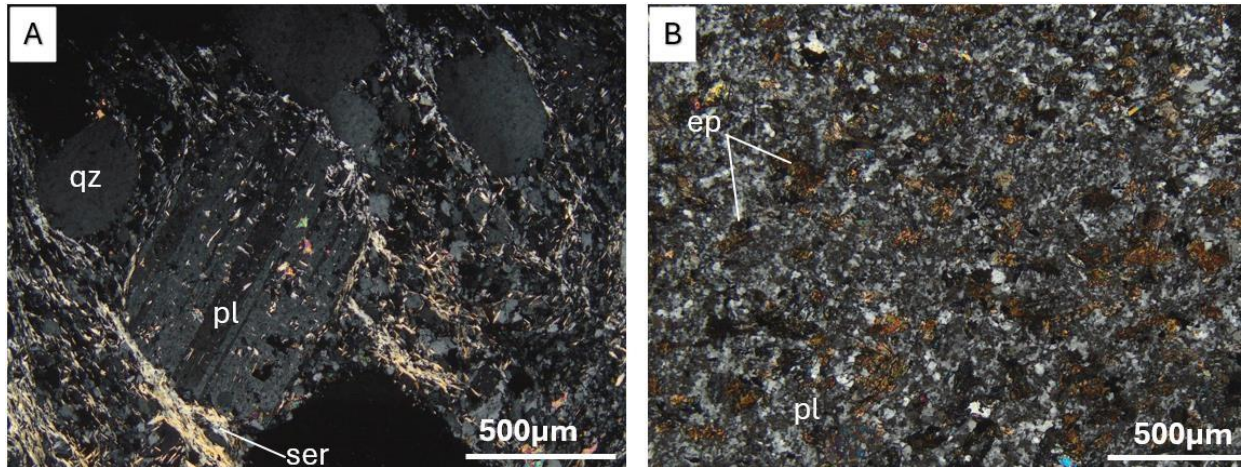


Fig. 4.4: Photomicrographs showing (a) medium-grained diorite (ML23-NM-083) and (b) fine-grained diorite (ML23-NM-067) under cross-polarized light.

Finer grains of plagioclase can be up to 100 micrometers; all plagioclase grains exhibit simple and polysynthetic twinning with weak to moderate sericite, chlorite, and epidote alteration. The quartz grains are up to 100 micrometers across, commonly ranging from 40 to 80 micrometers. The amphibole grains are anhedral up to 100 micrometers across; they are randomly oriented throughout the rock and are associated with plagioclase. Biotite occurs as fine grains up to 150 micrometers and is commonly associated with sericite and chlorite. The chlorite grains are up to 200 micrometers, commonly replacing amphibole and plagioclase. The epidote grains are up to 100 micrometers and strongly replace amphibole grains. The carbonate grains are up to 100 micrometers and occur pervasively in the host rock, commonly when the host rock is cut by veins.

4.1.3 Andesite

The andesites are moderately to strongly altered and comprise plagioclase, amphibole, quartz, chlorite, sericite, epidote, and pyrite (Fig. 4.4). Plagioclase is the dominant mineral within the andesites, and they are up to 200 micrometers across. The amphiboles are up to 150 micrometers across, commonly ranging between 20 to 60 micrometers. The quartz grains are anhedral and dominantly occur in the groundmass with a few recrystallized grains up to 100 micrometers across, commonly ranging between 30 to 80 micrometers. The chlorite grains are up to 200 micrometers across and strongly replace amphibole grains. The epidote grains are up

to 100 micrometers across. Sulfides consist of disseminated pyrite grains up to 100 micrometers across. The main distinguishing features between the diorite and andesite are the dominantly fine-grained texture of the andesites and the occurrence of quartzose groundmass.

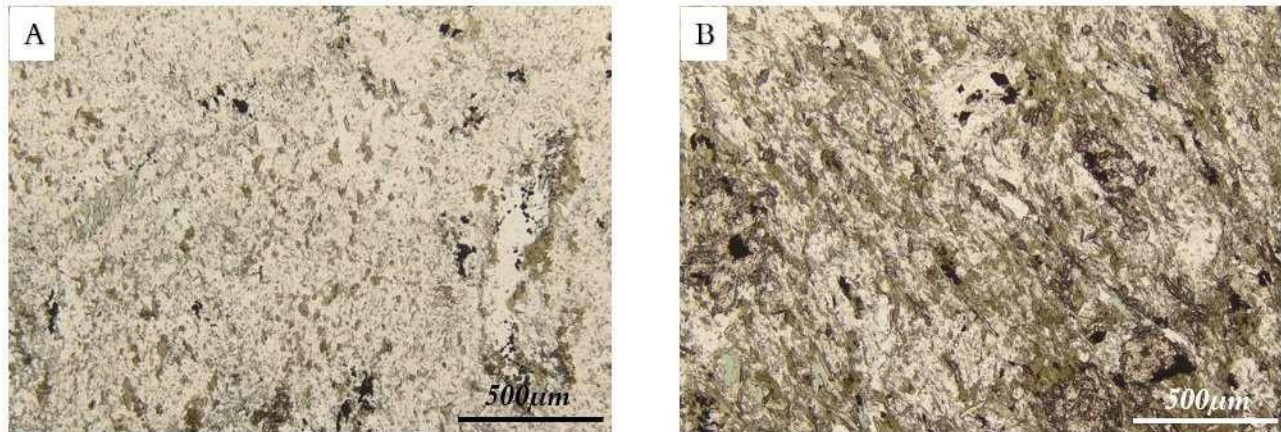


Fig. 4.5: Photomicrographs showing a less altered (ML23-NM-068) (a) and more altered (ML23- NM-074) (b) andesitic unit in plane-polarized light.

4.1.4 Sulfides

Within the host rocks, sulfides usually occur as individual grains of pyrite, chalcopyrite, and sphalerite or as sulfide mineral assemblages and show no obvious variation in the different host rocks. They comprise pyrite-chalcopyrite assemblages and pyrite-chalcopyrite-sphalerite assemblages (Fig. 4.5). The former is more common and has variable textures. The pyrite-chalcopyrite assemblages comprise anhedral chalcopyrite grains up to 200 micrometers across, commonly occurring on the grain boundaries of euhedral to subhedral pyrite grains, and the pyrite grains are up to 700 micrometers across.

The pyrite-chalcopyrite assemblages are mostly disseminated in the host rock, but are also present within veins. Pyrite-chalcopyrite-sphalerite assemblages are less abundant within the host rock. They comprise subhedral to anhedral grains of sphalerite up to 200 micrometers across, commonly occurring along the grain boundaries of pyrite, anhedral chalcopyrite grains up to 70 micrometers across, occurring as inclusions within pyrite grains, and along pyrite grain boundaries, and subhedral pyrite grains up to 400 micrometers across (Fig. 4.5).

The pyrite-chalcopyrite-sphalerite assemblages occur mostly as disseminated grains, but are also present in veins. Pyrite grains are the most common sulfide within the host rocks, and the grains can be up to 1mm, commonly 300 to 500 micrometers when they occur in a disseminated texture (Fig. 4.5c). Pyrite grains within veins can be larger up to 2mm, commonly 300 to 800 micrometers (Fig. 4.5d). Both assemblages are dominated by pyrite, chalcopyrite, and sphalerite, make up about 10% of the total observed sulfides at Moss Lake, and are both strongly associated with pyrite. Pyrite grains are mostly fractured and vein-related and are associated with gold mineralization.

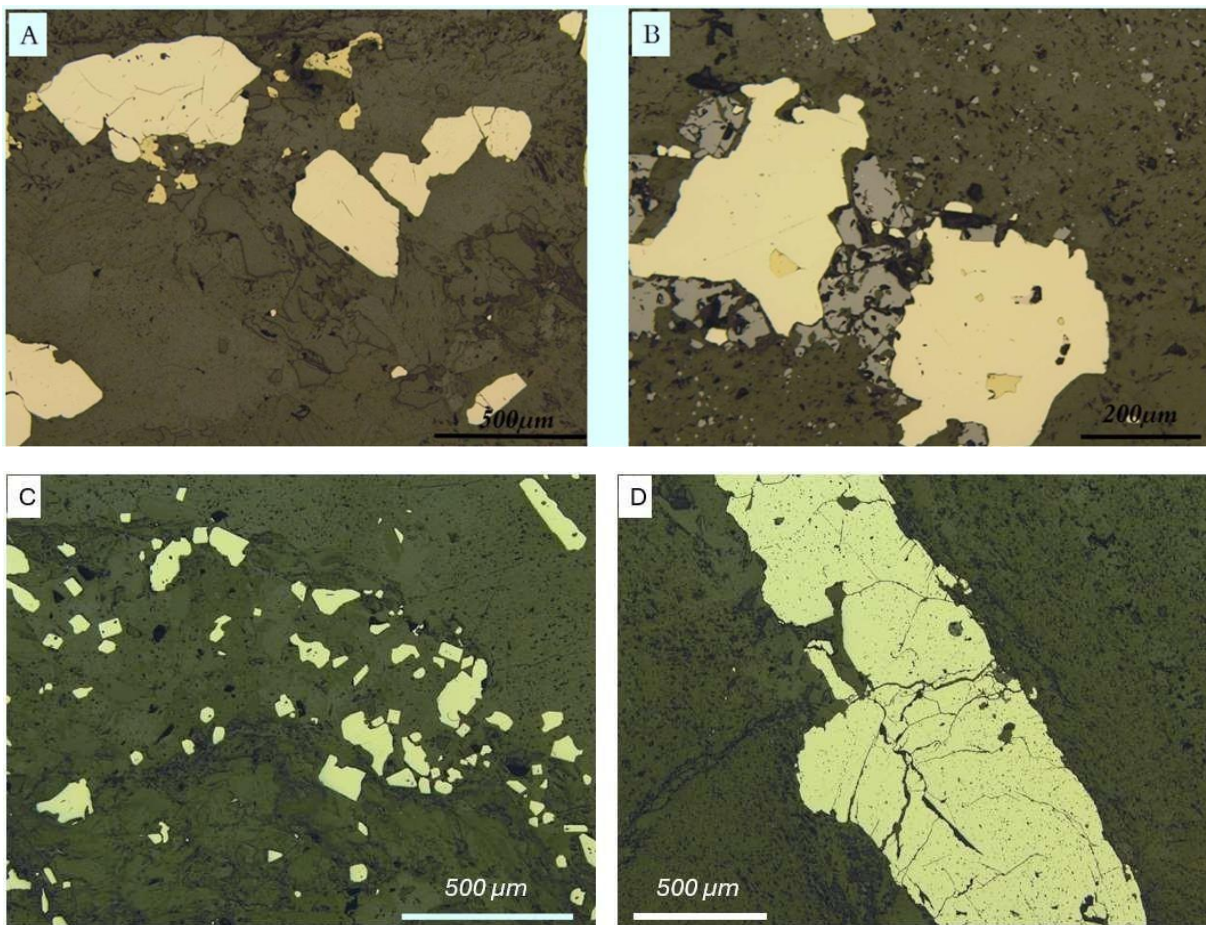


Fig. 4.6: Photomicrographs of sulfides in reflected light within the host rocks and the different textures of pyrite grains. Pyrite-chalcopyrite assemblage is shown in (a) (ML23-NM-014), and pyrite- chalcopyrite-sphalerite is shown in (b) (ML23-NM-070), image C (ML23-NM-030) shows disseminated pyrite grains with variable grain sizes occurring in the host rocks and image D (ML23-NM-078) shows pyrite within a pyrite-quartz-carbonate vein.

4.1.5 Alteration

Alteration is widespread within the host rocks at Moss Lake, ranging from weakly to strongly altered. In the weakly altered rocks, alteration minerals make up around 5 to 15 % of the mineralogy, whereas in the strongly altered rocks, alteration minerals make up about 45 to 60 % of the mineralogy, between 15 to 45 % alteration the rocks are grouped as moderately altered. The degree of alteration can be visible in hand sample as it was one of the criteria used during sampling (Fig. 4.6). Alteration minerals are comprised mainly of albite, biotite, sericite, chlorite, epidote, and carbonate. Albite and biotite alteration are the least observed alteration phase using petrography, sericite is the most common alteration mineral observed at Moss Lake, followed by chlorite and carbonate alteration, epidote alteration is also common, but less abundant than sericite, chlorite, and carbonate. Carbonate alteration occurs in association with quartz within veins and is prevalent within the dacite.

Biotite alteration is not very common among the host rocks and is barely observed in hand samples. In thin sections, they occur as dark brown elongate grains up to 80 micrometers across (Fig. 4.8a). Biotite is strongly replaced by chlorite and sericite alteration and is associated with dioritic units. Albite alteration is a common phase, but rarely observed in thin sections. In hand samples, however, albitization is observed as a pinkish-red hematite coloration (Fig. 4.8c), and the analysis of plagioclase grains in the SEM-EDX shows that they are mostly albite (Na-rich).

Sericite is the most common alteration mineral in hand samples, where it is a light greyish-green color (Fig. 4.6a;c). Sericite alteration within individual samples varies from weak to strong, with grains up to 30 micrometers across (Fig. 4.7a). Sericite alteration occurs as a localized replacement mineral within plagioclase phenocrysts as well as a pervasive replacement mineral within the host rock. Sericite grains are aligned in some samples; this alignment gives the sericite grains a foliated appearance, which is common in rocks with a high degree of sericitization (Fig. 4.8b).

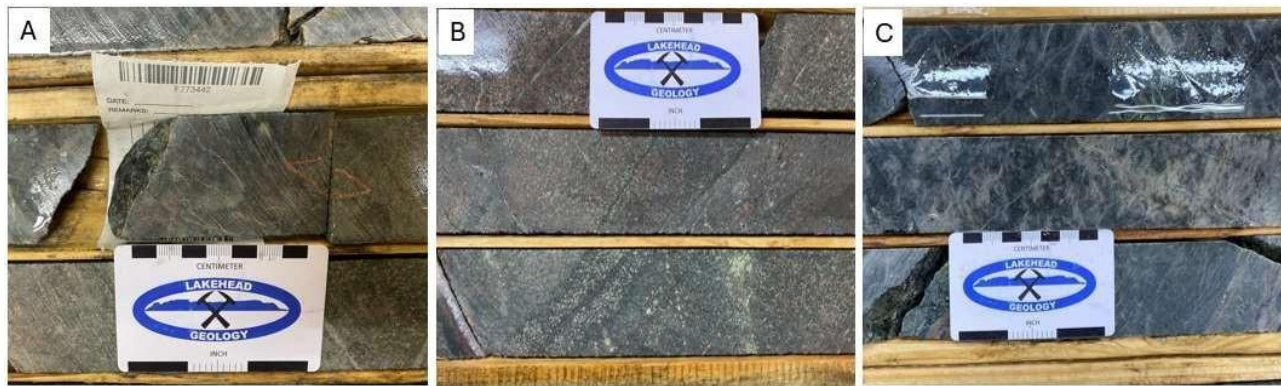


Fig. 4.7: Hand sample photos showing different intensities of alteration within the host rocks. Image A (ML23-NM-034) shows a weakly altered rock, image B (ML23-NM-004) shows a moderately altered rock, and image C (ML23-NM-075) shows a strongly altered rock.

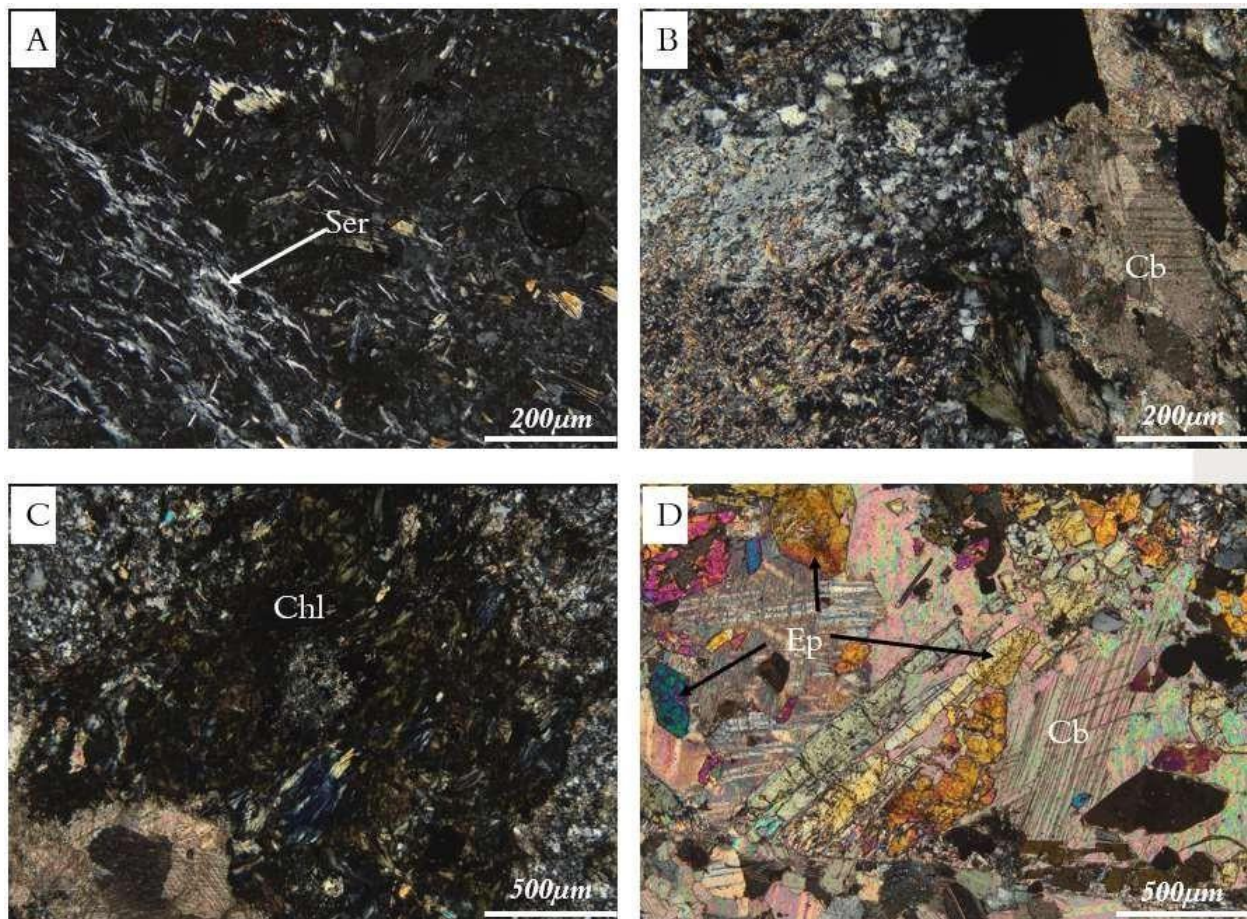


Fig. 4.8: Photomicrographs in cross-polarized light, showing the different alteration minerals occurring within the Moss Lake deposit. Images A (ML23-NM-014) and B (ML23-NM-064) show the occurrence of sericite and carbonate alteration, respectively, image C (ML23-NM-065) shows pervasive chlorite alteration and image D (ML23-NM-058) show epidote grains and their replacement of carbonates.

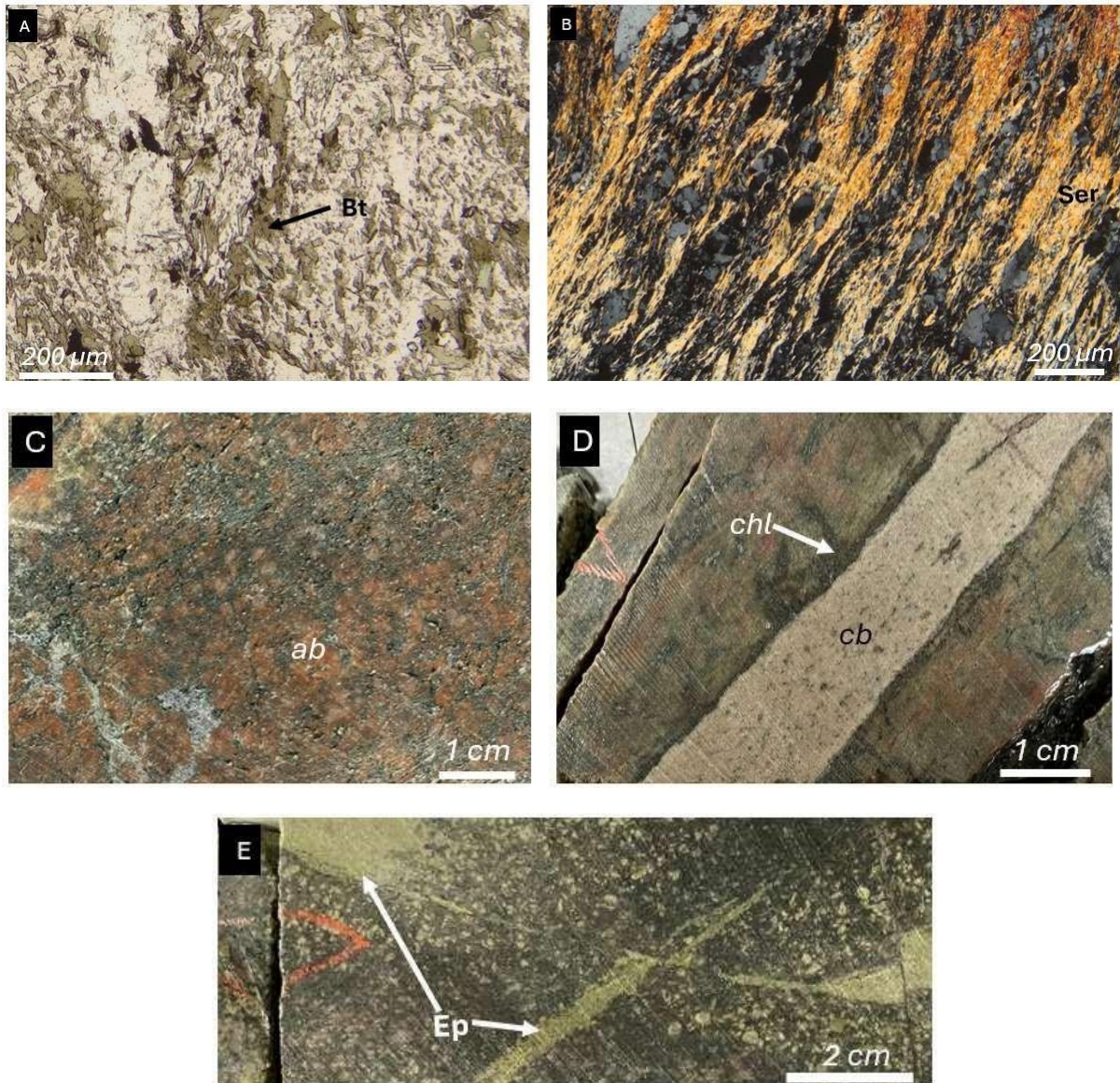


Fig. 4.9: Photomicrographs and hand sample images of various alteration minerals within the host rocks. Image A (ML23-NM-074) plane-polarized photomicrograph shows biotite alteration within a dioritic unit, image B (ML23-NM-046) cross-polarized photomicrograph showing strongly aligned sericite grains (sheared), image C (ML23-NM-009) hand sample photograph showing reddish coloration resulting from albite alteration, image D (ML23-NM-031) hand sample photograph showing carbonate vein associated with chlorite alteration on the rim of the vein, and Image E (ML23- NM-035) hand sample photograph shows pervasive epidote alteration and veinlets.

Carbonate alteration is present at Moss Lake and occurs within all rock types. Carbonate minerals are mainly observed as veins and veinlets in hand samples and are white to light grey in color (Fig. 4.8d). In thin section, carbonate alteration occurs weakly as pervasive alteration and strongly as vein infills; the grains can be up to 200 micrometers across, commonly larger up to 1 mm across within veins (Fig. 4.7b and 4.7d). SEM-EDX analysis shows carbonate minerals at Moss Lake are commonly calcite.

Chlorite is the predominant alteration mineral within the diorite units, noticeable in hand samples due to its dark green coloration (Fig. 4.8d). Chlorite alteration is also widespread in other rock types and dominantly occurs as a pervasive replacement mineral (Fig. 4.7c). Pervasive chlorite grains are up to 200 micrometers across, commonly ranging from 50 to 100 micrometers (Fig. 4.7c). Chlorite replaces sericite, plagioclase, carbonate, and biotite. Chlorite alteration also occurs in veins up to 50 to 100 micrometers wide (Fig. 4.10e).

Epidote alteration is present within the diorite intrusion. In hand sample epidote alteration is observed as greenish grains occurring pervasively within the rock and sometimes as epidote veinlets (Fig. 4.8e). In thin section, epidote grains are observed as colorless to light green grains up to 200 micrometers across (Fig. 4.7d), replacing plagioclase, chlorite, and amphibole grains. Epidote grains also occur within late veins associated with chlorite and carbonate (Fig. 4.7d).

4.1.6 Veins

At Moss Lake, veins play an important role in the mineralization process. Veins and their relationships were a key focus during sampling, and all the veins were studied in hand samples and thin sections. One or more veins are present within 60 of the 62 polished thin sections analyzed in this study. The size of the various veins vary from 0.1 to 3mm wide, commonly around 0.6 mm. The veins occur at different angles, with some veins parallel and some veins at an angle to the fabric of the rock (Fig. 4.9).

At least 12 different vein types were observed at the Moss Lake deposit, and they are grouped based on the main infills and the type of alteration associated with the vein minerals (Table 4.2). Most veins are quartz and carbonate-bearing; however, other vein infill minerals

Table 4.1: Vein types observed and their characteristics.

Vein ID	Vein infill	Alteration	Macro identification
QZ(1)	Quartz	No alteration, halo. Can be associated with epidote alteration when cut by type 7	Smoky quartz (Fig. 4.10d) No alteration halo
QC(2)	Quartz, carbonate		Greyish to white vein commonly at an angle to the fabric of the host rock (Fig. 4.9a)
CH(3)	Carbonate and hematite	Hematite halo	mm scale light grey veins with pinkish-red cm scale alteration halo (Fig. 4.9b)
QCC(4)	Quartz, carbonate, chlorite	Chlorite replacement of carbonates, sericite halo	Grey to green vein with off-white broad halo The vein is commonly undulating and can exhibit pinch and swell texture (Fig. 4.9f)
CB(5)	Carbonate	not common but can have chlorite replacement on rims of veins, sericite halo	Whitish vein commonly within dacite units and parallel to the fabric(Fig. 4.9a)
CCL(6)	Carbonate, chlorite	Chlorite infills and chlorite rim	Whitish vein with dark green rims when associated with chlorite alteration Halo is greyish to light pink (Fig. 4.10a)
ECL(7)	Chlorite, epidote	Sericite alteration on the rim of the vein, epidote halo	mm scale veins, not commonly visible Vein is greenish and common in diorite units (Fig. 4.10e)
SCL(8)	Sericite, chlorite	Chlorite replacement of sericite, chlorite halo	mm scale dark green vein Common in diorite unit (Fig. 4.10f)
QZ2(9)	Quartz, epidote	Epidote grains entrained in quartz-rich vein	Greenish to dark grey mm scale veins Common in diorite units (Fig. 4.10f)
QCP(10)	Quartz, carbonate, pyrite, minor chalcopyrite and sphalerite, gold	Sericite alteration in proximity to veins	Brassy-yellow pyrite grains in a matrix of quartz and carbonate (Fig. 4.10g)
QCP2(11)	Quartz, carbonate, pyrite, minor chalcopyrite, gold	Sericite shears within veins, parallel to vein fabric	Brassy-yellow pyrite grains within a smoky quartz matrix (Fig. 4.10c) commonly associated with sericite halo
QCP3(12)	Quartz, carbonate, pyrite, chalcopyrite, gold	Chlorite, epidote replacement of carbonate	mm scale veins with brassy-yellow color (Fig. 4.10b)

include pyrite, chlorite, epidote, and sericite. Vein types include (QZ) Quartz vein, (QC) Quartz-carbonate vein, (QCC) Quartz-carbonate vein with chlorite alteration, (QCP) Quartz-carbonate-pyrite vein, (QCP2) quartz-carbonate-pyrite ± sericite shears veins, (QCP3) quartz-carbonate-chlorite-pyrite vein with epidote alteration, (CB) carbonate vein, (CH) carbonate vein with hematite alteration, (CCL) carbonate-chlorite vein, (ECL) Chlorite vein with epidote alteration, (SCL) sericite-chlorite vein, (QZ2) epidote vein.

QC and QCP veins are the most dominant veins at the Moss Lake Au deposit. QC veins are deformed, and the major vein infill is recrystallized quartz grains up to 0.5 mm across (Fig. 4.9a). They also comprise carbonate grains up to 0.3 mm across. Within some QC veins, carbonate grains are altered by epidote and chlorite, with sericite alteration present outside the veins or at contact with other veins. QC veins typically have alteration halos when they are at an angle to the fabric of the host rock (Fig. 4.9a).

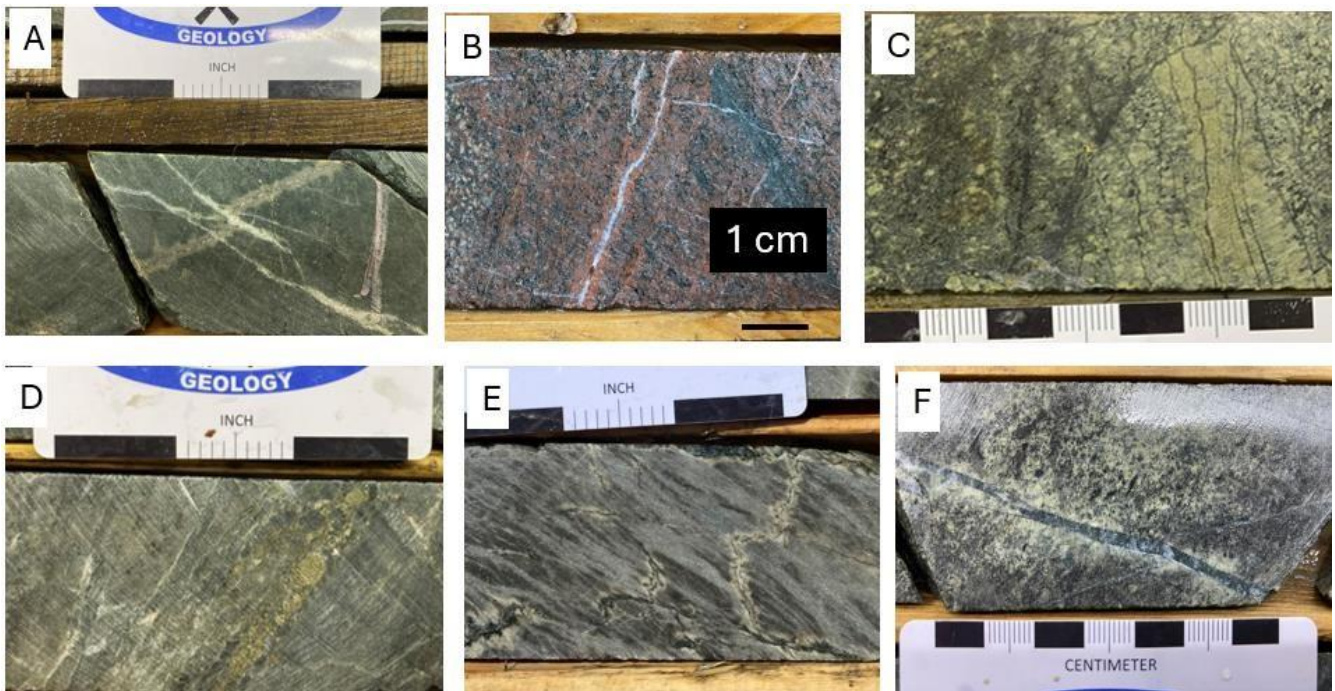


Fig. 4.10: Photographs of drill core sample of some vein types from the Moss Lake deposit and their relationship to the fabric of the host rock. A (ML23-NM-001) shows QC vein occurring at an angle to the fabric of the rock and cut by type CB, which is parallel to the fabric of the host rock, image B (ML23-NM-003) shows vein CH, image C (ML23-NM-035) shows vein QZ2, image D (ML23- NM- 010) shows vein QCP2, image E (ML23-NM-092) shows vein CCL and image F (ML23-NM-088) shows QCC vein with a sericite halo.

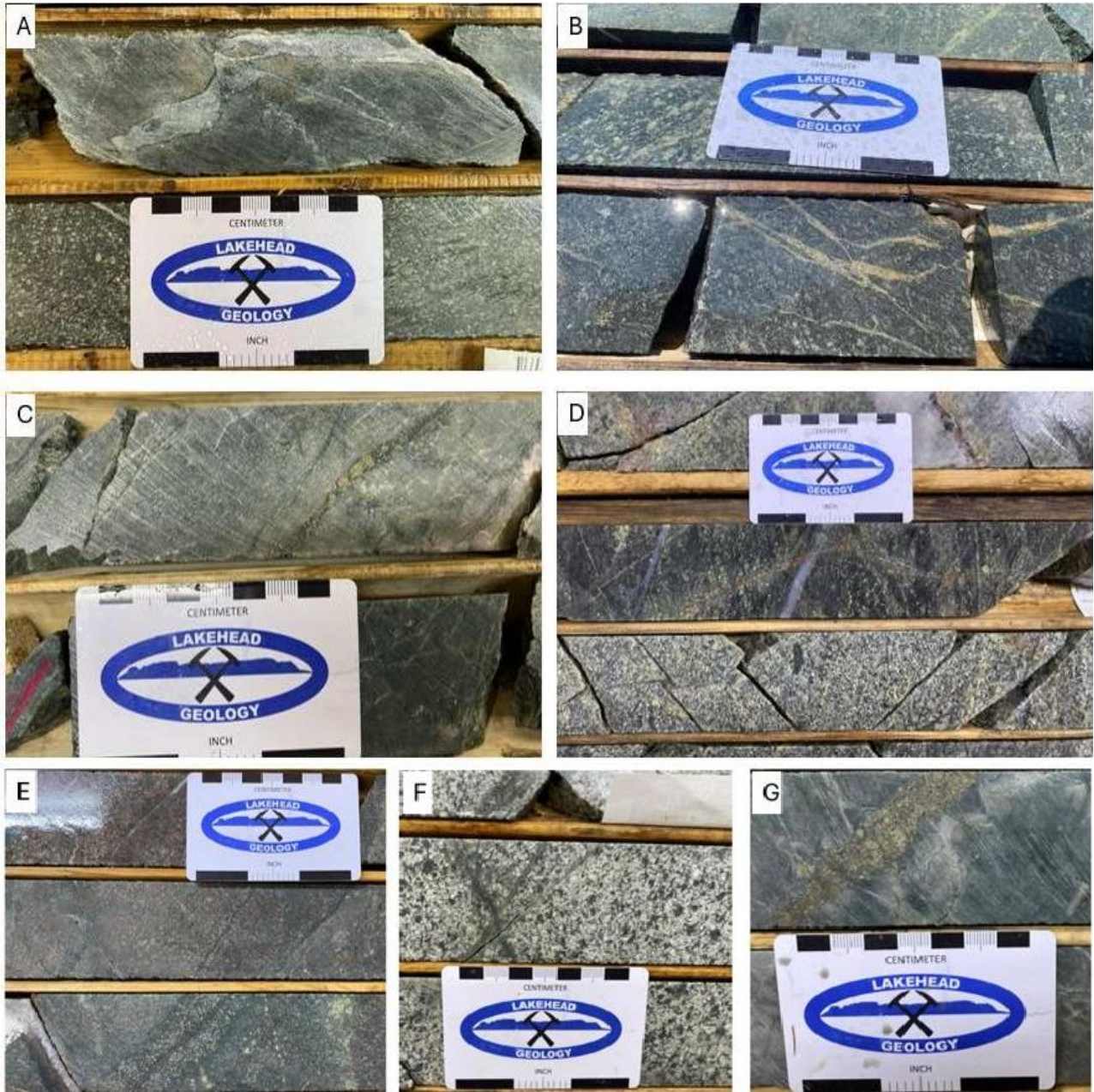


Fig. 4.11: Photographs of some major vein types at Moss Lake. Image A (ML23-NM-008) shows CB vein with chlorite alteration on the rims, image B (ML23-NM-097) is a QCP3 vein with epidote and chlorite alteration present within the vein, image C (ML23-NM-010) is a type QCP vein with sericite alteration present around the vein, the vein also contains traces of chalcopyrite and gold, image D (ML23-NM-085) is a QZ vein associated with epidote alteration on the rims of the vein, and cut by QZ2 veinlet. Image E (ML23-NM-005) and F (ML23-NM-089) are some of the less dominant vein types at Moss Lake, image E is ECL vein with a 1.5 cm epidote alteration halo around the vein, and F is a sample with two veins crosscutting, undulating SCL vein is cut across (MMD-22-070@628m) by a later ECL vein, image G (ML23-NM-033) shows QCP vein.

QCP veins at Moss Lake commonly contain trace amounts of sphalerite, chalcopyrite, and gold. The major vein infill is recrystallized quartz grains up to 0.4 mm. Carbonate grains within the veins are subhedral to anhedral and can be up to 0.8 mm, although commonly 0.5mm across (Fig. 4.10c). Pyrite grains are subhedral to euhedral and can be up to 1 mm across; they are commonly associated with minor chalcopyrite and sphalerite. QCP2 veins are similar to QCP but are associated with sericite alteration in very sheared host rocks (Fig. 4.9d). QCP3 veins are also similar to vein QCP but are associated with chlorite and epidote alteration (Fig. 4.10b).

QZ veins are also common at Moss Lake, the veins are deformed and are associated with QC and CB veins within some samples (Fig. 4.9d). QZ veins can be up to 1 mm wide, and recrystallized quartz grains are the major vein infill, they are up to up to 0.6 mm across. Within a few samples, QZ veins are associated with later chlorite and epidote alteration; Figure 4.10d shows QZ2 cut across vein QZ. This association of vein QZ with epidote alteration commonly occurs on the rim of the veins and within samples with a high intensity of chlorite and epidote alteration. CB veins are commonly associated with chlorite and, to a lesser degree, albite alteration (Fig. 4.9a); the veins are up to 0.8 mm wide, with carbonate grains up to 0.3 mm. CCL (Fig.4.9b) and CH (Fig. 4.9c) veins are varieties of CB veins that contain chlorite and albite alteration, respectively. Other veins observed at Moss Lake are moderately to strongly undulating and less common. These veins are usually narrower, up to 0.3 mm, and comprise fine-grained alteration minerals, they include SCL (Fig. 4.10f), QZ2 (Fig. 4.9c), and ECL veins (Fig. 4.10e).

4.1.7 Au Mineralization

Gold grains at the Moss Lake deposit are very fine-grained and difficult to observe and find in hand samples and microscope. By combining the microscope with the Scanning Electron Microscope (SEM), it was possible to observe the occurrence and textures of Au grains in thin sections. Gold grains within the Moss Lake deposit are strongly associated with pyrite, carbonate, and quartz. The grains are mostly subangular to subrounded and are commonly 2 to 20 micrometers across, with a few grains up to 45 micrometers (Fig. 4.11).

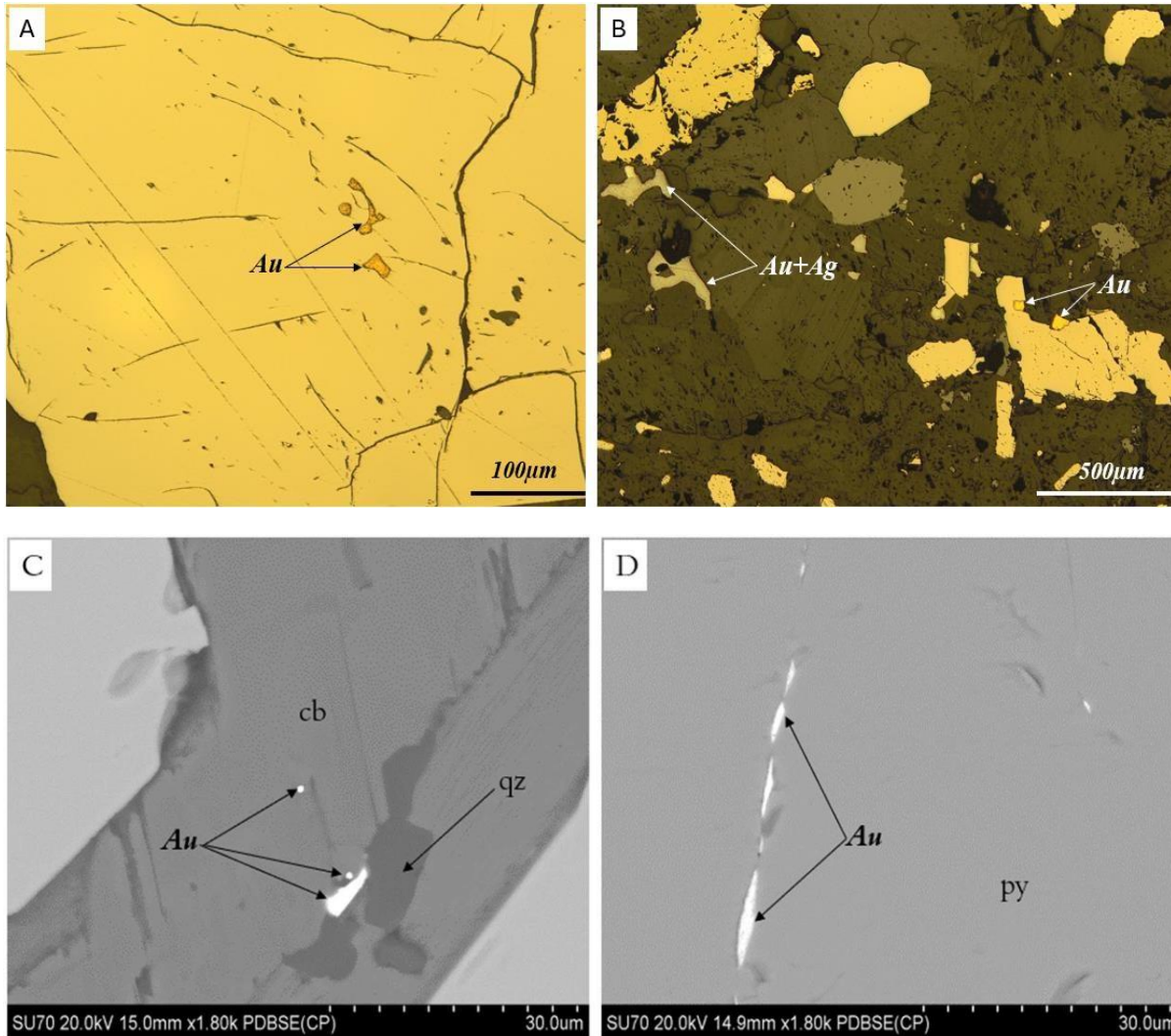


Fig. 4.12: Photomicrographs in reflected light showing Au grains within the Moss Lake deposit and the various textures and mineral associations in which they occur. A (ML23-NM-010) shows Au grains occurring within a pyrite grain, B (ML23-NM-046) shows Au grains occurring at the boundary of a pyrite grain and also an Au-bearing grain occurring away from pyrite grain, C (ML23- NM-074) shows Au grains occurring around calcite and quartz grains, and D (ML23-NM- 078) shows elongate Au grains exhibiting a pinch and swell texture within a pyrite grain.

Gold occurs in various textures at Moss Lake. In a few samples, the grains occur within pyrite grains (Fig. 4.11a), they were also observed on the boundary of pyrite grains (Fig. 4.11b), as well as away from pyrite grains within other minerals (Fig. 4.11c), mainly carbonate and quartz. Gold grains observed at Moss Lake dominantly occur within quartz, carbonate, and pyrite-bearing veins, such as QCP, QCP2 and QCP3 veins.

4.2 Re/Os Geochronology

Geochronological analysis was conducted to determine the age of the mineralizing event. Molybdenite was identified in sample E927263 from hole MMD-22-026 and was selected for Re/Os analysis. The sample is a smoky quartz-carbonate-pyrite vein that cuts across a dacitic volcanic wedge in the diorite complex; the quartz vein is associated with minor carbonate veinlets occurring dominantly at the vein rim (Fig. 4.12). Molybdenite hosted within the vein was dated, and the analysis suggests that the mineralizing event occurred at 2708 ± 12 Ma (Table 4.1).



Fig. 4.13: Drill core photo of sample E927263, black arrow shows type 3 vein from which molybdenite was analyzed.

Table 4.2: Re-Os isotopic and age data of molybdenite.

Sample	Re (ppm)	$\pm 2\sigma$	^{187}Re (ppm)	$\pm 2\sigma$	^{187}Os (ppb)	$\pm 2\sigma$	Modal age (Ma)	$\pm 2\sigma$ (with λ) Ma
MM22-026	281.6	0.8	177.0	0.5	8166	5	2708	12

4.3 Geochemistry and Spectral Data

4.3.1 Geochemistry

The geochemical results described here are from the 4-acid digest analyses conducted by Goldshore Resources on the drill cores prior to the commencement of this study. The data was provided for all 89 samples from the mineralized zone and consisted of major and minor elements (wt%), base metals, and a few trace elements (ppm); for clarity, the major elements described here have been converted to oxide wt%. The trace elements available in the database were insufficient for proper investigation of the trace element geochemistry, due to this limitation, it was mostly used to classify the host rocks into various geochemical compositions.

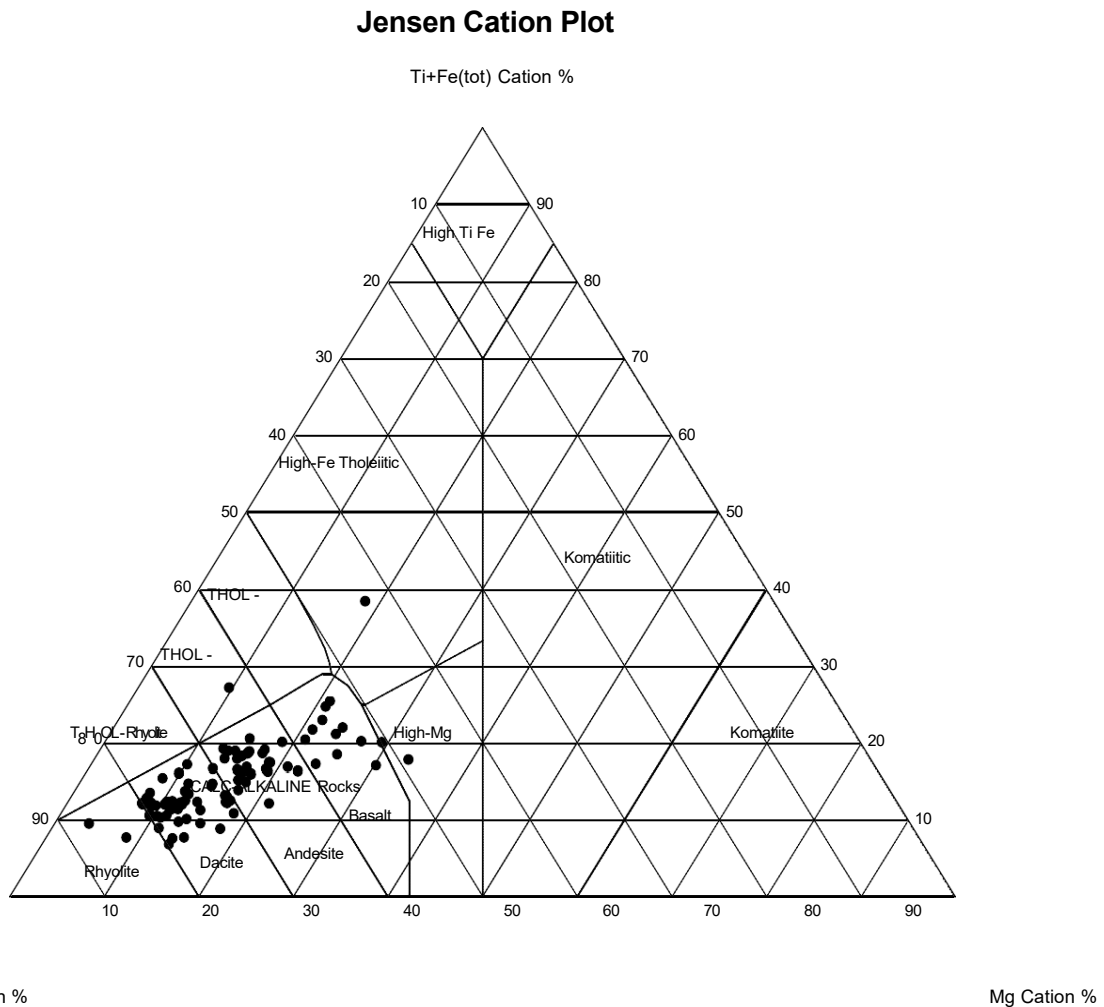


Fig. 4.14: Jensen Cation Plot showing the rock compositions of the Moss Deposit host rocks. The three main rock compositions are dacitic, andesitic, and basaltic.

Initial grouping of rock compositions based on geochemical data was done using the Jensen Cation plot, which showed that the host rocks in the study area fall into three main rock compositions with a few outliers (Fig. 4.13). The dominant rock compositions are dacitic, andesitic, and basaltic; among the outliers a total of six samples out of 89 plotted as rock types outside this range. Two samples plot as rhyolite and two as high-Mg tholeiitic basalt, one sample plot as tholeiitic dacite, and one as high-Fe tholeiitic basalt.

The most dominant rock composition based on the Jensen Cation Plot are dacites, with 45 samples of that composition. They are characterized by 0.9 to 2.9 wt.% MgO, 0.2 to 0.4 wt.% TiO₂, Sc content range from 4.0 to 12.5 ppm, Ni content range from 10.1 to 29.3 ppm, and Ti/Zr ratio from 10.7 to 48.1. The andesitic rocks are the second most abundant group by geochemistry, they are characterized by 2.02 to 4.37 wt.% MgO, 0.2 to 0.7 TiO₂, Sc content range from 8.0 to 18.6 ppm, Ni content from 11 to 43.7 ppm, and Ti/Zr ratio from 19.6 to 73.6. The basaltic rocks are characterized by 4.1 to 6.4 wt. % MgO, 0.4 to 0.7 wt.% TiO₂, Sc contents range from 15.8 to 27.2 ppm, Ni content from 16.4 to 199 ppm, and Ti/Zr ratio from 27.9 to 58.3. The two rhyolitic rocks are geochemically similar to the dacitic rocks, with the main difference being the lower MgO and Sc contents, which range between 0.4 to 1.1 wt% and 4.0 to 4.3 ppm, respectively. The two samples that plot as High-Mg tholeiitic basalt are geochemically similar to the samples with basaltic composition. The main distinguishing factor is the high MgO content of these samples, which ranges from 5.6 to 7.2 wt%.

4.3.2 Spectral data

Short-wave infrared analysis was conducted to determine the spectral features of chlorite and white mica at the Moss Lake deposit. The analysis was conducted on all 178 drill core samples, 89 samples from the mineralized zone and the other 89 from the NE zone, with the aim of investigating spectral characteristics in both chlorite and white micas within different zones of the deposit (Appendix III).

The data shows that the main spectral feature for white micas occurs between 2180 and 2228 nm wavelengths, which is the Al-OH absorption feature (Fig. 4.14). A total of 54 samples had no spectral feature for white mica, which suggests the absence of white mica alteration within these samples (Table 4.2). The exact position where the Al-OH absorption feature occurs is used to estimate what type of white mica occurs within the sample. The different ranges represent different white mica types or compositions: 2180 to 2190 nm (paragonitic white mica), 2190 to 2200 nm (mixed paragonitic and muscovitic white mica), 2200 to 2208 nm (muscovitic white mica), 2208 to 2216 nm (mixed muscovitic and phengitic white mica), 2216 to 2228 nm (phengitic white mica). The dominant white mica type among all the samples analyzed is a mix of muscovitic and phengitic white mica, which occurs within 82 samples. There were no spectra indicating the presence of paragonitic white mica.

Table 4.3: Distribution of different white mica types based on the wavelength of Al-OH absorption spectral feature.

Wavelength (nm)	Count	White mica type	Crystallinity	
			<1	>1
2180-2190	0	paragonitic	n.a	n.a
2190-2200	2	Mix (paragonitic + muscovitic)	2	0
2200-2208	36	Muscovitic	7	29
2208-2216	82	Mix (muscovitic + phengitic)	31	51
2216-2228	4	Phengitic	3	1
No white mica	54	n.a	n.a	n.a

Another important spectral feature in white micas is the H₂O absorption feature, which occurs around 1900 nm. The reflectance of this spectral feature is used to estimate the crystallinity of illite and white micas (Table 4.2). The crystallinity estimate is derived by dividing the depth of the Al-OH absorption feature by the depth of the H₂O absorption feature. The crystallinity estimates for each white mica type, reported as <1 or >1, which implies poorly

crystalline (lower temperatures) and highly crystalline (higher temperatures), are reported in Table 4.2. The crystallinity values range from 0.15 to 6.08.

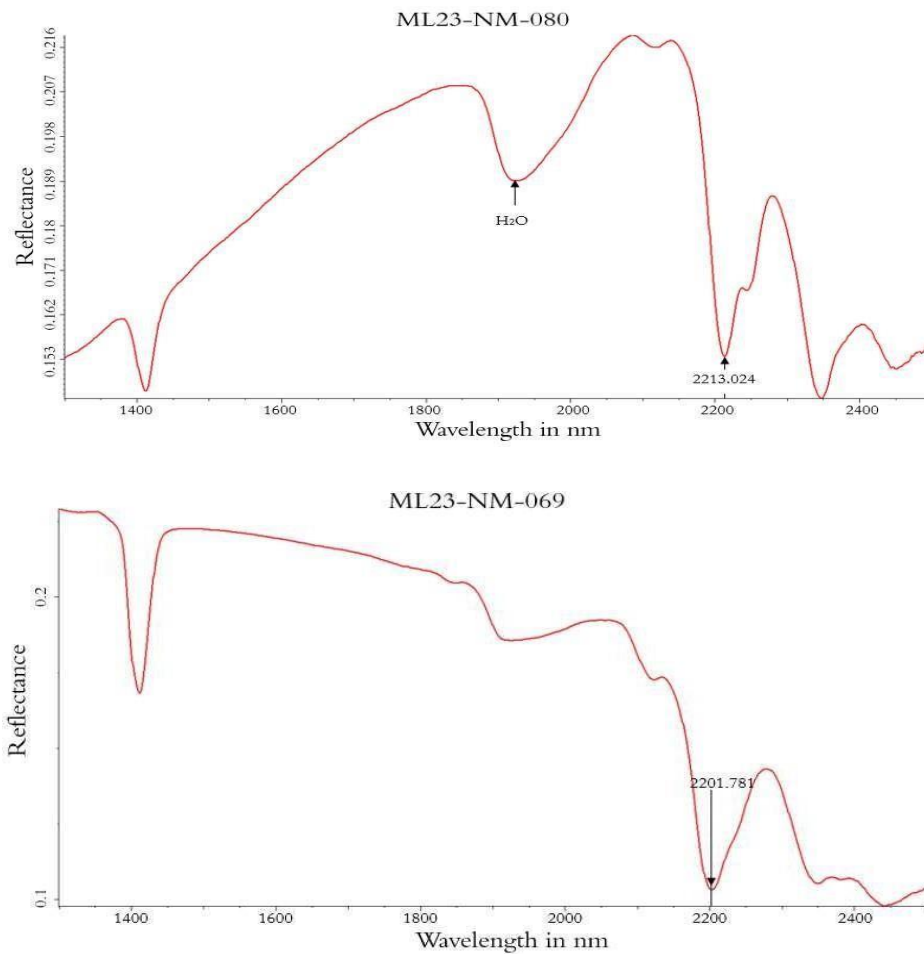


Fig. 4.15: White mica spectrum showing the position H₂O absorption features and the values of the Al-OH absorption feature. Sample ML23-NM-080 has an Al-OH absorption feature corresponding to a mixed composition of muscovite and phengite, and sample ML23-NM-069 has a pure muscovite spectral feature.

For chlorites, there are two important spectral features that are useful in identifying the different types; they occur around 2250 nm and 2340 nm and represent the Fe-OH and Mg-OH absorption features, respectively. Due to a stronger Fe-OH absorption feature than Mg-OH observed during the spectral interpretation and the influence other minerals can have on the Mg-OH absorption feature, the results reported are based on the chlorite Fe-OH absorption feature (Table 4.3).

Table 4.4: Distribution of different chlorite types based on the wavelength Fe-OH absorption feature

Wavelength (nm)	Count	Chlorite type
<2249	55	Mg chlorite
2250-2254	73	Mg-Fe chlorite
2254-2256	3	Fe-Mg chlorite
>2256	1	Fe chlorite
No chlorite	46	n.a

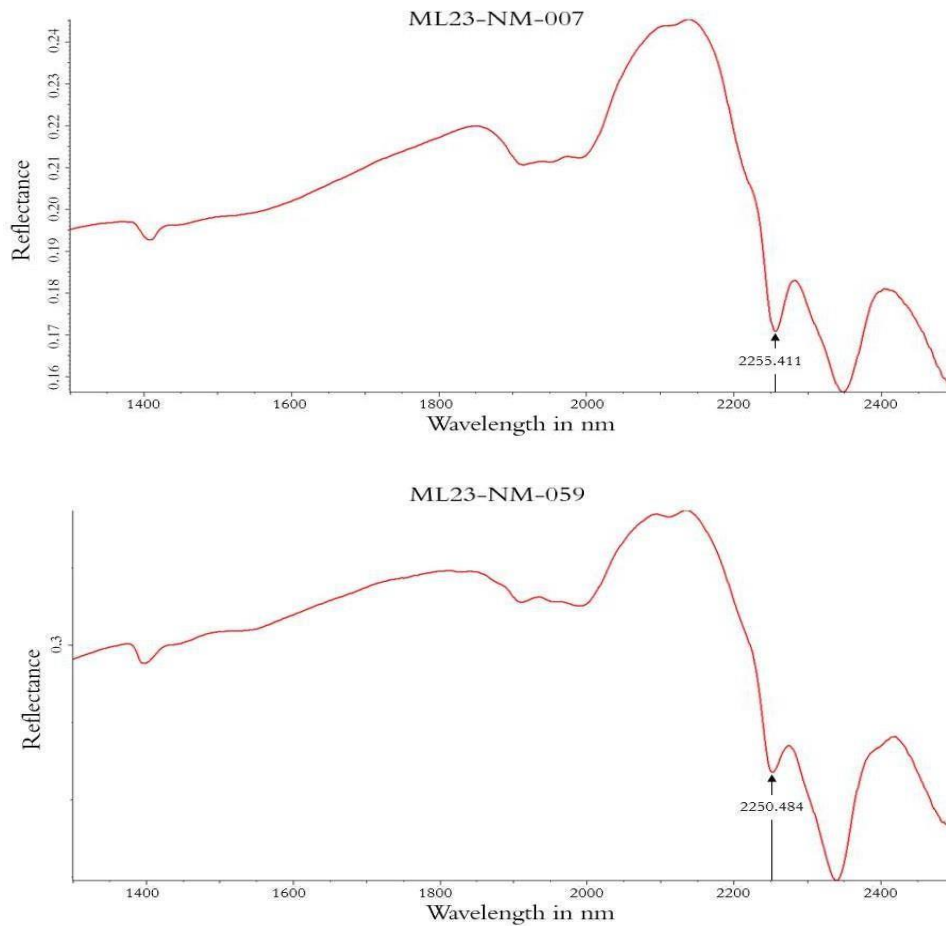


Fig. 4.16: Chlorite spectrum showing the position of the Fe-OH absorption feature. Sample ML23-NM-007 shows a sample with a Fe-OH absorption feature position corresponding with the Fe-Mg chlorite type, whereas sample ML23-NM-059 shows another sample with the Mg-Fe chlorite type.

A total of 46 samples had no spectral features for chlorite, implying the absence of chlorite alteration within these samples. The exact positions of the Fe-OH feature can be used to estimate the type of chlorite mineral present in a sample, based on their Fe or Mg abundance (Fig. 4.15). The different types by Fe-OH feature positions (nm) include >2249 (Mg-chlorite), 2250 to 2254 nm (Mg-Fe-chlorite), 2254 to 2256 (Fe-Mg-chlorite), and >2256 (Fe-chlorite). Based on the Fe- OH feature, most of the samples analyzed fall between 2240 and 2254 nm, corresponding to Mg and Mg-Fe chlorite. The most common chlorite type is the Mg-Fe chlorite, which is present in 73 samples.

In a number of samples, both white mica and chlorite spectral features were observed to occur together. Whole rock geochemical data of these samples shows that they are mostly intermediate in composition. On the Jensen Cation plot, the alteration mineralogy (defined by the spectral features) appears to be influenced by the composition of the parent rock. White mica alteration is dominantly present within rocks of rhyolitic to dacitic composition, whereas chlorite dominantly plots within rocks of andesitic to basaltic composition (Fig. 4.16).

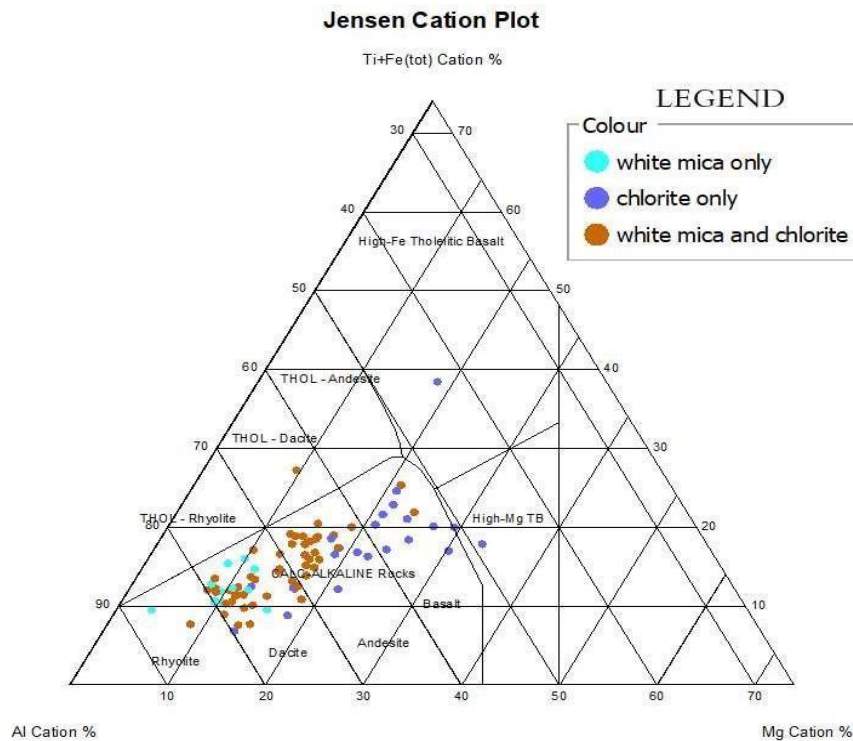


Fig. 4.17: Jensen Cation plot showing the distribution of rocks altered by white mica and chlorite (based on SWIR data) among the different host rock compositions.

4.4 Mineral Chemistry

Mineral chemistry analysis was conducted on white mica and chlorite grains from selected samples. The sample selection for white mica and chlorite Electron Probe Microanalysis (EPMA) from the various drill holes was spaced to cover different ranges of proximity to high Au assay values (Fig. 4.17). The analyses yielded major and minor element compositions for white mica and chlorite and are reported in Tables 4.4 and 4.5.

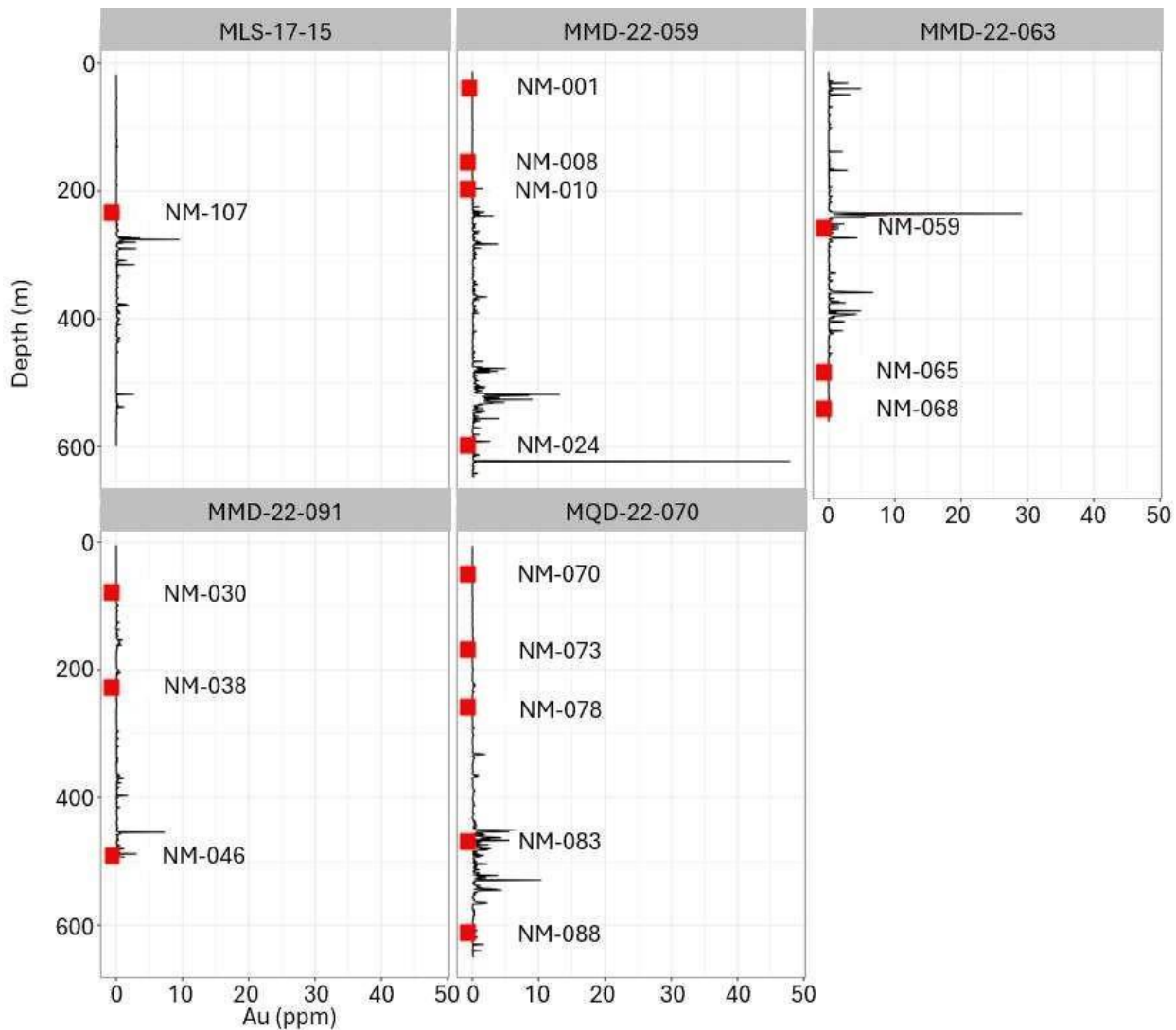


Fig. 4.18: Downhole plots showing the distribution of samples selected for EPMA analysis. The plots illustrate the depths of samples collected with respect to the downhole variations in Au (ppm) concentration in the sampled drill holes

Table 4.5: Sample mean values of EPMA analysis of white mica grains from Moss Lake Au deposit. The table shows the weight percent of major and minor oxides and the structural formulae of chlorites in APFU, calculated using 11 oxygen atoms.

Sample No.	NM-073	NM-046	NM-068	NM-107	NM-001	NM-008	NM-010	NM-078	NM-083	NM-038	NM-030	NM-065	NM-070
Hole ID	MQD-22-070	MMD-22-091	MMD-22-063	MLS-17-015	MMD-22-059	MMD-22-059	MMD-22-059	MQD-22-070	MQD-22-070	MMD-22-091	MMD-22-091	MMD-22-063	MQD-22-070
SiO ₂	46.16	46.97	45.98	45.69	49.48	46.37	47.49	48.04	47.65	46.89	47.06	47.70	46.37
ZrO ₂	0.00	0.00	0.00	0.05	0.00	0.03	0.00	0.23	0.04	0.03	0.00	0.00	0.11
TiO ₂	0.45	0.31	0.29	0.55	0.20	0.27	0.39	0.22	0.23	0.24	0.39	0.08	0.27
Al ₂ O ₃	33.36	33.14	34.97	32.76	33.14	34.40	34.11	30.59	31.45	31.70	32.81	32.91	34.13
Cr ₂ O ₃	0.09	0.07	0.09	0.03	0.02	0.06	0.02	0.02	0.04	0.03	0.04	0.02	0.03
FeO	3.89	2.41	3.23	4.57	2.42	3.33	2.29	3.85	3.23	3.87	3.21	3.19	3.53
MnO	0.00	0.05	0.03	0.04	0.03	0.03	0.02	0.04	0.04	0.00	0.03	0.03	0.03
MgO	1.34	2.37	1.09	1.49	0.97	1.27	1.91	2.17	2.63	1.81	1.57	1.32	1.00
CaO	0.17	0.17	0.06	0.03	0.14	0.04	0.03	0.18	0.03	0.03	0.02	0.04	0.06
Na ₂ O	0.69	0.27	0.57	0.32	1.45	0.34	0.37	1.15	0.39	0.34	0.33	0.39	0.47
K ₂ O	10.47	10.83	10.63	10.95	9.39	10.67	10.81	10.09	10.54	10.98	10.52	10.36	10.37
Cl	0.00	0.02	0.02	0.05	0.06	0.02	0.06	0.00	0.02	0.03	0.01	0.02	0.00
F	0.00	0.00	0.00	0.00	0.00	0.00	0.00	0.00	0.00	0.00	0.00	0.00	0.00
Total	92.73	96.60	96.95	96.46	97.24	96.81	97.44	96.58	96.28	95.92	95.99	96.04	96.37
Atom Per Formula Unit (APFU) based on 11 oxygen atoms													
Si	3.08	3.11	3.05	3.25	3.21	3.07	3.11	3.33	3.18	3.15	3.14	3.17	3.09
Ti	0.02	0.02	0.01	0.02	0.01	0.01	0.02	0.01	0.01	0.01	0.02	0.00	0.01
Al	2.63	2.59	2.73	2.39	2.56	2.69	2.63	2.27	2.47	2.51	2.58	2.58	2.68
Fe ²⁺	0.22	0.13	0.18	0.21	0.13	0.18	0.13	0.19	0.18	0.22	0.18	0.18	0.20
Mn	0.00	0.00	0.00	0.00	0.00	0.00	0.00	0.00	0.00	0.00	0.00	0.00	0.00
Mg	0.13	0.23	0.11	0.12	0.09	0.13	0.19	0.19	0.26	0.18	0.16	0.13	0.10
Ca	0.01	0.01	0.00	0.00	0.01	0.00	0.00	0.01	0.00	0.00	0.00	0.00	0.00
Na	0.09	0.03	0.07	0.04	0.22	0.04	0.05	0.13	0.05	0.04	0.04	0.05	0.06
K	0.89	0.92	0.90	1.01	0.77	0.90	0.90	0.93	0.90	0.94	0.90	0.88	0.88
Cr	0.00	0.00	0.00	0.00	0.00	0.00	0.00	0.00	0.00	0.00	0.00	0.00	0.00
Cl	0.00	0.00	0.00	0.00	0.00	0.00	0.00	0.00	0.00	0.00	0.00	0.00	0.00
Total	7.07	7.05	7.06	7.06	7.00	7.04	7.03	7.06	7.05	7.07	7.02	7.00	7.03

Table 4.6: Sample mean values of EPMA analysis of chlorite grains from Moss Lake Au deposit. The table shows the weight percent of major and minor oxides and the structural formulae of chlorites in APFU, calculated using 28 oxygen atoms, and the calculated temperatures based on De Caritat et al. (1993) (TDC1993) and El Sharkawy (2000) (TES2000).

Sample No.	NM 024	NM 038	NM 059	NM 088	MOSS 10	NM 001	NM 073	NM 046	NM 068	NM 107
Hole ID	MMD-22-059	MMD-22-091	MMD-22-063	MQD-22-070	OUTCROP	MMD-22-059	MQD-22-070	MMD-22-091	MMD-22-063	MLS-17-015
SiO ₂	29.46	28.29	28.55	27.60	26.14	25.65	26.80	28.90	25.83	28.17
Al ₂ O ₃	19.95	21.82	21.29	22.83	23.02	23.73	23.19	22.05	24.37	19.48
FeO	17.76	17.66	17.64	15.46	22.51	22.04	20.56	12.13	22.06	21.81
MnO	0.19	0.12	0.22	0.27	0.11	0.23	0.23	0.29	0.31	0.91
MgO	21.75	21.24	21.49	22.23	16.68	16.60	17.94	24.66	16.56	17.65
Na ₂ O	0.01	0.01	0.03	0.04	0.04	0.01	0.03	0.00	0.01	0.04
K ₂ O	0.14	0.06	0.04	0.04	0.06	0.04	0.04	0.05	0.04	0.06
TiO ₂	0.02	0.03	0.04	0.05	0.06	0.06	0.07	0.07	0.06	0.01
Cr ₂ O ₃	0.27	0.01	0.08	0.01	0.01	0.04	0.04	0.02	0.01	0.01
CaO	0.06	0.03	0.11	0.04	0.05	0.06	0.02	0.25	0.03	0.11
Total	89.62	89.29	89.48	88.56	88.68	88.46	88.91	88.44	89.27	88.23
Atom Per Formula Unit (APFU) on the basis of 28 oxygen atoms										
Si	5.79	5.57	5.73	5.43	5.33	5.24	5.38	5.63	5.28	5.77
Ti	0.00	0.01	0.05	0.01	0.01	0.01	0.01	0.01	0.01	0.00
Al	4.61	5.06	4.73	5.29	5.53	5.71	5.49	4.64	5.75	4.70
Cr	0.04	0.00	0.02	0.00	0.00	0.01	0.01	0.00	0.00	0.00
Fe ³⁺	0.12	0.12	0.13	0.08	0.11	0.11	0.15	0.17	0.17	0.13
Fe ²⁺	2.80	2.79	2.80	2.46	3.73	3.64	3.30	1.87	3.49	3.61
Mn	0.03	0.02	0.04	0.04	0.02	0.04	0.04	0.04	0.05	0.16
Mg	6.36	6.23	6.13	6.52	5.07	5.05	5.37	6.56	4.91	5.38
Ca	0.01	0.01	0.03	0.01	0.01	0.01	0.01	0.78	0.02	0.02
Na	0.01	0.02	0.03	0.04	0.04	0.02	0.03	0.12	0.09	0.04
K	0.07	0.03	0.20	0.02	0.03	0.02	0.02	0.34	0.02	0.03
Total	19.86	19.86	19.90	19.91	19.88	19.86	19.81	20.18	19.80	19.85
Geothermometry										
TDC1993 (°C)	269	278	281	285	275	281	264	272	273	266
TES2000 (°C)	235	258	253	277	272	283	270	265	285	227

A total of 13 major and minor elements and oxides were analyzed for the white mica chemical analysis; the results show that the white micas at Moss Lake are characterized by 45.6 to 49.4 wt % SiO₂, 30.6 to 34.9 wt % Al₂O₃, 2.3 to 4.5 wt % FeO, 0.9 to 2.6 wt% MgO, and 0.1 to 0.5 wt % TiO₂. A total of 10 major and minor oxides were analyzed for chlorite chemical analysis. The chlorites at Moss Lake are characterized by 25.6 to 29.4 wt % SiO₂, 19.5 to 24.3 wt% Al₂O₃, 12.1 to 22.5 wt% FeO, 16.5 to 24.6 wt% MgO, and very low TiO₂ content ranging from 0.01 to 0.07 wt %. Major and minor element compositions for both white mica and chlorite were used to recalculate the structural formulae in atoms per formula unit (APFU). APFU calculations were based on 11 and 28 oxygen atoms for white mica and chlorite, respectively (Tables 4.4 and 4.5). White mica chemistry was used to confirm the type of mica that occurs at the Moss Lake Au deposit and to investigate any chemical changes in white mica with increasing proximity to Au mineralization.

The sample averages for white mica composition were plotted on the Tischendorf et al. (2007) mica classification diagram, which is a common technique for classifying white mica based on the EPMA dataset. The diagram plots FeAl, which is $[(Fe_{tot} + Mn + Ti) - ^{IV}Al]$ on the y-axis versus MgLi (Mg - Li) on the x-axis (Fig. 4.18). Due to the absence of Li analysis in the white mica chemistry data, Mg (apfu) was used on the MgLi axis to classify the white mica type, under the assumption that Li is zero. On the mica classification diagram, all the data points plot within the muscovite field (Fig. 4.18).

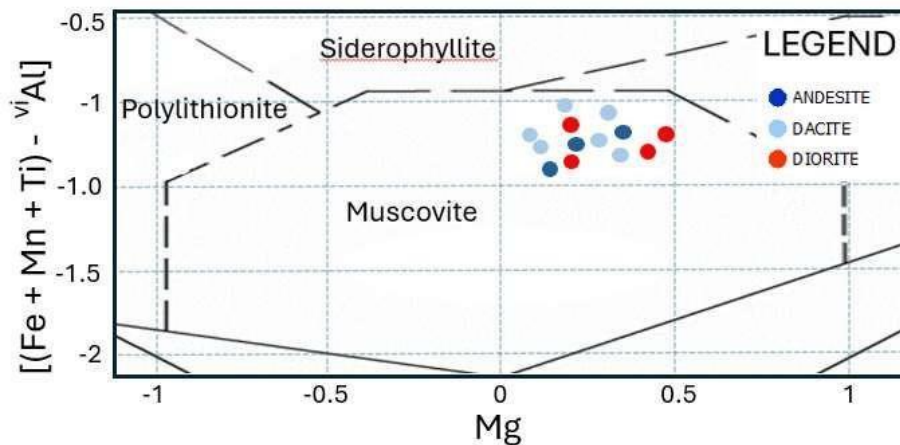


Fig. 4.19: Mica classification diagram showing that all the samples analyzed are muscovitic white mica. The points are colored by the host rock type (Tischendorf et al., 2007)

Based on the Si, Fe, and Mg (APFU) content of the chlorite, the classification diagram of Hey (1956) was used to classify the chlorites (Fig 4.19); the diagram shows that chlorites at Moss Lake are mostly sheridanite and clinochlore, which are Mg-dominant chlorite species.

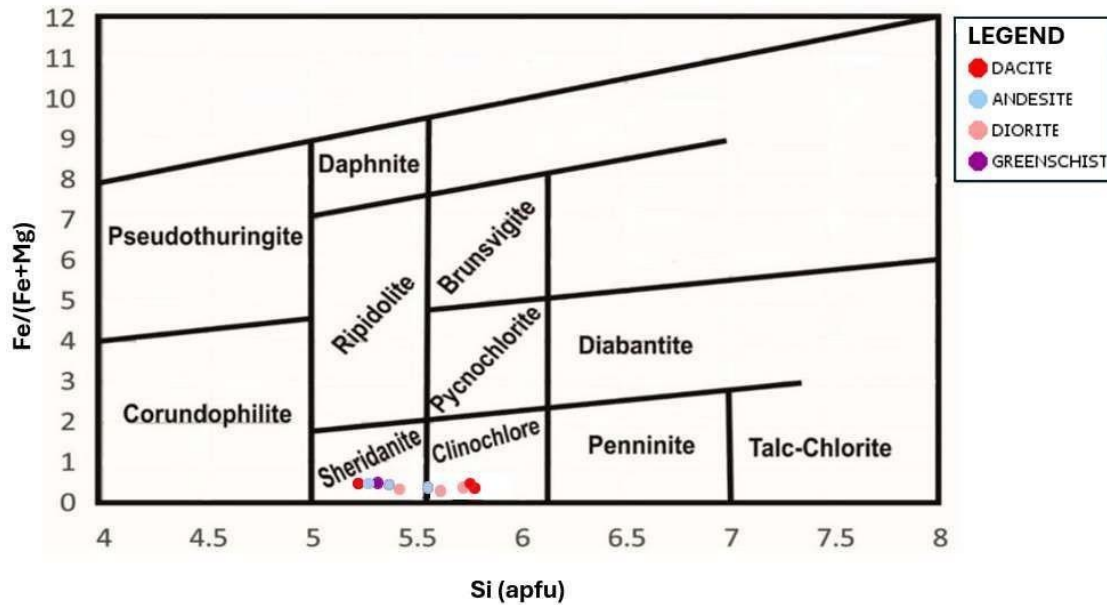


Fig. 4.20: Chlorite classification diagram showing the different species of chlorite that occur at the Moss Lake deposit (modified from Hey, 1956).

Chapter 5: Discussion

5.1 Age constraints on Au mineralization

A Re/Os date (2708 ± 12 Ma) was acquired during this study from the analysis of molybdenite within a quartz-carbonate \pm pyrite vein in the mineralized zone. This date is inferred to be the age for the Au mineralization event at Moss Lake based on the association of molybdenite with pyrite, which in turn is strongly associated with observed gold occurrences (Fig. 4.6). A compilation of previous ages (Corfu, 1986; 1998; 2000; Hart, 2007) from the Shebandowan greenstone belt yielded a total of 36 ages from volcanic and intrusive rocks across the greenstone belt (Fig. 5.1). There are two peak periods of rock formation within the belt, with most of the ages falling around an older age of ~ 2723 Ma and a younger age of ~ 2695 Ma. The older ages include rock from the central felsic-intermediate metavolcanic belt (CFB), whereas the younger ages include some of the intrusive rocks (Corfu, 1998).

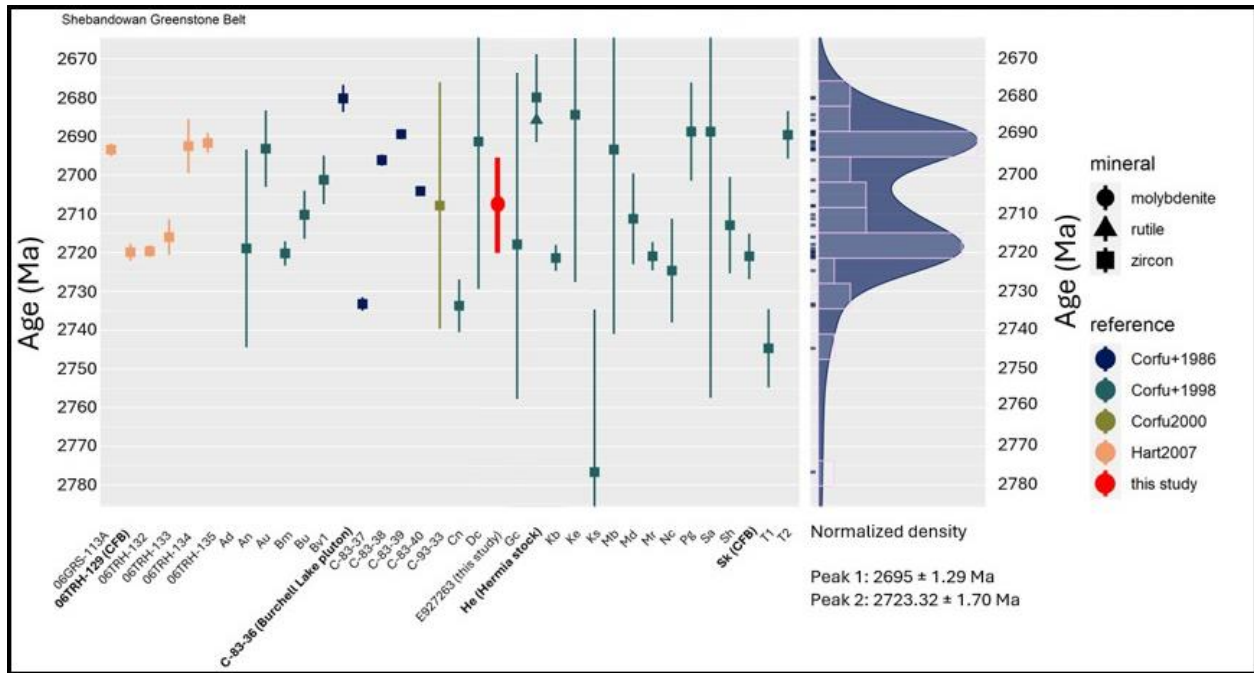


Fig. 5.1: Age distribution within the Shebandowan Greenstone Belt. The diagram shows the distribution of 36 ages determined for the rocks in the vicinity of the Moss Lake deposit; the normalized density chart shows the age range with the highest density, which is inferred to be the peak age of magmatic activity. The Re/Os age (2708 ± 12 Ma) for the gold mineralization within the Moss Lake deposit is highlighted by the bold red line.

South of the study area, within the Hamlin-Wye Lake area, Hart (2007) dated a volcanic rock of the CFB. The age (2720 ± 2 Ma) is around the older peak of published ages in the belt. This date is from a unit proximal to the Moss Lake deposit, and the dated rocks are of the same volcanic package as the Moss Lake host rocks. Similarly, to the east of the study area, a massive felsic flow within the CFB yielded an age of 2721 ± 6 Ma (Corfu, 1998); this is the most proximal date to the Moss Lake deposit and is considered in this study as the age of the host rocks. This age is close to the age determined by Hart (2007) in the southwest of the CFB and also corresponds with the older peak ages within the belt (Fig. 5.1). Although there are numerous dates for the metavolcanic rocks of the Shebandowan Greenstone Belt, the 2721 ± 4 Ma age (Corfu, 1998), from the Skimpole Lake area is taken as the age of the host rocks based on their proximity to the study area (Fig. 5.2).

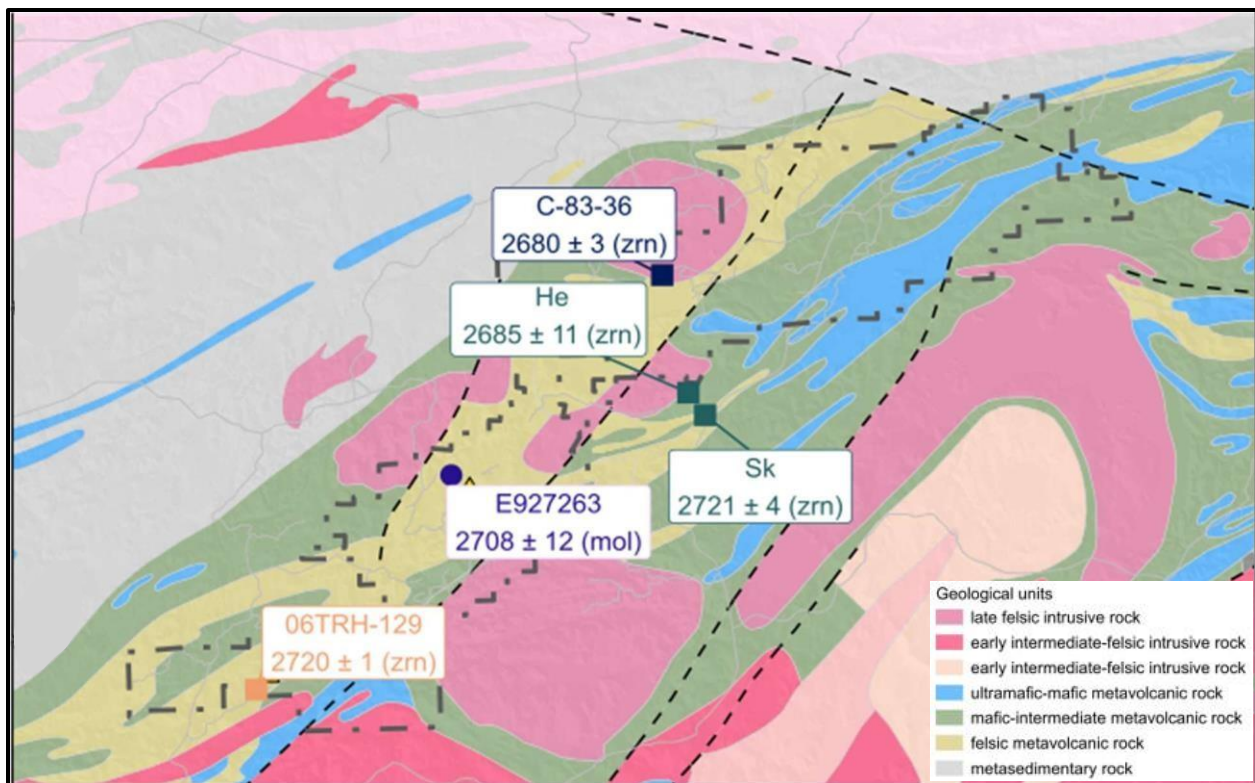


Fig. 5.2: Geological map showing the published ages of rocks in proximity to the Moss Lake deposit and age of gold mineralization obtained during this study (E927263). Sample 06TRH-129 and Sk are from volcanic rocks within the CFB, whereas samples C-83-36 and He are from the Burchell Lake and Hermia plutons, respectively, which are later intrusive rocks (modified from Goldshore Resources 2022).

The 2708 ± 12 Ma age for gold mineralization suggests that gold deposition occurred after the first magmatic event but prior to the second magmatic event. This age is within error of the ages of the host rocks. The CFB and the other metavolcanic belts of the Shebandowan Greenstone Belt are intruded by late felsic to plutons. The Burchell Lake pluton, which is located northeast of the Moss Lake deposit (Fig. 5.2), intrudes into the CFB. The pluton was dated by Corfu (1983) and yielded a zircon U/Pb age of 2680 ± 2 Ma. The Hermia stock, which is located south of the Burchell Lake pluton, also yielded a zircon U/Pb age of 2680 ± 11 Ma (Corfu, 1998). The late pluton within the vicinity of the Moss Lake deposit are also younger than the gold mineralization event (2708 ± 12 Ma), this implies that gold mineralization took place before the onset of the second magmatic event in the Shebandowan Greenstone Belt. Hence, gold mineralization is unrelated to the second magmatic event. There is no published date for the regional greenschist facies metamorphism within the Shebandowan Greenstone Belt, but due to the relatively undeformed state of the younger intrusive rocks (~ 2680 Ma), it is suggested that metamorphism took place between the two peaks of magmatic activity ($\sim 2720 - 2680$ Ma).

Overall, the two age groups determined for rocks in the vicinity of the Moss Lake deposit are (a) Older rocks (2715-2727 Ma; Corfu, 1998; Hart, 2007) and (b) younger intrusions (2657-2703 Ma; Corfu, 1983; Corfu, 1998), they represent two periods of magmatic activity. This is supported by the normalized density plot of all 36 published dates within the Shebandowan greenstone belt, which also indicates two peaks of age population (Fig. 5.1), an older peak (2723 ± 1.70 Ma), which comprises mainly ages from the metavolcanic rocks and a younger peak (2695 ± 1.3 Ma) representing the ages from felsic to mafic intrusive rocks. Gold mineralization took place after the older rocks were emplaced, but before the emplacement of the late plutons.

5.2 Paragenesis and gold occurrences

5.2.1 Paragenesis of the Moss Lake Deposit

Based on petrographic analysis, the rocks within the study area are composed of plagioclase and quartz, with minor amounts of amphibole, biotite, sulfides, and alteration assemblages. In this study the rocks have been classified based on the varying proportions of quartz, plagioclase, and amphibole, as well as their textural characteristics. They commonly comprise 15 – 40 % quartz, 30 – 70 % plagioclase, and 0 – 10 % amphibole, forming a range of rock types, including diorites, dacites, and andesites. This corresponds with previous work by Harris (1970), who described the rocks within the study area as mainly dacitic tuff, with other rocks such as diorite, andesite, and dacitic porphyries occurring in lesser abundance. All samples studied from both the mineralized and the northeast zones are petrographically similar, suggesting that they are an extension of the same suite of rocks to the northeast along the regional NE-SW strike (Osmani, 1997).

The veins and alteration at Moss Lake are strongly associated; carbonate, chlorite, sericite, and epidote alteration occur within many veins, either as major infills or as a replacement of the major vein infills. They also occur within the host rocks, replacing primary minerals, commonly plagioclase, and primary amphibole. Biotite occurs as a minor alteration phase in a few samples; it is rarely associated with veins, and when observed, it occurs as relict crystals that are strongly replaced by chlorite and sericite. Albite alteration is observed mostly as reddish coloration in hand samples and as Na enrichment in plagioclase. Biotite and albite are the least abundant alteration minerals and show the least relationship with other alteration minerals.

The sequence of alteration, determined based on the overprinting relationship, shows that the earliest phases of alteration were biotite, albite, and quartz, followed by sericite. Secondary quartz mostly occurs as veins or in proximity to veins and less as pervasive silicification. Sericite alteration occurs commonly as a replacement of plagioclase and is a dominant phase in the samples that display a high degree of shearing (Fig. 5.3a). Sericite

alteration is persistent through most of the samples observed and appears to be the most common alteration phase at the Moss Deposit.

Carbonate alteration is dominantly vein-related and replaces sericite alteration in a few samples. Precipitation of carbonate minerals suggests the introduction of CO₂-rich fluids into the host rocks (Lowenstern, 2001). Carbonate alteration is replaced by later phases which include chlorite and epidote (Fig 5.3b). Chlorite alteration replaces carbonates within veins as well as pervasive grains of carbonates (Fig. 5.3d), and chlorite also replaces sericite grains (Fig. 5.3c).

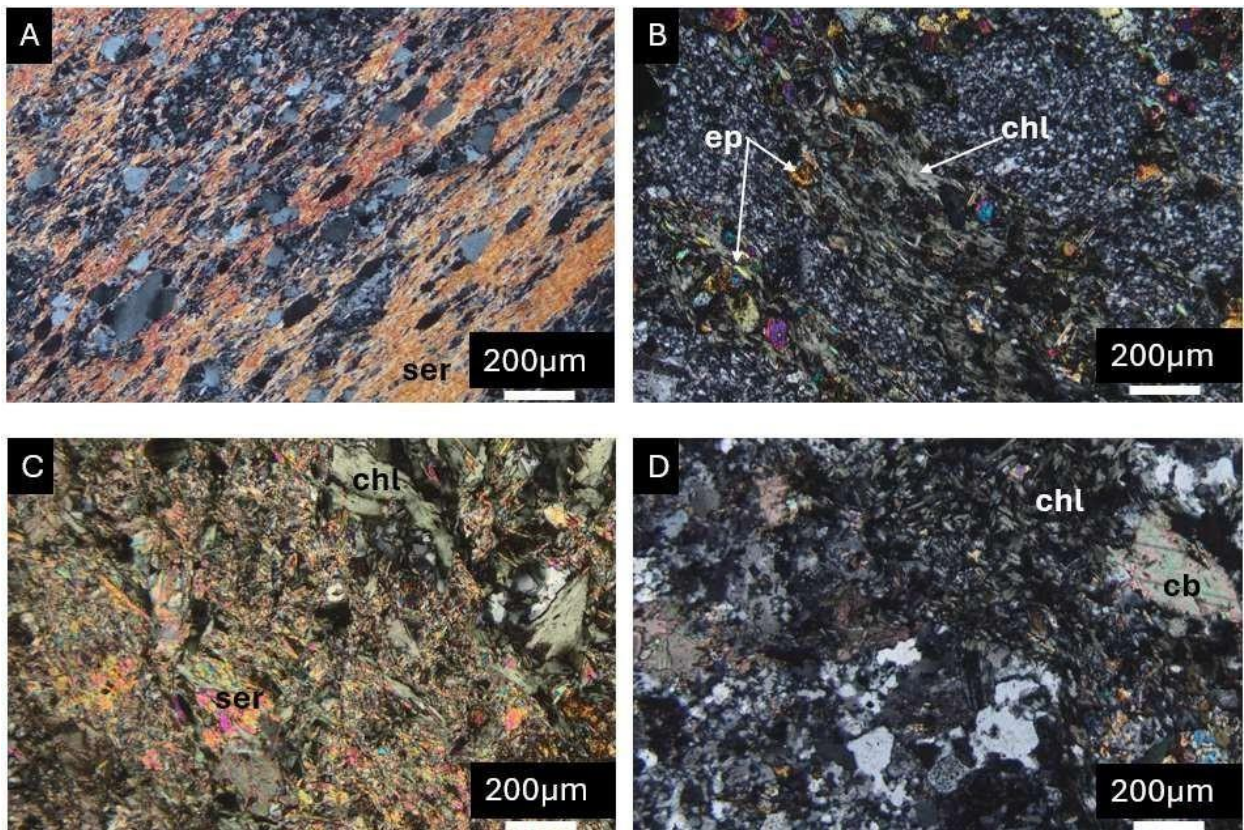


Fig 5.3: Photomicrographs under cross-polarized light of alteration assemblages and their overprinting relationship. Image A (ML23-NM-092) shows sericite-dominated lineation, which overprints other mineral within the sample except quartz; image B (ML23-NM-055) shows epidote crystals replacing chlorite; image C (ML23-NM-024) shows chlorite replacing sericite grains within a sericite-dominated sample, and image D (ML23-NM-070) shows the replacement of carbonate by chlorite within the host rock.

The occurrence of chlorite alteration is inferred to be earlier than epidote alteration, based on epidote replacement of chlorite grains in the few samples where they occur together (Fig. 5.3 b).

Characterizing the full paragenetic sequence of events at Moss Lake host required that all 12 vein types observed be considered with respect to their major infills and associated alteration minerals. Each vein type has been compared with others, and their crosscutting relationships have been considered in generating a paragenetic sequence. Quartz and carbonate are the most prevalent vein minerals, occurring together in 5 out of 12 vein types.

QZ veins are the earliest veins observed, and they are cut by most vein types. Quartz grains within all vein types are characterized by subgrain features, such as bulging grains and subgrain boundaries (Fig. 5.4a). These features imply that the grain has undergone dynamic recrystallization due to stress and elevated temperature during metamorphism (Stipp et al., 2002). The bulging features are stable around 250 to 400 °C (Stipp et al., 2002), which falls within the range of lower greenschist facies metamorphism. Later generations of QZ veins have been observed in a few samples cutting across earlier QZ veins (Fig 5.4b). QC veins are slightly younger than QZ veins, and they are cut by QCP3 and CB (Fig. 5.4c). The major infill is carbonate and quartz, and they are common within the host rocks. Vein type QCC is similar to vein QC, and are QC veins with chlorite alteration replacing carbonate grains.

QCP veins are more common in zones with higher gold occurrences; the major infills include quartz, carbonate, and pyrite. They are cut by vein CB and SCL; they cut vein CB (Fig. 5.4f), suggesting that they may be coeval. Pyrite within vein type 3 is associated with trace amounts of chalcopyrite, sphalerite, and gold. Re/Os age for the gold mineralization was acquired from molybdenite associated with QCP vein. Gold in QCP vein is associated mainly with pyrite. Gold is also associated with carbonate and quartz. Vein QCP2 and QCP3 are like vein QCP in terms of the 3 major infills. Vein QCP2 is associated with sericite alteration, which replaces carbonate grains and exhibits a linear texture around the veins (Fig. 5.3a). This linear texture of sericite is consistent with the deformation textures observed within the belt by Williams et al. (1991), who described the shear zones as dominated by shallow-plunging lineation.

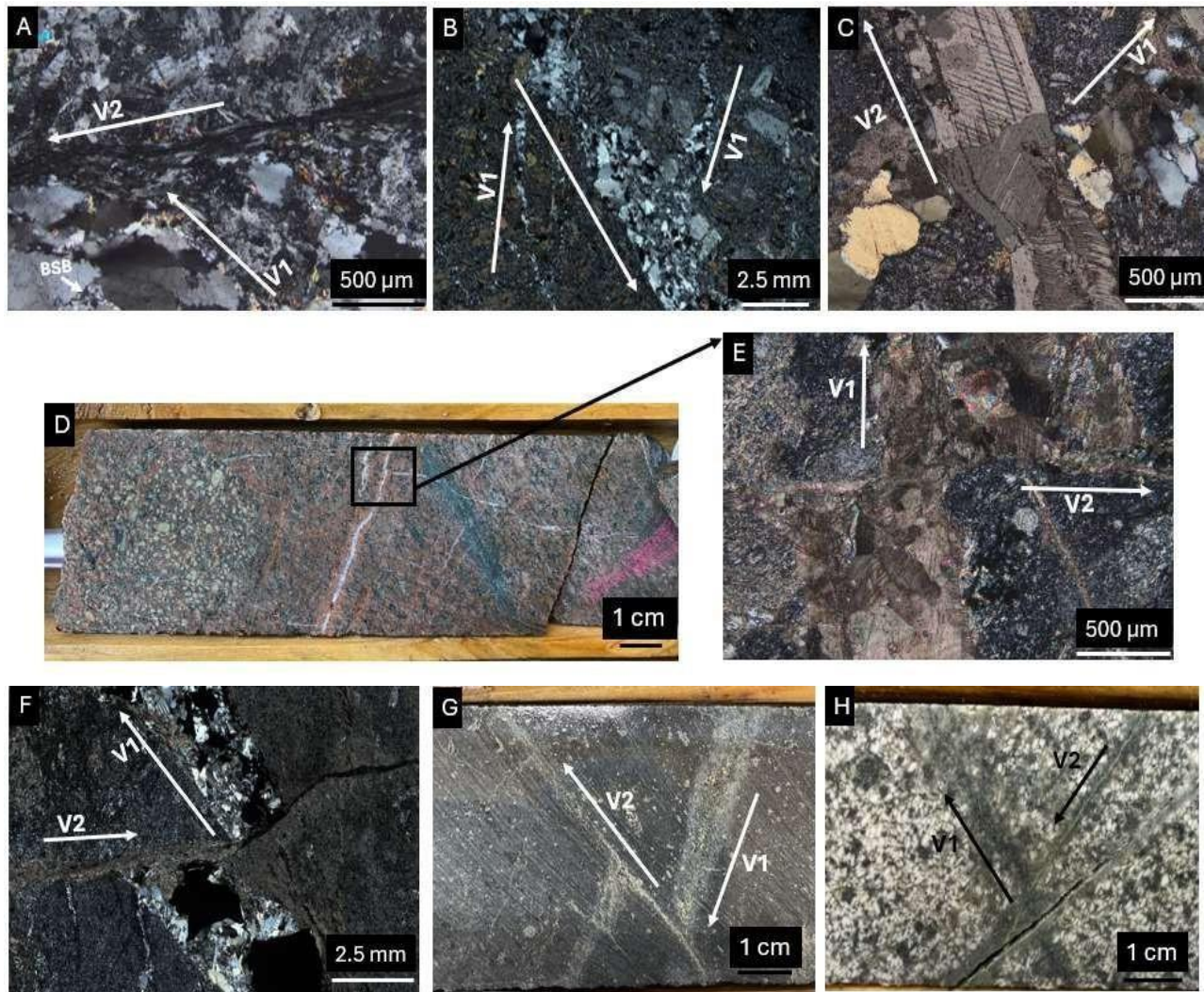


Fig. 5.4: Photomicrographs and hand sample images of some vein types, their crosscutting relationships, and textural features of infills. Image A (ML23-NM-023) shows QZ vein (v1) being cut by SCL vein (v2), quartz grains within v1 exhibit bulging subgrain boundary (BSB) typical of deformed quartz, image B (ML23-NM-025) shows the crosscutting relationship between two generations of QZ vein, image C (ML23-NM-001) shows vein QC (v1) being cut by vein CB (v2), image D (ML23-NM-003) shows the pinkish-red halo resulting from albitization of plagioclase, image E which is a zoom in on image D shows that the coloration only affected vein CH (v1), which is then cut by a later uncolored vein CB (v2) image F (ML23-NM-068) shows vein QCP (v1) being cut by vein CB (v2), image G (ML23-NM-074) shows a later vein QCP3 (v2) cutting an earlier one (v1), and image H (ML23-NM-089) shows vein ECL (v1) being cut by vein SCL (v2).

At Moss Lake, the lineation is sericite-dominated, and gold occurrences were observed within vein QCP2 associated with these features. Vein QCP3 differs from vein type 3 in that they are associated with chlorite and epidote alteration. Chlorite alteration replaces carbonates in the veins, and they are subsequently replaced by epidote alteration. At least two generations of vein QCP3 are observed in the rocks, and they cut one another (Fig. 5.3g); both generations are associated with gold mineralization and differ in terms of their alignment with the fabric of the host rocks.

CB veins are the most common vein type; they are among the early veins at Moss Lake and are cut by veins QZ, QC, QCP, QCP2, QCP3. CB veins also cut across CH, which are similar, but have a darker tint (Fig. 5.4e); in hand sample, vein CH is associated with a pinkish-red halo (Fig. 5.4d). This coloration is a product of the albitization of plagioclase, which can precipitate very fine hematite (Engvik et al., 2008). CCL veins are similar to vein CB, but some of the carbonate grains within them have been replaced by chlorite. They are common in the diorite units and broadly coeval with CB veins.

ECL veins are more common in the diorite samples, and the major infill is chlorite and epidote. Epidote occurs as a later phase, replacing chlorite grains within this vein type. Only a few crosscutting relationships were observed due to the paucity of vein ECL; but they cut vein SCL (Fig. 5.4h). Vein SCL is filled with sericite and chlorite and occurs mostly as an undulating veinlet; they are sericite-dominated, with chlorite replacing some of the sericite grains. Sericite-infilled veins are commonly surrounded by elongated sericite and chlorite grains. This fabric is typical around the contacts of diorite and dacite host rocks and is supporting evidence for the presence of a shear zone at Moss Lake. Vein QZ2 is the least abundant among the veins observed at Moss Lake; the major infill is quartz and epidote, and the quartz grains are strongly deformed than QZ veins.

Early phases of sulfides observed at Moss Lake comprise disseminated pyrite occurring pervasively within the host rock; most of the early pyrite occurrences are associated with chlorite and quartz. Pyrite, however, dominantly occurs within veins and is the most common

sulfide mineral at Moss Lake. They are closely associated with chalcopyrite within and in proximity to veins.

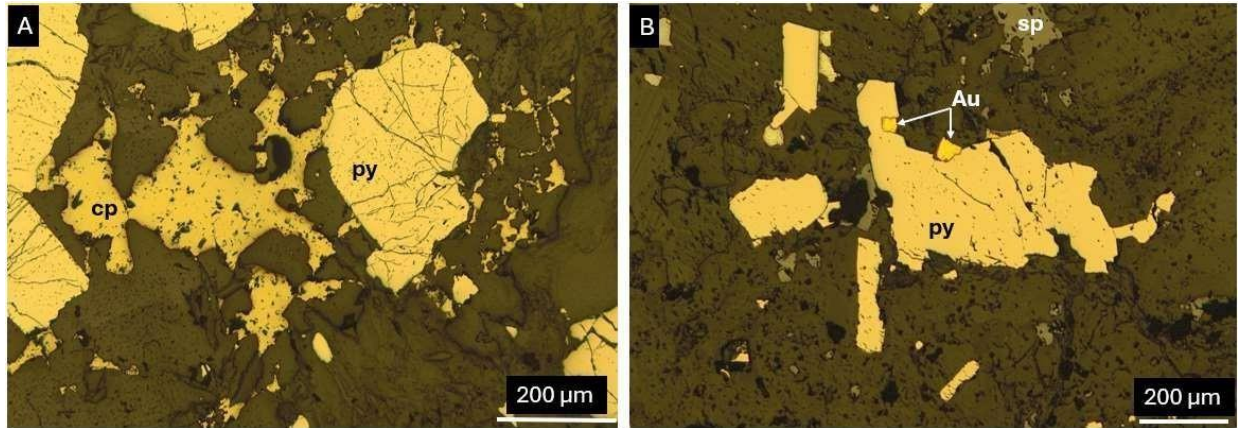


Fig. 5.5: Photomicrographs in reflected light of ore minerals association from a paragenetic standpoint. Image A (ML23-NM-010) shows the association of pyrite and chalcopyrite, where anhedral chalcopyrite is growing around pyrite grain boundaries, and image B (ML23-NM-046) shows one of the associations of pyrite and gold, with gold occurring at the pyrite grain boundary, it also shows subhedral sphalerite occurring in proximity to pyrite.

Based on the textural relationship, chalcopyrite is slightly later than pyrite in the paragenetic sequence and coeval with sphalerite (Fig. 5.5a). Pyrite is strongly associated with gold; the association is common within veins QCP, QCP2, QCP3. Within vein QCP2, the occurrence of gold on the pyrite grain boundary indicates that gold mobilization was effective after deposition, and based on this, gold is placed slightly later in the paragenetic sequence of ore minerals (Fig. 5.5b).

The paragenetic sequence of the Moss Lake deposit has been summarized in Figure 5.6; including alteration minerals, veins, and ore minerals. It has been broken into early, intermediate, and late stages. The early phase is dominated by quartz, albite, biotite, and sericite alteration, which are affected by the deformation (Fig. 5.4a). This deformation fabric persists throughout the paragenetic sequence as it also affects later phases. Studies have shown that the deformation within the study area occurred in two stages (D1 and D2), with D2 overprinting D1 (Corfu & Stott, 1986). Carbonate alteration is early to intermediate as it is a long-lived phase that forms multiple veins. It is strongly associated with pyrite and quartz and forms gold-bearing veins. Chlorite occurs in the intermediate stage and resurges in the later

phase in association with epidote, chlorite, and epidote replaces many earlier phases; chlorite replaces biotite, sericite, and carbonate, whereas epidote replaces chlorite and plagioclase. Earlier veins are dominated by quartz and carbonate, whereas later veins are dominated by epidote and chlorite. Gold is observed in veins QCP, QCP2, and QCP3, which are in the intermediate stage of the sequence; gold grains show a strong association with quartz, carbonate, and pyrite.



Fig. 5.6: Paragenesis of the Moss Lake deposit highlighting the sequence of alteration, veins, and mineralization; the dotted lines show the uncertainty in the positions. Sequence is divided into three stages early, intermediate, and late.

5.2.2 Sulfide and gold

Sulfide and gold are strongly associated at Moss Lake. Pyrite is the dominant sulfide phase, and the majority of the observed gold occurrences are within or proximal to pyrite grains. A total of six occurrences of gold were found within the samples (Fig. 5.7). They include (1) hosted in a dacite unit associated with vein QCP, where the gold occurs at a pyrite-chalcopyrite grain contact (Fig. 5.7a); (2) hosted in massive pyrite associated with vein QCP, where the gold occurs as inclusions within pyrite grain (Fig. 5.7b); (3) hosted in a deformed diorite unit associated with vein QCP2, where the gold occurs on the pyrite-sphalerite grain contact, associated with carbonate (Fig. 5.7c); (4) hosted in an andesite unit associated with vein QCP3, where the gold occurs at the contact of epidote and quartz in proximity to pyrite grains (Fig. 5.7d); (5) hosted in a diorite unit associated with vein QCP3, where the gold occurs on a pyrite-carbonate-quartz grain contact (Fig. 5.7e); (6) hosted in quartz associated with vein QC, where the gold occurs as an inclusion in quartz in proximity to vein QC (Fig. 5.7f).

The mineral most commonly associated with gold is pyrite, and based on their textural relationship, the gold occurrences were grouped into three styles, they include (1) gold as inclusions (Fig. 5.7b), (2) gold at the grain boundary (Fig. 5.7e), (3) gold grains occurring within gangue minerals in proximity to pyrite grains (Fig. 5.7d). The gangue minerals associated with gold occurrences include quartz, carbonate, sericite, epidote, and epidote. These three styles of gold occurrences can be linked to the deformation history of pyrite, as gold can be mobilized outwards from within pyrite grains through deformation-induced substructures (Dubosq et al., 2017). Hence, gold inclusions within pyrite could be the least mobilized grains, and gold grains on the pyrite grain boundary represent grains mobilized only to the edge of their host grain, whereas gold occurrence in gangue minerals represents the most mobilized grains that have been moved away from the host mineral. The fact that gold occurrence is related to pyrite suggests that gold enrichment at Moss Lake is coeval with deformation.

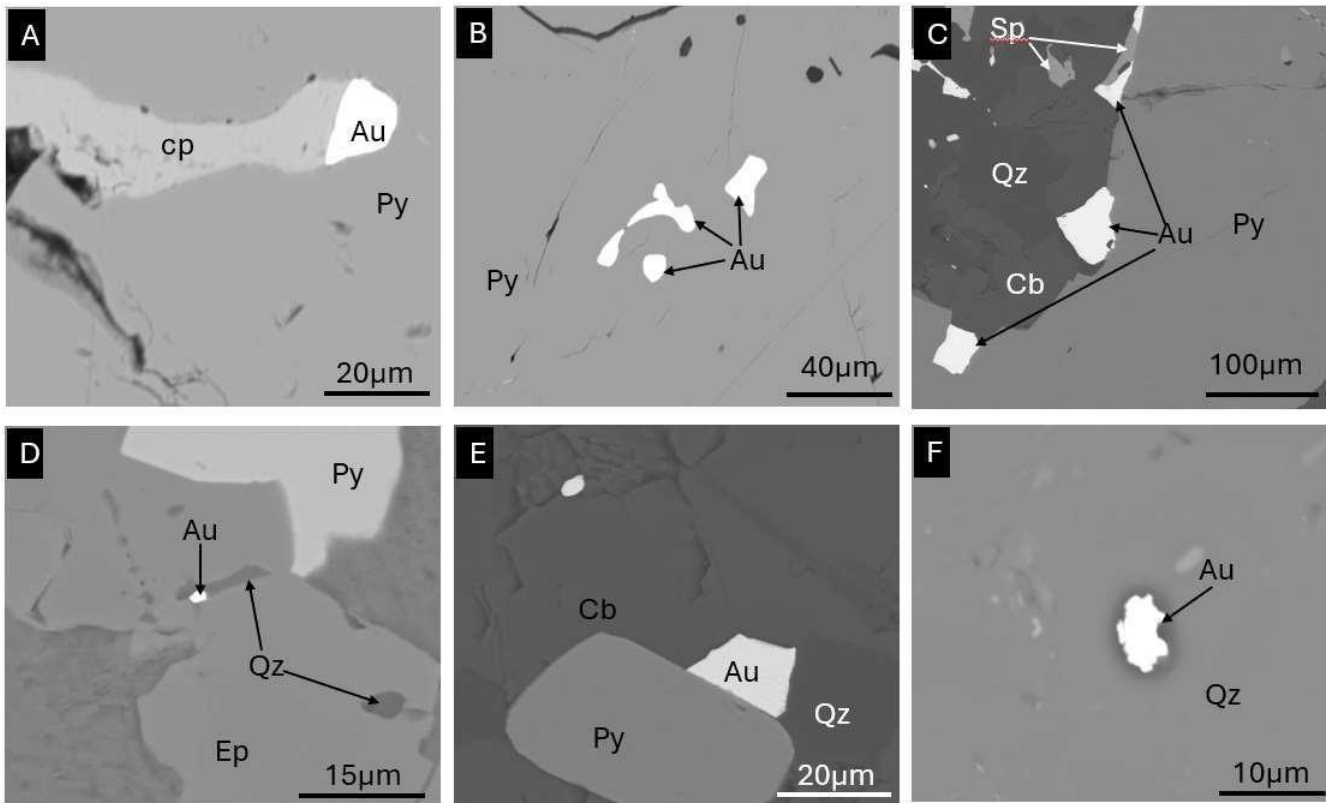


Fig. 5.7: SEM-BSE images of gold occurrences at Moss Lake Deposit and their associated minerals. Image A (ML23-NM-010) shows an occurrence of gold at chalcopyrite-pyrite grain contact, image B (ML23-NM-010) shows gold grains occurring as inclusions in pyrite, image C (ML23-NM-046) shows gold grains occurring at pyrite grain boundary in contact with sphalerite, quartz and carbonate, image D (ML23-NM-074) shows gold at the contact of two gangue minerals (epidote and quartz) in proximity to pyrite, image E (ML23-NM-046) shows gold occurring at pyrite-carbonate-quartz grain contact, and image F (ML23-NM-003) shows gold occurring as inclusion within quartz.

Gold was observed in all rock types at Moss Lake, but mostly within the diorite units and with only a few occurrences in the andesite units. Based on the assay values, within mineralized zones of individual drill holes, there are some barren sections within the same rock type as well as through different rock types (Fig. 4.16), suggesting that there are certain controls of gold localization. One such controls is veining, gold mineralization is localized in zones where the veining is dominant. The occurrence of quartz-carbonate-pyrite veining is a localizing factor for gold deposition. The most favorable vein types, which are strongly associated with gold, are pyrite-bearing QCP, QCP2, and QCP3 veins; vein QC is also associated with gold but only rarely.

Vein QCP2 and QCP3 are more likely to host gold when they are wider up to 0.5cm and associated with intense alteration. Vein QCP2 is also associated with strongly aligned sericite grains, and the vein is aligned parallel to the fabric of the surrounding alteration. Osmani (1997) reported that gold occurrences in the Moss Lake area are associated with rock units along a northeast-striking shear zone. Hence, this observed mineral alignment, which also affects the infills of vein QCP2, suggests that the vein occurs within a shear zone (Fig. 5.8). Shear zones are paths of high permeability and can facilitate the flow of mineralizing fluids (Alsop, 2004). The observation implies that gold mineralization at Moss Lake can be linked to the presence of shear zones, and these shear zones may represent fluid pathways.

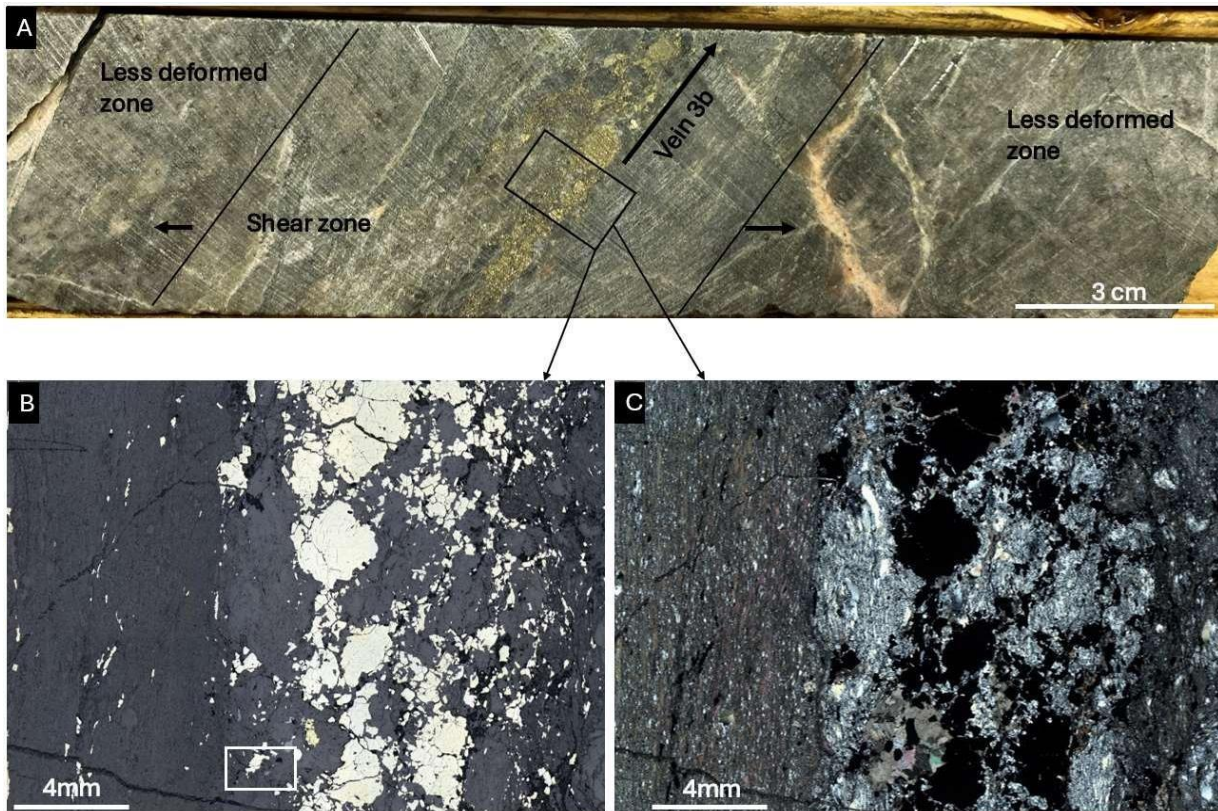


Fig. 5.8: Ductile deformation at Moss Lake and associated gold occurrences. Photographic image A from sample ML23-NM-046 shows an 8 cm wide shear zone @493.9m in drill hole MMD-22-091 occurring between two zones of less deformed rock. Vein QCP2 occurs within the shear zone and is parallel to the shear fabric. Image B is the reflected light image of vein QCP2, showing how the sulfides have responded to the ductile deformation by fracturing, and image C is the cross-polarized light image of the shear zone, showing how the alteration and vein minerals have been aligned to the fabric of the shear zone. The white box in Figure 5.8b represents the gold occurrence shown in Figure 5.7c.

5.3 Alteration and Mineralization

Alteration at Moss Lake comprises a variety of minerals, occurring in varying degrees of intensity, from the least-altered rocks with 5 – 15 % alteration minerals to strongly altered rocks with 45 - 60 % alteration minerals (Fig. 5.9a). They tend to occur in three main styles of alteration: the localized replacement of plagioclase and amphibole along cleavage planes and grain boundaries, pervasive alteration of discrete mineral grains within the host rock, and veins or replacement of vein infills. The alteration minerals include albite, sericite, calcite, epidote, and chlorite. Minor amounts of biotite were also observed but have been pervasively replaced by chlorite. Alteration is somewhat controlled by rock type, as chlorite and epidote are more dominant within the dioritic host rocks, whereas sericite and calcite are more dominant within the dacitic host rocks. In some samples, there appears to be strong lineation with a consistent orientation, suggesting the presence of a shear zone. Alteration within the shear zone occurs at a greater intensity from 50 – 60 % and is dominated by sericite and chlorite (Fig. 5.3a). Sericite and chlorite, which dominate the shear zones, are also the most widespread alteration phases observed in general within the samples.

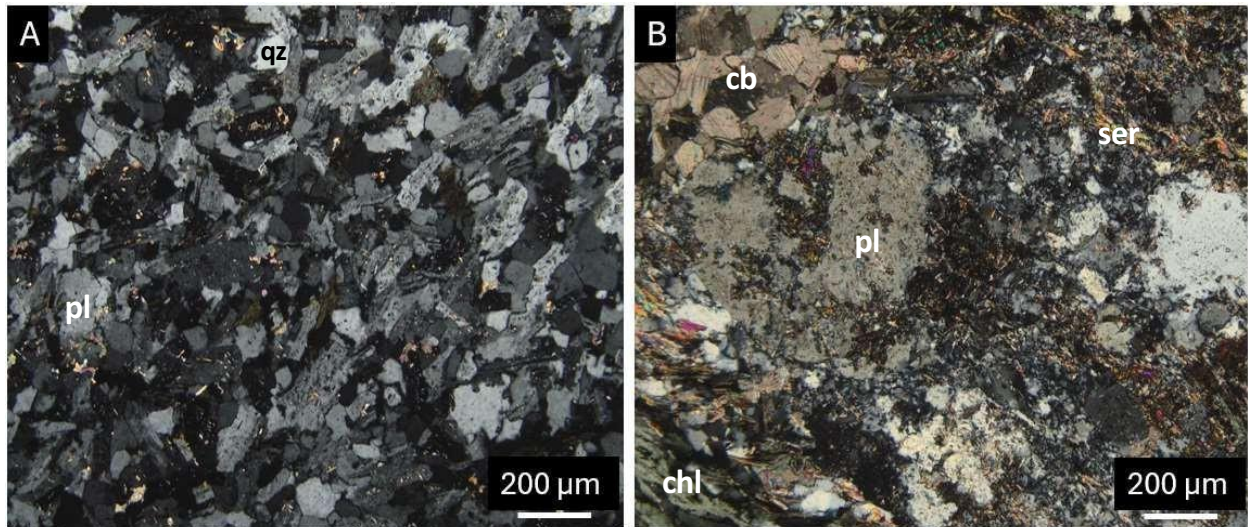


Fig. 5.9: Photomicrographs in cross-polarized transmitted light showing different degrees of alteration at Moss Lake. Image A (ML23-NM-026) is of a weakly altered fine-grained diorite, and image B (ML23-NM-016) shows a strongly altered fine-grained dacite.

Within the samples, the distribution of alteration minerals is widespread, but appears to be controlled by certain features, such as structures and rock types. For example, carbonate alteration is the most dominant phase within the veins, sericite, and chlorite are the most dominant pervasive alteration phase, albite alteration is localized to plagioclase grains, while epidote alteration is dominant within the dioritic host rocks. To investigate the controls of alteration, SWIR alteration data was compared with the geochemical composition of the host rock. Using SWIR data, the rocks were classified into three groups, based on the most dominant alteration phases: white mica only, chlorite only, and mixed white mica and chlorite samples. Due to the altered state of the host rocks, the plot of Sc vs. Mg was used to show the compositional changes in the host rocks. Scandium content can be used to classify altered rocks as a result of being relatively resistant to hydrothermal alteration and its correlation with the silicate-hosted component of Fe (Halley, 2020); this implies that Sc preferentially incorporates into mafic Fe-bearing silicates such as amphibole, rather than felsic silicates, such as plagioclase. The Sc vs. Mg plot groups the rocks into felsic and intermediate compositions, this was compared with the dominant alteration phase to observe for controls of rock composition on alteration (Fig. 5.10).

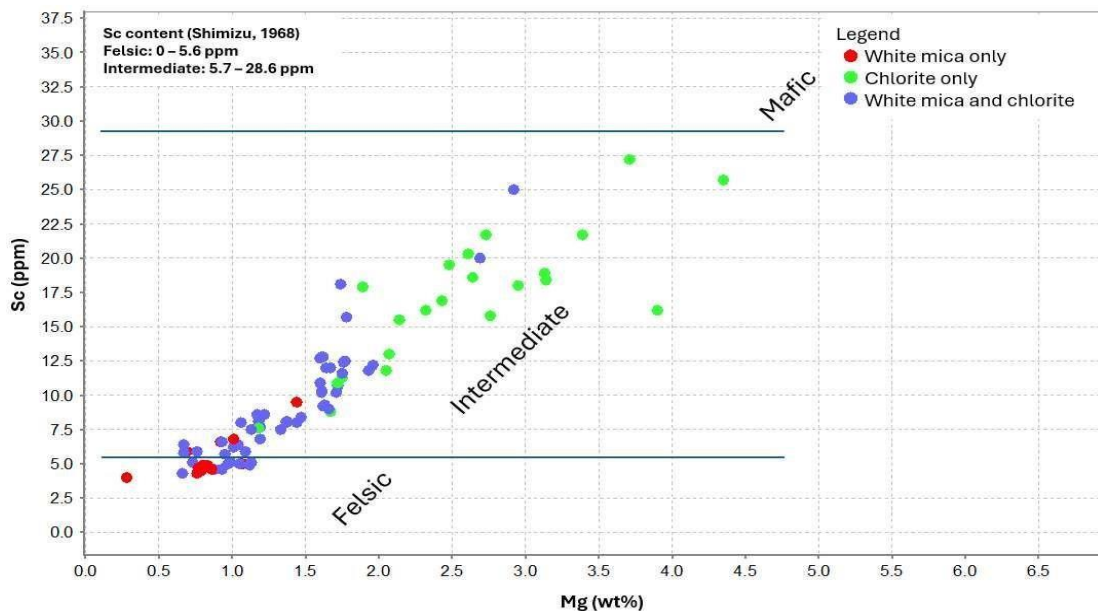


Fig. 5.10: Sc vs Mg plot showing the dominant compositions of the host rocks and their association with alteration phases. Chlorite-only samples are dominant in less fractionated rocks, whereas white mica dominant samples are dominant in more fractionated rocks, (dividing lines based on Shimizu, 1968).

The groups in Figure 5.10 are consistent with previous work that has described the study area as dominated by felsic to intermediate rocks (Harris, 1970). The SWIR data reveals that the dominant alteration phases were white mica and chlorite, but within individual samples, the dominant alteration phase provides insights on the parent rock composition. In the more felsic samples (low Sc and low Mg), white mica occurs as the sole alteration phase detected by SWIR, whereas in the more mafic rocks (high Sc and high Mg), chlorite is the sole alteration phase on the SWIR spectra, the rocks with the most intermediate values plots between the high and low and these rocks have a mix of chlorite and white mica as the dominant alteration phase (Fig. 5.10). Although the investigation reveals that rock composition has some control over the alteration of mineralogy, as shown by the association of chlorite dominant samples with high Sc and white mica dominant samples with low Sc, further investigation was needed to observe for controls of alteration intensity and gold distribution.

Using petrographic analysis alone, it was difficult to establish a correlation between alteration and gold mineralization, which was the aim of this study, this is because the gold occurrences are spatially associated with multiple mineral phases (Fig. 5.12d). Further investigation using geochemical data was completed to observe for any correlations between alteration intensity and gold distribution. As rocks undergo alteration processes, either by metamorphism or hydrothermal alteration, they are subjected to chemical changes, which are reflected as changes in the concentrations of mobile elements such as Na_2O , K_2O , CaO , FeO , and MgO (Pearce, 1976; Gélinas et al., 1982). Alteration indices can be a tool for investigating these chemical effects of alteration and their correlation with any minerals of interest (Large et al., 2001). The Ishikawa alteration index (Ishikawa et al., 1979), which shows the degree of sericite and chlorite alteration, was plotted against the gold concentration to investigate any trends with increasing degree of alteration. The Ishikawa alteration index plot shows that the degree of sericitization and chloritization has a weak correlation (r factor of 0.22 with gold content (Fig. 5.11a). The carbonate-chlorite-pyrite alteration index (CCPI) was also tested due to the relationship of gold with carbonate and pyrite; the index showed that the CCPI alteration has no correlation with gold (Fig. 5.11b).

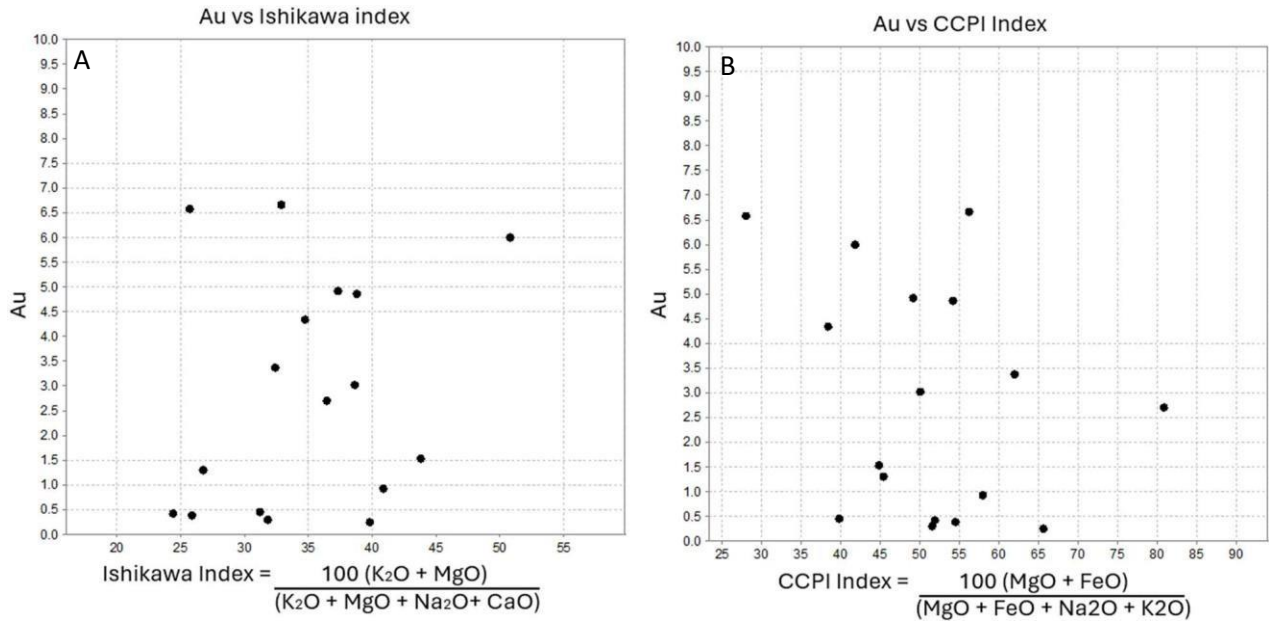


Fig. 5.11: Alteration indexes showing the degree of alteration in the host rocks compared to the gold distribution; for clarity, only Au values >0.2 ppm are reported. Image A shows the Ishikawa index, while image B shows the CCPI index.

However, this poor correlation does not mean alteration is unrelated to gold. The Moss Lake area has been subjected to multiple overprinting generations of alteration, including regional greenschist metamorphism-related alteration and metamorphic-hydrothermal alteration (Osmani, 1997), these can hinder the effectiveness of alteration indices, regarding comparisons with minerals of interest, in this case, gold. The weak positive correlation (0.22) of sericite and chlorite intensity with gold distribution suggests it may have a subtle relationship with the distribution of gold; this relationship may not be made obvious on the alteration index, but it may be revealed by further inquiry into the chemistry of sericite and chlorite; hence, a more detailed investigation of the chemistry of sericite and chlorite was carried out using SWIR and microprobe data in order to breach this limitation.

The variations in SWIR spectral features are a result of substitutions in the octahedral site cations, which causes subtle shifts in the position of the absorption wavelength; for white micas, the Al-OH bond produces an absorption around ~2200 nm, whereas for chlorite, the Al(Mg, Fe)-OH bond produces an absorption around 2250 nm (McLeod et al., 1987; Duke, 1994; Gaillard et al., 2018). The crystallinity of the white micas can be estimated by two spectral

features on the white mica spectrum (Depth 1900nm/Depth 2200nm); the 1900 nm feature represents the H₂O absorption of white mica, and its depth positively correlates with temperature (Chang et al., 2011; Yang et al., 2012; Zhang et al., 2017; Zuo et al., 2022). Spectral features of white mica suggest that at Moss Lake, muscovite (K-rich) and phengite (K-, Mg-rich) are the dominant white mica types, with most samples having a mixed composition of phengite and muscovite. Comparing the spectral composition of white mica and chlorite with the rock composition by plotting the wavelength position vs Sc, a weak trend was observed (Fig. 5.12a;b), which implies that the alteration style is influenced by rock composition, there is also a weak correlation with the spectral chemistry of the chlorite and white mica. Other processes, such as temperature and pressure, and interaction with hydrothermal fluids, can result in changes in the chemistry of the white mica and chlorite (Cloutier, 2021). When the spectral feature of white mica is compared with the gold concentrations of the samples, higher gold concentrations (>1.0 ppm) plot within a range of 2208 – 2214 nm (Fig. 5.12c); this range of wavelength represents white mica with a mixed composition of muscovite and phengite, no gold concentration above >1.0 ppm plot within white micas with a purely muscovite spectrum (2200 – 2208 nm; Fig. 5.12c). These variations in white mica spectral composition and its relationship to gold suggest that samples with mixed phengite and muscovite composition (2208 – 2214 nm) could be prospective for gold; hence, using SWIR data, it can be inferred that the presence of a phengitic component in white mica (K-Mg) could be an indicator for gold exploration.

The chlorite absorption feature position, when compared to Sc concentration in the individual samples, shows that most of the Mg-chlorite spectra plot in the low Sc field, suggesting a weak control of the rock composition on the spectral characteristics of chlorite (Fig. 5.12b). The crystallinity, which correlates with temperature, was compared with the chlorite wavelength position to observe for any correlation between changes in chlorite type with crystallinity. Figure 5.12d shows a negative correlation between crystallinity and chlorite wavelength position, suggesting that as crystallinity increases, chlorite wavelength decreases (a trend towards Mg-chlorite), and also higher crystallinity values (>1) were associated with samples with higher gold concentrations (Fig. 5.12d). The association of high white mica

crystallinity and Mg dominance in chlorite supports the idea that high crystallinity means high temperature, based on the preferential stability of Mg in chlorite at higher temperatures (Aja, 2015).

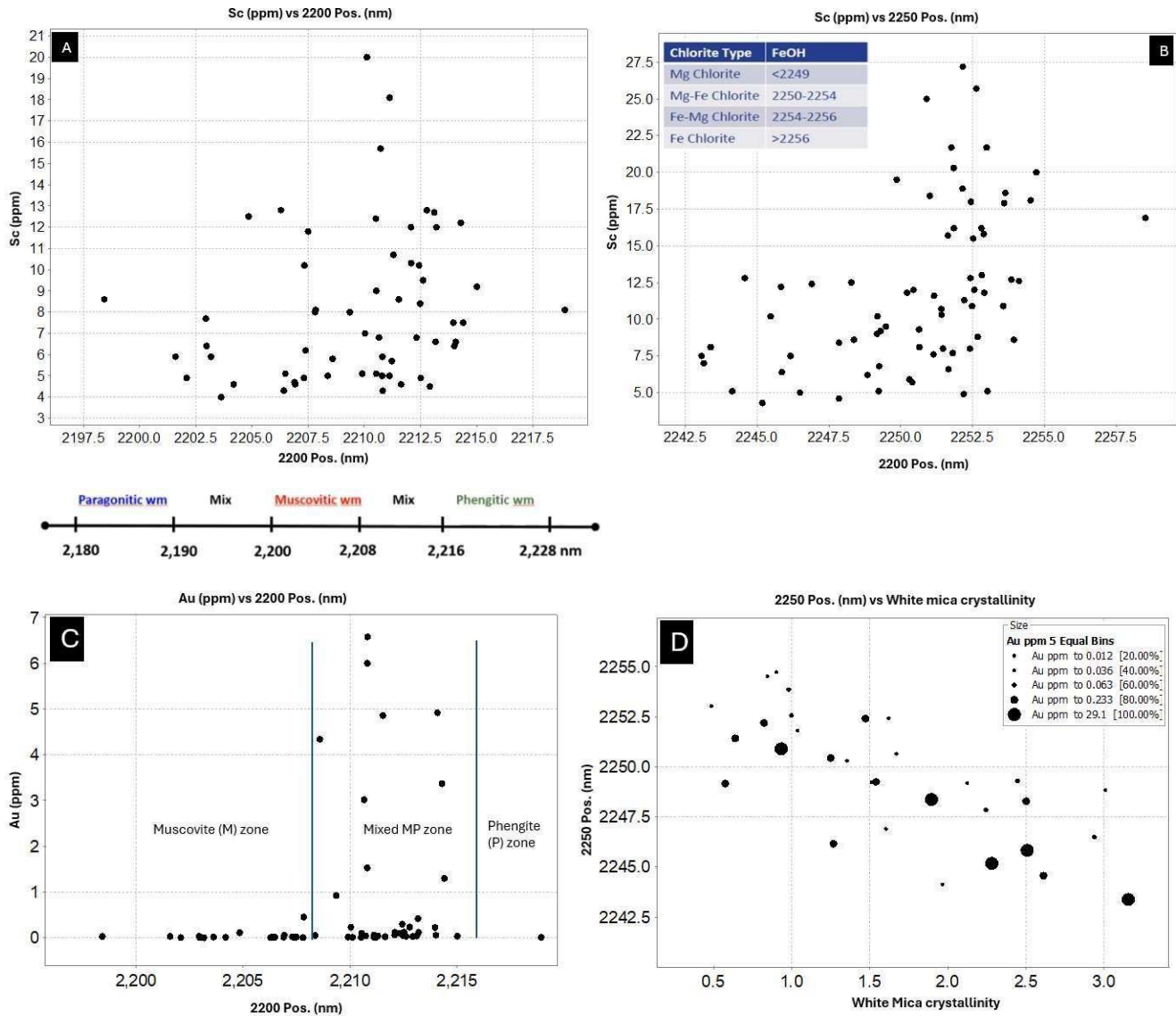


Fig. 5.12: Comparison of the spectral characteristics of white mica and chlorite with rock compositions and gold distribution. Images A and B show the variation in spectral chemistry (2200 pos. and 2250 pos.) of white mica and chlorite with increasing Sc in the host rock, image C shows the comparison of white mica chemistry with gold concentration where all Au values above 0.25 ppm plots within (2208 – 2214) nm. Image D compares the chlorite spectral chemistry with white mica crystallinity (temperature indicator) and gold distribution, where increasing crystallinity trends with decreasing wavelength (i.e., increasing Mg dominance in chlorite) and higher Au values occurred in Mg dominant chlorite samples.

The spectral data highlights chemical changes in the alteration minerals, such as the presence of a phengitic component in white micas, and the dominance of Mg over Fe in chlorite, and shows a subtle correlation with the distribution of gold. To investigate the changes in mineral chemistry with gold mineralization, the mineral chemistry was evaluated with respect to the deposit center. Although the dataset is limited, the chlorite chemistry shows an increase in Al and Fe moving away from the core of the deposit (Fig. 5.13a;b). This compositional variation is a result of the Tschermak substitution, where Mg or Fe substitutes for Al in the octahedral site of chlorite, at higher temperatures, Mg instead of Fe substitutes for Al (Bourdelle, 2021). Hence, the systematic increase in Al and Fe suggests a decrease in temperature as you move away from the core of the deposit. Silicon in chlorite also decreases away from the center of the deposit (Fig. 5.13d), this can also be attributed to the Tschermak substitution, where Si replaces Al in the tetrahedral sites of chlorite. Moss 10, a chlorite sample from a felsic metavolcanic outcrop in the Moss Lake area, was acquired from another study and analyzed for chlorite chemistry (A. Perez, Personal Communication, 2024); this sample yielded low Mg and Si values and high Fe and Al values, similar to samples that were farther away from the deposit center, supporting the idea that the observed chemical signature in the chlorites proximal to the ore center (high Mg and Si, low Fe and Al) was peculiar to them.

Using the chlorite mineral chemistry data, chlorite geothermometry was applied to evaluate the temperature of formation of the chlorite and to investigate for variation in chlorite temperature with respect to the ore center. The geothermometers of Bourdelle et al. (2013), De Caritat et al. (1993), and El Sharkawy (2000) were applied to compositional averages of individual samples from microprobe analyses. Bourdelle et al. (2013) is based on the Fe^{2+} , Mg, and Si (apfu), De Caritat et al. (1993) is based on the octahedral occupancy, and El Sharkawy (2000) is based on Al^{IV} (apfu). The chlorite temperature of formation based on De Caritat et al. (1993) and El Sharkawy (2000) ranges from 227 to 285 °C, with values reported in Table 4.5. This calculated temperature range showed some consistency when compared with the Bourdelle et al. (2013) plot, where the chlorite temperature ranged from 200 to 300 °C. When compared with distance from the ore center, the temperature changes did not show a trend, and this could result from the lack of precision of the geothermometers.

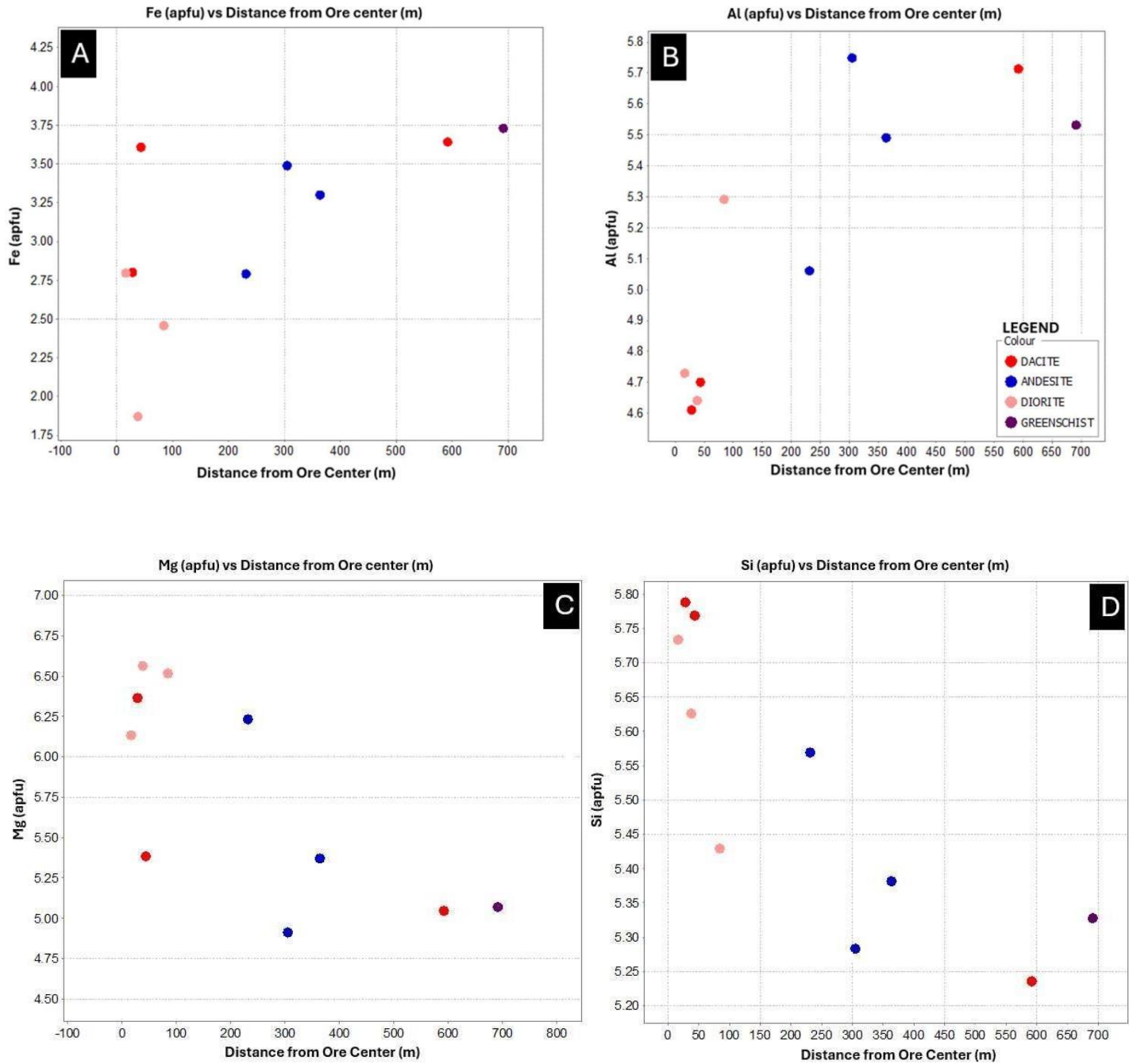


Fig. 5.13: Chlorite compositional variations with increasing distance away from the ore center. Image A and B shows the increasing Fe and Al concentrations in chlorite farther away from the deposit. Image C and D shows the decreasing Mg and Si concentrations in chlorite with increasing distance from the ore center.

The chemistry of white mica at Moss Lake also shows a correlation with distance from the center of the deposit. Magnesium in white mica decreases with increasing distance from the center of the deposit and has the strongest correlation with distance from ore as opposed to other elements in the white mica chemistry (Fig. 5.14a). This decrease away from the ore center indicates a trend towards muscovite end-member composition from a phengite end-member composition. The negative correlation in Figure 5.14b supports the idea of the Tschermak substitution reaction in white mica, where Al is replaced by Si in the tetrahedral sites, while Mg or Fe is incorporated in the octahedral sites (Duke, 1994).

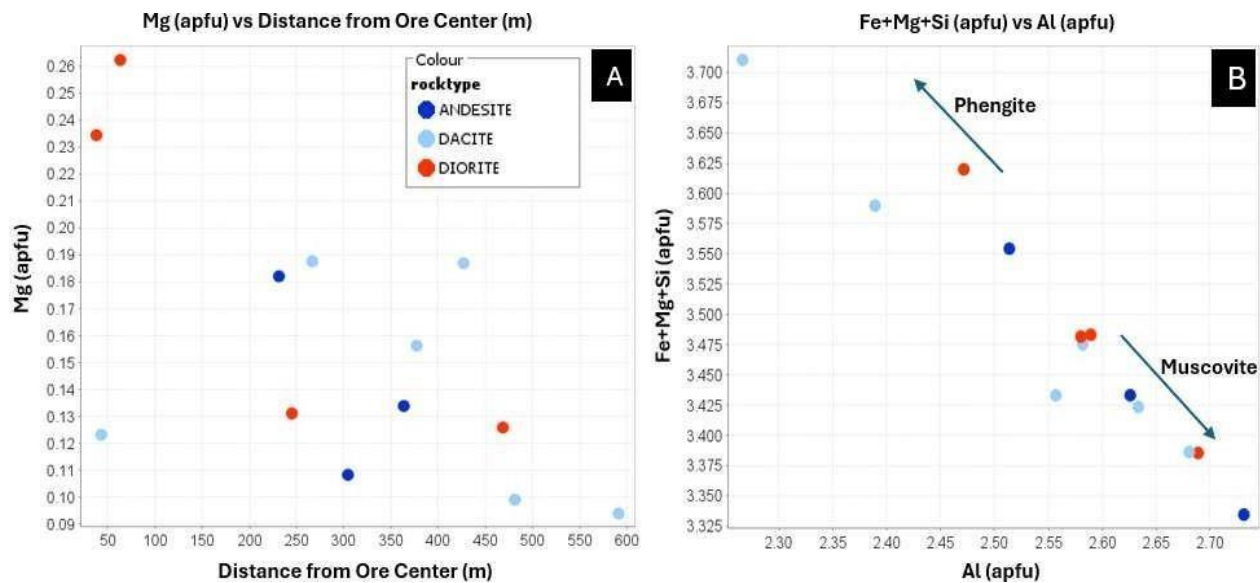


Fig. 5.14: Plots showing compositional changes in white mica. Image A shows the decreasing Mg concentration with increasing distance away from the ore center; Image B shows the negative correlation between Fe+Mg+Si and Al, which shows a trend from phengite to muscovite resulting from the Tschermak Substitution Reaction in white mica at higher temperature.

Fluid pathways are commonly zones of higher temperature, and such temperatures drive the Tschermak substitution (van Ruitenbeek et al., 2005; Wang et al., 2017), which can result in the compositional variations observed in the chemistry of chlorite and white mica. Magnesium enrichment in white mica and chlorite at the most proximal zone of the Moss Lake orebody may represent a fluid pathway, which is inferred to be a zone of higher temperature, such high temperature zone would facilitate the Tschermak substitution reaction leading to Mg

enrichment. Based on the chlorite and white mica chemistry, there is variation in alteration chemistry with increasing proximity to the ore center, and these changes can also be determined more subtly from the spectral features of these minerals, such as the association of gold-rich samples with white mica with a phengitic component (2208 – 2214 nm) and the association of high crystallinity with samples with Mg dominance over Fe. An important spectral feature that strongly correlates with the chemical data is the white mica crystallinity, which highlights trends of increasing temperature represented by a trend toward Mg-chlorite dominance (Fig. 5.12d). Mg-chlorite is also associated with higher Au values, implying that these higher-temperature samples are favorable for Au precipitation.

5.4 Summary

The objective of this study was to characterize the alteration at the Moss Lake deposit and compare it with the distribution of gold mineralization, with the aim of developing a vector to ore based on changes in the composition of alteration, particularly white mica and chlorite. Achieving this objective required the use of petrography, geochemistry, geochemistry, hyperspectral analysis, and mineral chemistry analysis on chlorite and white mica. A similar study was carried out at a larger scale by Gaillard et al. (2021) in the Malartic District using biotite and white mica spectral features and mineral chemistry

The changes observed in chlorite and white mica at the Moss Lake deposit are consistent with some of the compositional variations observed by Gaillard et al. (2021) in the Malartic District, where spectral data and mineral chemistry were also used. In this study, higher gold concentration occurred dominantly in samples with a phengitic component in their spectra. A similar trend was observed in the Malartic District, where white mica composition shifts from a muscovite end member composition in the distal metasedimentary rock to a phengitic composition in the hydrothermally altered host rocks (Gaillard et al., 2021). Similarly, in the white mica chemistry, the decrease in Mg content with increasing distance away from the center of the deposit is consistent with the trends observed at the Malartic District, where the Mg content in white mica is highest within the host rock and decreases with increasing distance from the ore body. In this study, chlorite is more abundant and widespread than

biotite. The spectral characteristics of chlorite and biotite are similar in a few aspects; for instance, biotite has a similar Al(Mg,Fe)-OH bond like chlorite, which produces an absorption feature around 2250 nm on the short-wave spectrum. In this study, higher gold concentrations occur within chlorite with Mg-chlorite spectra, and the composition of the chlorite showed a trend of decreasing Mg in chlorite with increasing distance from the center of the deposit, this is consistent with the chemistry of biotite studied in the Malartic District where the Mg in biotite decreases with increasing distance from the ore body (Gaillard et al., 2021). The compositional changes observed in chlorite in this study are consistent with that of biotite in the Malartic district. Such as decreasing Mg and Si and increasing Fe and Al in chlorite with increasing distance from the Moss Lake deposit, which is consistent with the changes in biotite with increasing distance from the ore body at the Malartic district. In this study, these compositional changes are attributed to the Tschermak-exchange reaction and deemed to define fluid pathways; a similar conclusion was reached at the Malartic District.

Chapter 6: Conclusions

The Moss Lake deposit is hosted within intermediate rocks of the central felsic to intermediate belt (CFB) of the Shebandowan Greenstone belt. Previous workers have dated the host rocks by zircon U/Pb at 2720 ± 2 Ma (Hart, 2007) and 2721 ± 6 Ma (Corfu, 1998). Numerous intrusions occur within the study area, such as the Burchell Lake Pluton, which is located northeast of Moss Lake, which was dated at 2680 ± 2 Ma (Corfu, 1983). In this study, gold mineralization was dated at 2708 ± 12 Ma (Re/Os), and this new age, despite being within error of the age for the CFB, provides a constraint for the mineralization. The age distribution within the Shebandowan Greenstone Belt highlights two peaks of magmatic activity, an older peak (~ 2720 Ma), which comprises mostly metavolcanic rocks, and a younger peak (~ 2680 Ma), which includes mostly late felsic to mafic intrusive rocks (Fig. 5.1). The Re/Os molybdenum age of this study places the mineralizing event between these two peak periods, but within error of the older peak, suggesting an association of the mineralizing event with the older peak.

Based on petrographic observations, plagioclase, quartz, and amphibole are the most common primary minerals among the host rocks. The diorites, dacites, and andesites are altered to varying degrees by sericite, chlorite, epidote, carbonate, biotite, and albite. Alteration intensity ranges from weakly altered to strongly altered and shows evidence of multiple overprinting alteration phases. The paragenesis of the Moss Lake deposit begins within the crystallization of a felsic to intermediate magma at ~ 2720 Ma. Subsequent alteration of plagioclase to albite and biotite replacement of amphibole were the early phases of alteration; these were coeval with the onset of quartz recrystallization and veining. Sericite alteration is widespread at Moss Lake and followed these earlier phases, replacing plagioclase and occurring pervasively within the rock. Sericite alteration is replaced by chlorite and epidote alteration. Carbonate alteration is also predominant within the rocks but mostly occurs within veins. A total of 12 vein types were observed within the samples; in five of the vein types, quartz and carbonate were the main infills. Vein QZ is the earliest vein; meanwhile, vein types CCL, ECL, and QZ2 are the late veins. Other vein types are in the intermediate stage, and their sequences are outlined in Figure 5.6. The intermediate-stage veins include vein QCP, QCP2 and QCP3

which are associated with sulfides and gold. These sulfides mainly include pyrite and chalcopyrite with minor sphalerite. The sulfides occur in the intermediate stage, and pyrite crystallized first, followed by chalcopyrite and sphalerite; gold is coeval or slightly later than pyrite formation due to textural association.

Several gold occurrences were observed, and they showed a strong spatial association with pyrite. Five out of six observed gold occurrences were in pyrite-bearing vein QCP, QCP2, and QCP3 and were associated with quartz and carbonate, with the other occurrence in a type 2 vein. Gold occurrences within the host rocks are localized within zones with strong shear fabric and zones of abundant veining; this implies that zones of structural activity are favorable for gold deposition. With vein QCP2, gold grains were observed within a shear zone. Within the shear zone, gold occurs on the boundary of a deformed pyrite grain. This textural association with deformed pyrite suggests that gold concentration at Moss Lake was coeval with deformation. These shear zones are also characterized by intense sericitization and chloritization aligned strongly with the shear fabric. The characteristics of the gold occurrences at Moss Lake are consistent with orogenic gold deposits. Generally, they comprise an array of quartz-carbonate veins with no significant zoning, with pyrite or pyrrhotite as the dominant sulfide and mineralization associated with shear zones, all within host rocks of greenschist facies metamorphism (Robert et al., 2007). These features are consistent with the observations made during this study and strongly suggest that the Moss Lake deposit is an orogenic gold deposit.

One major objective of the study was to investigate the relationship between the gold distribution and the alteration. From the petrological and geochemical investigations using the SEM and alteration indexes, it was observed that the alteration at Moss Lake weakly correlates with gold distribution. Several other factors control the intensity of alteration, such as veins, shears, and rock types. The key changes in the alteration were observed in their SWIR spectra and in the mineral chemistry data of white mica and chlorite. From the white mica SWIR data, it was observed that the wavelength position for mixed muscovite and phengite composition (2208 - 2216) correlates with higher gold assay values (Fig. 5.12c). This suggests that the presence of a phengitic (K-Mg) component in white mica could be favorable for gold

exploration. This observation was supported by the evaluation of white mica mineral chemistry, which showed that the white mica closer to the ore center had higher Mg (apfu) than those farther away from the deposit. This increase of Mg in white mica proximal to the ore center can be attributed to the Tschermak substitution reaction, which can be driven by high temperatures. The SWIR data of chlorite showed that the majority of the higher gold assay values occurred in samples with Mg-chlorite spectra (<2250 nm). This is consistent with the mineral chemistry data, which show that Mg in chlorite is highest in the samples proximal to the ore center and lowest in the distal samples. Other elements, such as Fe and Al, are lowest in proximal samples and higher farther away. The variation in chlorite chemistry can also be attributed to the Tschermak substitution in chlorite, which can be driven by higher temperatures. Geothermometry of chlorite shows that the chlorites at Moss Lake crystallized between 200 – 300 °C.

The objectives of the study were achieved by combining all the methods used. The petrographic studies were vital in the characterization of the rock types, veins, alteration assemblages, and gold mineralization, and a paragenetic sequence was built based on their overprinting relationships; geochronological studies were vital in understanding the genesis of gold in the system by constraining the mineralizing event to circa 2708 Ma. Using the changes in chlorite and white mica chemistry based on SWIR spectra and EPMA chemical composition, the main objective of this study was achieved as the data revealed a relationship between gold mineralization and alteration chemistry, and this provides insight into how the alteration minerals can be used as a vector toward the ore center. For white mica and chlorite, the occurrence of phengitic components (mixed phengite and muscovite white mica) and Mg-chlorite spectra, respectively, can indicate increasing proximity to ore centers. Relatively high Mg content in chlorite and white mica can indicate fluid pathways and serve as vectors to ore.

The results of this study are consistent with those of Gaillard et al. (2021) from the Malartic District, where a similar study was conducted to use white mica and biotite to develop a vector to ore, this consistency suggests that this method of vectoring can be applied in other mining districts for sustainable exploration. For exploration programs SWIR analysis can be the first approach in the utilization of this method for vectoring. SWIR analysis can be backed by

mineral chemistry analysis, which will provide exact compositional changes and can validate the SWIR observations. This can be a vital tool for the exploration of gold deposits. Hyperspectral data, when utilized properly, can track fluid pathways and temperature highs in chlorite and white mica spectra; these can be critical in mineral exploration. A next step for exploration at the Moss Lake Area should include a broader scale hyperspectral analysis of exploration targets or drills core in order to acquire spectral compositional data that will be invaluable in updating the exploration model and possibly expanding the deposit. By combining hyperspectral data with logging and geochemical data, exploration targets can be better understood.

References

- Aja, S., Omotoso, O., Bertoldi, C., 2015. The Structure and Thermochemistry of Three Fe-Mg Chlorites. *Clays Clay Miner.* 63, 351–367, <https://doi.org/10.1346/CCMN.2015.0630502>
- Alsop, G. I., Holdsworth, R. E., McCaffrey, K. J. W., Hand, M., 2004. Shear zones – an introduction and overview, *Flow Processes in Faults and Shear Zones*.
- Baltazar, O.F., Zucchetti, M, 2007. Lithofacies associations and structural evolution of the Archean Rio das Velhas greenstone belt, Quadrilátero Ferrífero, Brazil: a review of the setting of gold deposits. *Ore Geol Rev* 32, pp.471–499
- Burrows, D.R. & Spooner, E.T.C., 1987. Generation of a magmatic H₂O-CO₂ fluid enriched in Au, Mo, and W within an Archean sodic granodiorite stock, Mink Lake, northwestern Ontario. *Economic Geology*, 82, pp.1931-57.
- Cameron, E.M., 1988. Archean gold: relation to granulite formation and redox zoning in the crust. *Geology*, 16, pp.109-12.
- Card, K.D. and Ciesielski, A., 1986. DNAG #1, Subdivisions of the Superior Province of the Canadian Shield. *Geoscience Canada*, Vol. 13, pp.5-13.
- Card, K.D., Poulsen, K.H. & Robert, F., 1989. The Archean Superior Province and its lode gold deposits. *Economic Geology Monograph*, 6, pp.11-28.
- Chang, Z., Hedenquist, J. W., White, N. C., Cooke, D. R., Roach, M., Deyell, C. L., 2011. Exploration tools for linked porphyry and epithermal deposits: Example from the man Kayan intrusion-centered Cu-Au district, Luzon, Philippines. *Economic Geology*, 106(8), 1365–1398. <https://doi.org/10.2113/econgeo.106.8.1365>.
- Claoue-Long, J.C., King, R.W. & Kerrich, R., 1990. Archean hydrothermal zircons in the Abitibi greenstone belt: constraints on the timing of gold mineralization. *Earth Planetary Science*, 98, pp.109-28.
- Colvine, A.C., Fyon, J.A., Heather, K.B., Marmont, S., Smith, P.M., Troop, D.G., 1988. Archean lode gold deposits in Ontario. *Ontario Geological Survey Miscellaneous Paper*, 139, pp.136.
- Colvine, A.C., 1989. An empirical model for the formation of Archean gold deposits: products of final cratonization of the Superior Province, Canada. *Economic Geology Monograph*, 6, pp.37-53.
- Corfu, F. and Stott, G.M., 1998. Shebandowan Greenstone Belt, western Superior Province: U Pb ages, tectonic implications, and correlations. *GSA Bulletin*, Vol. 110, pp.1467-1484.

- Dube, B. & Gosselin, P., 2007. Greenstone-Hosted Quartz-Carbonate Vein Deposits. Geological Association of Canada, Mineral Deposits Division, Special Publication 5, pp.49-73
- Dubosq, R., Rogowitz A., Lawley, C., Schneider, D., Jackson, S., 2017. Pyrite deformation and connections to gold mobility: insight from microstructural analysis and trace element mapping.
- Duke, E.F., 1994; Near-infrared spectra of muscovite, Tschermak substitution, and metamorphic reaction progress: Implications for remote sensing. *Geology* 1994; 22 (7): 621–624. doi: [https://doi.org/10.1130/0091-7613\(1994\)022<0621:NISOMT>2.3.CO;2](https://doi.org/10.1130/0091-7613(1994)022<0621:NISOMT>2.3.CO;2)
- Engvik A.K., Putnis A., FitzGerald J.D., Austrheim H., 2008; Albitization of granitic rocks: the mechanism of replacement of oligoclase by albite. *The Canadian Mineralogist*, 46(6): 1401–1415 doi: <https://doi.org/10.3749/canmin.46.6.1401>
- Flindell, P., 2023. Goldshore Resources Inc. Corporate Presentation. Vancouver: Goldshore Resources Inc.
- Forslund, N., Laarman J., 2017. Wesdome Gold Mines Ltd Report on 2017 diamond drilling at the Moss Lake Property - Moss and Burchell Lake Townships, Thunder Bay Mining Division, Province of Ontario, Canada. N.T.S. 052 B/10
- Gaillard N., Williams-Jones A.E., Clark J.R., Lypaczewski P., Salvi S., Perrouty S., Piette-Lauzière N., Guilmette C., Robert L. Linnen R.L., 2018. Mica composition as a vector to gold mineralization: Deciphering hydrothermal and metamorphic effects in the Malartic district, Quebec. *Ore Geology Reviews*, Vol. 95, pp.789-820, ISSN 0169-1368, <https://doi.org/10.1016/j.oregeorev.2018.02.009>.
- Gélinas, L., Mellinger, M., Trudel, P., 1982. Archean mafic metavolcanics from the Rouyn Noranda district, Abitibi Greenstone Belt, Quebec. 1. Mobility of the major elements. *Canadian Journal of Earth Sciences*, Vol. 19, pp.2258-2275.
- Giblin, P.E., 1964. Geology of the Burchell Lake Area, District of Thunder Bay. Ontario Department of Mines, Geological Report No. 19, 39p.
- Goldfarb, R.J., Baker, T., Dube, B., Groves, D.I., Hart, C.J.R., Gosselin, P., 2005. Distribution, Character, and Genesis of Gold Deposits in Metamorphic Terranes. *Society of Economic Geologists*, 100th Anniversary Volume, pp.407-50.
- Google Earth. Location of Moss Lake Deposit from Thunder Bay, July 1, 2024. <https://earth.google.com/web/@48.49060365,89.31110959>.
- Groves, D., Barnicoat, A. C., Barley, M., Cassidy, K. F., Fare, R. J., Hagemann, S. G., Ho, S. E., Hronsky, J. M. A., Mikucki, E. J., Mueller, A. G., Mcnaughton, N., Perring, C. S., Ridley, J. R., Vearncombe, J. R., 1992. Sub-greenschist to granulite-hosted Archean lode-gold deposits of the Yilgarn Craton: a depositional continuum from deep-sourced hydrothermal fluids in the crustal-scale plumbing systems. J.E. Glover and S.E. Ho (Editors), *The Archaean: Terrains, Processes and Metallogeny*. Geol. Dep. (Key Centre) and Univ. Extension. Univ. West. Aust., 22, pp.325-37.

- Groves, D.I., Ridley, J.R., Bloem, E.M.J., Mintesnot, G., Hagemann, S., Hronsky, J.M.A., Knight, J.T., McNaughton, N.J., Ojala, J., Vielreicher, R.M., McCuaig, T.C., Holyland, P., 1995. Lode-gold deposits of the Yilgarn Block: Products of Late-Archean crustal-scale overpressured hydrothermal systems. *Journal of Geological Society of London*.
- Groves, D.I., Goldfarb, R.J., Gebre-Mariam, M., Hagemann, S.G., Robert F., 1998. Orogenic gold deposits: A proposed classification in the context of their crustal distribution and relationship to other gold deposit types. *Ore Geology Reviews*, 13, pp.7-27.
- Groves, D.I., Goldfarb, R.J., Robert, F., Hart, C.J.R., 2003. Gold Deposits in Metamorphic Belts: Overview of Current Understanding, Outstanding Problems, Future Research, and Exploration Significance. *Economic Geology*, 98, pp.1-29.
- Groves D.I., M. Santosh, Liang Zhang, 2020. A scale-integrated exploration model for orogenic gold deposits based on a mineral system approach. *Geoscience Frontiers*, Vol. 11, Issue 3, pp.719–738, ISSN 1674-9871, <https://doi.org/10.1016/j.gsf.2019.12.007>. (<https://www.sciencedirect.com/science/article/pii/S1674987119302415>)
- Halley, S 2020. Mapping Magmatic and Hydrothermal Processes from Routine Exploration Geochemical Analyses. *Economic Geology*, 115 (3): 489–503. doi: <https://doi.org/10.5382/econgeo.4722>
- Hanes, J.A., Archibald, D.A. & Hodgson, C.J., 1992. Dating of Archean auriferous quartz vein deposits in the Abitibi greenstone belt, Canada: $^{40}\text{Ar}/^{39}\text{Ar}$ evidence for a 70- to 100 m.y. time gap between plutonism-metamorphism and mineralization. *Economic Geology*, 87, pp.1849-61.
- Harris, F.R., 1970. Geology of the Moss Lake Area, District of Thunder Bay. Ontario Department of Mines and Northern Affairs, Geological Report 85, 61p.
- Hart, T.R., 2007. 9. Project Unit 06-003. Geochronology of the Hamlin and Wye Lakes Area, Shebandowan Greenstone Belt, Thunder Bay District *In* Summary of Field Work and Other Activities 2007, Ontario Geological Survey, Open File Report 6213, pp.9-1 to 9-8.
- Hodgkinson, J.M., 1968. Geology of the Kashabowie Area, District of Thunder Bay. Ontario Department of Mines, Geological Report 53, 35p.
- Hollings, P., Wyman, D. and Kerrich, R., 1999. Komatiite-basalt-rhyolite volcanic associations in Northern Superior Province greenstone belts: significance of plume-arc interaction in the generation of the protocontinental Superior Province. *Lithos*, Vol. 46, pp.137-161.
- Hodgson, C.J., Hamilton, J.V. & Hanes, J.A., 1989. The late emplacement of gold in the Archean Abitibi greenstone belt: a consequence of thermal equilibration following collisional orogeny. *Geological Association of Canada; Mineral Association of Canada*, 14, pp.8-45.
- Jamielita, R.A., Davis, D.W. & Krogh, T.E., 1990. U-Pb evidence for Abitibi gold mineralization postdating greenstone magmatism and metamorphism. *Nature*, 346, pp.831-34.

- Kerrick, R. & Cassidy, K.F., 1994. Temporal relationships of lode gold mineralization to accretion, magmatism, metamorphism and deformation - Archean to present: A review. *Ore Geology Reviews*, 9, pp. 263-310.
- Kerrick, R. & Wyman, D.A., 1993. The mesothermal gold-lamprophyre association: Significance for an accretionary geodynamic setting, supercontinent cycles, and metallogenic processes. *Mineralogy and Petrology*, 51, pp.147-172.
- Lowenstern, J.B., 2001. Carbon dioxide in magmas and implications for hydrothermal systems. *Mineral Deposits* 36, pp.490–502. <https://doi.org/10.1007/s001260100185>
- Markey, R., Stein, H.J., Hannah, J.L., Selby, D. and Creaser, R.A., 2007. “Standardizing Re-Os geochronology: A new molybdenite Reference Material (Henderson, USA) and the stoichiometry of Os salts”. *Chemical Geology*, Vol. 244, pp.74-87.
- McLeod, R.L., Gabell, A.R., Green, A.A., and Gardavsky, V., 1987. Chlorite infrared spectral data as proximity indicators of volcanic massive sulfide mineralization. Proc. PACRIM Congress, Gold Coast, Australia, pp. 321–324.
- Osmani, I.A., 1997. Geology and mineral potential: Greenwater Lake area, West-Central Shebandowan Greenstone Belt. Ontario Geological Survey, Report 296, 135p.
- Pearce, J.A., 1976. Statistical analysis of major element patterns in basalts. *Journal of Petrology*, Vol. 17, pp.15-43.
- Percival, J.A., Stern, R.A. and Skulski, T., 2001. Crustal growth through successive arc magmatism: reconnaissance U-Pb SHRIMP data from the northeastern Superior Province, Canada. *Precambrian Res.*, Vol. 109, p.203-238.
- Percival, J.A., Sanborn-Barrie, M., Skulski, T., Stott, G.M., Helmstaedt, H. and White, D.J. 2006. Tectonic evolution of the western Superior Province from NATMAP and Lithoprobe studies. *Canadian Journal of Earth Sciences*, Vol.43, pp.1085-1117.
- Poirier, S., Richard, P. L., Palich, J., Patrick, G. A., 2013. *Technical Report and Preliminary Economic Assessment For The Moss Lake Project, pp.52-61*. Val-D'Or: InnovExplo Consulting Firm Mines & Exploration.
- Risto, R.W. and Breede, K., 2010. An update to a technical review of the Moss Lake Gold property, including an updated mineral resource estimate, Moss Township, Northwestern Ontario. Report prepared for Moss Lake Gold Mines Ltd by Watts, Griffis, and McOuat Ltd, 100p.
- Stipp, M., Stünitz, H., Heilbronner, R., Schmid, S., 2002. The eastern Tonale fault zone: A 'natural laboratory' for crystal plastic deformation of quartz over a temperature range from 250 to 700 °C. *Journal of Structural Geology*, 24, 1861-1884. 10.1016/S0191-8141(02)00035-4.
- Stone, D., 2005. Geology of the northern Superior area, Ontario. Ontario Geological Survey, Open File Report 6140, 94p.

- Stott, G.M., Corkery, T., Leclair, A., Boily, M. and Percival, J., 2007. A revised terrane map for the Superior Province as interpreted from aeromagnetic data [abstract]; Institute on Lake Superior Geology Proceedings, 53rd Annual Meeting, Lutsen, MN, vol. 53, part 1, pp.74-75.
- Stott, G.M., Corkery, M.T., Percival, J.A., Simard, M. and Goutier, J., 2010. Project Units 98-006 and 98-007. A revised terrane subdivision of the Superior Province. Ontario Geological Survey, Open File Report 6260, pp.20.1-20.10.
- Thurston, P.C., 1991. Archean Geology of Ontario: Introduction; *in* Geology of Ontario, Ontario Geological Survey, spec. vol. 4, pt.1, pp.73-78.
- Thurston, P.C., 1991. Geology of Ontario: Introduction; *in* Geology of Ontario, Ontario Geological Survey, spec. vol. 4, pt.1, pp.3-25.
- Thurston, P.C., Osmani, I.A. and Stone, D., 1991. Northwestern Superior Province: review and terrane analysis. In: Thurston, P.C., Williams, H.R., Sutcliffe, H.R., Stott, G.M. (Eds.), Geology of Ontario. Ont. Geol. Surv., Spec. vol. 4, part 1, pp.81–141.
- Shimizu, T., 1969. Scandium Content of Igneous Rocks and Some Oceanic Sediments. Bulletin of the Chemical Society of Japan, Volume 42, Issue 6, Pages 1561-1569, <https://doi.org/10.1246/bcsj.42.1561>
- Sillitoe, R.H., 2020. Gold Deposit Types: An Overview. Society of Economic Geologists, 10, pp.1-28.
- Smoliar et al., 1996. "Re-Os ages of group IIA, IIIA, IVA, IVB iron meteorites". Science, 271, pp.1099-1102
- Whalen, J.B., Percival, J.A., McNicoll, V.J. and Longstaffe, F.J., 2002. A Mainly Crustal Origin for Tonalitic Granitoid Rocks, Superior Province, Canada: Implications for Late Archean Tectonomagmatic processes. Journal of Petrology, Vol.43, pp.1551- 1570.
- Williams, H.R., 1990. Subprovince accretion tectonics in the south-central Superior Province. Can. J. Earth Sci., Vol.27, pp.570-581.
- Williams, H.R., Stott, G.M., Heather, K.B., Muir, T.L. and Sage, R.P., 1991. Wawa Subprovince; *in* Geology of Ontario, Ontario Geological Survey, spec. vol. 4, pt.1, p.485-539.
- Wong, L., Davis, D.W., Krogh, T.E., Robert, F., 1991. U-Pb zircon and futile chronology of Archean greenstone formation and gold mineralization in the Val d'Or region, Quebec. Earth Planetary Science Letters, 104, pp.325-36.
- Wyman, D.A., Kerrich, R., 1988. Alkaline magmatism, major structures, and gold deposits: Implications for greenstone belt gold metallogeny. Economic Geology, 83, pp.451-58.
- Yang, K., Huntington, J. F., Gemmell, J. B., Scott, K. M., 2011. Variations in composition and abundance of white mica in the hydrothermal alteration system at Hellyer, Tasmania, as revealed by infrared reflectance spectroscopy. Journal of Geochemical Exploration, Vol.108(2), pp.143–156. <https://doi.org/10.1016/j.gexplo.2011.01.001>.

Zhang, S., Chen, H., Zhang, X., Zhang, W., Xu, C., Han, J., Chen, M., 2017. Application of short wavelength infrared (SWIR) technique to exploration of skarn deposit: A case study of Tonglvshan Cu-Fe-Au deposit, Edongnan (southeast Hubei) ore concentration area (in Chinese with English abstract). *Mineral Deposits*, Vol.36, no.6, pp.1263–1288. https://doi.org/10.16111/j.0258_7106.2017.06.002.

Zuo, L., Wang, G., Carranza, E.J.M., 2022. Short-Wavelength Infrared Spectral Analysis and 3D Vector Modeling for Deep Exploration in the Weilasituo Magmatic–Hydrothermal Li–Sn Polymetallic Deposit, Inner Mongolia, NE China. *Nat Resources Res* vol.31, pp.3121–3153 (2022). <https://doi.org/10.1007/s11053-022-10111-1>

Zweng, P.L., Mortensen, J.K., Dalrymple, G.B., 1993. Thermochronology of the Camflo Gold Deposit, Malartic, Quebec: implications for magmatic underplating and the formation of gold-bearing quartz veins. *Economic Geology*, 88, pp.1700-21.

Appendix I: Thin Section Descriptions

Sample ID: ML23-NM-001

Rock type: Andesite

Basic description:

The rock comprises plagioclase, quartz, sericite, carbonate, chlorite, and pyrite.

The rock is associated with various veins:

1 – Carbonate-quartz vein about 0.7mm wide, cut by a later vein

2 – Carbonate vein about 0.5mm wide cutting earlier vein.

The rock contains disseminated pyrite.

Paragenesis

Plagioclase -> quartz -> sericite -> pyrite -> chlorite -> vein 1 (carbonate, quartz) -> vein 2 (carbonate)

Mineralogy

Plagioclase (40%): The grains are fine, with sizes ranging from 300 – 600 micrometers. They show simple twinning and are altered by sericite.

Quartz (20%)

Within host rock (15%): The grains are very fine, with sizes ranging from 10 – 50 micrometers; they display undulatory extinction.

Within vein 1 (5%): Recrystallized grains up to 0.6mm occur in vein 1 along with carbonate.

Sericite (14%): Fine anhedral grains of sericite up to 20 micrometers. Most grains occur in plagioclase.

Carbonate (12%):

Within host rock (5%): Subhedral to anhedral grains up to 300 micrometers occur in the host rock. Most grains occur in proximity to carbonate-bearing veins.

Within vein (7%): Subhedral carbonate grains occur within both veins. The size is up to 400 micrometers.

Chlorite (7%): Anhedral grains of chlorite up to about 400 micrometers long can be seen in the host in an elongated texture.

Pyrite (7%): Subhedral grains up to 300 micrometers, disseminated within the rock.

Sample ID: ML23-NM-003

Rock type: Diorite

Basic description:

The rock comprises plagioclase, quartz, sericite, chlorite, and carbonate.

The rock is associated with multiple veins:

1 – Carbonate-chlorite vein cuts the rock. The vein is up to 0.6mm wide.

2 – Carbonate vein up to 1.2mm cuts the rock. The vein is aligned parallel to vein 1.

3 – Undulating vein filled with carbonate and chlorite cuts the rock.

4 – Carbonate vein up to 0.8mm wide cuts the host rock. The vein also cuts veins 1, 2, and 3.

Sulfides are present within the rock. They comprise of trace amounts of pyrite.

Paragenesis

Plagioclase -> quartz -> sericite -> Vein 1 (chlorite, carbonate) -> Vein 2 (carbonate) -> Vein 3 (carbonate, chlorite) -> Vein 4 (carbonate)

Mineralogy

Plagioclase (40%): Grains of plagioclase are up to 2mm in size. They are affected by sericite and chlorite alteration. Relict plagioclase grains dominate the sample in association with fine grains of quartz.

Quartz (28%): Very fine grains of quartz occur with undulatory extinction.

Sericite (8%): Very fine grains of sericite occur within the rock; they alter plagioclase. Sericite grains are also affected by later chlorite alteration.

Chlorite (10%):

Within host rock (7%): Chlorite grains are up to 400 micrometers and they occur pervasively throughout the rock. Chlorite grains alter plagioclase and sericite.

Within veins 1 and 3 (3%): Chlorite grains occur within veins 1 and 3 where they are associated with carbonate. Chlorite grains replace some carbonate within the veins.

Carbonate (14%): Carbonate grains up to 300 micrometers occur within veins 1, 2, 3, and 4. The grains are associated with chlorite in vein 1 and dominate the other veins.

Sample ID: ML23-NM-005

Rock type: Diorite

Basic description:

The rock comprises plagioclase, quartz, sericite, epidote, chlorite, and carbonate.

The rock is cut by a 300-micrometer-wide chlorite vein. The vein is associated with a 10mm alteration halo, which is dominated by epidote alteration.

Trace amounts of sulfides comprising pyrite are disseminated in the rock.

Paragenesis

Plagioclase -> quartz -> sericite -> carbonate -> chlorite vein -> epidote

Mineralogy

Plagioclase (30%): Grains are up to 1.5mm and they dominate the rock. Plagioclase grains that occur in close proximity to the vein are strongly affected by epidote alteration. Plagioclase grains that are distal from the vein are affected by sericite and chlorite alteration.

Quartz (15%): Very fine grains of quartz up to 100 micrometers occur within the rock in association with plagioclase.

Epidote (20%): Epidote grains are up to 0.7mm, and they occur as an alteration phase, forming a 20 mm halo around the chlorite vein that cuts the rock. Epidote grains within the halo strongly replace plagioclase, carbonate, and sericite grains. Epidote grains are also weakly distributed outside the halo.

Sericite (7%): Fine grains of sericite occur within the rock as an alteration phase affecting plagioclase. Sericite grains are replaced by later epidote and chlorite alteration.

Chlorite (8%): Chlorite grains make up the vein that cuts the rock. They also occur within the host rock, replacing plagioclase and sericite grains. Chlorite is associated with epidotes, which form haloes around the chlorite vein.

Carbonate (5%): Carbonate grains up to 150 micrometers occur pervasively within the rock. The grains are affected by epidote alteration.

Sample ID: ML23-NM-008

Rock type: Dacite

Basic description:

The rock comprises plagioclase, quartz, sericite, carbonate, and chlorite.

The host rock is cut by an undulating vein filled with quartz and carbonate; the vein is up to 10mm wide with a rim made up of chlorite.

Sulfides occur within the host rock comprising pyrite within the vein.

Paragenesis

Plagioclase -> quartz -> sericite -> vein (quartz, carbonate, chlorite, pyrite) -> chlorite

Mineralogy

Plagioclase (25%): Very fine grains of plagioclase occur within the host rock. Plagioclase grains are less than 50 micrometers and are strongly replaced by sericite and chlorite.

Quartz (20%):

Within host rock (15%): Very fine grains of quartz up to 50 micrometers occur in the rock associated with plagioclase.

Within vein (5%): Recrystallized quartz grains up to 100 micrometers occur within the vein. The grains are associated with carbonate, and they show undulatory extinction.

Sericite (15%): Sericite alteration is pervasive within the rock. It occurs in vein-like clusters throughout the rock, giving it a foliated texture. Some sericite grains are replaced by chlorite.

Carbonate (20%): Carbonate grains are the main constituent of the vein; they are up to 200 micrometers large and are associated with quartz and chlorite.

Chlorite (15%):

Within host rock (7%): Chlorite grains occur within the host rock as an alteration phase affecting plagioclase and sericite grains. The grains are up to 400 micrometers in size.

Within vein (8%): Anhedral elongated grains of chlorite occur within the vein dominantly at the rim of the vein. Chlorite grains alter the carbonate grains within the vein and alter the surrounding minerals in contact with the vein rim.

Pyrite (5%): Euhedral to subhedral grains of pyrite occur within the vein. Pyrite grains are up to 500 micrometers and are associated with carbonate.

Sample ID: ML23-NM-009

Rock type: Diorite

Basic description:

The rock comprises plagioclase, quartz, sericite, carbonate, and chlorite.

The rock is associated with various veins:

1 – Undulating vein infilled with carbonate and chlorite cuts the rock.

2 – Quartz-chlorite-carbonate vein cuts the rock. The vein is up to 5mm wide and cuts vein 1.

Sulfides are present in the rock comprising disseminated grains of pyrite.

Paragenesis

Plagioclase -> quartz -> sericite -> vein 1 (carbonate, chlorite) -> vein 2 (quartz, chlorite, carbonate)

Mineralogy

Plagioclase (30%): Plagioclase grains are up to 100 micrometers in size, and they dominate the rock. The grains can also be up to 1mm, and they are strongly affected by sericite and chlorite alteration.

Quartz (35%):

Within host rock (20%): Quartz grains up to 100 micrometers within the host rock. They are associated with plagioclase.

Within vein 2 (15%): Recrystallized quartz grains are up to 2mm within vein 2. The grains are associated with chlorite and carbonate within the vein.

Sericite (5%): Sericite grains occur within the rock altering plagioclase. The grains are very fine and are being replaced by later chlorite alteration.

Chlorite (12%):

Within host rock (5%): Grains are up to 150 micrometers and occur within the rock, replacing plagioclase and sericite grains.

Within veins 1 and 2 (7%): Chlorite grains occur within veins 1 and 2, and they are associated with carbonate and quartz. Within vein 1, chlorite replaces some carbonate grains. Within vein 2, chlorite replaces some quartz and carbonate grains.

Carbonate (7%): The grains are up to 250 micrometers, and they occur dominantly within veins 1 and 2. Carbonate grains are associated with chlorite and quartz. A few grains also occur within the host rock, replacing some sericite grains.

Pyrite (3%): Subhedral grains of pyrite up to 300 micrometers are disseminated within the host rock.

Sample ID: ML23-NM-010

Rock type: Dacite

Basic description:

The host rock comprises plagioclase, quartz, sericite, chlorite, and carbonate.

The rock is cut by a 2mm-wide undulating vein infilled with quartz, carbonate, sulfide, and sericite.

Sulfide is dominantly in veins, and a few grains are disseminated in the host rock. They include pyrite and chalcopyrite.

Paragenesis

Plagioclase -> quartz -> sericite -> carbonate -> vein (quartz, carbonate, pyrite, chalcopyrite, quartz, carbonate) -> chlorite.

Mineralogy

Plagioclase (20%): The grains are commonly about 200 to 400 micrometers with weak sericite alteration and display simple twinning.

Quartz (35%):

Within host rock (25%): Grains up to 300 micrometers dominate the host rock. They display undulatory extinction and bear some inclusions.

Within vein (10%): Recrystallized grains up to 500 micrometers occur in the vein.

Sericite (8%):

Within host rock (3%): Fine grains occur as inclusions in plagioclase within the host rock.

Within vein (5%): Grains up to 20 micrometers occur in clusters within the vein and are aligned parallel to the vein orientation.

Carbonate (12%)

Within host rock (6%): Fine grains of carbonate disseminated in the host rock and are up to 300 micrometers in size.

Within vein (6%): Grains up to 0.7mm are occurring in veins associated with quartz and sericite.

Chlorite (5%): Fine grains up to 100 micrometers occur in the host rock; they are associated with the edge of the vein.

Pyrite (15%): Euhedral to subhedral grains up to 1.5mm in size dominate the vein that cuts the host rock. Pyrite is associated with quartz and carbonate.

Chalcopyrite (5%): Anhedral grains of chalcopyrite up to 100 micrometers occur in the vein. They are dominantly present at pyrite grain boundaries.

Sample ID: ML23-NM-014

Rock type: Dacite

Basic description:

The host rock comprises plagioclase, quartz, sericite, carbonate, chlorite, and epidote.

The rock is associated with various veins:

1 – Early undulating vein infilled with carbonate, quartz, pyrite and epidote.

2 – Late undulating vein infilled with carbonate chlorite, epidote, and pyrite, cutting early vein.

The rock is associated with sulfides, which comprise pyrite and occur dominantly in the veins with minor grains disseminated in host rock.

Paragenesis

Plagioclase -> quartz -> sericite -> carbonate -> vein 1 (carbonate, quartz, pyrite, epidote) -> vein 2 (carbonate, epidote, chlorite, pyrite) -> chlorite

Mineralogy

Plagioclase (35%): Fine to medium grains of plagioclase up to 500 micrometers occur in the host rock; the grains are moderately altered by sericite.

Quartz (28%)

Within host rock (21%): Grains are up to 50 micrometers. The grains are associated with plagioclase grains, and they show undulatory extinction.

Within veins (7%): Recrystallized quartz within vein 1 is associated with carbonate and pyrite. Grains are up to 0.5mm.

Carbonate (10%)

Within host rock (3%): Fine grains up to 300 micrometers are disseminated in the host rock, and the grains are spatially associated with carbonate-rich veins.

Within veins (7%): Grains up to 1mm occur in both early and late veins. They are spatially associated with pyrite.

Sericite (5%): Weak sericite alteration present in the host rock. Grains are up to 100 micrometers and also occur as alteration of plagioclase grains.

Epidote (5%): Grains of up to 200 micrometers occur in vein 2, associated with chlorite.

Chlorite (7%):

Within host rock (3%): Fine grains up to 300 micrometers occur in the host rock, associated with relic plagioclase grains.

Within vein 2 (4%): Anhedral grains up to 0.5mm occur in vein 2.

Pyrite (10%): Euhedral to subhedral grains of pyrite up to 0.5mm occur within the veins, with minor occurrences in the host rock as well as in a disseminated texture.

Sample ID: ML23-NM-016

Rock type: Dacite

Basic description:

The host rock comprises plagioclase, quartz, sericite, carbonate, epidote, and chlorite.

The rock is associated with various veins:

1 – Carbonate vein up to 500 micrometers wide, cutting the host rock.

2 – Late quartz-carbonate vein up to 0.7mm wide cutting vein 1

3 – Late undulating vein infilled with quartz, carbonate, chlorite, pyrite, and sericite. The vein is up to 1.5 mm wide.

Sulfides occur within the rock comprising pyrite with trace amounts of chalcopyrite.

Paragenesis

Plagioclase -> quartz -> sericite -> vein 1 (carbonate) -> vein 2 (quartz, carbonate) -> vein 3 (carbonate, chlorite, pyrite, sericite) -> epidote

Mineralogy

Plagioclase (37%): Grains are up to 200 micrometers; they dominate the host rock and are mostly affected by sericite alteration. Larger grains up to 0.6mm are also present, and these grains are affected by sericite and epidote alteration.

Quartz (33%):

Within host rock (25%): Grains up to 100 micrometers occur in the host rock. Larger recrystallized grains, up to 400 micrometers, occur in proximity to veins. All quartz grains show undulatory extinction.

Within veins (8%): Recrystallized quartz grains up to 0.5mm wide occur in veins and are associated with carbonate grains.

Sericite (10%): Very fine grains of sericite occur as a product of alteration of plagioclase grains. Sericite also occurs as vein infill associated with quartz, carbonate, chlorite, and pyrite in late undulating vein 3.

Carbonate (7%): Carbonate grains occur in all 3 veins that cut the host rock with grain sizes ranging from 100 to 300 micrometers.

Chlorite (5%): Grains up to 200 micrometers wide occur pervasively in the host rock. Chlorite frequently replaces sericite and carbonate grains.

Epidote (3%): Grains up to 200 micrometers wide occur in the host rock. Epidote occurs as a replacement grain associated with a few chlorite and sericite grains in the host rock.

Pyrite (5%): subhedral grains up to 400 micrometers occur within vein 3. A few finer are disseminated within the host rock. Trace amount of chalcopyrite occurs on pyrite grain boundaries.

Sample ID: ML23-NM-017

Rock type: Diorite

Basic description:

The rock comprises plagioclase, quartz, carbonate, sericite, chlorite, and epidote.

The rock is associated with various veins:

1 – chlorite vein cuts the rock. The vein is less than 100 micrometers wide.

2 – Late chlorite-epidote vein up to 50 micrometers wide cuts the rock; the vein also cuts vein 1.

3 – Chlorite-pyrite vein less than 50 micrometers wide cuts the rock. The vein is aligned parallel to vein 1.

Sulfides are present in the rock. They comprise pyrite, which occurs within vein 3.

Paragenesis

Plagioclase -> quartz -> sericites -> carbonate -> vein 1 (chlorite) -> vein 2 (chlorite, epidote) -> vein 3 (chlorite, pyrite)

Mineralogy

Plagioclase (40%): The grains are up to 2mm, and they are strongly altered by epidote and sericite. Plagioclase grains display simple twinning.

Quartz (20%): Anhedral grains of quartz up to 400 micrometers occur within the rock; they are associated with plagioclase. Quartz grains display undulatory extinction.

Sericite (10%): The grains occur within the rock, they alter plagioclase; sericite grains also occur pervasively within the rock.

Epidote (12%): Epidote grains are up to 200 micrometers, and they occur as alteration minerals within plagioclase grains. Epidote also alters carbonate and chlorite grains.

Chlorite (8%): They form multiple veinlets that cut the rock, the veins are associated with epidote and pyrite.

Chlorite also occurs within the rock, replacing carbonate and plagioclase.

Carbonate (7%): Carbonate grains are up to 400 micrometers, and they occur pervasively in clusters within the rock. Carbonate grains alter some plagioclase and sericite grains.

Pyrite (3%): Subhedral grains of pyrite up to 150 micrometers occur within vein 3 in association with chlorite.

Sample ID: ML23-NM-022

Rock type: Diorite

Basic description:

The rock comprises plagioclase, quartz, sericite, chlorite, epidote, and carbonate.

The rock is associated with various veins:

1 – Carbonate vein up to 1mm wide cuts the rock.

2 – Carbonate-quartz vein up to 0.6mm wide cuts the rock. The vein cuts vein 1.

Paragenesis

Plagioclase -> quartz -> sericite -> amphibole -> chlorite -> vein 1 (carbonate) -> vein 2 (carbonate, quartz)

Mineralogy

Plagioclase (30%): Plagioclase grains are up to 400 micrometers, and they dominate the host rock. Plagioclase grains are strongly altered by epidote and chlorite.

Quartz (35%):

Within host rock (30%): Fine grains of quartz up to 100 micrometers occur within the rock. Quartz grains are associated with plagioclase and show undulatory extinction.

Within vein 2 (5%): Recrystallized grains of quartz up to 300 micrometers occur within vein 2. Quartz grains are associated with carbonate within the vein.

Epidote (10%): Epidote occurs as an alteration phase strongly affecting plagioclase grains within the rock. Epidote grains are also replaced by some chlorite alteration.

Amphibole (5%): Amphibole grains are rare within the rock, the grains are up to 200 micrometers. The grains are being replaced by later chlorite alteration.

Chlorite (8%): Chlorite grains occur pervasively throughout the rock. They can be seen replacing epidote, plagioclase, sericite, and carbonate grains. A few chlorite grains occur at the rim of vein 1, replacing carbonate grains.

Carbonate (7%): Carbonate grains in the rock are up to 150 micrometers. They are associated with quartz and chlorite. A few grains also occur pervasively within the rock.

Sericite (5%): Sericite grains are present, and they occur pervasively. They are replaced by chlorite and epidote alteration.

Sample ID: ML23-NM-023

Rock type: Diorite

Basic description:

The rock comprises plagioclase, quartz, sericite, muscovite, chlorite, and carbonate.

The rock is associated with various veins:

1 – Quartz vein cuts the rock, the vein is up to 1mm wide.

2 – Quartz-chlorite vein up to 100 micrometers wide cuts vein 1.

3 – Carbonate vein cuts the rock, the vein is aligned subparallel to vein 1, and the vein is about 0.5mm wide. Sulfides occur in trace amounts comprising disseminated pyrite grains.

Paragenesis

Plagioclase -> quartz -> sericite -> muscovite -> vein 1 (quartz) -> vein 2 (quartz, chlorite) -> vein 3 (muscovite, carbonate)

Mineralogy

Plagioclase (40%): Grains are up to 0.8mm and show simple twinning. Most grains are altered by sericite and some by muscovite grains.

Quartz (34%):

Within host rock (21%): Fine grains up to 200 micrometers make up the host rock. They show undulatory extinction.

Within vein 1 (11%): Recrystallized quartz grains up to 0.6mm. The vein rim is dominated by finer grains of about 300 micrometers.

Within vein 2 (2%): Recrystallized quartz grain up to 100 micrometers associated with thin chlorite vein.

Sericite (11%): Sericite grains are pervasively distributed in the host rock and dominantly present in plagioclase grains. Grains are up to 20 micrometers.

Muscovite (6%)

Within host rock (3%): Grains up to 100 micrometers occur in the host rock as a replacement mineral on plagioclase grains.

Within vein 3 (3%): Fine grains up to 80 micrometers are associated with carbonate in a late vein.

Chlorite (4%): Elongate grains up to 50 micrometers across occur in vein 2 in association with quartz.

Carbonate (4%): Grains up to 200 micrometers occurring in vein 3, associated with muscovite.

Pyrite (1%): Euhedral to subhedral grains disseminated in the host rock, grains are up to 150 micrometers.

Sample ID: ML23-NM-024

Rock type: Dacite

Basic description:

The rock comprises plagioclase, quartz, sericite, carbonate, chlorite, and epidote.

The rock is associated with various veins:

1 – Quartz-carbonate vein up to 7mm wide cuts the host rock. The vein is sheared at the contact with vein 2.

2 – Chlorite-carbonate vein up to 100 micrometers wide cuts the rock. The vein is sheared at the contact with vein 1.

Trace amounts of sulfides occur within the host rock, comprising disseminated pyrite grains.

Paragenesis

Plagioclase -> quartz -> sericite -> vein 1 (quartz, carbonate) -> vein 2 (chlorite, carbonate) -> epidote

Mineralogy

Plagioclase (35%): Fine grains of plagioclase occur within the host rock. Plagioclase grains are up to 100 micrometers and are strongly replaced by epidote, chlorite, and sericite.

Quartz (30%):

Within host rock (15%): Grains of quartz within the host rock are up to 100 micrometers and occur in the rock associated with plagioclase.

Within veins 1 and 2 (15%): Recrystallized quartz grains up to 200 micrometers occur within the veins. The grains are associated with carbonate, and they show undulatory extinction.

Carbonate (10%): Carbonate grains dominantly occur pervasively within the rock. They alter plagioclase. A few grains of carbonate occur within the veins that occur within the rock.

Sericite (5%): Sericite alteration is weak on plagioclase. Sericite grains are affected by later chlorite alteration.

Epidote (10%): Grains of epidote up to 300 micrometers occur pervasively within the host rock. Epidotes replace chlorite grains within the rock.

Chlorite (10%): Chlorite grains are pervasively distributed through the host rock. They occur on the rim of vein 1, replacing carbonates, and they make up vein 2 in association with carbonate.

Sample ID: ML23-NM-025

Rock type: Diorite

Basic description:

The rock comprises plagioclase, quartz, sericite, biotite, epidote, and chlorite.

The rock is associated with various veins:

1 – Multiple quartz veins up to 0.6mm wide cut the rock. The veins are all aligned parallel to each other and have a 2-3mm spacing between them.

2 – Quartz vein cuts the host rock. The vein is up to 2.5mm wide and cuts vein 1.

Sulfides within the rock comprise disseminated pyrite and chalcopyrite grains.

Paragenesis

Plagioclase -> quartz -> biotite -> sericite -> Vein 1 (quartz) -> Vein 2 (quartz) -> epidote -> chlorite

Mineralogy

Plagioclase (25%): Plagioclase grains are up to 2mm, and they dominate the host rock. Most of the plagioclase grains have been replaced by epidote alteration. Plagioclase grains are also affected by weak sericite alteration.

Quartz (30%):

Within host rock (15%): Fine grains of quartz up to 100 micrometers occur within the host rock. Quartz grains are associated with plagioclase.

Within Veins 1 and 2 (15%): Recrystallized grains of quartz make up veins 1 and 2. A cluster of multiple quartz veins with grains up to 0.5mm, spaced 3mm apart, make vein 1. Within vein 2, quartz grains are up to 0.8mm.

Sericite (5%): Sericite grains are up to 50 micrometers, and they occur pervasively within the rock. Sericite grains are strongly replaced by epidote alteration.

Biotite (15%): Biotite grains are up to 200 micrometers. The grains occur pervasively in the rock and are strongly replaced by chlorite grains.

Epidote (15%): Epidote grains occur pervasively in the rock. They strongly replace plagioclase and sericite.

Chlorite (5%): Chlorite grains are present within the rock. They alter biotite and plagioclase grains. Chlorite alteration is also present along the rims of vein 2.

Pyrite (3%): Subhedral grains of pyrite are disseminated within the rock, and the grains are associated with trace amounts of disseminated chalcopyrite grains.

Sample ID: ML23-NM-026

Rock type: Diorite

Basic description:

The host rock comprises plagioclase, quartz, sericite, carbonate, muscovite, and chlorite.

The host rock is highly fractured, with sericite occurring as a gouge, filling the fractures in a vein-like texture associated with carbonate.

Sulfides within the rock comprise disseminated pyrite grains.

Paragenesis

Plagioclase -> quartz -> pyrite -> carbonate -> sericite -> muscovite -> chlorite

Mineralogy

Plagioclase (45%): Grains up to 100 micrometers dominate the host rock. Plagioclase grains display simple twinning and are weakly altered by sericite grains.

Quartz (40%): Fine grains up to 100 micrometers dominate the host rock. Quartz grains are associated with plagioclase, and they display undulatory extinction.

Sericite (20%): Very fine grains up to 20 micrometers occur in the host as an alteration phase replacing plagioclase grains. Sericite also occurs in vein-like textures, filling fractures in the host rock, and is associated with carbonate.

Carbonate (7%): Fine grains up to 300 micrometers occur pervasively in the host rock. Larger carbonate grains up to 0.6mm also occur in association with sericite-dominated gouge zones.

Muscovite (5%): Elongated grains up to 100 micrometers associated with the fractures in the host rock. Muscovite is associated with sericitized zones of the host rock.

Chlorite (3%): Fine grains of chlorite occur pervasively in the host rock. Chlorite grains are associated with sericite and pyrite.

Pyrite (5%): Subhedral grains of pyrite up to 0.8mm are disseminated in the host rock. Pyrite grains are associated with sericite-dominated gouge zones.

Sample ID: ML23-NM-030

Rock type: Carbonate vein cutting a dacite.

Basic description:

The rock comprises plagioclase, quartz, sericite, carbonate, and chlorite.

The rock is cut by a 12mm carbonate-quartz-chlorite-pyrite vein.

Sulfides within the host rock comprise pyrite, which occurs within the carbonate vein.

Paragenesis

Plagioclase -> quartz -> sericite -> vein 1 (carbonate, chlorite, quartz)

Mineralogy

Plagioclase (25%): Fine grains of plagioclase occur within the rock. The grains are up to 400 micrometers and are altered by sericite and carbonate.

Quartz (30%):

Within host rock (25%): Quartz grains are up to 200 micrometers within the host rock. Quartz grains are coarser up to 400 micrometers in close proximity to the vein.

Within vein (5%): Grains up to 0.7mm occur within the main vein that cuts the rock. Quartz is associated with chlorite and carbonate within the vein.

Carbonate (25%):

Within host rock (5%): Carbonate grains occur as vein-like clusters around the vein and pervasively within the rock. The grains are up to 100 micrometers, and they alter plagioclase within the host rock.

Within carbonate vein (20%): Carbonate grains up to 2mm make up the vein that cuts the host rock. The grains are associated with pyrite and quartz. Chlorite alters some carbonate grains at the rim of the vein.

Sericite (8%): Sericite occurs pervasively within the host rock, with grains forming clusters throughout the rock. A few grains also alter plagioclase.

Chlorite (5%): Chlorite grains are up to 200 micrometers and dominantly occur within the vein. Chlorite grains within the vein are concentrated at the rim of the vein, and they are associated with quartz.

Pyrite (7%): Subhedral grains up to 0.6mm occur dominantly within the carbonate vein that cuts the host rock. Trace amount of pyrite also occurs disseminated in the rock.

Sample ID: ML23-NM-033

Rock type: Quartz-carbonate-pyrite vein cutting a dacite

Basic description:

The host rock comprises plagioclase, quartz, sericite, carbonate, and chlorite

The host rock is associated with various veins:

1 – Carbonate veinlet up to 400 micrometers wide cuts the rock.

2 – 14mm wide quartz-carbonate-pyrite vein cutting the host rock and cutting vein 1.

Sulfides within the host rock comprise pyrite, which occurs within veins.

Paragenesis

Plagioclase -> quartz -> sericite -> vein 1 (carbonate) -> vein 2 (carbonate, quartz, pyrite) -> chlorite

Mineralogy

Plagioclase (20%): Grains up to 100 micrometers dominate the host rock. Coarser grains up to 0.7mm also occur; they display simple twinning and are altered by sericite grains.

Quartz (30%):

Within host rock (20%): Fine grains of quartz up to 200 micrometers. Quartz grains are associated with plagioclase, and they display undulatory extinction.

Within vein 2 (10%): Recrystallized grains up to 0.6mm occurring within the vein in association with carbonate and pyrite.

Sericite (5%): Anhedral grains up to 50 micrometers are weakly distributed throughout the host rock. Sericite is dominantly present as alteration grains within coarser plagioclase grains.

Carbonate (10%): Grains up to 300 micrometers occurring within veins 1 and 2. Carbonate grains are associated with quartz and pyrite.

Chlorite (5%): Fine grains up to 100 micrometers occur as alteration grains within plagioclase grains and also pervasively in the groundmass.

Pyrite (15%): Subhedral grains up to 0.5mm occur within vein 1, associated with quartz and carbonate. Trace amount of pyrite is also disseminated within the host rock.

Chalcopyrite (5%): Anhedral grains of chalcopyrite occur within vein 1 in association with pyrite.

Sample ID: ML23-NM-036

Rock type: Dacite

Basic description:

The host rock comprises plagioclase, quartz, sericite, chlorite, and carbonate.

The rock is associated with various veins:

1 – Carbonate-quartz-pyrite vein up to 5mm wide cut the host rock.

2 – carbonate-quartz-pyrite vein of similar width cuts vein 1. The vein is aligned perpendicular to vein 1.

Sulfides are present within the rock, dominantly comprising pyrite.

Paragenesis

Plagioclase -> quartz -> chlorite -> vein 1(carbonate, quartz, pyrite) -> vein 1(carbonate, quartz, pyrite) -> sericite

Mineralogy

Plagioclase (25%): Grains of plagioclase up to 0.5mm dominate the host rock, and they are weakly altered by sericite and chlorite. Plagioclase grains show simple twinning.

Quartz (35%):

Within host rock (25%): Fine grains up to 100 micrometers occur within the host rock. Quartz grains are associated with plagioclase, and they display undulatory extinction.

Within veins (10%): Recrystallized grains up to 400 micrometers occurring within veins 1 and 2. Quartz grains are associated with pyrite and carbonate within veins.

Carbonate (10%): Grains up to 200 micrometers dominate veins 1 and 2. Carbonate and pyrite are the major components of veins 1 and 2,

Pyrite (20%): Subhedral grains of pyrite occur within the veins that cut the host rock. Pyrite grains can be up to 3mm and dominate the veins.

Chlorite (5%): Grains are up to 400 micrometers, and they occur pervasively through the host rock. A few grains occur within plagioclase grains as alteration minerals.

Sericite (5%): Very fine grains up to 50 micrometers occurring within plagioclase grains. Sericite alters plagioclase in association with chlorite.

Sample ID: ML23-NM-038

Rock type: Andesite

Basic description:

The host rock comprises plagioclase, quartz, sericite, epidote, chlorite, and carbonate

The rock is associated with various veins:

1 – Undulating vein infilled with epidote and minor carbonate. The vein is 2mm wide with a greenish halo.

2 – Quartz-carbonate-epidote-chlorite vein up to 1cm wide, cuts vein 1. The vein has an epidote-dominated rim.

3 – Carbonate-quartz vein cuts vein 2. Vein 3 is aligned parallel to vein 1.

The rock is associated with sulfides, which comprise trace amount of pyrite and chalcopyrite.

Paragenesis

Plagioclase -> quartz -> sericite -> carbonate -> chlorite -> vein 1 (epidote, carbonate) -> vein 2 (quartz, carbonate, epidote, chlorite) -> vein 3 (carbonate, quartz)

Mineralogy

Plagioclase (35%): Fine grains up to 150 micrometers dominate the host rock. They are mostly altered by epidote and sericite, and the grains display simple twinning.

Quartz

Within host rock (25%): Fine grains of quartz within the host rock are generally sized within 50 to 100 micrometers in size. They are associated with plagioclase, and they display undulatory extinction.

Within veins 2 and 3 (10%): Recrystallized grains up to 400 micrometers occur within the veins.

Sericite (5%): Very fine grains less than 50 micrometers occurring as alteration grains within plagioclase grains. They are also associated with quartz and chlorite.

Chlorite (10%): Grains are up to 150 micrometers and occur within vein 2. Chlorite grains are associated with quartz, carbonate, and epidote within veins. Some of the grains occur as inclusions within recrystallized quartz grains.

Carbonate (5%): Grains are up to 250 micrometers and occur in all veins that cut the host rock. Carbonate grains are associated with chlorite, epidote, and quartz.

Epidote (7%): Grains up to 0.6mm wide occur within veins 1 and 2. Epidote occurs as a replacement grain associated with quartz and carbonate within the veins. Epidote grains can be smaller to about 50 micrometers, and these grains dominantly occur at the edge of the veins.

Sample ID: ML23-NM-043

Rock type: Diorite

Basic description:

The rock comprises plagioclase, quartz, sericite, carbonate, epidote, and chlorite.

The rock is associated with multiple veins:

1 – Epidote quartz vein up to 0.6mm wide cuts the rock.

2 – Carbonate quartz vein up to 0.6mm wide cuts the rock. The vein also cuts vein 1.

Sulfides are present comprising pyrite, which are disseminated in the rock.

Paragenesis

Plagioclase-> quartz -> sericite -> Vein 1 (epidote, quartz) -> Vein 2 (carbonate, quartz) -> chlorite -> epidote

Mineralogy

Plagioclase (40%): Plagioclase grains have a bimodal distribution within the rock. They consist of phenocrysts up to 4mm and fine grains up to 100 micrometers. Plagioclase grains are strongly replaced by epidote and sericite alteration.

Quartz (30%):

Within host rock (25%): Fine grains of quartz occur within the host rock. The grains are up to 100 micrometers and are associated with plagioclase.

Within veins (5%): Quartz grains within the veins are larger, up to 350 micrometers. There are minor components of the veins and are associated with epidote and carbonate.

Sericite (5%): Sericite grains occur pervasively within the rock. They also occur as a weak alteration phase of plagioclase grains.

Carbonate (7%): Carbonate grains up to 150 micrometers occur within vein 2. Carbonate grains are associated with quartz in the vein. A few grains of carbonate are also pervasively distributed in the rock.

Chlorite (5%): Chlorite grains are up to 100 micrometers, and they occur pervasively within the rock. They replace sericite and plagioclase grains.

Epidote (10%): Epidote grains dominantly occur as an alteration phase, replacing plagioclase grains. They can be up to 200 micrometers in size and are also pervasively distributed in the rock, replacing plagioclase and chlorite grains.

Pyrite (3%): Subhedral grains of pyrite up to 200 micrometers are disseminated in the host rock.

Sample ID: ML23-NM-046

Rock type: Diorite

Basic description:

The rock comprises plagioclase, quartz, sericite, chlorite, and carbonate.

The rock is strongly sheared with a sericite-dominated shear texture.

Undulatory quartz-carbonate-pyrite vein up to 8mm wide cuts the rock. The vein is aligned parallel to the shear texture.

Ore minerals present within the host rock comprise pyrite, chalcopyrite, and trace amounts of gold.

Paragenesis

Plagioclase -> quartz -> sericite -> vein (quartz, carbonate, pyrite) -> chlorite

Mineralogy

Plagioclase (20%): Fine grains of plagioclase up to 150 micrometers dominate the sample. A few larger grains of plagioclase also occur; all plagioclase grains are affected by sericite alteration.

Quartz (33%):

Within host rock (20%): Fine grains of quartz up to 200 micrometers occur within the host rock associated with plagioclase. Quartz grains display undulatory extinction

Within vein (13%): Quartz grains within the vein range in size from 100 to 400 micrometers and are associated with carbonate and pyrite grains.

Sericite (15%): Sericite grains occur in a sericite-dominated shear texture that dominates the host rock. They also occur as alteration phases within plagioclase grains.

Carbonate (8%):

Within host rock (3%): Fine grains up to 200 micrometers occur within the host rock. Carbonate grains are associated with disseminated pyrite within the rock.

Within vein (5%): Carbonate grains within the vein are up to 0.8mm in size, and they are associated with quartz, pyrite, and gold.

Chlorite (5%): Fine grains of chlorite up to 200 micrometers occur pervasively distributed in the rock.

Pyrite (15%):

Within vein (10%): Subhedral pyrite grains up to 1mm occur dominantly within the vein. Pyrite grains are associated with carbonate, chalcopyrite, and trace amounts of gold.

Within host rock (5%): Pyrite grains range from 100 to 500 micrometers and are disseminated in the host rock. The grains are aligned parallel to the shear texture of the host rock.

Chalcopyrite (4%): Grains are up to 400 micrometers and are mostly disseminated within the host rock, with a few grains occurring within the vein.

Sample ID: ML23-NM-047

Rock type: Dacite

Basic description:

The rock comprises plagioclase, quartz, sericite, carbonate, and chlorite.

The rock is associated with various veins:

1 – Undulatory carbonate vein up to 400 micrometers wide cuts the rock.

2 – Quartz-carbonate veins up to 1.1mm cuts the rock. The vein cuts and offsets vein 1.

Paragenesis

Plagioclase -> quartz -> sericite -> chlorite -> vein 1 (carbonate) -> vein 2 (quartz, carbonate)

Mineralogy

Plagioclase (35%): Fine grains of plagioclase dominate the rock; they are up to 100 micrometers and display simple twinning. Plagioclase grains are affected by sericite and chlorite alteration.

Quartz (40%):

Within host rock (33%): The grains are up to 200 micrometers, and they are associated with plagioclase within the rock. Quartz grains show undulatory extinction.

Within vein 2 (7%): Recrystallized grains of quartz within vein 2 are up to 0.7mm, and they dominate the vein. Quartz grains occur in association with carbonate.

Sericite (15%): Sericite grains are present in the rock. They alter plagioclase grains. The grains are also pervasively distributed within the rock.

Carbonate (5%): Carbonate grains are up to 300 micrometers, and they occur within veins 1 and 2. Carbonate grains make up vein 1, and they are associated with quartz in vein 2. The grains have a dark reddish-brown tint, which is possibly a result of iron enrichment within the carbonate minerals.

Chlorite (5%): Chlorite occurs within the rock as elongated grains. They replace plagioclase and sericite grains.

Sample ID: ML23-NM-053

Rock type: Diorite

Basic description:

The rock comprises plagioclase, quartz, epidote, carbonate, and chlorite.

The rock is associated with multiple veins:

1 – Pyrite epidote vein up to 100 micrometers wide cuts the rock

2 – Undulating vein filled with carbonate, chlorite, and quartz cuts the rock. The vein exhibits a pinch and swell texture. The vein is up to 4mm at the widest point and about 200 micrometers at the narrowest point.

Sulfides are present within the rock comprising pyrite. Pyrite grains occur within veins and are also disseminated within the rock.

Paragenesis

Plagioclase -> quartz -> Epidote -> Vein 1 (pyrite, epidote) -> Vein 2 (chlorite, carbonate, pyrite)

Mineralogy

Plagioclase (43%): Plagioclase grains have a bimodal distribution. They comprise of phenocrysts up to 3.5mm and fine grains up to 100 micrometers. Plagioclase grains are strongly altered by epidote alteration.

Quartz (25%):

Within host rock (22%): Quartz grains are up to 50 micrometers within the host rock. The grains are associated with plagioclase and undulatory extinction.

Within vein 2 (3%): Quartz grains within vein 2 are up to 150 micrometers and they are associated with carbonate and chlorite grains.

Epidote (15%): Epidote grains occur within the rock as an alteration phase within plagioclase. Epidote grains also occur in vein 1 in association with pyrite.

Chlorite (7%): Chlorite grains occur within vein 2 in association with carbonate and quartz. A few grains of chlorite up to 100 micrometers are also present in the rock, replacing some epidote and plagioclase grains.

Carbonate (3%): Carbonate grains are up to 200 micrometers, and they occur within vein 2. Carbonate grains are associated with chlorite and quartz.

Pyrite (7%): Subhedral grains of pyrite up to 300 micrometers occur within the rock. Pyrite grains dominate vein 1 in association with epidote. Pyrite grains are also disseminated within the rock.

Sample ID: ML23-NM-055

Rock type: Diorite

Basic description:

The rock comprises plagioclase, quartz, sericite, epidote, chlorite, and carbonate.

The rock is associated with various veins:

1 – Undulatory epidote-chlorite-quartz vein cuts the rock. The vein is up to 1mm wide.

2 – Epidote vein cuts the rock. The vein is up to 0.8mm wide and is aligned subparallel to vein 1.

3 – Carbonate-quartz vein cuts the rock. The vein is up to 1mm wide and shrinks to about 150 micrometers, where it cuts veins 1 and 2.

Paragenesis

Plagioclase -> quartz -> sericite -> vein 1 (epidote, chlorite, quartz) -> vein 2 (epidote) -> vein 3 (carbonate, quartz)

Mineralogy

Plagioclase (30%): Grains are up to 1mm, and they dominate the rock. Plagioclase grains are strongly altered by sericite and epidote within the rock.

Quartz (40%):

Within host rock (35%): Quartz grains are up to 100 micrometers, and they are associated with plagioclase within the rock. Most of the grains are very fine and make up a groundmass texture around plagioclase grains.

Within veins 1 and 3 (5%): Recrystallized grains of quartz up to 200 micrometers occur within veins 1 and 3. Quartz grains occur in association with carbonate and epidote.

Sericite (15%): Sericite grains are present in the rock, and the grains are very fine, occurring dominantly within plagioclase grains. Sericite grains also form clusters in proximity to vein 2.

Carbonate (5%): Carbonate grains are up to 100 micrometers and occur within vein 3. Carbonate grains are associated with quartz in vein 2.

Epidote (7%): Anhedral grains of epidote up to 250 micrometers occur within the rock, dominantly within veins 1 and 2. Epidote grains also occur as an alteration phase on plagioclase.

Chlorite (5%): Chlorite is present in the rock as an alteration phase within plagioclase. Some chlorite grains are affected by later epidote alteration.

Sample ID: ML23-NM-058

Rock type: Diorite

Basic description:

The rock comprises plagioclase, quartz, sericite, epidote, carbonate, biotite, and chlorite.

The host rock is associated with various veins:

1 – Carbonate-quartz-epidote vein up to 5mm wide cuts the rock.

2 – Carbonate-epidote vein cuts the rock. The vein is 1.5mm wide and is aligned parallel to vein 1.

Sulfides are present within the host rock, comprising pyrite disseminated in the rock.

Paragenesis

Plagioclase -> quartz -> sericite -> biotite -> vein 1 (carbonate, quartz, epidote) -> vein 2 (carbonate, epidote)

Mineralogy

Plagioclase (30%): Grains are up to 300 micrometers, and they dominate the rock. Plagioclase grains are strongly altered by sericite and chlorite.

Quartz (23%):

Within host rock (20%): Quartz grains are up to 300 micrometers within the host rock and associated with plagioclase. Quartz grains show undulatory extinction.

Within vein 1 (3%): Recrystallized grains of quartz up to 200 micrometers occur within vein 1. Quartz grains occur in association with carbonate and epidote.

Biotite (10%): Anhedral grains of biotite are present within the rock. The grains are up to 250 micrometers. They are altered by epidote grains.

Sericite (5%): Sericite grains are present in the rock, and the grains are very fine, occurring dominantly within plagioclase grains.

Carbonate (10%): Carbonate grains are up to 0.6mm. They occur dominantly within veins 1 and 2. Carbonate grains are associated with epidote in the veins.

Epidote (7%): Anhedral grains of epidote up to 300 micrometers occur within the rock, dominantly within veins 1 and 2. Epidote grains also occur within the host rock, replacing biotite grains.

Chlorite (5%): Chlorite is present in the rock as an alteration phase within plagioclase. Some chlorite grains are affected by later epidote alteration.

Pyrite (5%): Subhedral grains of pyrite up to 200 micrometers are present, and the grains are disseminated in the rock.

Sample ID: ML23-NM-059

Rock type: Diorite

Basic description:

The rock comprises plagioclase, quartz, chlorite, epidote, sericite, and carbonate.

The rock is associated with various veins:

1 – Undulating vein filled with carbonate, pyrite, and quartz cuts the host rock. The vein is up to 3.5mm wide.

2 – Undulating vein up to 200 micrometers wide, filled with carbonate and chlorite. The vein cuts and offsets vein 1.

Sulfides occur within the host rock; they comprise pyrite, which occurs in veins.

Paragenesis

Plagioclase -> quartz -> sericite -> vein 1 (carbonate, pyrite, quartz) -> epidote -> vein 2 (carbonate, chlorite)

Mineralogy

Plagioclase (40%): Plagioclase grains are up to 0.6mm, and they dominate the host rock. Plagioclase grains are being altered by epidote, chlorite, and sericite. Plagioclase grains show simple twinning.

Quartz (25%): Quartz grains are up to 200 micrometers and comprise the host rock. A few recrystallized quartz grains up to 0.6mm occur within vein 1 in association with carbonate.

Epidote (10%): Grains are up to 300 micrometers and occur pervasively within the host rock. Some epidote grains alter plagioclase in association with chlorite.

Carbonate (7%): Carbonate grains are up to 200 micrometers and dominantly occur within veins 1 and 2. Carbonate grains also occur in vein-like clusters around the veins.

Chlorite (5%): Chlorite grains occur pervasively within the host rock; the grains are up to 300 micrometers in size and alter plagioclase and epidote. A few chlorite grains occur within vein 2 as vein infill associated with carbonate.

Sericite (3%): Grains of sericite occur within plagioclase grains as an alteration phase and are altered by chlorite.

Pyrite (10%): Pyrite grains up to 0.7mm occur dominantly within veins 1 and 2. Pyrite is the main constituent of vein 1 and is much less abundant in vein 2. A few grains also occur in a disseminated texture within the host rock.

Sample ID: ML23-NM-060

Rock type: Diorite

Basic description:

The rock comprises plagioclase, quartz, sericite, chlorite, carbonate, and epidote.

The rock is associated with various veins:

1 – Carbonate vein cuts the rock. The vein is up to 0.6mm wide.

2 – Chlorite-quartz-epidote vein cuts the rock. The vein is up to 7.5mm wide and cuts vein 1.

Sulfides are present in the rock comprising pyrite and trace amounts of chalcopyrite occurring within vein 2.

Paragenesis

Plagioclase -> quartz -> sericite -> vein 1 (carbonate) -> vein 2 (quartz, epidote)

Mineralogy

Plagioclase (40%): Plagioclase grains are up to 0.6mm, and they dominate the rock. Plagioclase is weakly altered by sericite and epidote grains.

Quartz (25%): Quartz grains within the rock are up to 150 micrometers. Quartz grains are associated with plagioclase, and they display undulatory extinction. A few grains of quartz occur on the rim of vein 2 in association with epidote and chlorite grains.

Sericite (5%): Sericite grains are present within the rock as an alteration phase affecting plagioclase. A few grains of sericite also occur pervasively in the rock, and they are altered by later chlorite alteration.

Epidote (12%):

Within the host rock (7%): Epidote grains occur within the rock as an alteration phase, replacing plagioclase grains. The grains are up to 150 micrometers.

Within vein 2 (5%): Epidote grains occur within vein 2 dominantly on the rims of the vein. Epidote veins occur in association with chlorite, carbonate, and quartz grains.

Chlorite (10%): Chlorite grains dominantly occur within vein 2, associated with epidote and quartz. Chlorite grains also occur within the rock, replacing sericite and epidote.

Carbonate (5%): Carbonate grains within the rock are up to 20 micrometers, and they make up vein 1.

Pyrite (3%): Pyrite grains are present within the rock. The grains are up to 0.6 micrometers, and they occur within vein 2. A few grains are disseminated within the rock and associated with trace amounts of chalcopyrite.

Sample ID: ML23-NM-061

Rock type: Diorite

Basic description:

The rock comprises plagioclase, quartz, sericite, epidote, carbonate, and chlorite.

The rock is associated with various veins:

1 – Chlorite- carbonate vein up to 100 micrometers wide cuts the host rock.

2 – Carbonate-quartz vein up to 3mm wide cuts the host rock. The vein also cuts vein 1.

Paragenesis

Plagioclase -> quartz -> sericite -> epidote -> vein 1 (chlorite, carbonate) -> vein 2 (carbonate, quartz)

Mineralogy

Plagioclase (35%): Plagioclase grains up to 300 micrometers dominate the rock. Plagioclase grains are strongly altered by epidote.

Quartz (25%):

Within host rock (20%): Fine grains of quartz up to 100 micrometers occur within the rock. The grains are associated with plagioclase and make up the host rock.

Within vein 2 (5%): Recrystallized grains of quartz occur within vein 2. Quartz grains within the vein are associated with carbonate grains.

Carbonate (10%): Carbonate grains are very fine, up to 50 micrometers, and they occur dominantly within vein 1. Within vein 1, carbonate grains are affected by a reddish tint, which could indicate a higher iron content of the carbonate mineral. A few carbonate grains are associated with chlorite in vein 2.

Epidote (15%): Epidote grains occur as an alteration phase replacing plagioclase grains. The grains can be up to 200 micrometers and also occur pervasive in the rock. Epidote grains are affected by later chlorite alteration.

Sericite (5%): Sericite grains are very fine and occur pervasively within the rock. They weakly alter plagioclase grains and are strongly replaced by later epidote and chlorite alteration.

Chlorite (10%): Chlorite grains occur pervasively within the rock, replacing sericite and epidote grains. Chlorite grains also make up vein 1, which cuts the rock. They are associated with carbonate grains.

Sample ID: ML23-NM-063

Rock type: Diorite

Basic description:

The rock comprises plagioclase, quartz, sericite, carbonate, chlorite, and epidote.

The rock is associated with various veins:

1 – Carbonate vein up to 1.2mm wide cuts the rock.

2 – Carbonate vein up to 0.8mm wide cuts the rock. The vein is aligned parallel to vein 1.

3 – Pyrite-carbonate vein cuts the rock. The vein is up to 7mm at the widest point and about 200 micrometers wide at the narrowest point.

Sulfides are present within the rock comprising of pyrite occurring within vein 3.

Paragenesis

Plagioclase -> quartz -> sericite -> epidote -> vein 1 (carbonate) -> vein 2 (carbonate) -> vein 3 (pyrite, carbonate) -> chlorite

Mineralogy

Plagioclase (35%): The grains are up to 2mm, and they dominate the rock. Plagioclase grains are affected by epidote and sericite alteration. The grains display simple twinning.

Quartz (30%): Quartz grains are up to 200 micrometers within the rock, and they display undulatory extinction. They are associated with plagioclase grains within the rock.

Sericite (5%): Fine grains of sericite occur pervasively within the rock. They are also present as an alteration phase within plagioclase. Sericite grains have been replaced by later carbonate and chlorite alteration.

Chlorite (5%): Chlorite grains occur pervasively within the rock. The grains are up to 100 micrometers and strongly replace plagioclase and sericite grains.

Carbonate (10%): Carbonate grains are up to 300 micrometers, and they make up veins 1 and 2. The grains also occur within vein 3 in association with pyrite.

Epidote (8%): Epidote grains are very fine and occur as an alteration phase within plagioclase grains. Epidote grains are associated with chlorite alteration.

Pyrite (7%): Pyrite grains are up to 3mm, and they occur entirely within vein 3. They are associated with carbonate and trace amounts of chalcopyrite, which also occurs in vein 3.

Sample ID: ML23-NM-064

Rock type: Diorite

Basic description:

The rock comprises plagioclase, quartz, sericite, carbonate, and chlorite.

The rock is associated with various veins:

1 – Quartz-pyrite-carbonate vein up to 5mm wide cuts the rock

2 – Carbonate vein up to 2mm wide cuts vein 1.

3 – Undulating vein infilled with carbonate and chlorite cuts vein 1.

Sulfides are present within the host rock comprising pyrite.

Paragenesis

Plagioclase -> quartz -> sericite -> vein 1 (quartz, carbonate, pyrite) -> vein 2 (carbonate) -> vein 3 (carbonate, chlorite).

Mineralogy

Plagioclase (40%): Plagioclase grains are up to 1mm, and they dominate the rock. Some grains are also less than 100 micrometers, and these are strongly replaced by sericite alteration. The coarser grains have sericite alteration within them.

Quartz (25%):

Within host rock (15%): Fine grains of quartz up to 50 micrometers occur within the host rock. Quartz grains are associated with plagioclase.

Within vein 1 (10%): Quartz grains up to 0.6mm occur within vein 1. They dominate the vein and are associated with carbonate and pyrite.

Sericite (10%): Sericite grains are present in the rock. The grains are very fine, and they strongly alter plagioclase. Sericite grains are replaced by chlorite alteration.

Carbonate (10%): Carbonate grains are up to 300 micrometers. They occur dominantly within veins 1 and 2. Carbonate grains are associated with chlorite in vein 2.

Chlorite (5%): Chlorite is present in the rock as an alteration phase affecting sericite and carbonate grains. Chlorite grains also occur within vein 3, where they replace some carbonate grains.

Pyrite (10%): Euhedral to subhedral grains of pyrite up to 1mm occur within the host rock. Pyrite grains occur dominantly within vein 1, with a few grains disseminated within the host rock.

Sample ID: ML23-NM-065

Rock type: Diorite

Basic description:

The rock comprises plagioclase, quartz, chlorite, sericite, and carbonate.

The host rock is associated with various veins:

1 – Undulating vein up to 150 micrometers. The vein is filled with quartz and chlorite.

2 – Carbonate-chlorite-quartz vein up to 0.6mm wide cuts the rock. The vein also cuts vein 1.

Sulfides are present and comprise trace amounts of pyrite disseminated in the host rock.

Paragenesis

Plagioclase -> quartz -> sericite -> vein 1 (quartz, chlorite) -> vein 2 (carbonate, chlorite, quartz)

Mineralogy

Plagioclase (40%): Plagioclase grains are up to 0.6mm and dominate the host rock. The grains are mostly altered by sericite and chlorite. Plagioclase grains can also be finer, with grains around 200 micrometers.

Quartz (25%):

Within host rock (20%): Quartz grains are up to 300 micrometers and dominate the host rock. Quartz grains tend to be larger up to 0.6mm near veins.

Within veins (5%): Recrystallized quartz grains up to 400 millimeters occur within veins 1 and 2. Quartz grains occur on the rims of the veins.

Chlorite (15%):

Within host rock (8%): Chlorite grains are present within the host, occurring as alteration phases within plagioclase grains and pervasively in the host rock.

Within veins (7%): Elongated chlorite grains are the dominant mineral in veins 1 and 2. They are associated with quartz and carbonate within the veins.

Sericite (15%): Very fine grains of sericite occur pervasively within the host rock and within plagioclase grains as an alteration phase. Some sericite grains are undergoing replacement by chlorite.

Carbonate (5%): Carbonate grains are fine with sizes less than 200 micrometers; they occur within vein 2 and in the surrounding groundmass. The grains are associated with quartz and carbonate.

Sample ID: ML23-NM-066

Rock type: Diorite

Basic description:

The rock comprises plagioclase, quartz, sericite, chlorite, carbonate, and epidote.

The rock is associated with various veins:

1 – Carbonate-chlorite undulating vein up to 7mm wide cuts the rock.

2 – Carbonate vein up to 1mm wide cuts the rock. The vein is aligned parallel to vein 1.

3 – Carbonate-chlorite up to 0.7mm wide cuts the rock. The vein is aligned parallel to veins 1 and 2.

4 – Undulatory carbonate-pyrite vein up to 1.2mm wide cuts the rock. The vein cuts and offsets veins 1, 2, and 3.

Sulfides are present within the rock, comprising disseminated pyrite grains.

Paragenesis

Plagioclase -> quartz -> sericite -> epidote -> vein 1 (carbonate, chlorite) -> vein 2 (carbonate) -> vein 3 (carbonate, chlorite) -> vein 4 (carbonate, pyrite)

Mineralogy

Plagioclase (40%): Plagioclase grains are up to 1.5mm, and they dominate the host rock. The grains are replaced by sericite and epidote.

Quartz (20%): Quartz grains are very fine, up to 50 micrometers, and they occur in association with plagioclase within the rock. The grains can be up to 200 micrometers near the veins.

Sericite (5%): Very fine grains of sericite are present within the rock. Sericite grains occur as an alteration phase affecting plagioclase.

Carbonate (17%): Carbonate grains are up to 300 micrometers, and they occur dominantly within veins 1, 2, 3, and 4. Carbonate grains are associated with chlorite within veins 1, 3, and 4.

Chlorite (8%): Chlorite grains are present within the rock, occurring within veins 1, 3, and 4. Chlorite grains within the veins are associated with carbonate.

Epidote (7%): Epidote grains are present within the rock. The grains are up to 200 micrometers, and they occur pervasively within the rock. Epidote grains replace plagioclase and chlorite grains in the rock.

Pyrite (3%): Subhedral grains of pyrite occur within the rock. A few grains are disseminated while other grains are present within vein 1.

Sample ID: ML23-NM-067

Rock type: Andesite

Basic description:

The host rock comprises plagioclase, quartz, sericite, chlorite, carbonate, and epidote. The rock is cut by a quartz-chlorite vein that is up to 5mm wide. The vein has a 10mm wide zone dominated by quartz, forming a halo around it.

Paragenesis

Plagioclase -> quartz -> sericite -> epidote -> quartz-chlorite vein

Mineralogy

Plagioclase (25%): grains are up to 200 micrometers and are altered by sericite and epidote. Plagioclase grains display simple twinning.

Quartz (40%):

Within host rock (20%): Quartz grains are up to 200 micrometers within the host rock. The grains occur dominantly around the vein, forming a 10mm wide quartz-rich halo on either side of the vein.

Within vein (20%): Recrystallized grains of quartz up to 4mm occur within the vein. Quartz grains are being replaced by chlorite grains, which occur within the vein.

Sericite (8%): Sericite grains are present in the rock. They alter plagioclase and are altered by some carbonate and chlorite grains.

Carbonate (5%): Carbonate grains are up to 200 micrometers. They dominantly affect plagioclase within the rock. Carbonate grains are associated with chlorite and sericite.

Epidote (7%): Grains of epidote up to 100 micrometers occur within the rock, dominantly as pervasive alteration grains. Some grains of epidote replace plagioclase and chlorite.

Chlorite (15%):

Within host rock (7%): Chlorite is present in the rock; the grains are up to 100 micrometers and occur pervasively. Chlorite grains are affected by later epidote alteration.

Within vein (8%): Anhedral grains of chlorite within the vein display a flaky texture and replace quartz grains within the vein.

Sample ID: ML23-NM-068

Rock type: Andesite

Basic description:

The rock comprises plagioclase, quartz, sericite, chlorite, carbonate, and epidote.

The rock is associated with various veins:

1 – Quartz-pyrite-carbonate vein up to 2mm wide cuts the host.

2 – Carbonate vein up to 150 micrometers wide cuts vein 1 and causes a 2mm offset to the earlier vein.

Sulfide grains are present within the rock and comprise pyrite, which occurs dominantly within vein 1.

Paragenesis

Plagioclase -> quartz -> sericite -> vein 1 (quartz, pyrite, carbonate) -> vein 2 (carbonate) chlorite -> epidote

Mineralogy

Plagioclase (30%): Grains of plagioclase up to 100 micrometers occur within the rock. The grains are very fine and strongly replaced by sericite and carbonate.

Quartz (20%):

Within host rock (13%): Quartz grains can be up to 200 micrometers within the host rock. The grains are slightly larger when they occur close to vein 1

Within vein 1 (7%): Grains up to 0.6mm occur within vein 1. Quartz grains are associated with pyrite and carbonate within vein 1.

Carbonate (10%):

Within host rock (5%): Carbonate grains are present, and they alter plagioclase grains within the rock. The grains are up to 1mm.

Within veins 1 and 2 (5%): Carbonate grains up to 0.6mm occur within vein 1. They are associated with pyrite and quartz. Finer grains less than 150 micrometers make up vein 2.

Sericite (15%): Sericite grains strongly alter plagioclase within the rock. Sericite grains also occur pervasively within the rock.

Chlorite (5%): Chlorite grains are up to 200 micrometers; they alter sericite, carbonate, and plagioclase grains within the host rock. Chlorite grains also occur around the rims of vein 1 associated with quartz.

Epidote (10%): Epidote grains occur pervasively within the rock. A few grains of epidote can be seen replacing chlorite grains within the rock.

Pyrite (10%): Subhedral grains of pyrite up to 2mm occur dominantly within vein 1. A few finer grains, up to 200 micrometers, are disseminated in the rock.

Sample ID: ML23-NM-070

Rock type: Dacite

Basic description:

The rock comprises plagioclase, quartz, sericite, amphibole, carbonate and chlorite.

The rock is associated with various veins:

1 – Carbonate-pyrite vein up to 7mm wide cuts the host rock.

2 – Carbonate-quartz vein up to 1.5mm wide, the vein is aligned parallel to vein 1.

Sulfides are present within the host rock, and they comprise pyrite, which occurs within vein 1.

Paragenesis

Plagioclase -> quartz -> amphibole -> sericite -> amphibole -> vein 1 (carbonate, pyrite) -> vein 2 (carbonate, quartz)

Mineralogy

Plagioclase (37%): Grains of plagioclase are up to 400 micrometers and dominate the rock. Finer grains of plagioclase that are less than 100 micrometers are strongly affected by sericite alteration.

Quartz (25%):

Within host rock (20%): Fine grains of quartz up to 100 micrometers occur within the rock in association with plagioclase. Quartz grains are larger up to 300 micrometers near vein 1.

Within vein 2 (5%): Grains are up to 400 micrometers and occur dominantly on the rims of vein 2.

Sericite (10%): Very fine grains of sericite occur pervasively within the rock. Sericite alteration affects fine plagioclase grains and is affected by later chlorite alteration.

Amphibole (5%): Anhedral grains of amphibole up to 200 micrometers occur pervasively within the rock.

Carbonate (15%): Carbonate grains up to 400 micrometers occur within veins 1 and 2 as the main components. The grains are affected by chlorite alteration from the rims of vein 1 and are associated with quartz grains in vein 2.

Chlorite (5%): Chlorite grains are up to 200 micrometers, and they alter amphibole within the rock. Chlorite also replaces carbonate grains within vein 1.

Pyrite (3%): Subhedral grains of pyrite occur within vein 1; the grains are up to 300 micrometers and are associated with trace amounts of sphalerite.

Sample ID: ML23-NM-073

Rock type: Andesite

Basic description:

The rock comprises plagioclase, quartz, sericite, epidote, chlorite, and carbonate.

The rock is associated with various veins:

1 – Undulating vein filled with sericite grains. The vein is up to 1mm at the widest point.

2 – Quartz-carbonate-chlorite vein up to 1.5mm wide cuts the rock. The vein also cuts and offsets vein 1.

Paragenesis

Plagioclase -> quartz -> vein 1 (sericite) -> vein 2 (quartz, carbonate, chlorite) -> epidote

Mineralogy

Plagioclase (55%): plagioclase grains dominate the rock; they are up to 250 micrometers and display simple twinning. Plagioclase grains are weakly altered by sericite and epidote grains.

Quartz (20%):

Within host rock (13%): Quartz grains up to 200 micrometers occur within the rock. Quartz grains are less abundant and display undulatory extinction.

Within vein 2 (7%): Grains are up to 400 micrometers and are associated with chlorite and carbonate within vein 2.

Sericite (10%):

Within host rock (3%): Sericite alteration is present within the rock. It occurs pervasively and as an alteration phase within plagioclase.

Within vein 1 (7%): Sericite grains make up vein 1. The grains are weakly affected by epidote alteration.

Chlorite (5%): Chlorite grains are dominantly within vein 2, where they replace carbonate. Few grains of chlorite also occur pervasively, and they are associated with epidote grains.

Epidote (5%): Epidote grains are present within the rock. The grains are up to 300 micrometers, and they occur in clusters, seemingly replacing relic mafic minerals, possibly amphibole.

Carbonate (5%): Anhedral carbonate grains occur within vein 2 and the surrounding rock. Carbonate grains are associated with quartz within vein 1 and are being replaced by chlorite.

Sample ID: ML23-NM-074

Rock type: Andesite

Basic description:

The rock comprises plagioclase, quartz, sericite, biotite, epidote and chlorite

The rock is associated with various veins

1 – Epidote-chlorite-pyrite-quartz-carbonate vein cuts the host rock. The vein is up to 3mm wide and has a chlorite-rich halo that extends its width to about 6mm.

2 – Pyrite-epidote-chlorite-quartz-carbonate vein up to 1.5mm wide cuts the rock. This vein cuts vein 1 and causes a dextral offset to the vein.

Sulfides are present within the rock comprising pyrite which occurs within the veins.

Paragenesis

Plagioclase -> quartz -> sericite -> vein 1 (epidote, chlorite, pyrite, quartz) -> vein 2 (pyrite, epidote, chlorite, quartz)

Mineralogy

Plagioclase (35%): Plagioclase grains within the rock are up to 200 micrometers, they are altered by sericite and chlorite and they display simple twinning.

Quartz (25%):

Within host rock (20%): Quartz grains are up to 300 micrometers within the host rock. The grains occur dominantly in association with plagioclase, and they display undulatory extinction

Within veins 1 and 2 (5%): Recrystallized grains of quartz up to 300 micrometers occur within veins 1 and 2. Quartz grains are associated with chlorite, pyrite, and epidote within the veins.

Biotite (5%): Anhedral grains of biotite up to 200 micrometers are present within the rock. They are altered by chlorite and epidote grains.

Sericite (5%): Sericite grains are present in the rock. They alter plagioclase and are altered by later epidote and chlorite.

Carbonate (3%): The grains are up to 300 micrometers, and they occur pervasively in the rock. Carbonate grains are associated with chlorite and sericite.

Epidote (12%):

Within host rock (5%): Grains of epidote are up to 200 micrometers, and they replace amphibole and chlorite grains within the rock.

Within veins 1 and 2 (7%): Epidote grains within the veins are up to 300 micrometers and are associated with chlorite, pyrite, and quartz within the vein.

Chlorite (7%) Anhedronal grains of chlorite up to 200 micrometers occur within the rock. A few chlorite grains are also present within veins 1 and 2, and they dominate the rims of the veins.

Pyrite (8%): Subhedral grains of pyrite up to 0.8mm occur within veins 1 and 2. They are associated with quartz and pyrite.

Sample ID: ML23-NM-078

Rock type: Dacite

Basic description:

The rock comprises plagioclase, quartz, sericite, chlorite, carbonate, and epidote.

The rock is associated with various veins:

1 – Pyrite-quartz vein cuts the rock. The vein is up to 1.5mm wide and is aligned parallel to the foliation fabric of the host rock.

2 – Undulating vein infilled with pyrite, quartz, carbonate, epidote, and sericite. The vein is up to 7mm wide and is aligned parallel to vein 1.

3 – Pyrite-quartz-carbonate vein cuts the rock. The vein is up to 1mm wide and is aligned parallel to veins 1 and 2.

4 – Pyrite-quartz-chlorite vein cuts the rock. The vein is up to 0.8mm wide and is aligned parallel with the other veins.

5 – Pyrite-chlorite-carbonate vein cuts the rock and cuts veins 1 to 4. The vein is up to 200 micrometers wide and is aligned at an angle to the earlier veins.

Sulfides are present within the rock; they comprise pyrite occurring within the veins.

Paragenesis

Plagioclase -> quartz -> sericite -> Vein 1 (pyrite-quartz) -> Vein 2 (pyrite, quartz, carbonate, epidote, sericite) -> Vein 3 (pyrite, quartz, carbonate) -> Vein 4 (pyrite, quartz, chlorite) -> Vein 5 (pyrite, chlorite, carbonate)

Mineralogy

Quartz (25%):

Within host rock (15%): fine grains of quartz occur within the host rock. The grains are up to 100 micrometers and are associated with plagioclase.

Within veins 1 to 4 (10%): grains are up to 0.6mm, and they occur in association with pyrite within veins 1 to 4.

Plagioclase (25%): Plagioclase grains up to 100 micrometers dominate the host rock; they are strongly altered by sericite and chlorite.

Sericite (10%): Very fine grains of sericite occur within the rock altering plagioclase. They also occur as clusters and infills within vein 2. Sericite grains are altered by later chlorite.

Carbonate (7%): Carbonate grains are up to 400 micrometers, and they occur dominantly within veins 2, 3, and 5. Carbonate grains in vein 5 are strongly altered by chlorite.

Chlorite (7%): Chlorite grains are up to 150 micrometers and occur within veins 4 and 5. They also occur within the host rock, replacing sericite grains.

Epidote (6%): The grains are up to 250 micrometers and occur dominantly within the host rock, replacing chlorite. They also occur as infill within vein 2.

Pyrite (20%): Subhedral grains of pyrite up to 5mm occur within veins 1 to 5. They are the main components of the veins. A few finer grains occur within the host rock disseminated around the veins.

Sample ID: ML23-NM-080

Rock type: Andesite

Basic description:

The rock comprises plagioclase, quartz, sericite, carbonate, and chlorite.

The rock is associated with various veins:

1 – Multiple interconnected chlorite veinlets up to 100 micrometers wide occur within the rock. They are cut by veins 2 and 3.

2 – Carbonate-chlorite vein cuts the rock. The vein is up to 4mm wide and cuts vein 1.

3 – Undulating vein infilled by carbonate, chlorite, and quartz. The vein is up to 2mm wide.

Sulfides are present in the host rock comprising disseminated grains of pyrite.

Paragenesis

Plagioclase -> quartz -> sericite -> vein 1 (chlorite) -> vein 2 (carbonate, chlorite) -> vein 3 (chlorite, carbonate, quartz)

Mineralogy

Plagioclase (60%): Plagioclase grains are dominant within the rock. The grains are up to 400 micrometers and weakly altered by sericite. Plagioclase grains display simple twinning.

Quartz (15%): Quartz grains are up to 300 micrometers and occur dominantly within the host rock. A few grains occur within vein 3 in association with chlorite and carbonate.

Sericite (5%): Sericite grains are present in the rock. They alter plagioclase and occur pervasively as clusters of sericite grains.

Carbonate (10%): Carbonate grains up to 200 micrometers occur dominantly within veins 1 and 2. They are associated with pyrite and chlorite within the veins. Some carbonate grains are being replaced by later chlorite alteration.

Chlorite (7%): Anhedral chlorite grains occur in clusters forming vein 1. The grains are dominantly elongated and interconnected. Chlorite grains also occur in veins 2 and 3, where they replace carbonate grains from the rims of the vein.

Pyrite (3%): Subhedral grains of pyrite up to 400 micrometers occur within the rock in a disseminated texture.

Sample ID: ML23-NM-083

Rock type: Diorite

Basic description:

The host rock comprises plagioclase, quartz, sericite, carbonate, chlorite, and epidote.

The rock is cut by a carbonate vein that is about 0.6mm wide.

Sulfides occur within the host rock, comprising pyrite and chalcopyrite disseminated through the rock.

Paragenesis

Plagioclase -> quartz -> sericite -> vein 1 (carbonate) -> chlorite -> epidote

Mineralogy

Quartz (27%): Subhedral grains of quartz up to 0.7mm in size occur within the rock. Finer grains of quartz up to 100 micrometers also commonly occur within the rock, and they display undulatory extinction.

Plagioclase (30%): Plagioclase grains can be up to 0.6mm in size, but most of the grains are finer, up to 200 micrometers in size, and they dominate the host rock. Plagioclase is strongly altered by sericite.

Sericite (15%): Sericite occurs pervasively throughout the host rock. Sericite also alters plagioclase grains. Sericite is associated with chlorite and carbonate as they replace some sericitized grains of plagioclase.

Carbonate (10%)

Within host rock (5%): Carbonate grains up to 300 micrometers occur within the host rock. They are associated with sericite and chlorite.

Within vein (5%): Larger grains of carbonate up to 0.7mm make up the vein that cuts the rock.

Chlorite (5%): Chlorite grains are very fine, less than 200 micrometers, and they occur pervasively throughout the host rock. They replace plagioclase, sericite, and carbonate grains.

Epidote (5%): Epidote grains are up to 300 micrometers and occur pervasively within the host rock. The grains are subhedral and are associated with chlorite.

Pyrite (5%): Subhedral grains of pyrite up to 400 micrometers in size are disseminated within the host rock.

Chalcopyrite (3%): Anhedral grains of chalcopyrite up to 350 micrometers are disseminated within the host rock.

Sample ID: ML23-NM-085

Rock type: Diorite

Basic description:

The rock comprises plagioclase, quartz, sericite, carbonate, amphibole, epidote and chlorite

The rock is associated with various veins:

1 – Quartz vein up to 6mm cuts the rock.

2 – Quartz vein up to 0.6mm wide cuts the rock. The vein is aligned parallel to vein 1.

3 – Carbonate vein up to 0.6mm wide cuts veins 1 and 2.

Sulfides within the host rock comprise disseminated grains of pyrite associated with trace amounts of chalcopyrite.

Paragenesis

Plagioclase -> quartz -> sericite -> vein 1 (quartz) -> vein 2 (quartz) -> vein 3 (carbonate) -> chlorite -> epidote

Mineralogy

Plagioclase (50%): Plagioclase grains are up to 1.5mm and dominate the rock. The grains are affected by sericite and epidote alteration.

Quartz (35%):

Within host rock (15%): Grains are up to 300 micrometers and occur within the rock. Quartz grains are associated with plagioclase.

Within veins 1 and 2 (20%): Recrystallized grains up to 1.5mm make up vein 1. Within vein 2, quartz grains are up to 400 micrometers in size.

Sericite (5%): Fine grains of sericite occur within the rock. Sericite grains alter plagioclase and are being replaced by later chlorite alteration.

Carbonate (5%): Carbonate grains are up to 350 micrometers and make up vein 3. A few carbonate grains are also pervasively distributed in the rock.

Amphibole (3%): A few grains of amphibole up to 400 micrometers are present within the rock. Amphibole grains are strongly replaced by chlorite and epidote.

Epidote (7%): Epidote grains are up to 200 micrometers and they occur within the rock as an alteration phase affecting amphibole grains. A few grains of epidote also occur within the rims of vein 1.

Chlorite (5%): Chlorite grains occur pervasively within the rock. They replace sericite, carbonate, and plagioclase grains.

Pyrite (5%): Pyrite grains up to 0.5mm are present within the rock. The grains are disseminated within the rock and are associated with trace amounts of chalcopyrite.

Sample ID: ML23-NM-088

Rock type: Diorite

Basic description:

The rock comprises plagioclase, quartz, sericite, amphibole, carbonate, epidote, and chlorite.

The host rock is cut by an undulating vein filled with quartz, carbonate, and chlorite.

Sulfides are present within the rock, comprising disseminated pyrite grains.

Paragenesis

Plagioclase -> quartz -> sericite -> amphibole -> quartz-carbonate-chlorite vein -> epidote

Mineralogy

Plagioclase (40%): Plagioclase grains are dominant within the rock. The grains are up to 400 micrometers and are replaced by strong sericite and epidote alteration.

Quartz (25%):

Within the host rock (20%): Fine grains of quartz up to 100 micrometers are present within the host rock.

Within the veins (5%): Recrystallized grains of quartz up to 0.7mm occur within the vein that cuts the rock. Quartz grains are associated with chlorite, carbonate, and epidote within the vein.

Amphibole (10%): Anhedral grains of amphibole up to 300 micrometers are present within the rock. Amphibole grains are strongly replaced by chlorite and epidote.

Epidote (7%): Epidote grains occur pervasively within the rock. They replace amphibole and sericite. A few epidote grains also occur within the vein that cuts the rock.

Chlorite (5%): Chlorite grains are present within the rock. They occur dominantly as infills within the vein that cuts the rock. Chlorite grains within the vein replace carbonate and quartz grains. A few chlorite grains replace amphiboles.

Sericite (5%): Fine grains of sericite are present within the rock. Sericite grains occur in the alteration phase within plagioclase grains. A few grains are also pervasively distributed in the rock.

Carbonate (5%): Carbonate grains are up to 2mm and occur dominantly within the vein that cuts the rock. Carbonate grains within the vein are associated with quartz and chlorite.

Pyrite (3%): Subhedral grains of pyrite up to 300 micrometers are disseminated within the host rock.

Sample ID: ML23-NM-089

Rock type: Diorite

Basic description:

The rock comprises plagioclase, quartz, sericite, amphibole, carbonate, epidote, and chlorite.

The rock is associated with various veins:

1 – Undulating vein infilled with sericite and chlorite cuts the rock. The vein is up to 100 micrometers wide.

2 - Epidote-chlorite vein up to 100 micrometers wide cuts the rock. The vein cuts vein 1.

Sulfides are present within the rock, comprising disseminated grains of pyrite and trace amounts of chalcopyrite.

Paragenesis

Plagioclase -> quartz -> sericite -> amphibole -> vein 1 (sericite, chlorite) -> vein 2 (epidote, chlorite)

Mineralogy

Plagioclase (50%): Plagioclase grains are up to 1.5mm, and they dominate the rock. Plagioclase grains are altered by sericite, chlorite, and epidote. Most plagioclase grains show dark color due to strong epidote and chlorite alteration.

Quartz (15%): Quartz grains show a bimodal distribution with grains up to 1.5mm, and grains are as fine as 100 micrometers, which is more common.

Sericite (5%): The grains are present within the rock and occur mainly as an alteration phase affecting plagioclase grains. They are replaced by later chlorite alteration.

Amphibole (5%): Anhedral grains of amphibole are present within the rock. They are associated with plagioclase and are being replaced by epidote and chlorite grains.

Chlorite (5%): Chlorite grains are present within the rock, occurring dominantly within veins 1 and 2. A few chlorite grains are also present as an alteration phase affecting plagioclase and sericite.

Epidote (8%): Epidote alteration is present within the rock. It replaces plagioclase and sericite grains within the rock. Epidote also occurs within vein 2 in association with chlorite.

Pyrite (3%): Subhedral grains of pyrite are present within the rock. Pyrite grains are associated with trace amounts of chalcopyrite and disseminated within the rock.

Sample ID: ML23-NM-092

Rock type: Dacite

Basic description:

The rock comprises plagioclase, quartz, sericite, carbonate, and pyrite.

The host rock exhibits a sheared texture with a sericite-dominated fabric.

The rock is associated with various veins:

1 – Quartz-carbonate vein wide up to 2 mm, cut and offset by vein 2.

2 – The quartz-carbonate vein is about 0.7mm wide and cuts and offsets vein 1.

Sulfides are present within the rock, comprising disseminated grains of pyrite.

Paragenesis:

Plagioclase -> quartz -> sericite -> vein 1 (quartz, carbonate) -> vein 2 (quartz, carbonate) -> deformation (shearing).

Mineralogy

Quartz (30%):

Within host rock (25%): Fine anhedral grains up to 250 micrometers dominate the mineralogy of the host rock.

They show undulatory extinction and are aligned mostly parallel to the shear fabric.

Within veins (5%): Recrystallized quartz grains up to 200 micrometers wide within veins 1 and 2. They are associated with carbonate grains.

Plagioclase (10%): Relic plagioclase crystals are in contact with quartz, and a few grains are altered to carbonate and sericite.

Sericite (40%): Fine grains of sericite in a sheared texture are dominant within host rock and overprint most primary textures.

Pyrite (10%): Pyrite is the dominant sulfide and occurs in a disseminated texture. The grains are up to 300 micrometers.

Carbonate (10%):

Within host rock (4%): Fine grains up to 100 micrometers occurring in the groundmass mainly occur in proximity to veins. They are associated with quartz and are slightly Fe-rich with a somewhat reddish tint.

Within veins (6%): Fine grains up to 200 micrometers occur within veins 1 and 2.

Sample ID: ML23-NM-097

Rock type: Diorite

Basic description:

The rock consists of relict plagioclase phenocrysts that have been pervasively altered, as well as quartz, carbonate, amphibole, chlorite, epidote, sericite, and pyrite.

This rock is associated with various veins:

1 – Undulating vein infilled with quartz, carbonate, chlorite, pyrite, and epidote. The vein is up to 3 mm wide and splits into smaller veins along its length.

2 – Similar to vein 1 but wide up to 0.8mm, and cuts and offsets vein 1.

Sulfide in the rock is mainly pyrite and occurs dominantly within the veins.

Paragenesis:

Plagioclase -> quartz -> amphibole -> sericite -> vein 1 (quartz-carbonate-chlorite-pyrite-epidote) -> vein 2 (quartz-carbonate-chlorite-pyrite-epidote)

Mineralogy:

Plagioclase (20%): Fine grains up to 50 micrometers, weakly altered by sericite. Coarser grains up to 200 micrometers show stronger alteration with the presence of more sericite inclusions.

Quartz (25%):

Within host rock (10%): Anhedral fine grains up to 100 micrometers are associated with plagioclase in host rock. Coarser grains of about 300 micrometers occur in proximity to veins.

Within vein (15%): Recrystallized quartz grains, dominantly around 400 micrometers, occur in both veins. They display subgrain features and undulatory extinction.

Amphibole (5%): Anhedral grains of secondary amphibole up to about 300 micrometers are commonly associated with chlorite. The grains are altered by chlorite.

Sericite (10%): Anhedral grains up to 50 micrometers are weakly distributed throughout the host rock. Sericite dominantly alters plagioclase grains.

Chlorite (10%): Anhedral grains up to 400 micrometers filling veins 1 and 2. The grains are associated with epidote and pyrite and are dominantly found on the edges of the veins.

Epidote (5%): Subhedral grains up to 300 micrometers fill veins 1 and 2. Grains are associated with pyrite and chlorite.

Carbonate (15%): Fine anhedral grains up to 500 micrometers are the main components of veins 1 and 2.

Pyrite (10%): Subhedral grains up to 400 micrometers fill veins 1 and 2. The grains are associated mostly with chlorite and epidote.

Sample ID: ML23-NM-107

Rock type: Carbonate vein cutting a dacite.

Basic description:

The rock consists of plagioclase, quartz, muscovite, sericite, carbonate, and chlorite.

The rock is associated with various veins:

- 1 – Sericite vein up to 200 micrometers wide that runs perpendicular to vein 3.
- 2 – Early carbonate vein up to 400 micrometers wide, with fabric parallel to vein 1.
- 3 – Carbonate vein about 2 cm wide cuts the host rock and earlier veins.

Paragenesis:

Plagioclase -> Quartz -> vein 1 (muscovite) -> sericite -> vein 2 (carbonate) -> vein 3 (carbonate) -> chlorite

Mineralogy:

Plagioclase (19%): Weakly sericite altered grains up to 0.5mm. Grains exhibit some simple twinning. Finer grains of about 100 micrometers are less altered by sericite and have fewer sericite grains within.

Quartz (15%): Fine anhedral grains of about 150 micrometers occurring within the host rock. They display undulatory extinction, and some of the grains show subgrain features.

Carbonate (40%):

Within host rock (1%): Grains up to 400 micrometers found proximal to veins and associated with quartz.

Within vein 2 (3%): Subhedral grains up to 300 micrometers.

Within vein 3 (36%): Fine grains up to 800 micrometers dominate in vein 3. Grains tend to be finer to about 300 micrometers closer to the rims of the vein.

Sericite (5%): Fine grains up to 100 micrometers distributed through the host rock, significantly occurring as alteration grains in plagioclase. They also occur as clusters of multiple grains exhibiting a shear fabric.

Chlorite (8%):

Within host rock (2%): Grains up to 100 micrometers. Associated with carbonate and replaces some carbonate grains.

Within vein 3 (6%): Fine anhedral grains of chlorite up to 200 micrometers occur on the rim of the vein and gradually into the surrounding host rock.

Epidote (5%): Fine grains up to 50 micrometers are weakly distributed through the host rock. The grains are associated with chlorite.

Muscovite (5%): Subhedral grains up to 200 micrometers within vein 1. The grains are fine up to 50 micrometers at the contact with vein 3.

Sample ID: ML23-NM-113

Rock type: Dacite

Basic description:

The host rock is composed of fine- to medium-grained quartz, plagioclase, carbonate, sericite, epidote, and chlorite.

The host rock is associated with various veins:

1 – Early quartz vein rimmed by disseminated sericite crystals, cut and offset by vein 4.

2 – Early carbonate quartz vein about 0.8mm wide, with quartz rim, cut and offset by vein 4.

3 – Similar and parallel to vein 2, slightly wider carbonate quartz vein, about 1.0mm wide with quartz at the rim of the vein, cut and offset by vein 4.

4 – Undulatory late vein infilled with sericite, carbonate, quartz, and epidote, the vein cuts all earlier veins and causes an offset.

Paragenesis

Plagioclase -> quartz -> muscovite -> sericite -> carbonate-> vein 1 ->vein 2 -> vein 3 -> chlorite -> epidote -> vein 4

Mineralogy

Plagioclase (37%): The grains are commonly less than 0.5mm, with a few crystals larger than 1 mm with moderately distributed sericite inclusions replacing the crystals. Muscovite also replaces some plagioclase phenocrysts and is less abundant in the host rock.

Quartz (23%)

Within host rock (16%): Grains up to 200 micrometers and some coarser recrystallized grains of about 1mm occur with minor inclusion. The coarser grains occur proximal to veins.

Within vein 1 (2%): Grains up to 1.5mm with undulatory extension, grains are finer in vein boundary, and the vein shows a pinch and swell texture.

Within veins 2 and 3 (3%): Grains occurring at the rims of veins 2 and 3, grains are up to 20 micrometers and display undulatory extinction.

Within vein 4 (2%): Recrystallized grains up to 1mm infill sheared undulating vein, grains have an elongate habit and are mostly equigranular.

Sericite (15%)

Within host rock (8%): Grains of about 20 - 100 micrometers disseminated in host rock and occur as inclusions in plagioclase crystals. Higher abundance in more altered and sheared zones of the host rock.

Within vein 4 (7%): Subhedral grains up to 50 micrometers cluster together within vein 4 and show a foliated texture, dominantly occurring on the rims of the vein and in the surrounding groundmass.

Carbonate (10%):

Within veins 2 and 3 (6%): Grains up to 400 micrometers within early carbonate quartz veins.

Within host rock (4%): Grains up to 300 micrometers disseminated in lower abundance in the host rock, with the highest concentration around late vein edges.

Muscovite (3%): Replaces some plagioclase phenocrysts. The grains are fine up to 500 micrometers.

Chlorite (5%): Minor chlorite is disseminated throughout the host rock with a slightly higher abundance around veins. The grains are fine up to 200 micrometers.

Epidote (7%): Fine grains up to 500 micrometers disseminated in the host rock and infilling late vein.

Sample ID: ML23-NM-115

Rock type: Diorite

Basic description:

The rock is composed of plagioclase, quartz, sericite, chlorite, epidote, hornblende, and carbonate.

The host rock is associated with various veins:

1 – Early carbonate-quartz-pyrite-chlorite vein with about 1.5mm width and grains up to 1mm, chlorite dominates the rims of the vein.

2 – Carbonate-chlorite-pyrite vein cutting early vein 1, the vein is about 200 micrometers wide and swells to about 0.5mm at the contact with vein 1, with carbonate grains up to 200 micrometers.

3 – Undulatory carbonate-chlorite-quartz-68

I am running a few minutes late; my previous meeting is running over 2 mm at the widest point and pinching to about 200 micrometers, the vein is aligned parallel to the fabric of vein 2.

4 – Chlorite-carbonate-pyrite veins with about 100 micrometers width and grains up to 100 micrometers, the vein is parallel to vein 2 and vein 3, and grains show an elongate habit.

Sulfides present in the rock include pyrite and minor chalcopyrite.

Paragenesis

Plagioclase -> quartz -> amphibole -> sericite -> epidote -> vein 1 (carbonate, chlorite, quartz)-> vein 2 (carbonate, chlorite) -> vein 3 (carbonate, chlorite, quartz) -> vein 4 (chlorite, carbonate).

Mineralogy

Plagioclase (27%): The grains are commonly 0.5-1mm with moderate to strong sericite alteration.

Quartz (21%)

Within host rock (15%): Fine grains up to 200 micrometers are sparsely distributed in the host rock, and finer grains less than 50 micrometers make up the groundmass.

Within veins 1 and 3 (6%): recrystallized medium grains up to 2mm with undulatory extinction.

Amphibole (3%): The grains can be up to 200 micrometers and are pervasively replaced by chlorite and epidote.

Sericite (20%): The grains are fine up to 50 micrometers and pervasively distributed in the host rock. Sericite is more abundant within plagioclase phenocrysts as inclusions.

Carbonate (11%)

Within host rock (3%): Grains up to 0.5mm occur in clusters randomly distributed in the host rock.

Within veins (8%): Grains up to 1.5mm occur in all veins in the host rock. Finer grains of about 200 micrometers also occur in more elongated textures in veins.

Epidote (5%): Grains up to 400 micrometers occur in parts of the host rock, replacing amphibole and other relic mafic minerals.

Chlorite (7%):

Within host rock (2%): Fine grains up to 0.5mm distributed in the host rock, abundant as replacement phase within plagioclase and amphibole grains.

Within veins 1, 2, and 3 (3%): Grains up to 100 micrometers dominate the rims of the veins. Grains are coarser up to 300 micrometers at contact with vein 4.

Within vein 4 (2%): Fine grains up to 100 micrometers dominate within vein 4, and the grains show an elongate habit.

Pyrite (5%):

Within host rock (1%): Subhedral fine grains up to 0.5mm disseminated in the host rock.

Within veins (4%): Euhedral to subhedral grains up to 2.5mm are distributed within the veins and are abundant at vein contacts associated with quartz and carbonate.

Chalcopyrite (1%): Fine grains up to 100 micrometers disseminated in the host rock, associated with disseminated pyrite.

Sample ID: ML23-NM-122

Rock type: Diorite

Basic description:

The rock is composed of plagioclase, quartz, sericite, muscovite, carbonate, and chlorite

The rock is associated with various veins:

1 – Undulating vein infilled with carbonate, chlorite, muscovite, quartz and pyrite.

2 – Carbonate veinlet rimmed by fine grains of sericite, vein 2 is parallel to the fabric of vein 1 and cuts it.

3 – Undulating vein infilled with carbonate, chlorite, quartz, and pyrite.

Sulfide occurs in disseminated texture and within veins; pyrite is the main sulfide observed.

Paragenesis

Plagioclase -> quartz -> sericite -> vein 1 (carbonate, chlorite, quartz, muscovite, pyrite) -> vein 2 (carbonate, sericite)-> vein 3 (carbonate, chlorite, quartz, pyrite)

Mineralogy:

Plagioclase (29%): The grains are up to 200 to 400 micrometers with moderate to strong sericite alteration and display simple twinning.

Quartz (21%)

Within host rock (15%): Grains are commonly 100 to 400 micrometers with minor inclusions of sericite. Finer grains less than 100 micrometers also occur and make up the groundmass.

Within veins 1 and 3 (6%): Recrystallized grains up to 500 micrometers occur on the edges of the undulating veins 1 and 2 in contact with carbonate.

Sericite (18%): Grains up to 50 micrometers moderately distributed within the host rock. They mostly occur as alteration grains in plagioclase.

Carbonate (14%): Grains of carbonate about 200-800 micrometers occur in all veins in the host rock.

Chlorite (8%): Fine, slightly elongated grains within veins 1 and 3. Grains are commonly 200 to 500 micrometers and dominantly occur on the rims of the veins.

Muscovite (3%): Anhedral grains up to 100 micrometers occurring as infills in vein 1, associated with plagioclase and carbonate.

Pyrite (8%): Pyrite grains up to 250 micrometers are disseminated through the host rock; grains are euhedral to subhedral and show no spatial association with any particular mineral.

Sample ID: ML23-NM-128

Rock type: Diorite

Basic description:

The host rock comprises plagioclase, quartz, carbonate, chlorite, and sericite.

Carbonate vein up to 3mm wide cuts across the rock.

Sulfides occur in the host rock comprising disseminated grains of pyrite.

Paragenesis

Plagioclase -> quartz -> sericite -> carbonate -> chlorite -> carbonate vein

Mineralogy

Plagioclase (18%): Anhedral grains up to 0.7mm, moderate to strong alteration by sericite and chlorite occurring within the grains, and carbonate alteration from the grain boundaries.

Quartz (17%): Anhedral grains up to 200 micrometers dominate the host rock, grains show undulatory extinction, and some grains bear chlorite inclusions. Recrystallized grains up to 1mm also occur in proximity to the carbonate vein.

Carbonate (35%)

Within host rock (27%): Fine grains up to 50 micrometers dominate the host rock. They are associated with plagioclase grains and are somewhat replaced by chlorite alteration.

Within vein (8%): Grains are up to 0.8mm in size and show simple twinning. The vein is somewhat altered by chlorite along the rims.

Chlorite (25%): Anhedral grains occurring pervasively through the host rock. They replace carbonate, sericite, plagioclase, and quartz.

Sericite (5%): Fine grains weakly altering plagioclase and subsequently replaced by chlorite.

Sample ID: ML23-NM-129

Rock type: Diorite

Basic description:

The rock consists of plagioclase, quartz, chlorite, carbonate, amphibole, and epidote.

The rock is associated with various veins:

1 – Carbonate-quartz-chlorite vein cuts host rock and is cut by a later vein. The vein is 4.5 mm wide.

2 – Late undulating vein infilled with carbonate, epidote, and quartz

The rock comprises disseminated pyrite.

Paragenesis

Plagioclase -> quartz -> amphibole -> vein 1 (carbonate-quartz-chlorite) -> vein 2 (carbonate-epidote-quartz)

Mineralogy

Quartz (2%):

Within host rock (15): Anhedral fine grains up to 50 micrometers make up the host rock.

Within veins (5%): Grains up to 500 micrometers occur in both veins that cut the host rock. Quartz grains are associated with carbonate grains in both veins.

Plagioclase (25%): Fine grains up to 50 micrometers occur in association with quartz in a groundmass texture.

Phenocrysts up to 1mm also occur and are moderately altered by sericite and chlorite.

Amphibole (7%): Anhedral amphibole grains can be seen in the host rock being altered to chlorite. They are usually up to 200 micrometers large.

Sericite (5%): Sericite alters plagioclase grains, dominantly occurring in coarser plagioclase grains.

Chlorite (15%):

Within host rock (3%): Grains up to 200 micrometers occur in the host rock. They often alter plagioclase and amphiboles.

Within vein 1 (7%): Fine grains of chlorite on the rims of vein 1 and some within the veins associated with carbonate.

Carbonate (20%):

Within vein 1 (15%): Fine grains up to 200 micrometers dominate vein 1. They are associated with quartz, pyrite, and chlorite.

Within vein 2 (5%): Very fine carbonate grains occur in vein 2 in association with epidote and quartz.

Epidote (3%): Minor amount of fine-grained epidote up to 100 micrometers is associated with vein 2 and a few pyrite grains.

Pyrite (5%): Subhedral grains of pyrite up to 400 micrometers are disseminated in the host. They are associated with some carbonate and epidote grains.

Sample ID: ML23-NM-135

Rock type: Dacite

Basic description:

Rock comprises plagioclase, quartz, sericite, carbonate, chlorite and muscovite.

The host rock is associated with various veins:

1 – Undulating vein infilled with carbonate, quartz, chlorite, and muscovite.

2 – Multiple sericite veinlets crosscut early veins. The veinlets are about 400 micrometers wide and are aligned parallel to one another.

Sulfides are present within the rock, comprising disseminated grains of pyrite.

Paragenesis

Plagioclase -> quartz -> vein 1 (carbonate, quartz, chlorite, muscovite) -> sericite veinlets -> chlorite

Mineralogy

Quartz (35%)

Within host rock (30%): Fine grains up to 100 micrometers dominate the rock, and grains show undulatory extinction.

Within vein 1 (5%): Recrystallized grains up to 1mm occur in vein 1, grains are deformed and display subgrain features.

Plagioclase (20%): Grains are up to 100 micrometers and show simple twinning. They occur in association with quartz and are moderately altered by sericite.

Sericite (15%): Fine grains of sericite occur as alteration phase in plagioclase. Grains are up to 50 micrometers and occur as sericite veins.

Carbonate (10%):

Within host rock (2%): Grains up to 100 micrometers are weakly distributed in the host rock.

Within vein 1 (8%): Carbonate grains up to 400 micrometers fill vein 1. They occur in association with quartz and muscovite.

Muscovite (8%): Muscovite grains dominantly occur as infills in vein 1. They occur in the offset portion of the vein and are commonly on the rims in association with carbonate and chlorite.

Chlorite (10%): Grains up to 0.6mm occur in veins and are spatially associated with quartz grain boundaries.

Pyrite (2%): Anhedral pyrite grains occur in vein 1 associated with the contact of vein 1 with later sericite veinlets.

Sample ID: ML23-NM-138

Rock type: Dacite

Basic description:

The host rock comprises plagioclase, quartz, sericite, muscovite and epidote.

Pyrite occurs in a disseminated texture through the host rock.

The host rock is sheared with sericite as the dominating the shear fabric.

Paragenesis

Plagioclase -> quartz -> sericite -> muscovite -> epidote

Mineralogy

Quartz (35%): Fine grains of quartz up to 200 micrometers dominate the host rock. Recrystallized quartz grains can be larger up to 0.5mm and show subgrain features. Quartz grains show undulatory extinction.

Plagioclase (30%): Grains are up to 300 micrometers and are weakly altered by sericite and epidote. Plagioclase grains are also larger, up to 0.6mm, and they display simple twinning.

Sericite (20%): Very fine grains of sericite occur pervasively in the host rock and also alter plagioclase crystals. Sericite also occurs dominantly as the shear fabric of the host rock and is associated with pyrite grains.

Muscovite (5%): Grains are up to 200 micrometers and are associated with sericite-dominated zones of the host rock. Muscovite grains are subhedral and show no alignment with the shear fabric of the host rock

Epidote (3%): Grains up to 300 micrometers occur pervasively in the host rock. Epidote grains show a spatial association with plagioclase grains.

Pyrite (7%): Euhedral to subhedral grains up to 0.5mm occur in the host rock. Pyrite is disseminated and the grains are oriented parallel to the shear fabric.

Sample ID: ML23-NM-139

Rock type: Andesite

Basic description:

The host rock comprises plagioclase, quartz, sericite, chlorite, carbonate, and epidote.

The rock is associated with various veins:

1 – Carbonate-chlorite vein up to 30 micrometers wide cuts the host rock

2 – Carbonate-pyrite-quartz vein up to 1.5mm wide cuts vein 1. The vein rim is dominated by quartz.

3 – Undulating vein infilled with pyrite, quartz, chlorite, epidote, and sericite. The vein is about 1cm wide and has a sheared sericite-dominated rim.

The rock is associated with sulfide minerals, which comprise pyrite.

Paragenesis Plagioclase -> quartz -> sericite -> carbonate -> vein 1 (carbonate, chlorite) -> vein 2 (carbonate, pyrite, quartz) -> vein 3 (pyrite, quartz, chlorite, epidote, sericite)

Mineralogy

Quartz (20%):

Within host rock (15%): Fine grains up to 200 micrometers occur within the host rock. Quartz grains are associated with plagioclase and show undulatory extinction.

Within veins 2 and 3 (5%): Recrystallized grains up to 0.5mm occur in association with carbonate and pyrite.

Plagioclase (30%): Grains are dominantly fine up to 250 micrometers and display simple twinning. Plagioclase grains are strongly altered by sericite and carbonate.

Sericite (15%): Grains are usually very fine, less than 20 micrometers, and occur pervasively through the host rock. Sericite also occurs around the rims of veins 2 and 3 as well as within plagioclase grains.

Carbonate (10%): Carbonate grains dominate all the veins that cut the host rock. The grain sizes range from 100 micrometers for vein 1 to 1mm for veins 2 and 3. They are associated with pyrite and quartz.

Chlorite (5%): Grains are up to 400 micrometers, and they mostly occur as vein 3 infill. Chlorite grains are associated with quartz, pyrite, and epidote.

Epidote (5%): Grains are up to 100 micrometers, and they are spatially associated with chlorite grains.

Pyrite (15%): Grains of pyrite are up to 0.6mm and dominantly occur within veins 2 and 3. Minor pyrite is also disseminated throughout the host rock.

Sample ID: ML23-NM-147

Rock type: Diorite

Basic description:

The host rock comprises plagioclase, quartz, sericite, chlorite, amphibole, carbonate, and epidote.

The rock is associated with various veins:

1 – Undulating vein infilled with carbonate, amphibole, quartz, and chlorite. The vein is 0.5mm wide and is cut by a later vein.

2 – Similar in composition with vein 1. Vein 2 is 1mm wide and cuts vein 1.

Sulfide minerals occur in trace amounts within the host rock, and they comprise pyrite.

Paragenesis

Plagioclase -> quartz -> sericite -> carbonate -> vein 1 (carbonate, amphibole, quartz and chlorite) -> vein 2 (carbonate, amphibole, quartz and chlorite)

Mineralogy

Plagioclase (40%): Grains are commonly 300 micrometers and are weakly altered by sericite and epidote.

Plagioclase grains are also larger up to 1.5mm, and these are more intensely altered by sericite, chlorite, and epidote.

Quartz (30%):

Within host rock (25%): Quartz grains are dominant in the host rock. Grains range from 200 – 400 micrometers.

Quartz grains show undulatory extinction.

Within veins (5%): Recrystallized quartz grains up to 300 micrometers occur within the veins. They are associated with carbonate and chlorite.

Chlorite (5%): Grains up to 0.5mm occur pervasively through the host rock. Chlorite grains are present as alteration phases on amphibole and plagioclase. They also occur on the rims of veins 1 and 2.

Sericite (5%): Fine grains up to 10 micrometers, they occur dominantly as alteration minerals within plagioclase grains.

Carbonate (10%): Grains are up to 500 micrometers, and they occur as the main constituents of veins 1 and 2. They are associated with quartz, chlorite and amphibole.

Amphibole (7%):

Within host rock (3%): Fine grains of secondary amphibole occur in the host rock, grains are up to 50 micrometers and are associated with chlorite and plagioclase.

Within veins (4%): Grains are up to 0.7mm and they occur in association with carbonate and quartz in veins 1 and 2. Amphibole grains are being altered by chlorite.

Epidote (5%): Grains are up to 100 micrometers and dominantly occur within veins 1 and 2 as infills. Minor epidote grains occur as alteration phases within plagioclase grains.

Sample ID: ML23-NM-149

Rock type: Dacite

Basic description:

The rock comprises plagioclase, quartz, sericite, chlorite, and carbonate

The rock is associated with various veins:

1 – Carbonate-quartz vein up to 1mm wide runs through the host rock and is cut by vein 3.

2 – Quartz vein up to 1mm wide runs through the host rock. Vein 2 is cut and offset by vein 3.

3 – Quartz-carbonate-chlorite vein up to 2.5mm wide runs through the host rock.

Paragenesis

Plagioclase -> quartz -> sericite -> vein 1 (sericite, quartz) -> vein 2 (carbonate, quartz) -> vein 3 (quartz, carbonate, chlorite)

Mineralogy

Plagioclase (25%): Grains are up to 300 micrometers and they are associated with quartz within the host rock.

Plagioclase grains are altered mainly by sericite grains and less by chlorite.

Quartz (45%):

Within host rock (35%): Fine grains of quartz up to 250 micrometers dominate the host rock. Quartz grains show undulatory extinction and are associated with plagioclase and sericite.

Within veins (10%): Recrystallized grains of quartz sized within 300 to 500 micrometers are present in all 3 veins that crosscut the host rock. Quartz grains are subrounded and display undulatory extinction.

Carbonate (10%): Grains are up to 1mm in size within vein 3 and up to 500 micrometers in vein 2. Carbonate grains are associated with quartz and chlorite.

Chlorite (5%): Fine grains of chlorite up to 50 micrometers occur dominantly within vein 3. A few grains, however, occur as an alteration phase on plagioclase.

Sericite (15%)

Within host rock (7%): Sericite grains occur pervasively through the host rock. The grains are very fine, less than 30 micrometers. They are mostly alteration products within plagioclase grains.

Within vein (8%): Clusters of sericite grains form vein 1. The grains are very fine, and they are spatially associated with quartz.

Sample ID: ML23-NM-154

Rock type: Dacite

Basic description:

The rock is associated with plagioclase, quartz, sericite, chlorite, and carbonate.

The rock is associated with various veins:

1 – Quartz vein up to 0.7mm wide cuts the host rock. The vein is cut by a later carbonate vein.

2 – Undulatory carbonate vein up to 1mm wide cuts the rock. The vein is aligned parallel to vein 1 and also cut by vein 3.

3 – Carbonate-quartz vein cuts the rock. The vein is up to 2mm wide and cuts veins 1 and 2

Sulfides are present within the host rock, comprising disseminated grains of pyrite.

Paragenesis

Plagioclase -> quartz -> sericite -> vein 1 (quartz) -> vein 2 (carbonate) -> vein 3 (carbonate, quartz) -> chlorite

Mineralogy

Plagioclase (40%): Few plagioclase phenocrysts up to 1.2mm occur within the rock, and they are strongly altered by sericite and chlorite. Plagioclase grains are commonly fine up to 100 micrometers, and they dominate the host rock.

Quartz (27%):

Within host rock (22%): fine grains of quartz occur within the rock; the grains are up to 50 micrometers and display undulatory extinction.

Within veins 1 and 2 (5%): grains are up to 300 micrometers, and they make up vein 1. Quartz grains within vein 2 are associated with carbonate and are commonly 100 micrometers.

Carbonate (15%): carbonate grains up to 200 micrometers are present within veins 2 and 3. They are associated with quartz and chlorite.

Chlorite (10%): Chlorite grains are up to 100 micrometers in size and occur pervasively in rock. They replace sericite and carbonate grains.

Sericite (5%): Very fine grains of sericite are present within the rock. Sericite grains occur as an alteration phase on plagioclase and also pervasively within the rock.

Pyrite (3%): Subhedral grains of pyrite up to 0.5mm occur within the host rock. Pyrite grains are disseminated within the host rock.

Sample ID: ML23-NM-158

Rock type: Diorite

Basic description:

The rock comprises plagioclase, quartz, amphibole, sericite, carbonate, chlorite and epidote

The rock is associated with various veins;

1 – Carbonate vein up to 5mm at widest point, the vein is undulatory and pinches to less than 1mm at contact with later vein.

2 – Quartz vein up to 6mm wide cuts the host rock.

3 – Late undulating veinlet, less than 1mm in width. The vein is infilled with sericite, epidote and chlorite.

The rock is associated with disseminated pyrite grains

Paragenesis

Plagioclase -> quartz -> sericite -> vein 1 (carbonate) -> pyrite -> vein 2 (quartz) -> amphibole -> chlorite -> vein 3 (sericite, epidote, chlorite)

Mineralogy

Quartz (30%):

Within host rock (15%): Grains are up to 500 micrometers, and they dominate the host rock. Quartz grains show undulatory extinction and are associated with plagioclase.

Within veins (15%): Recrystallized grains up to 0.6mm in size. They dominate vein 2, which is up to 6mm wide and is cut and offset by a later vein. The grains display undulatory extinction.

Plagioclase (15%): Grains are up to 1mm in size, and they are associated with quartz within the host rock.

Plagioclase grains are strongly altered by sericite grains. Most of the plagioclase grains are relict as they are almost completely replaced by alteration.

Sericite (25%): Very fine grains of sericite occur within the rock. Sericite dominantly alters plagioclase grains. A few sericite grains occur pervasively in association with carbonate.

Carbonate (15%): Grains are up to 500 micrometers, and they occur entirely within vein 1. The vein is cut and offset by vein 3 and pinches from 5mm to about 1mm at the contact with vein 3.

Amphibole (5%): Fine grains up to 300 micrometers occur within the rock. The grains are anhedral and associated with chlorite and pyrite.

Chlorite (5%): Grains are up to 200 micrometers. They are associated with some amphibole and plagioclase grains.

Epidote (5%): Grains are up to 150 micrometers, and they occur within vein 3.

Pyrite (10%): Subhedral grains of pyrite up to 300 micrometers in size occur predominantly in a disseminated texture within the host rock. Pyrite is associated with most of the silicate phases but is absent within vein 2.

Sample ID: ML23-NM-159

Rock type: Diorite

Basic description:

The rock comprises plagioclase, quartz, sericite, carbonate, chlorite and muscovite

The rock is associated with various veins:

1 – Quartz-carbonate vein up to 3mm wide cuts the host rock. The vein is cut and offset by vein 2.

2 – Undulating vein infilled with quartz, chlorite, carbonate, pyrite, and chalcopryrite. The vein is about 4mm wide and cuts vein 1.

Sulfides within the host rock include pyrite and chalcopryrite. They dominantly occur as disseminated grains throughout the host rock. Few grains are also concentrated within vein 2.

Paragenesis

Plagioclase -> Quartz -> sericite -> vein 1 (quartz, carbonate, muscovite) -> vein 2 (quartz, chlorite, carbonate, pyrite, chalcopryrite).

Mineralogy

Plagioclase (20%): Grains are up to 0.8mm in size. They are associated with quartz within the host rock. Plagioclase grains are strongly altered by sericite grains.

Quartz (35%):

Within host rock (20%): Grains are up to 200 micrometers. A few larger grains up to 1mm occur as well. Quartz grains show undulatory extinction and are associated with plagioclase.

Within veins 1 and 2 (15%): Recrystallized grains occur within veins 1 and 2. The grains are sized within 0.7 to 1.2mm in size. The grains display undulatory extinction.

Sericite (15%): Very fine grains of sericite occur within the rock. Sericite dominantly alters plagioclase grains. Sericite also occurs in vein-like clusters; these are interpreted as sericite-rich fluids filling fractures.

Carbonate (7%): Grains are up to 300 micrometers, and they occur entirely within veins 1 and 2. Carbonate grains in vein 1 are affected by a reddish alteration, which could be an effect of iron enrichment. They are associated with quartz within the veins.

Chlorite (5%): Grains are up to 0.5mm, and they occur within vein 2. Chlorite grains occur within the vein, with a few grains distributed close to the vein. They are associated with quartz and pyrite.

Muscovite (5%): Muscovite grains up to 400 micrometers occur within vein 1. The grains are associated with quartz and carbonate grains with vein 1.

Pyrite (10%): Subhedral grains up to 400 micrometers in size occur predominantly in a disseminated texture within the host rock. A few larger grains up to 0.7mm occur within vein 2 in association with chalcopyrite.

Chalcopyrite (3%): Anhedral grains of chalcopyrite up to 350 micrometers occur within the host rock in association with pyrite.

Sample ID: ML23-NM-164

Rock type: Diorite

Basic description:

The rock comprises plagioclase, quartz, carbonate, sericite, and chlorite.

The rock is associated with various veins:

1 – Quartz-pyrite-carbonate vein up to 4mm wide cuts the host rock.

2 – Carbonate veinlet up to 200 micrometer wide cuts vein 1.

3 – Undulating veinlet infilled with carbonate and chlorite cuts vein 2.

Sulfides occur within the host rock, dominated by pyrite associated with a few grains of chalcopyrite.

Paragenesis

Plagioclase -> quartz -> sericite -> vein 1 (quartz, pyrite, carbonate) -> vein 2 (carbonate) -> vein 3 (carbonate, chlorite) -> chlorite

Mineralogy

Plagioclase (35%): Plagioclase grain dominate the rock. A few grains are up to 1.5mm in size, while the majority of the grains are around 0.8mm. they are strongly affected by sericite alteration and much less by chlorite alteration. Plagioclase grains show simple twinning.

Quartz (35%):

Within host rock (25%): Anhedral grains up to 0.6mm in size occur within the rock, and they show undulatory extinction. Quartz grains are associated with plagioclase within the host rock.

Within vein 1 (10%): Recrystallized grains up to 400 micrometers occur within vein 1 in association with pyrite and carbonate grains.

Sericite (10%): Very fine grains less than 50 micrometers are present as alteration minerals within plagioclase grains.

Carbonate (5%): Grains of carbonate up to 300 micrometers occur within all the veins associated with the host rock. Carbonate grains are associated with quartz, chlorite and pyrite.

Chlorite (5%): Fine grains of chlorite occur within the host rock as alteration minerals around plagioclase grain boundaries. Very fine chlorite grains also occurs within vein 3.

Pyrite (10%):

Within host rock (5%): Pyrite grains occur in a disseminated texture within the host rock, they are up to 300 micrometers in size and are associated with plagioclase grains.

Within vein 1 (5%): Subhedral grains of pyrite up to 0.6mm occur within vein 1. Pyrite grains are associated with quartz within vein 1.

Sample ID: ML23-NM-169

Rock type: Dacite

Basic description:

The rock comprises plagioclase, quartz, sericite, carbonate, chlorite, muscovite and epidote.

The rock is associated with various veins:

1 – Epidote-sericite- pyrite-chlorite vein cuts the host rock; the vein is about 200 micrometers at its widest point.

2 – Undulating vein infilled with quartz, carbonate, and epidote. The vein is up to 2mm wide and cuts vein 1.

Sulfides within the host rock comprise pyrite, which is distributed within the veins.

Paragenesis

Plagioclase -> quartz -> sericite -> vein 1 (epidote, muscovite, pyrite, chlorite) -> vein 2 (quartz, carbonate, epidote)

Mineralogy

Plagioclase (35%): Fine grains up to 300 micrometers dominate the host rock. Plagioclase grains are altered mostly by sericite and much less intensely by epidote. The grains show simple twinning.

Quartz (35%):

Within host rock (32%): Anhedral grains of quartz up to 0.5mm occur within the rock. They are associated with plagioclase and show undulatory extinction.

Within vein 2 (3%): Quartz grains up to 1mm in size occur within vein 2. The grains are associated with carbonate and epidote within the vein.

Sericite (7%): Fine grains of sericite less than 50 micrometers are present as alteration minerals within plagioclase grains and pervasively distributed within the host rock.

Carbonate (5%): Grains of carbonate up to 0.7mm occur within vein 2. The grains are associated with quartz and epidote within vein 2.

Muscovite (5%): Muscovite grains up to 300 micrometers occur within vein 1. The grains are associated with epidote and chlorite.

Chlorite (5%): Fine grains of chlorite occur within vein 1. A few chlorite grains also occur pervasively in the host rock.

Pyrite (3%): Pyrite grains are distributed within the two veins that cut the host rock, the grains are up to 300 micrometers in size. A few grains also occur as disseminated grains.

Sample ID: ML23-NM-171

Rock type: Andesite

Basic description:

The rock comprises plagioclase, quartz, carbonate, and muscovite.

The rock is associated with various veins:

1 – Carbonate vein up to 0.7mm wide cuts the host rock. The vein cuts some plagioclase phenocrysts.

2 – Muscovite vein up to 0.8mm wide cuts the host rock. The vein also cuts and offsets vein 1.

Sulfides occur within the host rock. They comprise pyrite, which occurs in a disseminated texture.

Paragenesis

Plagioclase -> quartz -> vein 1 (carbonate) -> vein 2 (muscovite)

Mineralogy

Plagioclase (65%): Plagioclase dominates the host rock with a few phenocrysts up to 8mm in size. Most of the grains, however, are finer, with most grains around 0.5mm, and they are weakly altered by muscovite. Plagioclase grains display distinctive plagioclase twinning.

Quartz (10%): Quartz grains are very fine and subrounded, with sizes up to 150 micrometers. Quartz grains show undulatory extinction.

Muscovite (15%): Muscovite grains occur within vein 2, the grains are up to 400 micrometers. Muscovite grains from vein 2 alters plagioclase grains in contact with the vein.

Carbonate (8%): Carbonate grains are up to 0.5mm in size and they dominate vein 1. Carbonate grains are slightly altered by muscovite at vein 1 and 2 contact.

Pyrite (7%): Euhedral to subhedral pyrite grains up to 0.5mm occur within the host rock in a disseminated texture.

Sample ID: ML23-NM-176

Rock type: Dacite

Basic description:

The rock comprises plagioclase, quartz, sericite, chlorite, amphibole and carbonate.

The rock has a sericite-dominated shear texture.

The rock is associated with various veins:

1 – Quartz vein up to 1mm wide cuts the host rock

2 – Quartz-carbonate vein up to 0.6mm wide cuts the host rock. The vein is aligned parallel to vein 1 and shows no crosscutting relationship.

3 – Quartz-carbonate-chlorite vein up to 0.7mm wide. The vein parallels veins 1 and 2 and shows no crosscutting relationship with the earlier veins.

Paragenesis

Plagioclase -> quartz -> sericite -> amphibole -> chlorite -> vein 1 (quartz) -> vein 2 (quartz, carbonate) -> vein 3 (quartz, carbonate, chlorite)

Mineralogy

Plagioclase (25%): Very fine plagioclase grains up to 100 micrometers occur within the host rock. Plagioclase grains are altered by sericite and chlorite.

Quartz (30%):

Within host rock (20%): Very fine grains less than 100 micrometers make up the host rock. Quartz grains are anhedral and show weak extinction.

Within veins (10%): Recrystallized grains occur within veins 1,2 and 3. These are up to 300 micrometers in size and show undulatory extinction.

Sericite (25%): Sericite grains occur as pervasively distributed grains, and they occur in clusters, which creates a sericite-dominated shear texture of the host rock. Sericite clusters are altered by chlorite.

Chlorite (10%): Chlorite grains dominantly occur pervasively within the host rock. Chlorite grains alter sericite, plagioclase, and amphibole; the grains are up to 200 micrometers and are associated with a strongly sericitized zone. Few chlorite grains also occur within vein 3.

Amphibole (5%): Anhedral grains of amphibole occur within the rock. Amphibole grains are elongated and up to 0.6mm long, they occur mostly on the boundaries of vein 1.

Carbonate (5%): Grains are up to 300 micrometers, and they occur within veins 2 and 3. Carbonate grains are associated with quartz within the veins.

Sample ID: ML23-NM-178

Rock type: Dacite

Basic description:

The rock comprises plagioclase, quartz, sericite, chlorite, amphibole and carbonate.

The rock is associated with various veins:

1 – Undulating vein up to 0.7mm infilled with quartz, carbonate, and chlorite.

2 – later undulating vein infilled with quartz and chlorite. The vein is about 100 micrometers wide and cuts vein 1.

Trace amounts of sulfides occur within the host rock; they comprise pyrite.

Paragenesis

Plagioclase -> quartz -> sericite -> amphibole -> vein 1(quartz, carbonate, chlorite) -> vein 2 (quartz, chlorite, amphibole).

Mineralogy

Plagioclase (30%): Plagioclase grains are up to 0.6mm, and they dominate the host rock. Plagioclase grains are weakly altered by sericite, and they display simple twinning.

Quartz (40%):

Within host rock (35%): Quartz grains are up to 0.6mm, and they dominate the rock. Quartz grains are mostly subrounded and show undulatory extinction.

Within veins (5%): Recrystallized grains occur within veins 1 and 2. These are up to 0.8mm micrometers in size and show undulatory extinction.

Sericite (10%): Sericite grains occur as pervasively distributed grains. They also occur within plagioclase grains. Some of the grains pervasively distributed occur in vein-like clusters.

Chlorite (7%): Chlorite grains are up to 200 micrometers, and they dominantly occur as alteration phases replacing amphibole grains. A few grains occur as infills within the veins.

Amphibole (8%): Subhedral grains of amphibole up to 300 micrometers occur within the rock. Amphibole grains are strongly altered by chlorite. A few grains also occur within vein 2 in association with chlorite and quartz.

Carbonate (5%): Grains are up to 400 micrometers, and they occur within vein 1. Carbonate grains are associated with quartz and chlorite.

Appendix II: Whole-rock geochemistry

SAMPLE NO	NM-001	NM-002	NM-003	NM-004	NM-005	NM-006	NM-007	NM-008
Ag (ppm)	0.0	0.3	0.0	0.0	0.1	0.1	0.1	0.0
Al (wt %)	7.4	6.4	7.8	7.5	7.8	7.6	7.5	7.3
As (ppm)	0.1	1.0	0.8	1.0	1.0	1.8	5.1	1.4
Au (ppm)	0.0	0.0	0.0	0.0	0.1	0.0	0.0	0.0
Ba (ppm)	260.0	40.0	410.0	310.0	310.0	180.0	130.0	520.0
Be (ppm)	0.6	0.7	0.7	0.7	0.7	1.2	0.5	0.7
Bi (ppm)	0.0	0.1	0.1	0.1	0.1	0.1	1.2	0.1
Ca (wt %)	2.2	3.8	4.0	4.1	4.2	4.8	4.7	4.3
Cd (ppm)	0.0	0.2	0.0	0.1	0.1	0.1	0.1	0.0
Ce (ppm)	19.5	26.7	19.9	20.2	21.2	42.4	23.3	19.4
Co (ppm)	7.9	38.2	14.7	15.8	16.0	29.5	56.3	15.6
Cr (ppm)	26.0	51.0	89.0	88.0	93.0	251.0	109.0	89.0
Cs (ppm)	1.1	0.3	1.1	0.8	0.6	1.3	0.5	0.9
Cu (ppm)	18.6	39.6	1.4	3.0	4.4	39.6	56.3	18.9
Fe (wt %)	2.4	11.4	3.9	3.7	4.2	4.6	7.1	4.0
Ga (ppm)	17.3	14.7	16.8	17.2	17.5	18.6	15.1	16.3
Ge (ppm)	0.0	0.1	0.1	0.2	0.2	0.3	0.2	0.2
Hf (ppm)	2.1	2.4	1.5	1.5	1.5	2.2	2.2	1.5
In (ppm)	0.0	0.0	0.0	0.0	0.0	0.0	0.0	0.0
K (wt %)	1.1	0.1	1.1	0.8	0.7	0.5	0.7	1.3
La (ppm)	8.7	12.4	8.6	7.4	8.2	18.6	9.3	7.7
Li (ppm)	28.4	34.4	31.0	29.6	30.2	38.1	42.6	27.8
Mg (wt %)	1.1	2.4	2.1	2.0	2.1	3.9	2.7	1.9
Mn (ppm)	397.0	3830.0	774.0	711.0	771.0	783.0	1240.0	613.0
Mo (ppm)	0.2	0.9	0.4	0.8	0.8	0.2	2.4	0.4
Na (wt %)	3.4	1.3	2.9	3.1	2.9	3.2	2.4	2.4
Nb (ppm)	1.8	4.2	2.3	2.0	2.4	3.0	4.3	2.0
Ni (ppm)	18.6	83.2	30.6	37.9	38.2	152.0	199.0	31.3
P (ppm)	380.0	450.0	510.0	520.0	530.0	820.0	520.0	510.0
Pb (ppm)	0.9	19.4	4.0	5.1	5.6	5.7	2.1	2.5
Rb (ppm)	29.3	2.8	31.7	16.1	12.8	12.4	20.0	25.0
Re (ppm)	0.0	0.0	0.0	0.0	0.0	0.0	0.0	0.0
S (wt %)	0.0	1.1	0.1	0.0	0.1	0.0	0.6	0.1
Sb (ppm)	0.2	0.2	0.2	0.4	0.4	0.3	0.1	0.2
Sc (ppm)	5.9	16.9	11.8	12.6	13.0	16.2	20.0	11.8
Se (ppm)	0.5	1.0	0.5	0.5	0.5	0.5	0.5	0.5
Sn (ppm)	0.5	1.0	0.6	0.5	0.6	0.7	0.7	0.5
Sr (ppm)	251.0	85.1	480.0	510.0	664.0	704.0	114.5	422.0
Ta (ppm)	0.1	0.3	0.2	0.2	0.2	0.2	0.3	0.2
Te (ppm)	0.0	0.0	0.0	0.0	0.0	0.0	0.1	0.1
Th (ppm)	0.5	1.5	1.1	1.1	1.1	2.4	1.1	0.9
Ti (wt %)	0.2	0.3	0.2	0.2	0.2	0.4	0.3	0.2
Tl (ppm)	0.1	0.0	0.2	0.1	0.1	0.1	0.1	0.1
U (ppm)	0.1	0.4	0.3	0.3	0.3	0.7	0.3	0.3
V (ppm)	40.0	87.0	90.0	91.0	94.0	122.0	117.0	92.0
W (ppm)	1.0	0.3	0.8	0.6	0.8	0.7	0.7	0.8
Y (ppm)	3.8	17.4	8.9	8.4	8.6	9.4	14.6	8.3
Zn (ppm)	54.0	96.0	69.0	66.0	68.0	80.0	66.0	46.0
Zr (ppm)	88.7	104.0	56.5	62.4	59.4	89.9	111.5	57.3

SAMPLE NO	NM-009	NM-010	NM-011	NM-012	NM-013	NM-014	NM-015	NM-016
Ag (ppm)	0.1	2.8	0.1	1.2	0.0	1.7	0.4	0.4
Al (wt %)	7.1	7.4	7.4	7.9	8.1	8.3	7.3	7.2
As (ppm)	0.8	1.6	1.1	1.2	1.5	0.8	1.1	1.5
Au (ppm)	0.0	1.5	0.0	0.9	0.0	0.2	0.5	0.3
Ba (ppm)	510.0	550.0	320.0	250.0	170.0	230.0	250.0	300.0
Be (ppm)	0.7	0.6	0.8	0.7	0.7	0.7	0.8	0.8
Bi (ppm)	0.2	0.4	0.2	0.9	0.5	3.5	0.4	0.3
Ca (wt %)	3.4	2.1	3.6	2.7	2.8	2.9	4.1	3.7
Cd (ppm)	0.0	0.0	0.1	0.1	0.0	0.1	0.1	0.1
Ce (ppm)	15.8	9.8	14.2	9.3	15.9	31.7	13.0	16.1
Co (ppm)	13.2	24.8	12.9	53.3	29.7	17.6	5.5	7.8
Cr (ppm)	28.0	25.0	78.0	69.0	71.0	110.0	27.0	70.0
Cs (ppm)	1.3	1.8	1.0	1.4	1.0	1.3	1.9	1.5
Cu (ppm)	2.9	30.3	33.3	10.0	5.1	792.0	170.5	93.9
Fe (wt %)	3.2	2.3	3.2	4.4	4.2	4.6	1.8	2.8
Ga (ppm)	17.6	16.9	18.9	16.6	16.9	18.6	18.9	15.9
Ge (ppm)	0.2	0.1	0.2	0.1	0.1	0.1	0.2	0.2
Hf (ppm)	1.7	2.4	1.3	1.3	1.3	1.9	2.0	1.9
In (ppm)	0.0	0.0	0.1	0.0	0.0	0.0	0.0	0.0
K (wt %)	1.9	2.3	1.1	2.1	1.2	1.6	2.0	1.4
La (ppm)	5.8	4.1	5.9	4.2	7.0	16.0	4.4	7.2
Li (ppm)	16.1	12.7	16.8	16.5	17.4	17.2	12.8	17.1
Mg (wt %)	1.2	1.1	1.6	1.4	1.5	1.6	1.2	1.6
Mn (ppm)	462.0	134.0	319.0	256.0	180.0	289.0	380.0	337.0
Mo (ppm)	0.2	1.2	0.6	1.5	1.2	6.6	0.5	0.3
Na (wt %)	2.5	2.2	2.8	2.5	3.4	3.4	3.0	3.1
Nb (ppm)	1.9	1.3	1.7	1.3	1.7	1.4	2.1	1.6
Ni (ppm)	19.0	24.3	26.7	24.6	25.7	35.8	16.3	21.5
P (ppm)	440.0	280.0	460.0	450.0	450.0	470.0	470.0	580.0
Pb (ppm)	1.9	3.4	3.4	5.0	4.1	3.7	5.0	2.7
Rb (ppm)	37.4	70.6	25.4	68.5	44.1	46.5	53.0	41.2
Re (ppm)	0.0	0.0	0.0	0.0	0.0	0.0	0.0	0.0
S (wt %)	0.3	1.0	0.3	3.0	2.3	2.9	0.8	0.8
Sb (ppm)	0.1	0.1	0.2	0.1	0.2	0.4	0.2	0.8
Sc (ppm)	7.7	5.0	9.2	8.0	8.4	12.8	8.1	10.2
Se (ppm)	0.5	0.5	0.5	1.0	1.0	3.0	1.0	1.0
Sn (ppm)	0.7	0.7	0.6	0.7	0.7	1.3	0.9	0.7
Sr (ppm)	239.0	173.0	552.0	221.0	461.0	314.0	246.0	285.0
Ta (ppm)	0.2	0.1	0.1	0.1	0.1	0.1	0.2	0.2
Te (ppm)	0.1	3.4	0.2	2.9	0.3	3.0	1.0	0.5
Th (ppm)	1.0	0.4	0.7	0.7	0.7	0.7	1.1	1.5
Ti (wt %)	0.2	0.1	0.2	0.2	0.2	0.2	0.2	0.1
Tl (ppm)	0.2	0.3	0.2	0.3	0.2	0.2	0.3	0.2
U (ppm)	0.3	0.2	0.2	0.2	0.3	0.4	0.3	0.4
V (ppm)	81.0	37.0	80.0	76.0	75.0	111.0	88.0	82.0
W (ppm)	2.1	2.8	0.9	4.5	1.3	6.4	5.0	1.5
Y (ppm)	6.6	4.0	6.0	4.4	5.7	7.5	6.8	8.8
Zn (ppm)	40.0	22.0	31.0	40.0	29.0	26.0	27.0	35.0
Zr (ppm)	65.2	101.5	38.5	34.0	33.8	71.1	67.9	59.2

SAMPLE NO	NM-017	NM-018	NM-019	NM-020	NM-021	NM-022	NM-023	NM-024
Ag (ppm)	0.1	1.0	3.7	0.2	0.1	0.0	0.0	0.3
Al (wt %)	8.0	8.2	7.7	7.8	7.8	8.1	7.8	7.1
As (ppm)	2.4	1.7	2.4	1.4	0.7	0.9	0.6	0.5
Au (ppm)	0.0	0.1	4.9	0.2	0.0	0.0	0.0	0.1
Ba (ppm)	170.0	160.0	540.0	380.0	380.0	320.0	240.0	100.0
Be (ppm)	0.9	0.8	0.8	0.7	0.8	0.8	0.7	0.6
Bi (ppm)	0.4	0.4	1.9	0.2	0.1	0.0	0.1	0.1
Ca (wt %)	3.1	3.1	3.0	3.7	4.3	3.9	4.0	5.9
Cd (ppm)	0.0	0.0	0.4	0.1	0.0	0.0	0.1	0.1
Ce (ppm)	23.2	16.3	23.5	14.0	18.9	15.2	17.0	27.1
Co (ppm)	6.6	5.7	9.4	9.1	5.7	6.3	8.9	27.2
Cr (ppm)	57.0	31.0	28.0	49.0	43.0	49.0	54.0	322.0
Cs (ppm)	0.7	0.9	1.6	0.9	1.1	0.8	0.4	0.7
Cu (ppm)	30.2	949.0	140.0	26.5	26.1	4.1	10.4	132.5
Fe (wt %)	2.6	1.7	3.2	2.5	1.2	1.5	1.9	5.0
Ga (ppm)	18.6	19.4	19.3	17.6	19.7	18.5	17.8	17.1
Ge (ppm)	0.2	0.1	0.1	0.3	0.2	0.3	0.2	0.2
Hf (ppm)	1.8	1.9	2.3	1.4	1.9	1.4	1.5	1.6
In (ppm)	0.0	0.0	0.1	0.0	0.0	0.0	0.0	0.1
K (wt %)	0.9	1.1	2.3	1.4	1.4	1.2	0.9	0.5
La (ppm)	9.4	6.5	11.1	6.3	8.0	6.5	6.7	11.5
Li (ppm)	21.3	11.0	12.0	14.3	11.3	11.6	10.3	20.1
Mg (wt %)	1.7	1.0	0.9	1.3	1.2	1.4	1.4	4.4
Mn (ppm)	323.0	198.0	303.0	362.0	226.0	250.0	348.0	688.0
Mo (ppm)	0.4	6.7	1.0	0.4	10.4	1.1	2.4	1.2
Na (wt %)	3.9	4.7	2.3	3.1	3.9	3.8	3.5	2.6
Nb (ppm)	4.0	2.1	3.9	2.0	2.7	2.5	2.2	3.0
Ni (ppm)	20.4	17.4	11.4	21.0	20.7	22.9	23.6	116.0
P (ppm)	570.0	500.0	510.0	430.0	410.0	460.0	490.0	560.0
Pb (ppm)	2.3	4.8	8.3	7.4	1.4	0.9	5.2	2.4
Rb (ppm)	22.8	28.4	66.3	33.0	39.9	38.2	24.1	18.6
Re (ppm)	0.0	0.0	0.0	0.0	0.0	0.0	0.0	0.0
S (wt %)	0.2	0.5	1.8	0.5	1.1	0.8	0.3	0.7
Sb (ppm)	0.4	0.8	0.3	0.3	0.0	0.1	0.3	0.2
Sc (ppm)	10.7	6.4	6.6	7.0	7.6	8.0	9.5	25.7
Se (ppm)	0.5	1.0	1.0	0.5	0.5	1.0	0.5	1.0
Sn (ppm)	1.2	0.8	0.8	0.6	0.9	0.4	0.8	1.2
Sr (ppm)	480.0	429.0	375.0	496.0	418.0	458.0	521.0	425.0
Ta (ppm)	0.3	0.2	0.4	0.2	0.3	0.2	0.2	0.2
Te (ppm)	0.3	0.2	7.4	0.5	0.1	0.0	0.1	0.2
Th (ppm)	1.3	1.6	1.9	1.3	1.4	1.5	1.3	1.3
Ti (wt %)	0.2	0.2	0.2	0.2	0.2	0.2	0.2	0.3
Tl (ppm)	0.1	0.2	0.2	0.2	0.1	0.1	0.1	0.1
U (ppm)	0.4	0.4	0.5	0.3	0.5	0.3	0.4	0.4
V (ppm)	81.0	61.0	57.0	70.0	57.0	65.0	71.0	161.0
W (ppm)	1.6	1.7	4.0	1.1	1.7	0.9	0.9	1.4
Y (ppm)	9.8	6.6	9.1	6.6	8.0	6.1	7.3	15.5
Zn (ppm)	40.0	14.0	83.0	53.0	21.0	26.0	37.0	65.0
Zr (ppm)	60.2	61.5	80.4	54.0	67.6	44.0	53.4	63.2

SAMPLE NO	NM-025	NM-026	NM-027	NM-028	NM-029	NM-030	NM-031	NM-032
Ag (ppm)	0.1	0.1	0.1	0.1	0.1	0.1	0.4	0.2
Al (wt %)	8.1	7.8	6.5	7.3	8.1	7.5	7.0	6.4
As (ppm)	1.0	0.1	0.6	1.0	0.4	0.5	1.0	0.4
Au (ppm)	0.0	0.0	0.0	0.0	0.0	0.0	0.1	0.0
Ba (ppm)	280.0	310.0	210.0	210.0	200.0	190.0	440.0	390.0
Be (ppm)	0.7	0.6	0.5	0.6	0.7	0.6	0.7	0.7
Bi (ppm)	0.0	0.1	0.1	0.1	0.2	0.1	0.1	0.3
Ca (wt %)	5.1	2.6	3.6	2.2	4.2	1.9	3.0	3.5
Cd (ppm)	0.1	0.0	0.0	0.1	0.1	0.0	0.1	0.0
Ce (ppm)	22.3	13.2	13.2	10.9	16.1	13.8	10.7	32.6
Co (ppm)	21.3	5.5	4.8	9.9	13.8	4.3	6.6	7.1
Cr (ppm)	122.0	27.0	23.0	28.0	60.0	27.0	27.0	21.0
Cs (ppm)	1.2	1.5	1.4	1.3	1.8	1.1	1.9	1.3
Cu (ppm)	175.0	2.4	3.0	34.3	15.4	3.6	32.3	34.1
Fe (wt %)	4.2	2.0	1.7	2.3	4.0	1.8	2.2	1.9
Ga (ppm)	16.6	17.7	16.5	18.2	16.8	18.2	17.3	17.3
Ge (ppm)	0.1	0.1	0.1	0.0	0.1	0.2	0.2	0.2
Hf (ppm)	1.6	2.3	2.2	2.4	2.0	2.6	2.6	2.5
In (ppm)	0.0	0.0	0.0	0.0	0.0	0.0	0.0	0.0
K (wt %)	0.9	1.4	1.7	1.3	1.3	1.4	2.8	1.9
La (ppm)	9.7	6.3	5.8	5.0	7.2	6.7	4.8	11.2
Li (ppm)	16.4	11.8	10.8	11.4	21.7	14.3	11.3	6.9
Mg (wt %)	2.6	0.8	0.8	0.9	1.7	1.1	1.0	0.6
Mn (ppm)	611.0	296.0	423.0	152.0	413.0	188.0	338.0	440.0
Mo (ppm)	2.1	0.2	0.3	1.1	0.9	1.0	1.1	1.2
Na (wt %)	3.0	3.5	2.7	3.3	2.9	3.6	1.7	3.1
Nb (ppm)	2.7	0.8	0.7	0.9	1.4	1.1	1.0	1.2
Ni (ppm)	43.7	20.8	16.8	18.3	24.5	25.7	15.9	15.3
P (ppm)	560.0	290.0	280.0	290.0	500.0	290.0	320.0	1680.0
Pb (ppm)	2.9	1.8	1.5	3.1	2.6	4.3	3.0	3.5
Rb (ppm)	22.6	39.7	37.7	33.1	31.9	42.0	69.1	47.7
Re (ppm)	0.0	0.0	0.0	0.0	0.0	0.0	0.0	0.0
S (wt %)	0.6	0.3	0.3	0.7	0.6	0.2	0.5	0.9
Sb (ppm)	0.4	0.1	0.1	0.1	0.1	0.2	0.3	0.2
Sc (ppm)	18.6	4.9	4.3	4.6	10.2	5.1	5.1	4.0
Se (ppm)	1.0	1.0	1.0	1.0	1.0	1.0	1.0	1.0
Sn (ppm)	0.8	0.4	0.4	1.0	0.9	0.5	0.6	0.6
Sr (ppm)	654.0	244.0	159.5	251.0	320.0	244.0	170.5	278.0
Ta (ppm)	0.2	0.1	0.1	0.1	0.1	0.1	0.1	0.1
Te (ppm)	0.1	0.1	0.1	0.2	0.3	0.1	0.5	0.2
Th (ppm)	1.2	0.5	0.4	0.5	1.1	0.5	0.5	0.7
Ti (wt %)	0.3	0.1	0.1	0.1	0.1	0.1	0.1	0.1
Tl (ppm)	0.1	0.2	0.2	0.2	0.2	0.2	0.4	0.2
U (ppm)	0.4	0.1	0.1	0.1	0.3	0.2	0.2	0.2
V (ppm)	118.0	36.0	35.0	37.0	85.0	37.0	43.0	38.0
W (ppm)	2.1	0.7	1.4	0.8	1.0	1.7	2.1	1.4
Y (ppm)	11.1	3.8	4.7	3.1	7.2	3.8	4.0	6.1
Zn (ppm)	51.0	38.0	30.0	22.0	44.0	27.0	27.0	13.0
Zr (ppm)	66.2	88.5	83.3	89.0	70.4	100.0	93.8	94.2

SAMPLE NO	NM-033	NM-034	NM-035	NM-036	NM-037	NM-038	NM-039	NM-040
Ag (ppm)	0.1	0.1	0.2	0.6	0.2	0.2	0.1	0.1
Al (wt %)	7.5	7.5	7.9	7.8	7.3	8.0	7.7	7.6
As (ppm)	0.9	0.5	1.3	3.1	0.7	1.2	0.8	0.8
Au (ppm)	0.1	0.1	0.0	0.1	0.0	0.0	0.0	0.0
Ba (ppm)	390.0	260.0	240.0	380.0	230.0	200.0	240.0	210.0
Be (ppm)	0.6	0.6	0.7	0.7	0.5	0.7	0.8	0.6
Bi (ppm)	0.6	0.1	0.2	0.5	0.1	0.1	0.1	0.1
Ca (wt %)	2.0	1.9	4.4	2.8	2.0	5.5	3.3	1.8
Cd (ppm)	0.1	0.0	0.0	0.4	0.0	0.1	0.0	0.0
Ce (ppm)	15.3	11.2	20.8	27.0	11.3	21.8	42.3	18.8
Co (ppm)	37.1	7.9	14.4	105.0	12.6	18.4	27.0	6.3
Cr (ppm)	26.0	29.0	79.0	53.0	30.0	48.0	146.0	25.0
Cs (ppm)	1.5	0.9	0.8	0.9	0.6	2.5	1.5	0.9
Cu (ppm)	6.3	16.6	59.3	28.1	137.5	421.0	147.0	97.2
Fe (wt %)	2.4	2.7	4.4	6.7	2.2	5.9	4.9	1.9
Ga (ppm)	18.2	17.5	19.6	19.5	19.4	18.3	18.6	18.2
Ge (ppm)	0.2	0.1	0.1	0.2	0.1	0.1	0.1	0.1
Hf (ppm)	2.6	2.4	2.2	2.7	2.5	2.0	2.2	2.7
In (ppm)	0.0	0.0	0.1	0.0	0.0	0.1	0.0	0.0
K (wt %)	1.8	1.3	0.9	1.3	0.8	1.1	1.1	1.2
La (ppm)	6.6	5.0	8.9	12.8	5.2	8.7	18.5	8.7
Li (ppm)	11.1	14.3	23.6	16.7	8.5	32.3	32.9	10.6
Mg (wt %)	1.0	1.1	1.7	1.1	0.7	3.1	3.1	0.9
Mn (ppm)	145.0	219.0	521.0	271.0	134.0	375.0	362.0	140.0
Mo (ppm)	2.2	1.2	1.2	4.3	1.0	0.5	0.8	3.1
Na (wt %)	3.2	3.3	2.9	3.6	4.0	2.1	2.7	3.8
Nb (ppm)	0.9	1.1	1.9	1.8	1.3	3.5	3.5	1.5
Ni (ppm)	23.9	25.1	29.4	45.9	28.2	24.3	45.8	19.5
P (ppm)	280.0	300.0	610.0	440.0	300.0	970.0	960.0	320.0
Pb (ppm)	3.5	2.7	4.5	8.7	3.3	5.2	2.1	1.6
Rb (ppm)	52.5	37.0	14.2	34.4	24.2	21.5	28.2	43.3
Re (ppm)	0.0	0.0	0.0	0.0	0.0	0.0	0.0	0.0
S (wt %)	1.2	0.5	0.3	5.1	0.6	0.2	1.5	0.2
Sb (ppm)	0.1	0.2	0.4	0.6	0.2	0.4	0.2	0.2
Sc (ppm)	5.0	5.0	10.9	8.0	5.1	18.9	18.4	4.6
Se (ppm)	1.0	0.5	3.0	8.0	1.0	1.0	2.0	2.0
Sn (ppm)	0.7	0.4	0.8	0.9	0.6	1.3	1.2	0.5
Sr (ppm)	258.0	233.0	641.0	273.0	348.0	672.0	436.0	226.0
Ta (ppm)	0.1	0.1	0.2	0.1	0.1	0.3	0.3	0.1
Te (ppm)	0.6	0.2	0.4	1.2	0.1	0.1	0.2	0.1
Th (ppm)	0.5	0.5	1.1	1.0	0.6	1.2	1.2	0.6
Ti (wt %)	0.1	0.1	0.2	0.2	0.1	0.4	0.3	0.1
Tl (ppm)	0.2	0.2	0.1	0.2	0.1	0.3	0.2	0.2
U (ppm)	0.2	0.1	0.3	0.4	0.2	0.4	0.3	0.2
V (ppm)	35.0	39.0	98.0	60.0	38.0	161.0	137.0	33.0
W (ppm)	2.6	7.0	0.9	2.7	0.6	1.5	1.3	0.8
Y (ppm)	3.6	3.7	8.9	9.8	4.1	17.4	12.9	3.5
Zn (ppm)	25.0	25.0	50.0	33.0	21.0	39.0	39.0	18.0
Zr (ppm)	101.5	89.2	89.4	102.5	94.3	79.4	86.2	109.0

SAMPLE NO	NM-041	NM-042	NM-043	NM-044	NM-045	NM-046	NM-047	NM-048	NM-049
Ag (ppm)	0.1	0.5	0.2	0.1	3.0	1.4	0.2	22.3	0.2
Al (wt %)	7.9	7.6	7.9	8.0	6.7	7.6	7.7	7.1	6.8
As (ppm)	1.0	0.9	1.7	0.9	1.1	1.9	0.7	2.4	0.6
Au (ppm)	0.0	0.1	0.1	0.1	3.0	1.3	0.0	4.9	0.1
Ba (ppm)	240.0	440.0	360.0	180.0	430.0	430.0	570.0	200.0	380.0
Be (ppm)	0.8	1.1	0.8	0.9	1.0	0.8	0.7	0.7	0.8
Bi (ppm)	0.1	0.1	0.1	0.1	1.3	0.5	0.2	0.9	0.2
Ca (wt %)	3.8	5.6	3.8	3.6	3.4	3.8	2.3	2.5	4.2
Cd (ppm)	0.0	0.1	0.0	0.1	0.2	2.4	0.0	0.0	0.0
Ce (ppm)	14.3	71.5	15.6	19.6	11.5	15.6	16.9	22.6	14.7
Co (ppm)	10.9	11.6	11.0	5.8	9.0	7.9	7.3	13.6	12.0
Cr (ppm)	82.0	69.0	77.0	76.0	49.0	55.0	29.0	27.0	49.0
Cs (ppm)	0.4	1.9	1.0	0.4	2.1	1.0	1.7	1.7	1.4
Cu (ppm)	156.5	266.0	98.1	21.3	38.9	11.8	13.8	397.0	7.7
Fe (wt %)	2.6	2.6	2.8	1.7	2.7	2.2	2.2	3.9	3.9
Ga (ppm)	18.9	17.3	18.7	19.7	15.4	17.0	23.6	21.5	18.2
Ge (ppm)	0.1	0.2	0.1	0.1	0.1	0.2	0.1	0.1	0.1
Hf (ppm)	1.5	1.7	1.3	1.9	1.3	1.4	3.0	2.0	2.6
In (ppm)	0.0	0.0	0.0	0.0	0.0	0.1	0.0	0.0	0.0
K (wt %)	0.6	1.2	0.9	0.6	2.3	1.2	2.4	2.0	1.6
La (ppm)	5.9	31.5	6.2	6.7	5.0	6.0	8.1	10.4	6.0
Li (ppm)	10.8	14.0	15.7	11.5	15.5	13.2	16.8	18.1	24.0
Mg (wt %)	1.7	1.7	1.6	1.8	1.2	1.3	1.0	1.2	1.7
Mn (ppm)	325.0	472.0	361.0	276.0	352.0	337.0	196.0	242.0	393.0
Mo (ppm)	2.6	2.9	3.4	5.8	4.7	1.5	1.1	0.5	0.6
Na (wt %)	3.6	4.4	3.4	4.8	2.0	3.4	2.7	2.6	2.9
Nb (ppm)	2.6	3.5	2.5	3.1	1.6	2.6	1.6	2.5	3.4
Ni (ppm)	26.5	28.2	25.6	26.4	21.6	20.1	26.4	20.0	20.3
P (ppm)	470.0	1130.0	450.0	570.0	420.0	460.0	320.0	430.0	660.0
Pb (ppm)	2.2	3.9	3.2	3.6	3.5	4.0	2.5	3.0	1.9
Rb (ppm)	13.6	35.1	25.3	10.0	58.9	27.3	78.6	76.8	47.5
Re (ppm)	0.0	0.0	0.0	0.0	0.0	0.0	0.0	0.0	0.0
S (wt %)	0.1	0.4	0.3	0.1	1.6	0.7	0.1	1.2	0.4
Sb (ppm)	0.3	0.2	0.8	0.2	0.1	0.2	0.1	0.1	0.3
Sc (ppm)	8.8	9.0	9.3	11.3	6.8	7.5	6.2	8.6	12.0
Se (ppm)	2.0	1.0	1.0	1.0	1.0	1.0	1.0	1.0	1.0
Sn (ppm)	0.7	0.7	0.8	1.5	0.7	0.8	0.6	0.8	1.1
Sr (ppm)	598.0	790.0	566.0	520.0	183.0	480.0	188.5	227.0	297.0
Ta (ppm)	0.2	0.2	0.2	0.2	0.1	0.2	0.1	0.2	0.3
Te (ppm)	0.0	0.5	0.2	0.1	4.9	1.7	0.2	13.5	0.3
Th (ppm)	0.6	1.3	0.7	1.1	1.2	1.4	0.6	1.3	1.4
Ti (wt %)	0.2	0.2	0.2	0.3	0.1	0.2	0.1	0.2	0.2
Tl (ppm)	0.1	0.2	0.1	0.1	0.3	0.1	0.3	0.3	0.3
U (ppm)	0.2	0.3	0.2	0.4	0.2	0.3	0.2	0.3	0.5
V (ppm)	78.0	87.0	77.0	91.0	70.0	69.0	42.0	77.0	94.0
W (ppm)	0.5	1.5	1.4	1.4	6.0	3.4	1.3	3.3	3.1
Y (ppm)	5.6	9.1	6.1	9.7	5.4	7.1	4.8	7.7	9.9
Zn (ppm)	35.0	45.0	37.0	43.0	68.0	208.0	26.0	33.0	36.0
Zr (ppm)	45.5	61.1	45.3	70.3	43.2	47.4	122.5	73.5	102.5

SAMPLE NO	NM-050	NM-051	NM-052	NM-053	NM-054	NM-055	NM-056	NM-057
Ag (ppm)	0.1	2.2	0.1	0.0	0.5	0.5	0.4	27.3
Al (wt %)	7.7	8.0	7.3	8.1	6.9	7.3	7.2	7.2
As (ppm)	1.0	1.6	0.4	0.9	2.0	2.0	1.0	2.2
Au (ppm)	0.0	0.1	0.0	0.0	0.4	0.1	0.1	10.0
Ba (ppm)	450.0	170.0	480.0	180.0	190.0	330.0	190.0	310.0
Be (ppm)	0.9	0.6	0.6	0.6	0.7	0.7	0.6	0.6
Bi (ppm)	0.3	4.4	0.1	0.1	0.1	0.1	0.8	7.8
Ca (wt %)	3.1	2.2	2.3	4.8	4.0	3.6	2.7	4.2
Cd (ppm)	0.0	0.0	0.0	0.1	0.0	0.0	0.0	0.1
Ce (ppm)	22.5	11.5	13.2	18.9	17.2	20.8	18.8	30.0
Co (ppm)	10.4	34.8	11.6	26.6	8.8	14.1	11.3	31.7
Cr (ppm)	39.0	26.0	25.0	175.0	76.0	60.0	25.0	93.0
Cs (ppm)	0.9	0.9	1.1	0.3	0.4	0.7	1.0	1.1
Cu (ppm)	1.6	97.5	5.4	18.1	11.4	710.0	315.0	904.0
Fe (wt %)	3.0	3.2	1.9	4.6	2.9	3.5	2.8	5.8
Ga (ppm)	19.2	17.4	18.7	20.0	17.9	20.8	20.8	16.9
Ge (ppm)	0.2	0.2	0.2	0.1	0.2	0.2	0.1	0.1
Hf (ppm)	1.8	2.8	2.2	1.9	1.9	2.1	2.7	1.6
In (ppm)	0.0	0.0	0.0	0.0	0.0	0.0	0.0	0.1
K (wt %)	1.3	1.7	1.5	0.7	0.7	1.1	1.5	1.3
La (ppm)	10.3	4.9	6.4	8.5	7.5	9.3	9.1	12.7
Li (ppm)	18.3	10.1	10.5	23.4	14.6	12.5	11.1	28.6
Mg (wt %)	1.4	0.8	1.0	3.0	1.6	1.6	1.0	2.9
Mn (ppm)	320.0	175.0	138.0	524.0	343.0	285.0	129.0	624.0
Mo (ppm)	0.5	0.8	1.5	1.4	0.3	15.0	20.3	2.7
Na (wt %)	3.5	3.9	3.3	2.7	3.3	2.9	3.1	2.1
Nb (ppm)	2.5	1.4	1.2	2.7	3.4	3.0	1.9	1.8
Ni (ppm)	16.5	26.0	26.8	61.2	21.1	26.4	22.5	39.6
P (ppm)	550.0	300.0	290.0	460.0	540.0	530.0	350.0	720.0
Pb (ppm)	2.4	2.8	1.8	2.8	3.7	4.4	2.3	4.6
Rb (ppm)	45.8	78.8	46.8	15.7	14.7	33.5	65.4	45.8
Re (ppm)	0.0	0.0	0.0	0.0	0.0	0.0	0.0	0.0
S (wt %)	0.5	2.2	0.4	0.6	0.2	0.3	0.6	2.7
Sb (ppm)	0.3	0.1	0.1	0.4	0.4	0.4	0.4	1.3
Sc (ppm)	8.1	4.9	5.7	18.0	10.9	12.0	6.8	25.0
Se (ppm)	1.0	2.0	1.0	2.0	2.0	3.0	1.0	2.0
Sn (ppm)	0.7	0.5	0.4	0.7	0.8	1.0	0.5	1.0
Sr (ppm)	454.0	150.0	187.5	593.0	553.0	500.0	266.0	275.0
Ta (ppm)	0.2	0.1	0.1	0.2	0.3	0.2	0.1	0.2
Te (ppm)	0.4	4.6	0.1	0.1	0.6	0.2	0.4	37.0
Th (ppm)	1.6	0.5	0.5	0.9	1.4	1.5	0.5	1.7
Ti (wt %)	0.2	0.1	0.1	0.3	0.2	0.2	0.2	0.2
Tl (ppm)	0.2	0.3	0.2	0.1	0.1	0.1	0.2	0.2
U (ppm)	0.5	0.3	0.2	0.3	0.5	0.3	0.2	0.5
V (ppm)	63.0	33.0	35.0	138.0	82.0	95.0	56.0	158.0
W (ppm)	1.0	2.5	0.7	0.9	0.9	0.8	1.9	3.3
Y (ppm)	9.4	4.8	4.1	8.3	10.3	10.2	5.1	14.7
Zn (ppm)	37.0	19.0	15.0	43.0	33.0	26.0	16.0	51.0
Zr (ppm)	61.9	109.0	79.9	68.2	68.2	69.3	112.5	62.7

SAMPLE NO	NM-058	NM-059	NM-060	NM-061	NM-062	NM-063	NM-064	NM-065
Ag (ppm)	3.1	0.5	0.1	0.1	4.2	0.2	6.3	0.1
Al (wt %)	6.5	8.0	7.4	7.6	8.0	7.6	7.1	7.9
As (ppm)	1.4	1.2	3.1	1.8	0.9	1.2	0.8	0.9
Au (ppm)	2.7	0.2	0.0	0.0	6.7	0.1	3.4	0.0
Ba (ppm)	220.0	170.0	150.0	140.0	290.0	120.0	260.0	570.0
Be (ppm)	0.4	0.7	0.8	0.7	0.7	0.7	0.7	0.7
Bi (ppm)	1.2	0.4	0.2	0.1	1.9	0.2	0.7	0.3
Ca (wt %)	7.2	6.0	4.8	5.7	3.4	3.7	4.1	4.1
Cd (ppm)	0.1	0.0	0.0	0.0	0.0	0.0	0.1	0.0
Ce (ppm)	27.5	33.4	19.9	23.9	20.7	15.6	30.1	25.9
Co (ppm)	21.8	28.7	8.7	15.0	13.6	8.7	16.7	18.2
Cr (ppm)	83.0	119.0	48.0	48.0	65.0	60.0	85.0	68.0
Cs (ppm)	0.9	1.1	0.4	0.3	0.9	0.9	1.5	2.0
Cu (ppm)	108.0	138.5	97.2	56.1	633.0	34.9	170.5	130.5
Fe (wt %)	5.1	6.0	2.4	3.9	3.7	2.2	4.6	4.1
Ga (ppm)	15.3	18.0	18.2	18.4	20.9	20.1	18.1	19.0
Ge (ppm)	0.1	0.1	0.2	0.2	0.2	0.2	0.1	0.1
Hf (ppm)	1.4	1.4	1.6	1.5	1.8	1.8	1.9	2.0
In (ppm)	0.1	0.1	0.1	0.1	0.0	0.0	0.0	0.1
K (wt %)	0.9	1.1	0.8	0.8	1.3	0.7	1.2	1.6
La (ppm)	12.0	14.8	8.2	10.3	9.3	6.2	12.9	10.7
Li (ppm)	30.3	36.0	15.9	14.3	18.2	18.9	21.4	30.0
Mg (wt %)	3.4	3.7	2.1	2.3	1.8	1.8	2.0	1.6
Mn (ppm)	986.0	829.0	442.0	617.0	428.0	370.0	527.0	995.0
Mo (ppm)	1.1	0.9	22.1	1.4	1.1	1.5	2.8	0.2
Na (wt %)	1.3	2.0	4.1	3.0	3.3	4.1	3.1	2.6
Nb (ppm)	1.8	2.9	3.6	3.7	2.4	3.0	2.6	2.4
Ni (ppm)	31.7	43.4	15.4	20.3	24.9	20.0	32.1	28.0
P (ppm)	610.0	760.0	690.0	680.0	610.0	580.0	770.0	620.0
Pb (ppm)	3.1	4.3	2.4	6.7	2.4	2.1	4.1	2.5
Rb (ppm)	33.3	33.8	18.9	17.1	34.8	22.1	39.9	34.1
Re (ppm)	0.0	0.0	0.1	0.0	0.0	0.0	0.0	0.0
S (wt %)	0.8	0.4	0.1	0.2	0.6	0.2	1.8	0.2
Sb (ppm)	1.3	1.5	0.8	0.7	0.4	0.3	0.3	0.2
Sc (ppm)	21.7	27.2	15.5	16.2	11.6	12.5	12.2	12.7
Se (ppm)	1.0	1.0	1.0	2.0	1.0	2.0	1.0	1.0
Sn (ppm)	0.8	1.1	2.3	1.7	0.8	1.6	1.2	0.8
Sr (ppm)	326.0	683.0	374.0	596.0	423.0	385.0	277.0	419.0
Ta (ppm)	0.2	0.2	0.3	0.3	0.2	0.3	0.2	0.2
Te (ppm)	3.6	0.4	0.2	0.1	10.8	0.4	5.5	0.1
Th (ppm)	1.4	1.7	1.4	1.5	1.2	1.4	1.6	1.3
Ti (wt %)	0.2	0.3	0.4	0.4	0.2	0.2	0.2	0.2
Tl (ppm)	0.1	0.2	0.1	0.1	0.1	0.1	0.1	0.2
U (ppm)	0.4	0.5	0.3	0.4	0.3	0.3	0.4	0.3
V (ppm)	145.0	183.0	106.0	134.0	87.0	63.0	92.0	107.0
W (ppm)	2.7	2.0	2.7	1.7	2.0	1.4	4.7	1.5
Y (ppm)	13.8	16.7	12.3	12.3	9.4	10.1	8.5	11.4
Zn (ppm)	59.0	54.0	32.0	52.0	45.0	32.0	80.0	91.0
Zr (ppm)	52.4	56.9	53.7	50.9	65.7	60.3	64.8	73.1

SAMPLE NO	NM-066	NM-067	NM-068	NM-069	NM-070	NM-071	NM-072	NM-073
Ag (ppm)	0.0	0.1	0.2	0.3	0.2	0.1	0.2	0.1
Al (wt %)	7.7	8.0	7.7	7.6	7.3	7.6	7.1	7.9
As (ppm)	1.4	0.4	0.4	2.4	1.2	1.6	1.1	0.7
Au (ppm)	0.0	0.0	0.0	0.0	0.0	0.0	0.1	0.0
Ba (ppm)	360.0	130.0	260.0	250.0	260.0	290.0	410.0	320.0
Be (ppm)	0.7	0.6	0.5	0.7	0.6	0.6	0.6	0.6
Bi (ppm)	0.6	0.3	0.1	0.4	0.0	0.0	0.2	0.1
Ca (wt %)	4.3	4.6	3.8	2.8	3.6	2.5	1.7	1.9
Cd (ppm)	0.1	0.1	0.0	9.9	0.3	0.2	0.1	0.0
Ce (ppm)	26.3	23.7	22.9	21.3	16.4	7.5	16.9	15.6
Co (ppm)	18.0	19.8	23.2	10.0	10.1	6.0	6.7	6.6
Cr (ppm)	72.0	31.0	31.0	27.0	32.0	14.0	28.0	26.0
Cs (ppm)	1.6	1.2	1.6	1.9	2.2	1.4	1.3	0.9
Cu (ppm)	4.9	39.0	76.0	44.2	26.8	6.0	10.6	39.3
Fe (wt %)	4.2	4.3	4.3	2.3	2.3	1.6	2.2	2.3
Ga (ppm)	19.0	18.5	18.2	20.4	19.4	18.4	18.6	19.3
Ge (ppm)	0.1	0.1	0.1	0.1	0.1	0.1	0.2	0.2
Hf (ppm)	2.1	2.0	2.8	2.1	2.3	1.9	2.5	2.6
In (ppm)	0.1	0.0	0.0	0.1	0.0	0.0	0.0	0.0
K (wt %)	1.0	1.0	1.2	2.1	2.0	1.5	1.4	0.9
La (ppm)	12.7	11.5	10.5	8.9	7.1	3.4	7.6	7.5
Li (ppm)	30.5	27.8	34.7	27.3	27.5	11.5	18.6	21.2
Mg (wt %)	1.6	1.7	1.9	0.7	0.7	0.3	0.9	1.1
Mn (ppm)	990.0	1125.0	804.0	657.0	577.0	364.0	325.0	363.0
Mo (ppm)	0.6	0.6	1.0	1.5	2.0	0.2	0.5	0.3
Na (wt %)	2.8	2.4	2.3	2.2	2.0	3.4	3.4	3.6
Nb (ppm)	1.8	3.9	4.3	2.2	2.3	1.0	1.5	1.3
Ni (ppm)	27.3	29.5	28.1	19.8	29.3	13.0	23.4	24.0
P (ppm)	600.0	430.0	430.0	410.0	390.0	240.0	320.0	310.0
Pb (ppm)	3.0	2.9	1.7	8.8	14.2	4.8	3.9	2.4
Rb (ppm)	29.2	28.1	28.5	51.0	45.9	31.5	33.8	18.7
Re (ppm)	0.0	0.0	0.0	0.0	0.0	0.0	0.0	0.0
S (wt %)	0.7	0.2	0.1	0.6	0.0	0.1	0.7	0.0
Sb (ppm)	0.2	0.1	0.1	0.1	1.2	0.1	0.1	0.2
Sc (ppm)	12.8	18.1	17.9	5.9	6.4	4.0	4.6	4.9
Se (ppm)	1.0	0.5	1.0	1.0	1.0	1.0	1.0	1.0
Sn (ppm)	0.7	0.9	0.8	0.5	0.5	0.3	0.4	0.4
Sr (ppm)	402.0	310.0	202.0	239.0	263.0	351.0	395.0	339.0
Ta (ppm)	0.2	0.3	0.4	0.1	0.2	0.1	0.1	0.1
Te (ppm)	0.3	0.1	0.1	0.0	0.0	0.0	0.2	0.0
Th (ppm)	1.6	1.7	1.6	0.5	0.4	0.4	0.5	0.6
Ti (wt %)	0.2	0.3	0.3	0.2	0.2	0.1	0.1	0.1
Tl (ppm)	0.2	0.1	0.1	0.2	0.2	0.2	0.2	0.1
U (ppm)	0.5	0.4	0.4	0.1	0.1	0.2	0.2	0.2
V (ppm)	94.0	113.0	113.0	43.0	47.0	27.0	38.0	35.0
W (ppm)	0.5	0.7	0.5	0.5	0.3	0.4	0.4	0.4
Y (ppm)	11.8	15.0	14.9	3.5	3.7	2.8	3.9	4.0
Zn (ppm)	87.0	74.0	67.0	369.0	83.0	46.0	41.0	30.0
Zr (ppm)	68.7	85.4	122.0	91.0	81.3	65.3	100.5	103.0

SAMPLE NO	NM-074	NM-075	NM-076	NM-077	NM-078	NM-079	NM-080	NM-081
Ag (ppm)	0.3	0.1	0.4	0.1	0.5	0.0	0.2	1.5
Al (wt %)	7.8	7.2	7.6	7.5	7.9	8.0	7.3	7.3
As (ppm)	4.3	0.9	1.7	0.8	1.5	1.8	1.0	0.1
Au (ppm)	0.1	0.0	0.1	0.0	0.2	0.0	0.0	6.6
Ba (ppm)	610.0	460.0	530.0	190.0	480.0	110.0	250.0	240.0
Be (ppm)	0.8	0.7	0.8	0.7	0.8	0.8	0.6	0.7
Bi (ppm)	1.0	0.1	0.2	0.1	0.8	0.1	0.1	0.8
Ca (wt %)	4.0	2.1	2.8	1.7	4.9	4.6	2.0	1.8
Cd (ppm)	0.1	0.0	0.1	0.0	0.4	0.1	0.1	0.0
Ce (ppm)	37.7	15.4	27.6	18.2	28.8	24.1	14.0	9.1
Co (ppm)	27.1	6.6	5.3	9.0	31.2	11.3	8.0	4.5
Cr (ppm)	46.0	25.0	36.0	29.0	224.0	73.0	21.0	20.0
Cs (ppm)	3.1	1.4	2.5	0.8	3.1	0.9	1.2	1.2
Cu (ppm)	56.0	12.3	215.0	4.4	160.0	8.0	80.2	245.0
Fe (wt %)	6.8	1.9	4.7	2.2	6.4	4.6	2.1	1.3
Ga (ppm)	20.1	18.8	18.7	19.2	18.1	21.1	18.6	17.4
Ge (ppm)	0.2	0.2	0.2	0.1	0.1	0.1	0.2	0.1
Hf (ppm)	2.9	2.4	2.8	2.3	2.1	1.9	2.4	2.2
In (ppm)	0.1	0.0	0.1	0.0	0.1	0.1	0.0	0.0
K (wt %)	1.8	1.8	1.9	1.1	2.0	0.6	1.5	1.3
La (ppm)	15.8	6.4	12.0	8.3	13.2	10.1	6.1	4.2
Li (ppm)	41.9	16.5	33.4	15.9	27.8	22.9	11.8	6.2
Mg (wt %)	2.7	0.8	1.6	1.0	2.8	1.8	0.8	0.7
Mn (ppm)	553.0	199.0	432.0	181.0	843.0	450.0	189.0	151.0
Mo (ppm)	0.8	1.3	1.8	1.0	2.5	0.9	0.6	2.8
Na (wt %)	1.9	2.7	2.4	3.5	1.4	2.5	3.3	4.0
Nb (ppm)	4.0	1.4	4.0	1.0	2.8	3.0	1.3	1.1
Ni (ppm)	26.3	25.3	16.1	26.6	72.8	25.0	21.1	10.6
P (ppm)	1300.0	300.0	730.0	320.0	860.0	650.0	290.0	300.0
Pb (ppm)	4.6	2.3	4.2	2.6	4.0	6.7	3.2	3.9
Rb (ppm)	39.1	45.9	50.5	32.3	52.3	15.2	47.8	40.8
Re (ppm)	0.0	0.0	0.0	0.0	0.0	0.0	0.0	0.0
S (wt %)	1.7	0.4	0.5	0.7	2.2	0.2	0.3	0.2
Sb (ppm)	0.3	0.1	0.1	0.2	0.2	0.4	0.1	0.1
Sc (ppm)	21.7	4.7	10.3	5.1	15.8	12.4	4.5	4.3
Se (ppm)	1.0	0.5	1.0	1.0	1.0	0.5	1.0	1.0
Sn (ppm)	1.2	0.4	1.1	0.5	1.0	0.7	0.6	0.3
Sr (ppm)	527.0	256.0	324.0	310.0	264.0	625.0	232.0	249.0
Ta (ppm)	0.3	0.1	0.4	0.1	0.2	0.2	0.1	0.1
Te (ppm)	0.4	0.1	0.2	0.2	0.7	0.1	0.1	7.9
Th (ppm)	1.8	0.5	2.1	0.6	1.7	1.1	0.5	0.5
Ti (wt %)	0.4	0.1	0.3	0.1	0.3	0.2	0.1	0.1
Tl (ppm)	0.3	0.2	0.3	0.2	0.4	0.1	0.2	0.2
U (ppm)	0.4	0.1	0.6	0.2	0.4	0.3	0.2	0.1
V (ppm)	162.0	36.0	95.0	40.0	123.0	92.0	32.0	34.0
W (ppm)	0.4	0.6	1.3	0.5	1.2	1.0	0.9	1.3
Y (ppm)	21.1	3.8	11.2	4.2	14.6	11.4	3.6	3.2
Zn (ppm)	58.0	19.0	59.0	20.0	81.0	30.0	31.0	22.0
Zr (ppm)	117.5	96.2	107.5	93.5	81.8	68.1	101.5	76.7

SAMPLE NO	NM-082	NM-083	NM-084	NM-085	NM-086	NM-087	NM-088	NM-089
Ag (ppm)	4.5	12.7	0.8	0.4	0.7	1.9	0.3	0.3
Al (wt %)	7.4	7.4	7.6	7.4	7.8	7.7	7.5	7.7
As (ppm)	0.9	2.2	1.7	1.5	4.6	3.2	2.0	2.5
Au (ppm)	4.3	6.0	0.2	0.4	0.1	0.2	0.0	0.0
Ba (ppm)	520.0	560.0	480.0	410.0	230.0	360.0	230.0	130.0
Be (ppm)	0.9	0.8	0.8	0.7	1.0	1.0	1.1	1.0
Bi (ppm)	2.1	0.7	0.3	0.1	0.8	1.1	0.3	0.1
Ca (wt %)	3.0	2.4	3.0	3.2	5.3	5.1	4.5	4.1
Cd (ppm)	0.1	13.0	0.1	0.0	0.1	0.1	0.1	0.1
Ce (ppm)	17.6	19.8	18.4	16.7	31.9	31.6	31.5	12.2
Co (ppm)	7.7	6.3	8.2	9.7	21.3	20.6	12.3	4.7
Cr (ppm)	23.0	26.0	42.0	40.0	44.0	48.0	27.0	55.0
Cs (ppm)	2.2	2.0	2.1	1.1	2.5	2.2	1.2	0.4
Cu (ppm)	308.0	281.0	211.0	68.1	332.0	1105.0	87.6	174.5
Fe (wt %)	2.2	2.2	2.6	3.4	5.7	5.1	3.2	1.3
Ga (ppm)	17.8	17.4	19.5	21.2	17.3	16.8	17.6	17.7
Ge (ppm)	0.1	0.1	0.1	0.2	0.2	0.2	0.2	0.2
Hf (ppm)	1.8	1.8	1.5	1.7	2.3	2.3	2.6	2.0
In (ppm)	0.0	0.0	0.0	0.0	0.1	0.1	0.0	0.0
K (wt %)	2.4	3.2	1.8	1.0	1.7	2.2	1.1	0.5
La (ppm)	7.7	9.3	7.7	7.9	14.1	14.4	10.8	4.6
Li (ppm)	7.2	9.5	13.0	12.8	23.1	24.0	13.2	7.3
Mg (wt %)	0.7	0.8	1.1	0.9	2.6	2.5	1.8	1.2
Mn (ppm)	349.0	753.0	273.0	279.0	770.0	767.0	488.0	265.0
Mo (ppm)	0.4	0.6	0.6	1.1	2.8	83.1	1.7	9.8
Na (wt %)	2.5	1.3	3.0	3.1	2.4	2.2	3.3	3.8
Nb (ppm)	1.4	1.9	3.3	2.8	3.0	2.9	5.2	3.1
Ni (ppm)	10.6	10.1	16.2	17.6	16.4	18.7	11.0	12.2
P (ppm)	440.0	430.0	500.0	460.0	1060.0	1020.0	1120.0	600.0
Pb (ppm)	7.2	844.0	4.0	3.3	7.2	5.4	6.8	3.8
Rb (ppm)	69.8	92.8	46.3	31.0	59.0	70.6	31.0	11.7
Re (ppm)	0.0	0.0	0.0	0.0	0.0	0.0	0.0	0.0
S (wt %)	0.9	1.1	0.3	0.4	1.7	1.8	0.5	0.1
Sb (ppm)	0.2	2.4	0.3	0.9	0.7	0.5	0.4	0.4
Sc (ppm)	5.8	5.9	7.5	6.6	20.3	19.5	15.7	8.6
Se (ppm)	1.0	1.0	2.0	1.0	1.0	2.0	1.0	1.0
Sn (ppm)	0.5	0.5	0.5	0.3	1.0	1.1	1.4	0.8
Sr (ppm)	431.0	237.0	585.0	644.0	767.0	493.0	683.0	723.0
Ta (ppm)	0.1	0.2	0.3	0.3	0.2	0.2	0.4	0.3
Te (ppm)	8.0	6.2	0.4	0.3	0.6	1.3	0.3	0.1
Th (ppm)	1.6	1.8	1.6	1.8	1.9	1.9	2.0	1.7
Ti (wt %)	0.1	0.1	0.2	0.2	0.4	0.4	0.4	0.2
Tl (ppm)	0.3	0.3	0.2	0.1	0.4	0.4	0.2	0.1
U (ppm)	0.6	0.6	0.3	0.2	0.6	0.6	0.5	0.4
V (ppm)	47.0	49.0	63.0	81.0	189.0	170.0	125.0	67.0
W (ppm)	2.7	47.5	1.7	0.7	5.2	7.7	3.2	1.2
Y (ppm)	5.5	5.9	7.8	6.0	20.6	18.6	19.7	9.1
Zn (ppm)	25.0	1190.0	36.0	35.0	49.0	48.0	35.0	21.0
Zr (ppm)	64.1	66.0	53.8	57.7	88.2	90.7	94.0	70.9

Appendix III: Short Wave Infra-red data

Sample Number	Mineral 1	Mineral 2	2200 POS (nm)	2250 POS (nm)	1900 POS (nm)	1900 Depth
ML23NM001	Chlorite-FeMg	Muscoviticillite	2203.17	2250.3	1913.25	0.196
ML23NM002	Chlorite-Fe	Siderite	n/a	2258.52	n/a	n/a
ML23NM003	Chlorite-FeMg	Siderite	n/a	2252.91	1911.06	0.103
ML23NM004	Epidote	Ankerite	n/a	2254.12	n/a	n/a
ML23NM005	Chlorite-FeMg	Epidote	n/a	2252.82	1915.78	0.134
ML23NM006	Chlorite-FeMg	Siderite	n/a	2251.85	1916.01	0.0756
ML23NM007	Chlorite-FeMg	Muscovite	2210.11	2254.72	1915.16	0.124
ML23NM008	Chlorite-FeMg	Muscovite	2207.49	2250.22	n/a	n/a
ML23NM009	Chlorite-FeMg	Muscovite	2202.94	2251.81	1921.45	0.149
ML23NM010	Muscovite	Ankerite	2210.79	n/a	1911.73	0.084
ML23NM011	Phengite	Chlorite-FeMg	2215.01	2249.3	1912.67	0.107
ML23NM012	Muscovite	Chlorite-Mg	2209.35	n/a	1911.96	0.143
ML23NM013	Chlorite-FeMg	Muscovite	2212.48	2247.85	1912.37	0.102
ML23NM014	Phengite	Chlorite-Mg	2212.78	2244.57	1915.65	0.12
ML23NM015	Muscovite	Chlorite-FeMg	2207.83	2243.38	1916.71	0.0756
ML23NM016	Muscovite	Chlorite-FeMg	2212.43	2245.47	n/a	n/a
ML23NM017	Phengite	Chlorite-FeMg	2211.29	2251.41	n/a	n/a
ML23NM018	Phengite	Chlorite-Mg	2214	2245.86	n/a	n/a
ML23NM019	Phengite	Ankerite	2214.07	n/a	n/a	n/a
ML23NM020	Siderite	Muscovite	2210.03	2243.14	n/a	n/a
ML23NM021	Chlorite-FeMg	Siderite	n/a	2251.14	n/a	n/a
ML23NM022	Chlorite-Mg	Muscovite	2207.8	2251.47	n/a	n/a
ML23NM023	Muscovite	Epidote	2212.61	2249.48	n/a	n/a
ML23NM024	Chlorite-FeMg	Ankerite	n/a	2252.63	n/a	n/a
ML23NM025	Chlorite-FeMg	Epidote	n/a	2253.64	n/a	n/a
ML23NM026	Muscoviticillite	-	2202.09	n/a	1908.96	0.126
ML23NM027	Muscovite	Ankerite	2206.41	n/a	1921.41	0.511
ML23NM028	Muscovite	Chlorite-Mg	2204.18	n/a	1915.36	0.0799
ML23NM029	Chlorite-FeMg	Muscovite	2207.33	2249.19	1910.97	0.106
ML23NM030	Muscovite	Chlorite-FeMg	2209.9	2244.13	1912.53	0.147
ML23NM031	Dolomite	-	n/a	n/a	n/a	n/a
ML23NM032	Dolomite	-	n/a	n/a	n/a	n/a
ML23NM033	Muscovite	Chlorite-FeMg	2211.12	2246.49	1921.84	0.0698
ML23NM034	Muscovite	Chlorite-FeMg	2208.36	n/a	1912.44	0.105
ML23NM035	Chlorite-FeMg	Epidote	n/a	2253.57	1911.92	0.116
ML23NM036	Chlorite-FeMg	Muscovite	n/a	2252.41	1912.41	0.0881
ML23NM037	Chlorite-FeMg	Phengiticillite	2210.53	2253.02	1913	0.227
ML23NM038	Chlorite-FeMg	-	n/a	2252.15	1922.32	0.171
ML23NM039	Chlorite-FeMg	-	n/a	2251.01	1915.43	0.12
ML23NM040	Chlorite-FeMg	Muscovite	2211.63	2247.85	n/a	n/a
ML23NM041	Chlorite-Mg	Epidote	n/a	2252.68	1914.82	0.0803
ML23NM042	Chlorite-FeMg	Muscovite	2210.53	2249.17	1911.92	0.133
ML23NM043	Chlorite-FeMg	Phengite	n/a	2250.64	1913.95	0.11
ML23NM044	Chlorite-FeMg	Hornblende	n/a	2252.21	1914.15	0.114
ML23NM045	Muscovite	Chlorite-Mg	2210.65	n/a	n/a	n/a
ML23NM046	Phengite	Chlorite-Mg	2214.4	2243.06	n/a	n/a

Sample Number	Mineral 1	Mineral 2	2200 POS (nm)	2250 POS (nm)	1900 POS (nm)	1900 Depth
ML23NM047	Chlorite-Fe	Muscovite	2207.38	2248.84	1913.39	0.0843
ML23NM048	Muscovite	Chlorite-FeMg	2211.53	2248.37	1915.51	0.0893
ML23NM049	Chlorite-FeMg	Muscovite	2212.07	2252.56	1908.91	0.0932
ML23NM050	Phengite	Chlorite-FeMg	2218.92	2250.65	1917.39	0.118
ML23NM051	Phengite	Siderite	2212.51	n/a	1912.87	0.0858
ML23NM052	Chlorite-FeMg	Muscovite	2211.22	2250.4	1910.8	0.104
ML23NM053	Chlorite-FeMg	Epidote	n/a	2252.44	1915.71	0.124
ML23NM054	Chlorite-FeMg	Phengite	n/a	2252.48	1923.57	0.173
ML23NM055	Phengiticllite	Chlorite-Mg	2213.2	2250.44	1911.9	0.176
ML23NM056	Phengiticllite	Epidote	2212.32	2249.25	1911.45	0.192
ML23NM057	Chlorite-FeMg	Phengite	n/a	2250.9	1908.88	0.121
ML23NM058	Chlorite-FeMg	-	n/a	2251.76	1883.32	0.103
ML23NM059	Chlorite-FeMg	Calcite	n/a	2252.16	1911.36	0.0889
ML23NM060	Chlorite-Mg	Epidote	n/a	2252.52	1912.54	0.121
ML23NM061	Chlorite-FeMg	Epidote	n/a	2252.81	n/a	n/a
ML23NM062	Chlorite-FeMg	Phengite	n/a	2251.16	1909.62	0.12
ML23NM063	Chlorite-FeMg	Muscovite	2204.84	2248.28	1915.97	0.125
ML23NM064	Phengite	Chlorite-FeMg	2214.29	2245.83	1914.48	0.0877
ML23NM065	Chlorite-FeMg	Muscovite	2213.11	2253.85	1907.91	0.136
ML23NM066	Chlorite-FeMg	Muscovite	2206.28	2252.43	1911.49	0.132
ML23NM067	Chlorite-FeMg	Muscovite	2211.12	2254.52	1879.75	0.153
ML23NM068	Chlorite-FeMg	-	n/a	2253.6	1876.79	0.144
ML23NM069	Muscovite	-	2201.59	n/a	1915.38	0.0887
ML23NM070	Muscovite	Chlorite-Mg	2202.97	n/a	1914.09	0.0893
ML23NM071	Chlorite-FeMg	Epidote	n/a	2252.99	1921.82	0.0646
ML23NM072	Muscovite	Siderite	2203.62	n/a	1921.63	0.11
ML23NM073	Muscovite	-	2206.92	n/a	1913.75	0.14
ML23NM074	Chlorite-FeMg	Muscovite	2207.3	2252.19	1912.89	0.168
ML23NM075	Muscovite	Ankerite	2206.89	n/a	1915.69	0.129
ML23NM076	Chlorite-FeMg	Muscovite	2212.08	2251.42	1912.42	0.139
ML23NM077	Chlorite-FeMg	Muscovite	2206.48	2249.23	1915.16	0.204
ML23NM078	Chlorite-FeMg	Epidote	n/a	2252.89	1881.99	0.101
ML23NM079	Muscovite	Chlorite-FeMg	2210.51	2246.9	1912.68	0.101
ML23NM080	Phengite	Ankerite	2212.91	n/a	n/a	n/a
ML23NM081	Muscovite	Chlorite-FeMg	2210.81	2245.18	1918.61	0.151
ML23NM082	Muscovite	Chlorite-FeMg	2208.58	n/a	1914.21	0.0659
ML23NM083	Muscovite	Chlorite-Fe	2210.8	n/a	1915.28	0.053
ML23NM084	Phengite	Chlorite-FeMg	2213.96	2246.16	1915.44	0.23
ML23NM085	Chlorite-FeMg	Phengite	2213.17	2251.66	n/a	n/a
ML23NM086	Chlorite-FeMg	Epidote	n/a	2251.84	n/a	n/a
ML23NM087	Chlorite-FeMg	Biotite	n/a	2249.86	n/a	n/a
ML23NM088	Chlorite-FeMg	Phengite	2210.72	2251.64	n/a	n/a
ML23NM089	Chlorite-Mg	Muscovite	2198.42	2253.94	n/a	n/a
ML23NM090	Phengiticllite	Chlorite-Mg	2212.61	n/a	1911.11	0.123
ML23NM091	Chlorite-FeMg	Montmorillonite	2210.59	2249.65	1907.96	0.211
ML23NM092	Muscoviticllite	Montmorillonite	2210.68	n/a	1907.67	0.284

Sample Number	Mineral 1	Mineral 2	2200 POS (nm)	2250 POS (nm)	1900 POS (nm)	1900 Depth
ML23NM093	Hornblende	Chlorite-FeMg	2202.06	2251.99	1907.91	0.106
ML23NM094	Chlorite-FeMg	Montmorillonite	2207.91	2251.52	1907.44	0.215
ML23NM095	Chlorite-FeMg	Epidote	n/a	2252.17	1907.5	0.164
ML23NM096	Chlorite-FeMg	Epidote	n/a	2252.11	1909.64	0.113
ML23NM097	Chlorite-FeMg	Tourmaline-Fe	n/a	2251.3	n/a	0.0988
ML23NM098	Gypsum	-	2214.62	n/a	n/a	0.147
ML23NM099	Epidote	Chlorite-FeMg	n/a	2253.73	n/a	0.102
ML23NM100	Chlorite-FeMg	Phengite	2213.5	2246.66	n/a	0.264
ML23NM101	Chlorite-FeMg	Gypsum	2218.22	2251.02	n/a	0.263
ML23NM102	Chlorite-FeMg	Phlogopite	n/a	2249.14	n/a	0.224
ML23NM103	Chlorite-FeMg	Muscovite	2205.05	2251.79	1918.32	0.13
ML23NM104	Muscovite	-	2206.37	n/a	1911.27	0.0576
ML23NM105	Chlorite-FeMg	Phlogopite	n/a	2250.77	1914.24	0.0953
ML23NM106	Siderite	Phengite	2214.07	2244.82	n/a	0.0753
ML23NM107	Phengite	Chlorite-FeMg	2212.24	n/a	1919.37	0.0753
ML23NM108	Chlorite-FeMg	-	n/a	2252.14	1878.07	0.111
ML23NM109	Muscovite	-	2209.72	n/a	n/a	0.0606
ML23NM110	Phengite	-	2211.62	n/a	n/a	0.0715
ML23NM111	Phengite	Siderite	2210.17	n/a	n/a	0.124
ML23NM112	Calcite	Chlorite-FeMg	n/a	2253.65	n/a	0.0803
ML23NM113	Phengite	-	2211.61	n/a	1917.11	0.0599
ML23NM114	Muscovite	-	2211.07	n/a	n/a	0.183
ML23NM115	Chlorite-FeMg	Phengite	n/a	2251.77	1879.29	n/a
ML23NM116	Muscovite	Chlorite-FeMg	2208.65	2248.28	n/a	0.118
ML23NM117	Chlorite-FeMg	Muscovite	2208.7	2247.86	n/a	0.244
ML23NM118	Chlorite-FeMg	Muscovite	2210.3	2248.25	n/a	0.157
ML23NM119	Muscovite	Chlorite-FeMg	2211.78	2247.17	n/a	0.153
ML23NM120	Phengite	Chlorite-Mg	2212.69	n/a	1909.71	0.182
ML23NM121	Muscoviticillite	Chlorite-FeMg	2210.85	2243.55	1910.2	0.172
ML23NM122	Muscoviticillite	Chlorite-FeMg	2210.47	n/a	1909.62	0.0877
ML23NM123	Chlorite-FeMg	Calcite	n/a	2252.06	1908.19	0.13
ML23NM124	Phengite	Chlorite-FeMg	2210.94	2247.68	1909.17	0.106
ML23NM125	Chlorite-FeMg	Montmorillonite	n/a	2250.22	1910.24	0.128
ML23NM126	Chlorite-FeMg	Phengiticillite	n/a	2249.55	1908.97	0.197
ML23NM127	Chlorite-FeMg	Muscoviticillite	2204.11	2250.11	1908.41	0.134
ML23NM128	Chlorite-FeMg	-	n/a	2252.06	1910.27	0.145
ML23NM129	Chlorite-FeMg	Ankerite	n/a	2252.02	1919.54	0.14
ML23NM130	Chlorite-FeMg	-	n/a	2250.26	n/a	0.0654
ML23NM131	Chlorite-FeMg	Phengite	2226.08	2249.53	1923.46	0.123
ML23NM132	Chlorite-FeMg	-	n/a	2250.1	n/a	0.126
ML23NM133	Phengite	Chlorite-Mg	2214.46	2247.01	n/a	0.19
ML23NM134	Chlorite-FeMg	Epidote	n/a	2253.34	n/a	0.104
ML23NM135	Muscovite	-	2207.6	n/a	1911.12	0.0927
ML23NM136	Montmorillonite	Chlorite-FeMg	2210.59	2249.25	1909.32	0.217
ML23NM137	Hornblende	Epidote	2199.83	2253.42	1913.27	0.0631
ML23NM138	Muscovite	-	2206.77	n/a	1911.73	0.0851

Sample Number	Mineral 1	Mineral 2	2200 POS (nm)	2250 POS (nm)	1900 POS (nm)	1900 Depth
ML23NM139	Muscovite	-	2205.33	n/a	1911.84	0.0505
ML23NM140	Phengite	Tourmaline-Fe	2210.05	2240.23	1911.05	0.0988
ML23NM141	Muscovite	Chlorite-FeMg	2208.41	n/a	1923.22	0.1
ML23NM142	Phengiticillite	Chlorite-FeMg	2210.48	2248.7	1910.46	0.103
ML23NM143	Chlorite-FeMg	Calcite	n/a	2250.17	n/a	0.101
ML23NM144	Chlorite-FeMg	-	n/a	2251.33	1922.19	0.0757
ML23NM145	Muscovite	Chlorite-Mg	2210.48	2240.62	n/a	0.127
ML23NM146	Phengite	Siderite	2209.03	2243.52	1923.46	0.0733
ML23NM147	Chlorite-FeMg	Phengite	2211.56	2251.21	n/a	n/a
ML23NM148	Chlorite-FeMg	Phengite	n/a	2250.81	1913.42	0.151
ML23NM149	Muscovite	Chlorite-FeMg	2212.03	2245	1910.3	0.148
ML23NM150	Muscovite	Chlorite-FeMg	2206.46	n/a	1917.73	0.1
ML23NM151	Muscovite	Chlorite-FeMg	2211.52	2244.24	1909.17	0.1
ML23NM152	Chlorite-FeMg	Phengite	2213.77	2249.65	1915.12	0.117
ML23NM153	Chlorite-FeMg	Phengiticillite	2210	2249.14	1907.33	0.182
ML23NM154	Chlorite-FeMg	Montmorillonite	2211.35	2249.67	1909.85	0.217
ML23NM155	Muscoviticillite	Chlorite-FeMg	2208.38	2248.45	1910.32	0.107
ML23NM156	Epidote	Montmorillonite	n/a	2253.2	1908.19	0.204
ML23NM157	Muscoviticillite	Chlorite-FeMg	2206.37	n/a	1909.52	0.234
ML23NM158	Muscoviticillite	Chlorite-FeMg	2207.45	2246.42	1906.61	0.143
ML23NM159	Muscoviticillite	Chlorite-FeMg	2208.22	n/a	1907.85	0.0916
ML23NM160	Muscoviticillite	Chlorite-Mg	2210.62	n/a	1907.82	0.148
ML23NM161	Montmorillonite	Chlorite-Mg	2208.52	n/a	1906.77	0.286
ML23NM162	Muscoviticillite	Chlorite-FeMg	2210.49	n/a	1908.91	0.128
ML23NM163	Muscovite	Siderite	2206.15	n/a	n/a	0.105
ML23NM164	Muscovite	Chlorite-FeMg	2208.06	2248.65	n/a	0.148
ML23NM165	Muscovite	-	2207.43	n/a	1916.36	0.0827
ML23NM166	Chlorite-FeMg	Ankerite	n/a	2252.17	1908.48	0.144
ML23NM167	Chlorite-FeMg	Phengite	n/a	2249.42	1915.13	0.121
ML23NM168	Muscovite	Siderite	2209.8	n/a	1911.29	0.0761
ML23NM169	Chlorite-FeMg	Muscovite	2209.96	2248.57	1913.95	0.128
ML23NM170	Chlorite-FeMg	Muscovite	2205.56	2250.03	n/a	0.0894
ML23NM171	Phengite	Siderite	2210.15	n/a	n/a	0.0893
ML23NM172	Phengite	Chlorite-Mg	2210.83	2246.35	n/a	0.055
ML23NM173	Chlorite-FeMg	Phengite	2208.46	2248.58	1913.35	0.109
ML23NM174	Chlorite-FeMg	Gypsum	2217	2250.25	n/a	0.285
ML23NM175	Chlorite-FeMg	Muscovite	2207.72	2251.23	1922.11	0.0797
ML23NM176	Chlorite-FeMg	Biotite	n/a	2251.58	1877.29	0.18
ML23NM177	Muscovite	-	2204.72	n/a	n/a	0.0677
ML23NM178	Chlorite-FeMg	Muscovite	2205.64	2249.52	1879.42	0.129

n/a: not analyzed, no spectral peak, not calculated, - : no data

Appendix IV: Mineral chemistry of chlorite and white mica

Chlorite composition (wt %)

Sample ID	SiO ₂	Al ₂ O ₃	FeO	MnO	MgO	Na ₂ O	K ₂ O	TiO ₂	Cr ₂ O ₃	CaO	Total (-OH)
NM-24_chl-1	28.72	22.62	14.25	0.17	23.43	bdl	0.25	bdl	0.06	0.10	89.58
NM-24_chl-1	28.85	23.14	14.46	0.13	23.72	bdl	0.09	bdl	0.02	0.12	90.53
NM-24_chl-2	30.03	18.20	18.44	0.20	20.84	bdl	0.42	bdl	0.39	0.06	88.60
NM-24_chl-2	29.50	18.54	19.22	0.24	20.78	bdl	0.08	bdl	0.26	0.06	88.67
NM-24_chl-3	30.47	18.69	18.63	0.22	21.68	0.04	0.08	bdl	0.48	0.08	90.36
NM-24_chl-3	29.78	18.07	19.72	0.19	21.22	bdl	0.08	bdl	0.36	0.07	89.50
NM-24_chl-4	29.82	18.27	19.26	0.19	21.09	bdl	0.09	bdl	0.11	0.04	88.87
NM-24_chl-4	29.79	18.57	19.61	0.21	21.10	0.04	0.15	0.19	0.20	0.05	89.90
NM-24_chl-5	29.25	22.09	16.63	0.19	22.12	bdl	0.17	bdl	0.21	0.01	90.67
NM-24_chl-5	28.44	21.26	17.41	0.19	21.55	bdl	0.04	bdl	0.62	0.02	89.52
NM-38_chl-1	27.40	23.16	17.88	0.14	20.56	bdl	0.04	bdl	bdl	0.03	89.22
NM-38_chl-2	28.47	22.36	17.62	0.11	21.67	bdl	0.03	bdl	bdl	bdl	90.25
NM-38_chl-2	28.47	22.04	17.50	0.12	21.85	0.03	0.02	bdl	bdl	0.01	90.05
NM-38_chl-3	27.05	22.94	17.67	0.09	20.71	bdl	0.04	bdl	0.05	0.05	88.59
NM-38_chl-3	27.44	23.02	17.70	0.09	20.84	bdl	0.03	0.31	0.05	0.07	89.55
NM-38_chl-4	29.18	20.45	16.55	0.09	22.28	bdl	0.03	bdl	bdl	0.02	88.60
NM-38_chl-4	28.00	22.16	17.16	0.12	21.25	0.04	0.03	bdl	bdl	0.02	88.77
NM-38_chl-5	28.17	22.49	17.84	0.09	21.05	bdl	0.06	bdl	bdl	0.03	89.73
NM-38_chl-5	30.47	17.74	19.06	0.20	21.00	0.03	0.28	bdl	0.02	0.06	88.84
NM-59_chl-2	28.08	23.36	16.84	0.16	21.56	0.08	0.05	bdl	0.04	0.19	90.35
NM-59_chl-3	28.98	19.72	18.30	0.31	21.27	0.07	0.05	bdl	0.05	0.12	88.86
NM-59_chl-3	29.32	19.98	18.74	0.22	21.19	bdl	0.04	0.29	0.04	0.08	89.90
NM-59_chl-4	28.88	19.91	18.21	0.25	21.46	bdl	0.04	bdl	0.17	0.04	88.97
NM-59_chl-4	27.95	23.44	16.94	0.17	21.44	bdl	0.04	bdl	0.03	0.02	90.04
NM-59_chl-5	28.80	20.17	17.84	0.24	22.18	0.05	0.03	bdl	0.08	0.15	89.53
NM-59_chl-5	27.88	22.46	16.59	0.20	21.31	bdl	0.04	bdl	0.11	0.15	88.73
NM-88_CHL-1	27.33	22.99	16.00	0.27	21.93	bdl	0.04	0.07	bdl	0.02	88.65
NM-88_CHL-1	27.24	22.70	16.10	0.27	21.77	bdl	0.04	0.05	bdl	0.02	88.19
NM-88_CHL-1	27.51	23.40	15.62	0.26	21.73	bdl	0.04	0.05	bdl	0.01	88.64
NM-88_CHL-2	28.44	22.64	16.10	0.29	21.73	0.25	0.04	0.04	0.02	0.04	89.60
NM-88_CHL-2	27.48	22.84	16.02	0.26	22.05	bdl	0.03	bdl	bdl	0.04	88.72
NM-88_CHL-2	27.35	22.76	15.67	0.27	21.73	0.05	0.04	bdl	0.02	0.02	87.92
NM-88_CHL-3	27.59	22.82	15.59	0.24	22.16	0.03	0.03	bdl	0.01	0.02	88.50
NM-88_CHL-3	27.27	22.84	15.70	0.25	21.80	bdl	0.03	0.06	0.02	0.02	87.98
NM-88_CHL-4	27.63	22.82	15.79	0.24	22.17	bdl	0.04	0.06	bdl	0.02	88.75
NM-88_CHL-4	27.80	22.62	16.12	0.32	22.04	bdl	0.04	0.04	0.02	0.02	89.02
NM-88_CHL-4	27.47	23.54	15.75	0.23	22.08	bdl	0.04	0.04	bdl	0.02	89.17
NM-88_CHL-5	27.90	22.40	13.19	0.28	23.75	0.14	0.10	0.23	0.03	0.17	88.20
NM-88_CHL-5	27.84	22.34	13.29	0.26	24.02	0.07	0.06	0.05	bdl	0.04	87.97
MOSS-10_CHL-1	26.02	22.74	22.09	0.08	17.01	0.06	0.05	0.06	0.02	0.02	88.16

Sample ID	SiO ₂	Al ₂ O ₃	FeO	MnO	MgO	Na ₂ O	K ₂ O	TiO ₂	Cr ₂ O ₃	CaO	Total (-OH)
MOSS-10_CHL-1	26.33	22.49	22.29	0.11	16.89	0.05	0.04	0.06	0.02	0.01	88.30
MOSS-10_CHL-2	26.27	22.65	22.21	0.09	17.10	0.05	0.04	0.09	bdl	0.01	88.50
MOSS-10_CHL-2	27.72	22.57	22.18	0.13	16.41	bdl	0.04	0.06	0.01	bdl	89.12
MOSS-10_CHL-2	26.04	22.38	22.53	0.12	16.31	0.04	0.06	0.09	bdl	0.02	87.59
MOSS-10_CHL-3	26.09	23.02	22.85	0.14	16.70	0.09	0.07	0.02	0.02	0.08	89.09
MOSS-10_CHL-3	26.92	22.89	22.36	0.09	16.12	0.13	0.15	0.06	bdl	0.29	89.01
MOSS-10_CHL-4	25.75	22.87	22.70	0.12	16.97	bdl	0.04	0.05	bdl	0.05	88.56
MOSS-10_CHL-4	25.48	24.13	22.01	0.11	16.85	0.05	0.02	0.09	bdl	bdl	88.74
MOSS-10_CHL-4	26.82	23.07	23.08	0.07	16.95	bdl	0.10	0.06	bdl	0.04	90.18
MOSS-10_CHL-5	25.25	23.64	22.36	0.11	16.44	0.07	0.09	0.04	bdl	0.06	88.07
MOSS-10_CHL-5	25.76	23.11	22.82	0.12	16.75	bdl	0.04	0.08	0.02	0.02	88.71
MOSS-10_CHL-5	25.34	23.72	23.10	0.09	16.40	0.05	0.03	0.06	bdl	0.02	88.80
NM-01_CHL-1	25.55	23.50	22.37	0.24	16.68	0.04	0.04	0.06	0.03	0.03	88.54
NM-01_CHL-1	25.88	23.04	22.21	0.20	16.97	bdl	0.03	0.06	0.10	0.05	88.54
NM-01_CHL-1	25.59	23.50	22.07	0.25	16.78	bdl	0.03	0.05	0.14	0.11	88.51
NM-01_CHL-2	25.16	24.43	22.31	0.28	15.68	bdl	0.09	0.03	0.03	0.02	88.02
NM-01_CHL-3	25.62	24.02	21.89	0.25	16.32	bdl	0.02	0.06	0.06	0.07	88.30
NM-01_CHL-3	25.73	23.38	21.28	0.21	16.69	0.05	0.05	0.08	0.04	0.03	87.54
NM-01_CHL-3	25.42	23.34	22.37	0.23	16.63	0.04	0.05	0.09	0.03	0.08	88.27
NM-01_CHL-4	25.76	24.30	22.48	0.20	16.85	bdl	0.03	0.04	0.02	bdl	89.67
NM-01_CHL-4	26.39	23.49	22.14	0.24	17.21	bdl	0.02	0.06	bdl	0.02	89.57
NM-01_CHL-4	25.83	23.47	22.09	0.28	16.22	bdl	0.03	0.08	bdl	0.04	88.04
NM-01_CHL-5	25.44	23.98	21.84	0.18	16.66	bdl	0.04	0.04	bdl	0.17	88.35
NM-01_CHL-5	25.47	24.37	21.38	0.21	16.51	bdl	0.06	0.04	0.02	0.07	88.13
NM-073_CHL-1	26.84	23.53	20.85	0.24	17.82	0.10	0.04	0.03	0.02	0.03	89.50
NM-073_CHL-2	26.52	22.96	20.78	0.21	17.97	0.04	0.03	0.05	bdl	0.02	88.58
NM-073_CHL-2	27.30	23.86	19.93	0.26	18.18	bdl	0.04	0.07	bdl	0.03	89.67
NM-073_CHL-2	27.29	22.69	19.96	0.25	17.90	0.05	0.03	0.05	bdl	0.03	88.25
NM-073_CHL-3	27.05	23.57	20.84	0.18	17.95	0.05	0.04	0.06	0.07	0.03	89.85
NM-073_CHL-3	26.48	23.21	20.40	0.23	17.80	bdl	0.04	0.16	0.11	bdl	88.43
NM-073_CHL-3	26.41	22.76	21.03	0.23	17.59	bdl	0.04	0.08	0.06	0.03	88.22
NM-073_CHL-4	27.05	23.36	21.05	0.21	17.99	bdl	0.04	0.05	0.12	0.01	89.89
NM-073_CHL-4	27.39	23.03	20.65	0.23	18.09	bdl	0.03	0.09	0.10	bdl	89.60
NM-073_CHL-4	26.42	23.41	20.89	0.20	17.49	0.04	0.04	bdl	0.12	0.02	88.64
NM-073_CHL-5	26.46	23.36	21.27	0.27	17.26	0.04	0.02	0.05	bdl	0.03	88.75
NM-073_CHL-5	26.18	22.95	21.07	0.21	17.70	0.05	0.02	0.22	bdl	0.03	88.43
NM-073_CHL-5	26.75	23.46	21.04	0.24	17.49	bdl	0.03	0.05	bdl	0.08	89.15
NM-073_CHL-6	27.04	22.59	19.75	0.20	18.87	0.05	0.04	0.06	bdl	0.02	88.61
NM-073_CHL-6	26.76	23.09	19.87	0.24	18.27	bdl	0.05	0.07	bdl	0.03	88.36
NM-073_CHL-6	26.79	23.30	19.59	0.26	18.67	bdl	0.03	bdl	bdl	0.01	88.65
NM-046_CHL-1	28.98	21.08	12.28	0.30	25.13	bdl	0.05	0.03	0.02	0.36	88.23
NM-046_CHL-2	28.83	23.02	11.99	0.29	24.20	bdl	0.06	0.12	0.02	0.13	88.65
NM-068_CHL-1	26.03	24.58	22.12	0.29	16.87	bdl	0.04	0.07	bdl	0.01	90.01

Sample ID	SiO ₂	Al ₂ O ₃	FeO	MnO	MgO	Na ₂ O	K ₂ O	TiO ₂	Cr ₂ O ₃	CaO	Total (-OH)
NM-068_CHL-1	25.22	24.14	21.41	0.30	16.54	bdl	0.03	0.08	bdl	0.02	87.74
NM-068_CHL-1	25.61	24.82	21.96	0.32	16.83	0.04	0.04	0.07	0.01	0.02	89.72
NM-068_CHL-2	26.28	23.56	21.50	0.28	17.22	bdl	0.05	0.05	bdl	0.03	88.98
NM-068_CHL-2	25.85	24.45	21.64	0.33	16.41	bdl	0.09	0.07	bdl	0.03	88.88
NM-068_CHL-2	25.87	24.54	21.49	0.30	16.88	bdl	0.03	0.05	bdl	0.03	89.19
NM-068_CHL-3	25.57	24.29	21.44	0.32	16.73	bdl	0.04	0.04	0.01	0.11	88.54
NM-068_CHL-3	25.90	23.91	21.80	0.31	16.86	0.06	0.05	0.08	0.03	0.03	89.02
NM-068_CHL-4	26.15	24.39	23.02	0.33	16.13	0.04	0.02	bdl	bdl	0.01	90.10
NM-068_CHL-4	26.21	24.66	22.73	0.33	16.06	bdl	0.04	0.04	bdl	0.02	90.09
NM-068_CHL-4	25.46	24.72	23.57	0.31	15.59	bdl	0.02	0.06	bdl	0.02	89.74
NM-107_CHL-1	28.20	19.02	24.46	0.19	15.63	0.06	0.03	bdl	bdl	0.07	88.65
NM-107_CHL-1	27.25	19.49	25.79	0.18	14.90	bdl	0.04	bdl	bdl	0.05	88.71
NM-107_CHL-1	28.36	18.83	25.00	0.26	15.58	bdl	0.03	bdl	bdl	0.07	89.14
NM-107_CHL-2	28.27	20.25	20.37	0.69	18.80	bdl	0.05	bdl	bdl	0.03	88.45
NM-107_CHL-2	28.16	19.97	21.59	0.78	18.25	bdl	0.03	bdl	bdl	0.04	88.82
NM-107_CHL-2	28.35	19.98	21.47	0.72	18.27	bdl	0.06	0.06	0.02	0.05	88.97
NM-107_CHL-3	27.92	19.35	20.85	0.91	17.78	0.07	0.06	bdl	0.02	0.05	87.01
NM-107_CHL-3	28.20	19.61	19.75	0.85	18.80	0.05	0.07	bdl	0.02	0.13	87.48
NM-107_CHL-3	28.32	19.77	20.54	0.79	18.68	0.07	0.05	0.03	bdl	0.08	88.33
NM-107_CHL-4	28.63	19.62	20.58	0.80	18.50	0.10	0.09	0.08	0.02	0.22	88.65
NM-107_CHL-4	27.65	19.10	20.62	0.85	18.04	0.09	0.10	bdl	bdl	0.32	86.77
NM-107_CHL-4	28.71	18.71	20.64	0.88	18.51	0.10	0.06	bdl	0.02	0.17	87.81

Bdl: below detection limits

Detection limits: Na₂O> 0.03, TiO₂> 0.02, Cr₂O₃, CaO> 0.01, ZrO₂

White mica composition (wt %)

SAMPLE	SiO ₂	ZrO ₂	TiO ₂	Al ₂ O ₃	Cr ₂ O ₃	FeO	MnO	MgO	CaO	Na ₂ O	K ₂ O	Cl	Total (-OH)
NM-073_WM-1	50.00	bdl	0.09	33.42	bdl	2.29	bdl	0.91	0.36	2.44	9.17	bdl	98.68
NM-073_WM-1	56.23	bdl	0.11	28.74	bdl	1.62	bdl	0.37	0.69	6.07	5.37	bdl	99.20
NM-073_WM-2	45.25	bdl	0.47	33.71	0.04	3.99	bdl	1.29	0.07	0.37	10.95	bdl	96.14
NM-073_WM-2	45.35	bdl	0.27	34.13	0.03	3.86	bdl	1.27	0.03	0.44	10.65	bdl	96.04
NM-073_WM-2	45.41	bdl	0.47	33.34	0.03	4.19	bdl	1.43	0.05	0.32	10.65	bdl	95.89
NM-073_WM-3	45.93	bdl	0.61	33.74	0.18	4.08	bdl	1.22	bdl	0.36	10.79	bdl	96.90
NM-073_WM-3	45.32	bdl	0.23	33.58	0.16	4.87	bdl	1.38	bdl	0.33	10.74	bdl	96.61
NM-073_WM-3	45.81	bdl	1.27	32.76	0.14	4.56	bdl	1.47	bdl	0.36	10.78	bdl	97.16
NM-073_WM-4	49.36	bdl	0.08	33.61	bdl	2.30	bdl	0.83	0.11	2.17	9.36	bdl	97.81
NM-073_WM-5	45.49	bdl	0.35	32.48	bdl	4.38	bdl	1.82	bdl	0.31	10.80	bdl	95.62
NM-073_WM-5	45.75	bdl	0.56	32.93	0.02	3.93	bdl	1.58	bdl	0.31	10.71	bdl	95.81
NM-073_WM-5	45.27	bdl	0.27	33.31	bdl	4.42	bdl	1.55	0.03	0.37	10.71	bdl	95.93
NM-073_WM-5	44.98	bdl	0.72	33.32	bdl	3.80	bdl	1.33	0.55	0.46	10.35	bdl	95.52
NM-046_WM-1	46.82	bdl	0.37	33.56	bdl	2.35	bdl	2.23	bdl	0.28	11.04	bdl	96.64
NM-046_WM-1	48.00	bdl	0.21	32.21	bdl	2.17	bdl	2.53	0.01	0.27	11.13	0.01	96.54
NM-046_WM-1	47.04	bdl	0.29	33.44	bdl	2.45	bdl	2.26	0.01	0.26	11.09	bdl	96.84
NM-046_WM-2	48.25	bdl	0.26	32.72	bdl	2.00	bdl	2.32	bdl	0.26	11.07	bdl	96.88
NM-046_WM-2	47.44	bdl	0.36	32.74	0.12	2.25	bdl	2.55	0.02	0.26	11.07	bdl	96.81
NM-046_WM-3	46.31	bdl	0.42	33.89	0.03	2.42	bdl	2.01	bdl	0.26	10.91	bdl	96.26
NM-046_WM-3	46.82	bdl	0.29	34.12	0.02	2.42	bdl	2.09	0.02	0.30	10.89	bdl	96.96
NM-046_WM-3	46.17	bdl	0.32	34.24	bdl	2.36	bdl	1.99	bdl	0.25	11.00	bdl	96.32
NM-046_WM-4	46.75	bdl	0.20	34.20	bdl	2.22	bdl	2.05	0.01	0.29	10.84	bdl	96.57
NM-046_WM-4	46.42	bdl	0.24	33.89	0.01	2.23	bdl	1.97	0.01	0.29	10.88	bdl	95.95
NM-046_WM-4	47.18	bdl	0.30	34.17	bdl	2.29	0.03	1.96	0.01	0.33	10.86	bdl	97.12
NM-046_WM-5	46.21	bdl	0.43	33.33	0.07	2.48	bdl	2.37	0.04	0.26	10.81	0.04	96.04
NM-046_WM-5	47.25	bdl	0.44	33.42	0.09	2.41	bdl	2.21	0.01	0.29	10.80	bdl	96.92
NM-046_WM-5	46.11	bdl	0.24	29.51	0.19	3.77	0.07	4.21	1.77	0.14	8.87	0.02	94.92
NM-046_WM-6	46.36	bdl	0.43	33.06	0.07	2.61	0.04	2.43	bdl	0.28	10.94	bdl	96.21
NM-046_WM-6	48.49	bdl	0.21	31.72	0.05	2.20	bdl	2.72	0.01	0.25	11.08	bdl	96.74
NM-068_WM-1	46.90	bdl	0.36	34.09	bdl	2.99	bdl	0.95	0.05	1.05	10.17	bdl	96.57
NM-068_WM-1	46.03	bdl	0.44	32.39	0.04	4.63	bdl	1.80	bdl	0.43	10.66	0.01	96.44
NM-068_WM-1	48.38	bdl	0.29	32.31	0.02	3.39	0.03	1.47	0.19	1.21	9.96	0.01	97.28
NM-068_WM-2	46.09	bdl	0.18	36.37	0.02	2.77	bdl	0.79	0.01	0.52	10.58	bdl	97.34
NM-068_WM-2	45.75	bdl	0.15	36.35	0.02	2.70	bdl	0.77	bdl	0.47	10.85	bdl	97.06
NM-068_WM-2	45.56	bdl	0.27	34.42	bdl	4.06	0.02	1.79	0.02	0.31	10.55	bdl	97.01
NM-068_WM-3	44.50	bdl	0.34	34.86	0.08	3.15	0.03	0.94	0.03	0.39	10.75	bdl	95.06
NM-068_WM-3	45.85	bdl	0.39	35.18	0.02	3.23	bdl	1.01	bdl	0.36	11.11	bdl	97.15
NM-068_WM-4	46.19	bdl	0.27	36.64	0.03	2.94	bdl	0.76	bdl	0.50	10.88	0.02	98.23
NM-068_WM-4	47.64	bdl	0.47	34.28	bdl	3.65	bdl	1.43	bdl	0.46	10.77	0.02	98.72
NM-068_WM-5	45.31	bdl	0.18	36.58	0.12	2.66	bdl	0.64	bdl	0.64	10.43	0.01	96.57
NM-068_WM-5	44.85	bdl	0.15	35.80	0.31	2.89	0.03	1.00	bdl	0.50	10.74	0.03	96.31
NM-068_WM-5	44.74	bdl	0.27	35.36	0.23	2.95	bdl	0.87	bdl	0.54	10.72	0.04	95.73

SAMPLE	SiO ₂	ZrO ₂	TiO ₂	Al ₂ O ₃	Cr ₂ O ₃	FeO	MnO	MgO	CaO	Na ₂ O	K ₂ O	Cl	Total (-OH)
NM-107_WM-1	46.33	bdl	0.78	31.60	bdl	4.51	bdl	1.79	bdl	0.25	11.13	bdl	96.39
NM-107_WM-1	45.53	bdl	0.59	33.81	0.05	4.20	0.03	1.15	bdl	0.32	10.96	0.05	96.68
NM-107_WM-1	46.23	bdl	0.57	31.56	0.01	4.60	bdl	1.86	bdl	0.26	11.00	bdl	96.83
NM-107_WM-1	46.08	bdl	0.58	32.34	0.02	4.35	0.05	1.54	bdl	0.28	11.09	bdl	96.10
NM-107_WM-2	43.76	bdl	0.60	35.70	0.02	4.09	0.04	0.82	bdl	0.36	10.58	bdl	96.32
NM-107_WM-2	44.55	0.02	0.60	33.40	0.05	5.00	0.06	1.69	0.04	0.42	10.55	bdl	95.98
NM-107_WM-2	44.37	bdl	0.44	37.64	bdl	2.98	bdl	0.42	0.03	0.52	10.69	bdl	96.37
NM-107_WM-3	46.41	bdl	bdl	31.99	0.02	4.64	0.04	1.73	0.01	0.24	11.10	bdl	97.09
NM-107_WM-3	45.55	bdl	0.45	31.48	bdl	5.22	0.04	1.81	bdl	0.27	11.03	bdl	96.18
NM-107_WM-3	46.24	bdl	0.64	31.34	0.01	5.13	0.03	1.71	0.05	0.39	10.80	bdl	95.84
NM-107_WM-4	46.10	bdl	0.33	31.80	0.02	4.90	0.04	1.69	bdl	0.28	11.08	bdl	96.35
NM-107_WM-4	46.32	bdl	0.36	31.45	0.02	4.84	0.05	1.66	bdl	0.28	11.18	bdl	96.24
NM-107_WM-4	46.12	bdl	0.28	31.85	0.03	5.01	0.04	1.59	bdl	0.26	11.12	bdl	96.14
NM-001_WM-1	48.32	bdl	0.17	28.97	bdl	2.01	bdl	0.94	0.20	1.36	8.35	bdl	96.33
NM-001_WM-1	46.57	bdl	0.25	35.14	0.02	2.91	0.03	1.03	0.02	0.56	10.33	bdl	96.32
NM-001_WM-2	46.56	bdl	0.19	31.84	bdl	2.39	bdl	1.01	bdl	0.42	10.69	bdl	94.25
NM-001_WM-2	45.58	bdl	0.17	33.54	0.02	2.94	bdl	1.35	0.04	0.52	10.36	bdl	97.10
NM-001_WM-3	53.09	bdl	0.28	32.32	0.02	2.14	bdl	0.86	0.15	3.54	8.02	bdl	94.53
NM-001_WM-3	51.24	bdl	0.12	28.93	bdl	1.87	bdl	0.68	0.35	4.31	7.31	bdl	95.43
NM-001_WM-3	45.32	bdl	0.36	33.48	0.02	2.70	bdl	0.82	0.21	1.81	8.79	0.06	99.81
NM-001_WM-4	50.02	bdl	0.20	31.82	bdl	2.43	bdl	0.95	0.24	2.40	8.85	bdl	93.56
NM-001_WM-4	47.65	bdl	0.26	34.45	bdl	2.71	bdl	0.98	0.10	1.15	10.04	bdl	96.91
NM-001_WM-5	47.01	bdl	0.17	36.22	bdl	2.28	bdl	0.88	0.03	0.72	10.10	bdl	97.35
NM-001_WM-5	47.06	bdl	0.14	35.65	bdl	2.45	bdl	1.04	bdl	0.51	10.40	bdl	97.41
NM-001_WM-5	47.67	bdl	0.12	34.23	bdl	2.50	bdl	1.37	bdl	0.45	10.59	bdl	97.25
NM-001_WM-6	58.10	bdl	0.19	28.23	bdl	2.15	0.03	0.66	0.08	1.11	8.27	bdl	96.92
NM-001_WM-6	53.85	bdl	0.11	28.68	bdl	1.67	bdl	0.60	0.31	5.05	5.97	bdl	98.81
NM-001_WM-6	66.17	bdl	0.15	22.98	bdl	1.67	0.05	0.52	0.08	0.68	6.44	0.01	96.24
NM-008_WM-1	45.49	bdl	0.31	33.92	0.03	3.55	0.03	1.19	0.06	0.36	10.74	bdl	95.68
NM-008_WM-1	46.66	bdl	0.30	35.07	0.02	3.43	bdl	1.19	0.01	0.33	10.74	bdl	97.75
NM-008_WM-1	46.63	bdl	0.26	34.56	0.03	3.30	bdl	1.25	bdl	0.32	10.70	bdl	97.06
NM-008_WM-2	46.37	0.03	0.22	33.75	0.27	3.39	0.02	1.31	0.04	0.32	10.67	0.04	96.42
NM-008_WM-2	74.47	bdl	0.15	15.11	0.06	1.57	bdl	0.67	0.14	0.18	4.98	0.02	97.34
NM-008_WM-2	47.50	bdl	0.20	33.97	0.24	2.84	bdl	1.45	0.04	0.33	10.71	0.03	97.31
NM-008_WM-3	45.99	bdl	0.17	35.73	0.04	2.86	bdl	0.93	bdl	0.48	10.66	bdl	96.86
NM-008_WM-3	46.44	bdl	0.36	34.35	0.05	3.53	bdl	1.29	bdl	0.30	10.67	0.01	97.01
NM-008_WM-3	46.01	bdl	0.36	34.11	0.02	3.94	bdl	1.35	0.03	0.38	10.58	bdl	96.78
NM-008_WM-4	47.60	bdl	0.31	34.95	0.04	3.46	bdl	1.35	0.03	0.35	10.64	bdl	98.73
NM-008_WM-4	46.11	bdl	0.26	34.31	0.02	3.15	bdl	1.33	0.06	0.31	10.66	bdl	96.21
NM-008_WM-4	47.02	bdl	0.23	34.90	bdl	3.03	0.03	1.35	0.03	0.35	10.71	bdl	97.65
NM-008_WM-5	47.00	bdl	0.18	34.62	0.03	3.06	bdl	1.31	0.03	0.31	10.29	bdl	96.83

SAMPLE	SiO ₂	ZrO ₂	TiO ₂	Al ₂ O ₃	Cr ₂ O ₃	FeO	MnO	MgO	CaO	Na ₂ O	K ₂ O	Cl	Total (-OH)
NM-008_WM-5	45.92	bdl	0.25	34.11	0.05	3.38	0.02	1.27	0.03	0.39	10.78	0.02	96.22
NM-008_WM-5	46.11	bdl	0.21	34.33	0.03	3.11	bdl	1.19	0.03	0.32	10.48	bdl	95.80
NM-008_WM-6	46.18	bdl	0.32	34.37	bdl	3.52	bdl	1.28	0.02	0.33	10.89	0.01	96.92
NM-008_WM-6	44.75	bdl	0.32	33.53	0.02	3.58	bdl	1.27	0.08	0.30	10.70	bdl	97.10
NM-010_WM-1	47.35	bdl	0.28	35.54	bdl	2.01	bdl	1.60	bdl	0.35	10.87	bdl	94.54
NM-010_WM-1	46.42	bdl	0.48	34.07	bdl	2.55	bdl	2.05	0.01	0.32	10.49	bdl	98.01
NM-010_WM-1	47.31	bdl	0.33	34.75	0.02	2.19	bdl	1.71	bdl	0.28	10.88	bdl	96.39
NM-010_WM-2	47.34	bdl	0.20	34.89	0.02	2.11	bdl	1.66	bdl	0.29	10.97	bdl	97.47
NM-010_WM-2	47.72	bdl	0.31	34.11	bdl	2.39	bdl	1.99	bdl	0.29	11.17	bdl	97.49
NM-010_WM-3	47.42	bdl	0.42	34.43	bdl	2.31	bdl	1.82	bdl	0.42	10.84	bdl	97.99
NM-010_WM-3	47.65	bdl	0.49	34.28	bdl	2.38	0.02	1.90	bdl	0.30	10.79	bdl	97.65
NM-010_WM-3	48.30	bdl	0.47	34.40	bdl	2.18	bdl	1.96	0.01	0.28	10.67	bdl	97.81
NM-010_WM-4	47.54	bdl	0.45	34.24	0.02	2.30	0.03	1.89	0.01	0.28	10.91	bdl	98.28
NM-010_WM-4	46.94	bdl	0.60	33.41	bdl	2.79	bdl	2.55	bdl	0.26	10.78	bdl	97.66
NM-010_WM-4	47.19	bdl	0.50	33.56	bdl	2.39	bdl	2.10	0.01	0.23	11.07	bdl	97.32
NM-010_WM-5	47.71	bdl	0.24	34.92	0.02	2.04	bdl	1.73	bdl	0.35	10.89	bdl	97.06
NM-010_WM-5	47.23	bdl	0.40	33.72	bdl	2.24	bdl	1.90	0.01	0.27	11.29	bdl	97.89
NM-010_WM-5	48.01	bdl	0.41	34.52	bdl	2.51	bdl	1.99	0.02	0.21	10.99	bdl	97.06
NM-010_WM-6	47.02	bdl	0.32	32.97	bdl	2.14	bdl	1.99	0.03	0.24	10.92	0.05	98.66
NM-010_WM-6	48.71	bdl	0.33	31.93	bdl	2.03	bdl	1.77	0.11	1.52	9.43	0.07	95.69
NM-078_WM-2	49.17	bdl	0.33	29.38	bdl	4.50	bdl	2.31	0.18	2.28	9.08	bdl	96.10
NM-078_WM-2	46.82	0.05	0.12	32.18	bdl	3.47	bdl	1.69	0.12	0.38	11.04	bdl	97.24
NM-078_WM-3	51.06	bdl	0.20	28.50	bdl	3.82	bdl	1.97	0.51	2.65	9.04	bdl	95.86
NM-078_WM-3	48.09	bdl	0.28	29.75	bdl	4.61	bdl	2.40	0.04	0.91	10.44	bdl	97.75
NM-078_WM-3	46.63	bdl	0.37	30.22	bdl	4.98	bdl	2.38	0.03	0.35	10.68	bdl	96.51
NM-078_WM-4	47.45	0.42	0.18	31.17	bdl	3.35	bdl	2.18	0.11	0.54	10.67	bdl	95.63
NM-078_WM-4	46.79	bdl	0.18	31.61	0.02	3.20	bdl	2.02	0.02	0.41	10.93	bdl	96.06
NM-078_WM-4	47.29	bdl	0.19	32.02	bdl	3.12	bdl	2.08	0.03	0.33	10.94	bdl	95.19
NM-078_WM-5	45.23	bdl	0.31	30.74	0.02	4.69	bdl	3.09	0.12	0.38	10.37	bdl	95.99
NM-078_WM-5	47.01	bdl	0.13	31.20	0.02	4.32	0.04	2.97	0.10	0.36	10.34	bdl	94.95
NM-078_WM-5	53.03	bdl	0.11	28.91	bdl	2.36	bdl	1.21	0.78	4.43	7.35	bdl	96.49
NM-083_WM-1	47.03	bdl	0.23	33.20	bdl	3.18	0.02	1.54	0.03	0.36	10.91	bdl	98.18
NM-083_WM-1	51.49	bdl	0.22	30.26	bdl	2.42	bdl	1.98	0.13	1.97	9.52	bdl	96.51
NM-083_WM-1	50.51	bdl	bdl	29.57	0.01	2.73	0.03	2.96	0.01	0.24	10.85	bdl	97.98
NM-083_WM-2	46.89	bdl	0.15	32.11	0.01	3.07	0.03	1.86	bdl	0.26	11.25	0.02	96.92
NM-083_WM-2	48.05	bdl	0.16	33.42	bdl	3.13	bdl	1.78	0.01	0.29	10.83	bdl	95.66
NM-083_WM-2	48.97	0.04	0.09	31.21	bdl	2.79	bdl	2.49	0.01	0.22	10.74	bdl	97.67
NM-083_WM-3	42.49	bdl	0.36	30.67	0.07	5.32	0.09	5.46	bdl	0.28	8.76	bdl	96.57
NM-083_WM-3	44.07	bdl	0.31	31.16	0.08	5.33	0.04	5.07	bdl	0.27	9.13	bdl	93.51
NM-083_WM-3	47.43	bdl	0.59	32.76	0.02	3.13	0.03	1.86	bdl	0.37	10.95	bdl	95.46
NM-083_WM-4	46.83	bdl	0.28	32.58	0.03	3.26	bdl	1.94	0.02	0.27	10.88	bdl	97.14
NM-083_WM-4	49.23	bdl	bdl	30.03	bdl	2.52	bdl	2.86	bdl	0.24	10.99	bdl	96.07

SAMPLE	SiO ₂	ZrO ₂	TiO ₂	Al ₂ O ₃	Cr ₂ O ₃	FeO	MnO	MgO	CaO	Na ₂ O	K ₂ O	Cl	Total (-OH)
NM-083_WM-4	48.51	bdl	0.06	30.61	0.03	2.77	0.04	2.62	bdl	0.23	10.98	bdl	95.86
NM-083_WM-5	48.92	bdl	bdl	29.35	bdl	2.83	bdl	2.89	bdl	0.22	10.75	0.03	94.98
NM-083_WM-5	46.51	bdl	0.19	33.05	bdl	3.21	bdl	1.76	bdl	0.34	10.80	bdl	95.87
NM-083_WM-5	47.85	bdl	0.16	31.68	bdl	2.78	bdl	2.30	bdl	0.36	10.82	bdl	95.95
NM-038_WM-1	46.84	bdl	0.28	31.94	0.03	3.75	bdl	1.94	0.03	0.39	10.81	0.02	95.48
NM-038_WM-1	65.48	bdl	bdl	18.54	bdl	0.58	bdl	0.44	0.02	0.17	15.88	bdl	96.04
NM-038_WM-2	46.24	0.03	0.35	31.53	bdl	4.02	bdl	1.88	0.01	0.29	11.16	bdl	96.57
NM-030_WM-1	45.81	bdl	0.31	32.39	0.02	3.21	bdl	1.73	0.01	0.45	10.84	bdl	95.51
NM-030_WM-1	46.38	bdl	0.37	32.08	bdl	3.92	bdl	2.16	0.01	0.20	10.59	bdl	94.77
NM-030_WM-1	46.62	bdl	0.35	34.02	0.02	3.14	bdl	1.29	bdl	0.38	10.37	bdl	95.70
NM-030_WM-3	46.65	bdl	0.53	33.38	0.05	3.31	bdl	1.53	0.04	0.33	10.73	bdl	96.20
NM-030_WM-3	45.50	bdl	0.55	33.04	0.08	3.14	bdl	1.60	0.02	0.38	10.38	bdl	96.54
NM-030_WM-4	46.77	bdl	0.37	33.09	bdl	3.22	bdl	1.67	0.01	0.28	10.51	bdl	94.68
NM-030_WM-4	47.28	bdl	0.51	33.04	bdl	3.08	bdl	1.60	0.03	0.41	10.46	bdl	95.92
NM-030_WM-5	52.69	bdl	0.29	30.12	bdl	2.87	bdl	1.29	bdl	0.25	9.79	0.01	96.41
NM-030_WM-5	46.70	bdl	0.36	33.28	bdl	3.06	bdl	1.48	bdl	0.30	10.87	bdl	97.30
NM-030_WM-5	46.23	bdl	0.30	33.69	bdl	3.09	0.03	1.35	bdl	0.37	10.65	bdl	96.06
NM-065_WM-1	46.90	bdl	0.06	32.84	0.02	3.57	bdl	1.36	bdl	0.25	10.64	bdl	95.71
NM-065_WM-1	48.86	bdl	0.03	32.63	0.02	2.83	bdl	1.28	0.03	0.80	10.20	bdl	95.64
NM-065_WM-1	47.39	bdl	0.03	32.51	bdl	3.44	0.03	1.54	0.02	0.32	10.14	0.02	96.69
NM-065_WM-2	47.44	bdl	0.09	34.21	bdl	2.78	bdl	1.04	0.03	0.39	10.27	bdl	96.26
NM-065_WM-2	48.22	bdl	0.10	31.37	bdl	3.80	bdl	1.55	0.03	0.27	10.41	bdl	95.75
NM-065_WM-2	46.45	bdl	0.07	32.76	bdl	3.08	bdl	1.34	bdl	0.32	10.47	bdl	94.50
NM-065_WM-3	47.36	bdl	0.09	35.01	bdl	2.65	bdl	0.92	bdl	0.48	10.50	bdl	97.01
NM-065_WM-3	49.31	bdl	0.03	32.40	bdl	2.88	0.04	1.58	0.04	0.92	9.87	bdl	97.08
NM-065_WM-3	47.30	bdl	0.26	31.91	bdl	3.53	bdl	1.62	0.01	0.39	10.47	bdl	95.50
NM-065_WM-4	47.07	bdl	0.05	33.00	0.02	3.54	bdl	1.21	0.02	0.33	10.58	bdl	95.81
NM-065_WM-4	47.17	bdl	0.09	33.41	bdl	3.22	bdl	1.25	0.01	0.26	10.52	bdl	95.94
NM-065_WM-4	46.35	bdl	0.09	34.54	bdl	3.06	bdl	0.97	0.02	0.35	10.63	bdl	96.00
NM-065_WM-5	48.25	bdl	0.08	32.32	bdl	3.22	0.03	1.29	0.07	0.24	10.21	bdl	95.69
NM-065_WM-5	49.69	bdl	bdl	31.83	bdl	3.08	bdl	1.57	0.10	0.19	10.12	bdl	96.58
NM-070_WM-1	48.59	bdl	0.32	31.41	0.02	3.49	bdl	1.61	0.06	0.53	10.52	bdl	96.55
NM-070_WM-1	47.01	bdl	0.39	34.12	0.06	3.52	bdl	0.99	bdl	0.39	10.50	bdl	96.98
NM-070_WM-1	46.07	bdl	0.24	34.44	0.05	3.50	bdl	0.85	bdl	0.45	10.63	bdl	96.23
NM-070_WM-2	46.88	bdl	0.37	34.72	bdl	3.31	bdl	1.00	0.03	0.45	10.34	bdl	97.09
NM-070_WM-2	46.21	bdl	0.28	34.57	0.01	3.43	bdl	0.82	0.01	0.51	10.43	bdl	96.28
NM-070_WM-2	45.35	bdl	0.22	34.17	bdl	4.04	0.03	1.13	0.01	0.38	10.48	bdl	95.83
NM-070_WM-3	46.02	bdl	0.24	34.79	0.03	3.46	bdl	0.73	0.05	0.50	10.30	bdl	96.10
NM-070_WM-3	45.70	bdl	0.19	35.82	bdl	3.20	bdl	0.51	bdl	0.57	10.56	bdl	96.54
NM-070_WM-3	46.19	bdl	0.34	34.43	0.02	3.75	bdl	0.94	0.03	0.41	10.68	bdl	96.80
NM-070_WM-4	46.20	bdl	0.28	34.55	0.02	3.43	bdl	0.87	bdl	0.41	10.51	bdl	96.27
NM-070_WM-4	46.89	0.04	0.34	34.78	0.02	3.32	bdl	0.91	0.03	0.42	10.58	bdl	97.34
NM-070_WM-4	46.15	bdl	0.16	35.43	0.03	2.84	bdl	0.64	0.01	0.61	10.48	bdl	96.37
NM-070_WM-5	46.28	0.11	0.32	32.29	0.06	3.38	bdl	1.18	0.14	0.77	10.12	bdl	94.64

SAMPLE	SiO ₂	ZrO ₂	TiO ₂	Al ₂ O ₃	Cr ₂ O ₃	FeO	MnO	MgO	CaO	Na ₂ O	K ₂ O	Cl	Total (-OH)
NM-070_WM-5	45.22	bdl	0.21	33.10	0.02	3.49	bdl	1.03	0.18	0.35	10.00	bdl	93.59
NM-070_WM-5	46.86	0.17	0.16	33.39	0.01	4.77	bdl	1.76	0.08	0.33	9.44	bdl	96.97

Bdl: below detection limits

Detection limits: TiO₂> 0.03, Cr₂O₃, CaO, Cl> 0.01, ZrO₂ >0.02, MnO> 0.02